UNIVERSITY OF CALIFORNIA

Santa Barbara

Smartphone-based Molecular Pathogen Identification, and Host-mediated Antimicrobial Susceptibility

A Dissertation submitted in partial satisfaction of the requirements for the degree Doctor of Philosophy in Molecular, Cellular and Developmental Biology

by

Lucien Barnes

Committee in charge:

Professor Michael J. Mahan, Chair

Professor David A. Low

Professor Christopher S. Hayes

September 2021

The dissertation of Lucien Barnes is approved.

_____

Professor David A. Low

_____

Professor Christopher S. Hayes

_____

Professor Michael J. Mahan, Committee Chair

September 2021

Smartphone-based Molecular Pathogen Identification,

and Host-mediated Antimicrobial Susceptibility

By

Lucien Barnes

Dedicated to my Mom.

For always being there.

And for encouraging me to ask “Why?”

ACKNOWLEDGEMENTS

My graduate career has been an incredible experience, and I am deeply thankful for the support I have received from all of the amazing people I have been lucky enough to have in my life. To begin, I would like to thank my advisor, Dr. Michael Mahan, for his guidance, encouragement, and support, and for allowing me to work on projects with immediate applications against infectious disease. I would like to deeply thank Dr. Douglas Heithoff, for his constant support, for sharing his scientific excellence, and for his friendship. Thank you to my colleague in the lab for many years, Dr. Selvi Ersoy, for your positive energy and brilliant insights! To all of my other friends from the Mahan Lab, Geneva Tripp, Scott Mahan, Jakob Harrison-Gleason, David Finkelson, and David Baskin, thank you for the countless happy memories you have left me with. I would like to sincerely thank the members of my committee, Dr. David Low, and Dr. Christopher Hayes for your phenomenal advice and continual support. Thank you also to the amazing professors I have been able to TA courses for, Dr. Charles Samuel, Dr. Seng-Hui Low, and Dr. Douglas Thrower. And a very large thank you to Dr. Kathy Foltz, for being a role-model as a brilliant and caring scientist.

My family and friends are the center of my life, and I want to thank them all for their extreme support and kindness during these last seven years. To my dear, late mother and father, I owe everything to you, and I miss you every day. To my loving stepdad Bob, thank you for being there for me, I am truly blessed to have you in my life. And thank you to my Aunt Connie, Uncle Gary, Uncle Keith, and my wonderful cousins for being a cherished part of my life.

VITA OF LUCIEN BARNES

September 2021

EDUCATION

Bachelor of Science in Cellular and Molecular Biology/Biochemistry,
minors in Chemistry, English
Department of Biology
Western Washington University, Bellingham, WA, 2006-2010

Doctor of Philosophy in Molecular, Cellular and Developmental Biology
Department of Molecular, Cellular and Developmental Biology
University of California, Santa Barbara, 2014-2021

AWARDS AND HONORS

Recipient of Chang Fellowship, University of California, Santa Barbara, 2017

Recipient of Siff Foundation Fellowship, University of California, Santa Barbara, 2016

Recipient of Storke Fellowship, University of California, Santa Barbara, 2015

Recipient of Rathmann Fellowship, University of California, Santa Barbara, 2014

RESEARCH EXPERIENCE

Graduate Student Researcher, University of California, Santa Barbara
Santa Barbara, CA, 2014-2021

- Advisor: Professor Michael Mahan
- Research: Development of point-of-care smartphone-based diagnostics for bacterial and viral pathogens, as well as antimicrobial susceptibility tests in host mimicking and ex vivo media

Process Development Specialist, Infectious Disease Research Institute, Seattle
Seattle, WA, 2010-2014

- Supervisors: Dr. Ryan Kramer, Dr. Thomas Vedvick, Dr. James Chesko
- Research: Biophysical characterization of recombinant vaccine formulations, and vaccine lyophilization process development

RESEARCH EXPERIENCE (Continued)

Undergraduate Research Assistant, Western Washington University, Bellingham
Bellingham, WA, 2008-2010

- Supervisor: Professor Marion Brodhagen
- Research: Development of molecular diagnostics and discovery of antimicrobial compounds against the fungal pathogen *Aspergillus flavus*

TEACHING EXPERIENCE

Teaching Assistant, University of California, Santa Barbara:
MCDB 138 – Medical Immunology (summer 2021)
MCDB 21 – The Immune System and AIDS (spring 2021)
MCDB 132L – Bacterial Pathogenesis Laboratory
(winter 2016, 2017, 2020, 2021)
MCDB 139 – Medical Microbiology (spring 2018)
MCDB 134 – Animal Virology (spring 2016)
MCDB 101A – Bacterial Genetics (summer session 2015, fall 2015)
MCDB 101B – Eukaryotic Genetics (summer 2015)
MCDB 1AL – Introductory Biology Laboratory (fall 2014)

PUBLICATIONS

Peer-Reviewed

Douglas M. Heithoff, **Lucien Barnes**, Scott P. Mahan, Gary N. Fox, Katherine E. Arn, Lynn N. Fitzgibbons, Jeffery C. Fried, David A. Low, Charles E. Samuel, and Michael J. Mahan. Transforming the smartphone into a stand-alone point-of-care diagnostic for SARS-CoV-2 and influenza. *In submission* (2021).

Lucien Barnes, Douglas M. Heithoff, Scott P. Mahan, Gary N. Fox, Andrea Zambrano, Jane Choe, Lynn N. Fitzgibbons, Jamey D. Marth, Jeffrey C. Fried, H. Tom Soh, and Michael J. Mahan. Smartphone-based pathogen diagnosis in urinary sepsis patients. *EBioMedicine* 36 (2018): 73-82.

Selvi C. Ersoy, Douglas M. Heithoff, **Lucien Barnes**, Geneva K. Tripp, John K. House, Jamey D. Marth, Jeffrey W. Smith, Michael J. Mahan. Correcting a Fundamental Flaw in the Paradigm for Antimicrobial Susceptibility Testing. *EBioMedicine*, 20(2017):173-181.

Lucien Barnes, Dawn M. Fedor, Simon Williams, Quinton M. Dowling, Michelle C. Archer, Sylvain Cloutier, Sarah Parker, Thomas S. Vedvick, Christopher B. Fox, Ryan M. Kramer. Lyophilization of an adjuvanted Mycobacterium tuberculosis

vaccine in a single-chamber pharmaceutical cartridge. AAPS *PharmSciTech* 18, no. 6 (2017): 2077-2084.

Mark T. Orr, Ryan M. Kramer, **Lucien Barnes**, Quinton M. Dowling, Anthony L. Desbien, Elyse A. Beebe, John D. Laurence, Christopher B. Fox, Steven G. Reed, Rhea N. Choler, Thomas S. Vedvick. Elimination of the cold-chain dependence of a nanoemulsion adjuvanted vaccine against tuberculosis by lyophilization. *Journal of Controlled Release,* 177:20-26. 2014.

Christopher B. Fox, Ryan M. Kramer, **Lucien Barnes**, Quinton M. Dowling, Thomas S. Vedvick. Working together: interactions between vaccine antigens and adjuvants. *Therapeutic Advances in Vaccines,*1:7-20. 2013.

Christopher B. Fox, **Lucien Barnes**, Tara Evers, James D. Chesko, Thomas S. Vedvick, Rhea N. Choler, Steven G. Reed, Susan L. Baldwin. Adjuvanted pandemic influenza vaccine: variation of emulsion components affects stability, antigen structure, and vaccine efficacy. *Influenza and Other Respiratory Viruses,* 7:815-826. 2013.

PUBLICATIONS

Textbook Chapters and Patents

Michael J. Mahan, Douglas M. Heithoff, **Lucien Barnes**, Robert L. Sinsheimer. Epigenetic Programming by Microbial Pathogens and Impacts on Acute and Chronic Disease. In *Epigenetics of Infectious Diseases*, pp. 89-112. Springer International Publishing, 2017.

Michelle Y. Chan, Dawn M. Fedor, Tony Phan, **Lucien Barnes**, Ryan M. Kramer. Interactions Between Antigens and Nanoemulsion Adjuvants: Separation and Characterization Techniques. In *Vaccine Adjuvants*, pp. 285-294. Humana Press, New York, NY, 2017.

Christopher B. Fox, Thomas S. Vedvick, **Lucien Barnes,** Ryan M. Kramer, Steven G. Reed. Single Vial Vaccine Formulations. US. Pat. Appl. US20160324783A1, 2014.

ABSTRACT

Smartphone-based Molecular Pathogen Identification,

and Host-mediated Antimicrobial Susceptibility

by

Lucien Barnes

Bacterial and viral infections represent an urgent and dynamic threat to human health. Infections with antibiotic resistant pathogens are increasing at an alarming rate, and emergent zoonotic viruses have again demonstrated the potential severity of their impact on society during the SARS-CoV-2 pandemic. In this dissertation, we develop unique approaches to both diagnose pathogen identity and treat antibiotic-resistant infections. We first describe a smartphone-based point-of-care pathogen nucleic acid diagnostic. This method accurately and quantitatively diagnoses important infections, including SARS-CoV-2, influenza, and urinary sepsis pathogens, directly from human patient specimens. To address antibiotic resistance, the second part of this dissertation develops testing methods that utilize host microenvironmental signals and more accurately identify effective antibiotics during prescription selection. During an infection, bacterial pathogens frequently adopt physiological changes in response to the host microenvironment, which can sometimes render them more (or less) susceptible to a given antibiotic. The first approach uses host signals (such as sodium bicarbonate) to mimic the host

environment within culture media. These conditions identified clinically significant differences in antibiotic susceptibility across a wide variety of human bacterial pathogens, and were predictive of treatment outcome in murine models of sepsis. We next developed a method of testing antimicrobial susceptibility directly in human urine and serum, which provides a more complete assortment of host signals than is available with contrived growth media. This assay also identified many clinically significant differences in susceptibility, and now requires confirmation in murine and human patient infections. Collectively, these molecular diagnostic and antibiotic testing approaches provide additional options for rapid pathogen diagnosis, and selection of effective antimicrobial treatments.

TABLE OF CONTENTS

LIST OF TABLES AND FIGURES

ABBREVIATIONS

AIDS	acquired immunodeficiency syndrome
AST	antimicrobial susceptibility test
AZM	azithromycin
BIP	backwards inner primer
BL	backwards loop primer
CDC	Centers for Disease Control and Prevention
CLSI	Clinical and Laboratory Standards Institute
CFU	colony forming unit
CFX	ceftriaxone
CoNS	coagulase negative *Staphylococcus*
COVID-19	coronavirus disease 2019
CRAB	carbapenem-resistant *Acinetobacter baumannii*
CRKP	carbapenem-resistant *Klebsiella pneumoniae*
CRPA	carbapenem-resistant *Pseudomonas aeruginosa*
CRE	carbapenem-resistant *Enterobacteriaceae*
CSBA	Columbia Sheep's Blood Agar
Ct	Threshold cycle
d	days
DMEM	Dulbecco's Modified Eagle Medium
dNTP	deoxyribonucleotide triphosphate
EC	*Escherichia coli*
ERY	erythromycin
ESBL	extended-spectrum β-lactamase
ESKAPE	*Enterococcus, Staphylococcus, Klebsiella, Acinetobacter, Pseudomonas*, and *Enterobacter*
EUA	emergency use authorization
FDA	food and drug administration
FIP	forward inner primer
FL	forward loop primer
IVAS	in vivo altered susceptibility
h	hours
HIV	human immunodeficiency virus
ID	identification
i.p.	intraperitoneal
i.v.	intravenous
KPN	*Klebsiella pneumoniae*
LAMP	loop-mediate isothermal amplification
LB	Luria-Bertani medium

LD_{50}	lethal dose 50 (dose required to kill 50% of animals tested)
LED	light emitting diode
LHB	Lysed Horse Blood
LOD	limit of detection
LPM	low-phosphate, low-magnesium medium
m	minutes
MALDI-TOF	matrix-assisted laser desorption ionization time of flight
MERS	middle east respiratory syndrome
MHB	Mueller Hinton Broth
MIC	minimum inhibitory concentration
MLM	modified Lacks medium
MRSA	methicillin-resistant *Staphylococcus aureus*
MSSA	methicillin-sensitive *Staphylococcus aureus*
NEAR	nicking-enzyme amplification reaction
PA	*Pseudomonas aeruginosa*
PBS	phosphate buffered saline
PC	personal computer
PCR	polymerase chain reaction
PK/PD	pharmacokinetic/pharmacodynamic
POC	point-of-care
SA	*Staphylococcus aureus*
SARS	severe acute respiratory syndrome
smaRT-LAMP	smartphone-based loop-mediated isothermal amplification
SE	*Salmonella* Enteritidis
SPN	*Streptococcus pneumoniae*
ST	*Salmonella* Typhimurium
$TCID_{50}$	tissue culture infectious dose 50 (dose required to infect 50% of cultures)
THB	Todd-Hewitt Broth
TS	tryptic soy
Tt	time to threshold
UTI	urinary tract infection
VRSA	vancomycin-resistant *Staphylococcus aureus*
WHO	World Health Organization
YP	*Yersinia pseudotuberculosis*

Chapter 1

General Introduction

1.1. THE DUAL THREATS OF EMERGING PATHOGENS AND ANTIMICROBIAL RESISTANCE

Despite humanity's valiant efforts to defend itself against infectious disease, novel pathogens will continue to emerge, requiring constant vigilance and the ability to rapidly respond to new threats when they arise. Further, existing pathogens are gradually escaping our best therapeutic strategies following decades of inadequate antibiotic stewardship, via the evolution and accumulation of resistance genes (*1*). Our society thus faces two concurrent microbial threats, one from organisms that we have never encountered, and the other from more familiar pathogens that now evade our control. To address these threats, we must develop adaptable and scalable molecular pathogen diagnostics that can identify novel pathogens or variants as they emerge. In addition, we must develop therapeutic prescription strategies against antibiotic resistance to leverage the large existing arsenal of antimicrobials, instead of relying on the waning discovery of additional novel molecules (*2*). The focus of this dissertation is to address these issues, by introducing a novel nucleic acid pathogen diagnostic (termed "smaRT-LAMP" in Chapters 2 and 3) and methods of identifying efficacious antimicrobials using host microenvironmental susceptibility signals (Chapters 4 and 5).

RNA viruses represent an enormous pandemic threat to humanity from novel zoonotic pathogens (*3*). Although secondary bacterial infections are often closely associated with viral pandemics (*4*) and bacterial pathogens or emergent strains can frequently result in extensive tragic outbreaks (*5*-*7*), novel RNA virus pandemics have proven to be particularly dire over the past century. The high genomic diversity

and speed of transmission among such RNA viruses create significant challenges for development and deployment of diagnostics in a timely manner.

The most severe viral pandemic within the last several generations was caused by avian influenza A (H1N1) in 1918, which rapidly spread across the globe, and killed an estimated 50 – 100 million people (*8*). This occurred long before the advent of molecular diagnostics, and serves as a dire warning of the potential mortality of future pandemics. In the 1980s, Human Immunodeficiency Virus (HIV) was discovered, and began a global epidemic which by 2015 had infected an estimated 76 million people, and killed 35 million people (*9*). Molecular diagnostics for this pathogen emerged slowly (*10*) and a high prevalence of untested asymptomatic individuals still contributes to the continued transmission occurring today.

In 2002 another novel viral pathogen, the coronavirus SARS-CoV-1 (severe acute respiratory syndrome coronavirus 1), emerged in China and was relatively well contained, causing only 8,089 reported infections and 774 deaths (*11*). In this case, a nucleic acid diagnostic (nasopharyngeal aspirate reverse transcription-PCR) was developed rapidly (*12*), and facilitated timely infection control efforts. At the end of the decade, the world was faced with another novel viral pandemic – an H1N1 influenza A, which was far less lethal than the 1918 strain, but still caused 60.8 million cases and 12,469 deaths in the United States between 2009 and 2010 (*13*). During this pandemic, a PCR assay was approved by the CDC two weeks after the pandemic was recognized in 2009, and multiple other assays were developed by clinical laboratories (*14*), helping to reduce transmission and improve treatment.

Two years later in 2012, another more lethal novel coronavirus was identified – MERS-CoV (Middle East respiratory syndrome coronavirus) – which had infected 2000 patients globally, and had a mortality rate above 30%. Nucleic acid diagnostics were developed shortly after identification, but this pathogen remains a future pandemic risk (*15*). The next noteworthy viral epidemic in 2014 was caused by Ebola virus, and occurred in West Africa. Although the first recorded outbreak of this virus occurred in 1976, the 2014 epidemic caused global concern due to a high mortality rate and large scale, with 28,646 cases and 11,323 deaths (*16*). Commercial RT-PCR assays became available in 2014 (*17*), which contributed to the eventual containment of this pathogen.

At the end of 2019, the latest novel viral threat was identified in China, when the SARS-CoV-2 (severe acute respiratory syndrome coronavirus 2) coronavirus began to spread, shortly before the COVID-19 respiratory disease pandemic. The SARS-CoV-2 virus disseminated rapidly around the globe, due in part to its high transmissibility, long (2-14 day) asymptomatic incubation period, and high percentage (> 40%) of asymptomatic spreaders (*11*). Although molecular diagnostics emerged quickly, an exceedingly high demand for reagents resulted in minimal testing occurring in the initial months of the pandemic (*18*). Widespread testing has become easier in well-developed regions, but it remains a challenge for areas with limited healthcare resources. This issue may re-emerge globally during upcoming cold and flu seasons, when social distancing will be less common. Molecular differentiation between influenza and SARS-CoV-2 will likely become

important, and unfortunately, manufacturers are struggling to produce the complex probe-based diagnostics required for large-scale differential testing (*19*).

The viral epidemics and pandemics of the previous century underscore the importance of rapid development and deployment of molecular diagnostics for novel pathogens. Such diagnostics must not only be developed expeditiously, but must also be scalable enough for immediate deployment during the early stages of a pandemic. Chapters 2 and 3 describe a method to enable this (termed “smaRT-LAMP”), which permits rapid assay development for novel pathogens, and does not rely on molecular probes or expensive equipment. SmaRT-LAMP can be performed anywhere in the world using little more than a cell phone, hot plate, and a cardboard box, to test up to 96 total reactions with quantitative results in 25 minutes.

The emergence of novel antibiotic resistant strains of known bacterial pathogens represents an equally dire threat to humanity as novel viral pathogens. However, this process has been occurring over longer timescales, and without intervention, will likely result in a “post-antibiotic era”, in which even minor bacterial infections could prove lethal without effective antibiotic therapies. Currently in the United States, there are estimated to be more than 2.8 million antibiotic-resistant infections and 35,000 deaths annually (*20*) which is expected to increase as the emergence of new resistant strains continues to outpace antibiotic discovery. This resistance has largely been caused by a combination of poor antibiotic stewardship, subtherapeutic clinical treatment, agricultural antibiotic abuse, environmental contamination, and patients with recurring infections.

Antibiotic stewardship refers to the practice of optimizing antibiotic use in order to best treat a patient, yet avoid selection of antibiotic resistance within bacterial pathogens (*21*). In a clinical setting, rapid prescription often involves the selection of empirical therapies based on disease presentation and epidemiology, without specifically identifying the causative pathogen or characterizing its unique antibiotic resistance profile (*22, 23*). If an inappropriate antibiotic is thusly administered, the patient fails to respond, and the patient's microbiota are also exposed to a selective pressure that selects for antibiotic resistance gene evolution or acquisition (*24*). When this occurs on a large scale, with many patients, in many hospitals, pathogenic and commensal organisms can gradually develop substantial resistance to the antibiotic.

In addition to poor stewardship, subtherapeutic or incomplete treatment can also select for antibiotic resistance, when a susceptible pathogen is exposed to a low concentration of an antibiotic, but is not killed. This can occur for multiple reasons, including imperfect drug penetration into an infected organ, such as during treatment with a combination therapy, which provides a microenvironment that selects for resistance to individual drugs in the cocktail (*25*). Resistance can also occur as a result of poor patient compliance (when a patient prematurely ends a course of antimicrobial therapy), and is common when treatment regimens include long-term administration of toxic antibiotic chemotherapies, such as for tuberculosis (*26*). In this case, the pathogen is exposed to an antibiotic, but not for enough time to be killed, which selects for resistance.

Antibiotic resistance can also emerge due to antibiotic misuse in the agricultural industry, and from environmental contamination with antibiotics. The poultry industry represents an unfortunate example of agricultural overuse of antibiotics, leading to antibiotic resistance. In this industry, antibiotics are administered in extremely large quantities for both disease treatment and growth promotion; in 2016 alone an estimated 1,265,420 kg of “medically important” antimicrobials were used, providing an enormous opportunity for resistance genes to emerge and enter the environment (*27*). Environmental contamination with low-concentration antimicrobials also provides a serious risk of antimicrobial resistance evolution, and in one study, ciprofloxacin was detected at 2.5 mg/L in an Indian river downstream of a wastewater treatment plant. Such anthropogenic contamination with nearly therapeutic concentrations of antimicrobials provides a considerable opportunity for resistance genes to both evolve de novo, and to be accumulated by potential human pathogens (*28*).

Treatment of chronic and recurring infections are another important source for antimicrobial resistance to emerge. This includes treatment of immunocompromised individuals, cystic fibrosis patients, and recurring urinary tract infections. Patients with a compromised immune system (such as AIDS patients, or those who are undergoing treatment with immunosuppressing cancer chemotherapies) often require frequent treatments with antimicrobials, but have a lower chance of clearing the pathogen due to immune dysfunction. This can result in antibiotic resistance due to disruptive selective pressures and exposure to prophylactic therapies to prevent opportunistic infection (*29*). Antibiotic resistance can also emerge when treating

cystic fibrosis patients, who cannot easily clear lung pathogens and must be provided prophylactic antimicrobials beginning at an early age to minimize infection-related loss of lung function. Because cystic fibrosis patients are surviving longer than ever and are frequently on prophylactic antimicrobials, the opportunity for multi-drug resistant pathogens to emerge within these patients is also increasing (*30*). Treatment of asymptomatic bacteriuria in patients with recurring urinary tract infections provides an additional potential route for selection of antibiotic resistant pathogens due to frequent and unnecessary exposure to antibiotics; this has been associated with an increased prevalence of antibiotic resistant infections in these patients (*31*).

Due to the processes described above, a wide variety of multi-drug resistant pathogens have emerged, which are poised to inflict substantial human harm. Some of the more noteworthy drug resistant pathogens currently include Methicillin-Resistant *Staphylococcus aureus* (MRSA), Vancomycin-Resistant *Staphylococcus aureus* (VRSA), Carbapenem-Resistant *Enterobacteriaceae* (CRE) and other Carbapenem-resistant bacteria such as Carbapenem-Resistant *Acinetobacter baumannii* (CRAB), Carbapenem-Resistant *Klebsiella pneumoniae* (CRKP) and Carbapenem-Resistant *Pseudomonas aeruginosa* (CRPA). Some of these (such as MRSA) can be frequently acquired in the community, while others are more often associated with hospitalization or long-term care facilities.

MRSA was first detected in the 1960s, and has since become a major cause of antibiotic resistant infections. Acquisition of the *mecA* or *mecC* penicillin binding protein PBP2/2a is a hallmark of MRSA, which is commonly transferred as part of

the staphylococcal cassette chromosome (SSC*mec*) and confers resistance to *β*-lactam antibiotics, although the SSC can harbor numerous other antibiotic resistance genes as well. MRSA colonization and infection can cause a wide range of disease, including asymptomatic carriage, skin abscesses, septicemia, pneumonia, endocarditis, and urinary tract infections, among others (*32*). More recently, VRSA is resistant to the primary antibiotic used to treat MRSA – vancomycin – and was first detected in the United States in 2002. VRSA vancomycin resistance is mediated by the *vanA* operon, and associated peptidoglycan ligase gene, and is much less prevalent than MRSA, primarily infecting diabetic wounds (*32*).

Carbapenem-resistant *Enterobacteriaceae* (CRE) and other Gram-negative carbapenem resistant pathogens are another rapidly emerging antibiotic resistance threat. The carbapenem antibiotics are typically last-line therapeutics, and resistance in CRE is usually caused by β-lactamase activity or carbapenemase production. Noteworthy carbapenemase-resistance genes include New-Delhi β-lactamase ($bla_{\text{NDM-1}}$), *Klebsiella pneumoniae* carbapenemase (bla_{KPC}), OXA β-lactamases (including $bla_{\text{OXA-48}}$), Verona integron-encoded metallo-β-lactamase (bla_{VIM}) and an imipenem-active group of β-lactamases (bla_{IMP}) (*33*). Beyond *Enterobacteriaceae*, other Gram-negative carbapenem-resistant pathogens are also emerging frequently, including carbapenem-resistant *Acinetobacter baumannii* (CRAB) and carbapenem-resistant *Pseudomonas aeruginosa* (CRPA) (*34*).

The evolution of antibiotic resistance is a natural process, and the by-product of an ancient microbial arms race, wherein bacteria evolved to produce antibiotics to inhibit their microbial competitors, which then subsequently evolve resistance

mechanisms against these antibiotics. In the relatively recent history of human antimicrobial use since the first sulfa drug, sulfamidochrysoidine was patented in the 1930s (*1*), microbes have made short work of evolving and disseminating resistance genes. This process is outpacing current antibiotic discovery efforts, and there is no reason to believe it will stop before the majority of therapeutics are rendered useless. We must therefore devise strategies that more effectively use the large array of molecules we have already discovered. Chapters 4 and 5 introduce methods of evaluating antimicrobial efficacy against patient isolates using a new paradigm – mimicking the host microenvironment – to more accurately select antimicrobials that are efficacious in vivo during personalized antimicrobial susceptibility testing (AST) before therapy prescription.

1.2. CLINICAL AND POINT-OF-CARE DIAGNOSTICS FOR PATHOGEN IDENTIFICATION

Pathogen identification (ID) is an important part of infectious disease diagnosis, and can guide the clinician to an appropriate empirical therapy. However, due to current limitations in diagnostic availability (cost, time, distribution), clinicians will frequently make treatment decisions without definitive pathogen identification, based instead on personal experience and local epidemiological data (*23*). This practice has been reasonable for much of the last century because first-line antimicrobial “wonder drugs” were efficacious against a majority of bacterial or eukaryotic infections, and there were very few options for antiviral therapeutics. However, now that many bacterial infections are multi-drug resistant, and there are different treatment options for common viral pathogens (*35, 36*) with overlapping disease symptoms (e.g., SARS-CoV-2 vs influenza), precision pathogen ID is becoming increasingly important.

ID diagnostics are available with a wide range of accuracy and cost, depending on the technology employed. Some tests are well suited for rapid detection at the point-of-care (UTI “dipsticks” and antigen tests). Other tests, including molecular assays (genome sequencing, PCR, isothermal amplification) typically require an advanced clinical laboratory, and are not well suited for rapid results or point-of-care diagnosis. Chapters 2 and 3 attempt to bridge this gap, by introducing an assay (smaRT-LAMP) that is affordable, rapid, and portable (like non-molecular assays) yet provides the accuracy and specificity of expensive gold-standard molecular tests.

Dipstick urinalysis is a frequently used, non-nucleic-acid-based assay for diagnosis of urinary tract infections (UTI). In this test, abnormal leukocyte esterase, and/or nitrate levels in urine can suggest UTI, however these results do not identify the specific pathogen (often assumed to be *Escherichia coli)*, nor the load. Dipstick urinalysis thus requires further urine culture to determine if the bacterial burden is high enough to indicate infection ($>10^5$ CFU/mL) vs subclinical bacteriuria or non-clean catch that typically does not require therapeutic intervention in healthy adults (*37*). Rapid antigen tests are another commonly used non-molecular ID-diagnostic, and can specifically identify a pathogen, but often have relatively poor accuracy. The widely used Group-A *Streptococcus* tests have an estimated detection sensitivity of 86% (*38*), which is clinically useful, but still misdiagnoses a large percentage of patients. Rapid antigen testing has also been widely employed during the SARS-CoV-2 pandemic, with similarly poor sensitivity, as low as 83% with moderate viral loads of 10^6 genome copies/mL (*39*).

Nucleic acid diagnostics are a far more specific, accurate, and quantitative method of determining pathogen ID, and RT-PCR assays are considered the “gold-standard”. The Bio-Fire FilmArray system is a popular clinical RT-PCR option, which is able to perform multiplex sample analysis on patient specimens, against panels of ~20 pathogens designed for blood or respiratory pathogens, among others (*40*). These systems are excellent for clinical pathology labs, but equipment and test kits are expensive, which limits testing capacity to wealthy regions. Recently, isothermal nucleic acid tests have become popular for SARS-CoV-2 ID, such as the Abbott ID Now (which uses “nicking-enzyme amplification reaction” or NEAR) (*41*). The ID

Now platform is rapid for a single patient, but is not scalable, and can only characterize up to 4 patients/hour/device. Additionally, LAMP (loop-mediated isothermal amplification) is a highly sensitive and increasingly utilized isothermal nucleic-acid amplification reaction (*42*). During a LAMP reaction, a polymerase with isothermal strand-displacement activity (*Bst*) amplifies gene targets using 4-6 oligonucleotide primers to detect 6-8 sites within a ~200 nucleotide amplicon region (*43*). LAMP-based diagnostics have been successfully utilized within this dissertation because the reaction has excellent performance and is easily modified for specific applications.

Perhaps the ultimate molecular assay for pathogen ID is genomic sequencing, which has only recently become affordable enough for routine identification, and has been heavily utilized during the SARS-CoV-2 pandemic (*44*). This approach requires expensive sequencing infrastructure, but enables complex genotypic analysis, and in conjunction with machine-learning phylogenic tools such as PANGO (*45*), has proven invaluable for identification and monitoring of coronavirus variants with enhanced transmissibility and pathogenicity. Although powerful, this method is currently limited to advanced medical facilities with access to state-of-the-art sequencing technology.

To address the pressing need for affordable and scalable molecular ID diagnostics, Chapter 2 establishes a smartphone-based real-time loop-mediated isothermal amplification method, termed “smaRT-LAMP”. In this assay, a smartphone camera monitors the fluorescence emitted during LAMP reactions. A custom-built smartphone application (Bacticount) analyzes the reaction images to

generate real-time LAMP traces, from which the app determines the timing of exponential amplification (Time-to-threshold, Tt). The app then calculates the pathogen genomic concentration within a sample, by comparing sample Tt to a spiked standard curve. The smaRT-LAMP platform is inexpensive and easy to construct, requiring only a hotplate, cardboard box, LED lights, and a sample holder, and costs under $100 USD (in addition to the phone). The experiments in Chapter 2 provide a proof of principle for 8 diverse bacterial pathogens, in blood, urine, and feces. SmaRT-LAMP was able to correctly determine ID and quantify bacterial loads from urinary sepsis patients, as well as blood, urine, and feces from murine models of sepsis.

Due to an urgent need for affordable and rapid virus ID during the SARS-CoV-2 pandemic, Chapter 3 optimizes smaRT-LAMP for the detection of SARS-CoV-2 and influenza A and B viruses from human saliva. The assay demonstrated excellent specificity and sensitivity, and was able to correctly ID and quantify CoV-2 from 20 positive patient saliva specimens, and did not detect 30 negative saliva specimens. SmaRT-LAMP CoV-2 and influenza assays were perfectly specific (it did not inappropriately amplify any other respiratory pathogens), and had quantitative sensitivity (limit of detection) that matched or exceeded CDC RT-qPCR “gold-standard” assays for these pathogens. Further, this assay can be performed on up to 96 total reactions, for < $7/sample, with a turn-around time of 25 minutes – making this assay uniquely suited to regular CoV-2 and influenza screening across the globe, with performance that matches gold-standard methodologies.

1.3. ANTIMICROBIAL SUSCEPTIBILITY TESTING AND THE HOST MICROENVIRONMENT

To treat serious or persistent infections, clinicians will commonly order an antimicrobial susceptibility test (AST) to be performed, wherein a bacterial pathogen is isolated from the patient, and tested for sensitivity against a panel of empirically relevant antimicrobials. For clinical decision making, it is often helpful to quantify the antimicrobial susceptibility of the pathogen, which has typically been performed using gradient (E-test), disk-diffusion, agar, and broth dilution assays (*46*). Additionally, four automated systems are currently cleared by the FDA, including the VITEK2 (bioMérieux), which reduce the labor and improve the speed of AST (*46*). The goal of AST is to classify a pathogen as “Susceptible”, “Intermediate” or “Resistant” to a given antimicrobial, based on the measured susceptibility concentration (known as the minimal inhibitory concentration; MIC), and a clinical “breakpoint” value. These clinical breakpoint values are determined based on factors such as the typical MIC range for the organisms, pharmacokinetics/dynamics of the antimicrobial, and patient clinical outcome data (*47*). The central assumption is that when a pathogen is grown in standard in vitro conditions, an antimicrobial with a low MIC (below the “susceptible” or “intermediate” breakpoint values) will be able to treat the patient.

Unfortunately, predicted “sensitive” antimicrobials frequently fail to treat the patient, in what has been termed the “90-60 rule”, where susceptible antimicrobials are only effective 90% of the time (and resistant antimicrobials are still effective 60% of the time) (*48-50*). The impact of the host microenvironment on antimicrobial

susceptibility has recently come into focus; the limitations of the standard rich media used in dilution AST likely contributes to the unexpected treatment failure because it does not provide important host signals to the pathogen (*51*).

Although there are many potential microenvironmental signals that modulate antimicrobial resistance in the host (*52*), some of the more noteworthy signals and conditions include the macrophage phagosome microenvironment, bicarbonate, osmolality, and biofilm-formation. The conditions within a macrophage phagosome can be mimicked by low pH (pH 5.5), low phosphate (337 μM) and low magnesium (8 μM) concentrations (*53*). When tested in conditions that mimic this phagosome environment, the intracellular pathogen *Salmonella* Typhimurium demonstrated a markedly increased MIC to polymyxin B when compared to testing in MHB, which accurately predicted treatment failure in a murine model of *Salmonella* sepsis (*54*). Bicarbonate is another important signal, which is present in mammalian blood and has been demonstrated to enhance antibiotic susceptibility via membrane permeabilization and downregulation of resistance genes including *mecA* (*55, 56*). The osmolarity of the host environment has also been shown to be important, as decreased urine osmolality has been shown to enhance susceptibility of *E. coli* to a β-lactam antibiotic (mecillinam) (*57*). Finally, in response to the host environment, many pathogens form complex biofilms, which have also been shown to contribute to antimicrobial resistance within the host (*58*).

In response to the emerging need for more accurate AST methodologies that can mimic the host microenvironment, Chapter 4 details the impacts of multiple host-mimicking media on antimicrobial susceptibility against a large panel of diverse

human pathogens, and important antimicrobial therapeutics. Substantial changes in susceptibility were frequently observed in a strain-specific manner, suggesting that such host-mimicking testing needs to be performed on a patient's individual isolate. Further, these alterations in resistance predicted the treatment outcomes in several murine sepsis models, indicating that these alterations also occur in vivo. Finally, bicarbonate was identified as a common host-mimicking signal in these media, and was successfully used as an additive to the standard MHB media, to create an enhanced host-mimicking testing medium that is inexpensive and widely available.

Although host-mimicking media represent a substantial improvement in the accuracy of AST, the abundance of potential signaling molecules in host fluids precludes the possibility of formulating a perfectly host-mimicking artificial medium. In light of this, Chapter 5 develops an AST method which uses human fluids (serum and urine) as the culture and testing media, to enable susceptibility testing of a patient's pathogen isolate ex vivo, directly in human body fluid specimens. Consistent growth in human fluids to high cell densities required for dilution AST is a substantial hurdle in the development and deployment of such assays. We have resolved these issues, using a supplementation and aggregate-disruption strategy that has been successfully utilized on a diverse panel of human pathogens. This ex vivo AST identified a wide range of susceptibility changes in urine and serum, which will enable further validation with murine sepsis models, and eventually human therapeutic interventions.

Chapter 2

Smartphone-based Pathogen Diagnosis in Urinary Sepsis Patients†

†This chapter contains excerpts, reproduced with permission, from Barnes L, Heithoff DM, Mahan SP, Fox GN, Zambrano A, Choe J, Fitzgibbons LN, Marth JD, Fried J, Soh HT, and Mahan MJ. (2018). Smartphone-based pathogen diagnosis in urinary sepsis patients. *EBioMedicine*. 36(2018) 73-82.

ABSTRACT

Background: There is an urgent need for rapid, sensitive, and affordable diagnostics for microbial infections at the point-of-care. Although a number of innovative systems have been reported that transform mobile phones into potential diagnostic tools, the translational challenge to clinical diagnostics remains a significant hurdle to overcome.

Methods: A smartphone-based real-time loop-mediated isothermal amplification (smaRT-LAMP) system was developed for pathogen ID in urinary sepsis patients. The free, custom-built mobile phone app allows the phone to serve as a stand-alone device for quantitative diagnostics, allowing the determination of genome copy-number of bacterial pathogens in real time.

Findings: A head-to-head comparative bacterial analysis of urine from sepsis patients revealed that the performance of smaRT-LAMP matched that of clinical diagnostics at the admitting hospital in a fraction of the time (~1 h vs. 18–28 h). Among patients with bacteremic complications of their urinary sepsis, pathogen ID from the urine matched that from the blood – potentially allowing pathogen diagnosis shortly after hospital admission. Additionally, smaRT-LAMP did not exhibit false positives in sepsis patients with clinically negative urine cultures.

Interpretation: The smaRT-LAMP system is effective against diverse Gram-negative and -positive pathogens and biological specimens, costs less than $100 US to fabricate (in addition to the smartphone), and is configurable for the simultaneous detection of multiple pathogens. SmaRT-LAMP thus offers the potential to deliver

rapid diagnosis and treatment of urinary tract infections and urinary sepsis with a simple test that can be performed at low cost at the point-of-care.

2.1. INTRODUCTION

The World Health Organization and the U.S. Department of Health and Human Services have recently prioritized the development of rapid, accurate, and cost-effective diagnostics that can be used by healthcare providers at the point-of-care (POC) to diagnose bacterial infections (*59, 60*). Such diagnostic systems are especially needed in less developed countries, where bacterial infections are more prevalent and medical resources are limited (*61, 62*). The microbial diagnosis of pathogens directly from whole blood has been constrained by the low number of circulating organisms – typically just 1–100 colony forming units (CFU)/mL during infection – and the frequency of false positive results (*63*). Moreover, standard culturing practices for pathogen identification (ID) from blood can take 2 to 3 days (*64*). To expedite the process, there are numerous molecular methods for the detection of bacteria – including PCR, probe-based direct detection, peptide nucleic acid-based fluorescence in situ hybridization, and matrix-assisted laser desorption ionization–time of flight mass (MALDI) spectrometry analysis (*65-67*) . However, these clinical techniques require prior sub-culturing in blood culture bottles for bacterial detection (8–24 h), followed by pathogen ID (1.5–24 h), resulting in a total time of ~10–48 h from inoculation to time to pathogen ID (*68-71*). Additionally, these methods generally require access to specialized laboratory equipment, which can be excessively costly and technologically complex for POC or resource limited settings.

Among different types of clinical samples, urine samples are particularly

attractive because they can be obtained without invasive procedures (such as a blood draw) and the clinically relevant break point defining a positive clinical culture result for urinary tract infections (UTIs) is ≥ 10^5 CFU/mL (*37, 72*), making timely diagnostic detection potentially simpler. UTIs are among the most common type of infection, and are associated with recurrent illnesses, pyelonephritis with sepsis, renal damage, pre-term birth, and complications from prolonged antimicrobial therapy that include high-level resistance and *Clostridium difficile* colitis (*73, 74*). Unfortunately, there are presently no direct urine testing methods for pathogen ID approved for human clinical diagnostics (*75*). Instead, urine specimens must be cultured before biochemical characterization, and such culture methods are routinely confounded by false positive results due to contamination at collection or false negative results due to culture failure (*72*). Thus, improved urine-based tests for the rapid detection of pathogens would be highly valuable for improving patient outcomes for UTIs and in potentially fatal conditions arising from septicemia (e.g., pyelonephritis) (*76*).

A number of innovative systems have recently been reported that transform mobile phones into potential clinical POC diagnostic tools based on various detection modalities. Examples include optical and fluorescence imaging (*77*), microtiter assay interpretation (*78*), immunologic detection (e.g. microfluidic chips (*79-81*); antibody-conjugated strips (*82*)) and nucleic acid detection (e.g., microfuge tubes (*83, 84*); microtiter plates (*85*); microfluidic chambers (*86*); microfluidic chips (*87-93*)). Although these are notable advances in terms of broadening access to sophisticated molecular diagnostics, translation to clinical utility using patient-derived

samples has been limited (e.g., HIV blood samples (*81*), influenza throat swabs (*82*), *Chlamydia trachomatis* swabs (*93*)).

We have developed a rapid, quantitative and accessible smartphone-based detection system with clinical utility, achieving timely diagnosis of bacteriuria from human patients. SmaRT-LAMP performance matched that of standard clinical diagnostics, but within a substantially shorter time-frame and lower cost, thus providing a means for inexpensive and accurate diagnosis of UTIs and urinary sepsis directly from clinical specimens at the POC.

2.2. RESULTS

2.2.1. Overview of the SmaRT-LAMP system

The smaRT-LAMP procedure can be performed with freshly collected biological specimens (e.g., blood, urine, or feces), which are then lysed with a simple NaOH and detergent treatment and subsequent heating procedure (**Figure 2.1a**). The resultant lysate is combined with a pre-mixed LAMP reaction mixture that will generate a fluorescent signal in response to successful amplification (see Methods). These samples are then placed in an inexpensive apparatus consisting of a platform that can simultaneously accommodate up to 36 samples, a single-temperature heat block, and an LED light source (**Figure 2.6**). The entire detection system can be fabricated for less than $100 US, not including the smartphone (**Table 2.3**).

The streaming image data from smaRT-LAMP are collected in real time and analyzed by a smartphone running the Bacticount app (**Figure 2.1b**, **Figure 2.7**), which we developed for the Android operating system and have made freely available through the Google Play store. We derive the template DNA copy number by using a 'coarse derivative' algorithm (*94*) to convert the fluorescence data into a time-to-threshold parameter (Tt) – the time at which the rate of fluorescence increase is fastest. This Tt measurement indicates the exponential phase of the LAMP reaction and is linearly proportional to the logarithm of the template DNA copy number (*95*). Thus, we can quantitatively determine the concentration of gDNA in a sample based on a standard curve of Tt measurements derived from samples of known concentration. As shown below, our coarse derivative algorithm is robust and produces highly reproducible data, even with fluctuations in background

fluorescence, camera recalibrations, and shifts in the relative position between the sample and the smartphone camera.

2.2.2. SmaRT-LAMP sensitivity and intra- and interspecies detection

We tested whether the sensitivity of smaRT-LAMP can match that of a LAMP assay performed in a real-time quantitative PCR instrument (qPCR) for detecting gDNA of *Salmonella* Typhimurium (*ST*). We used a set of six primers designed to target the highly conserved *recF* gene (*96, 97*). These primers are specific to *Salmonella* sp., and thus are not expected to hybridize to DNA of unrelated pathogens. We compared the smaRT-LAMP and qPCR instrument for measuring the gDNA of ST over a broad range, from5×10^1 –5×10^4 copies of the genome. SmaRT-LAMP and qPCR instruments showed equivalent performance in this assay, as evidenced by the Tt dose dependency, trace quality and reaction time (**Figure 2.8**).

Strain discrimination is imperative for clinical diagnostics and treatment, and we demonstrated that the smaRT-LAMP platform is compatible with both intra- and interspecies detection and strain discrimination. We tested this by employing primer sets specific to gDNA templates from eight different Gram-negative and -positive pathogens, including *ST*, *S. enteritidis* (*SE*), *Escherichia coli* (*EC*), *Klebsiella pneumoniae* (*KPN*), *Pseudomonas aeruginosa* (*PA*), *Yersinia pseudotuberculosis* (*YP*), *Streptococcus pneumoniae* (*SPN*) and *Staphylococcus aureus* (*SA*) (**Table 2.4**). SmaRT-LAMP achieved robust interspecies detection and strain discrimination of these Gram-negative and -positive pathogens, with each of the eight primer sets

amplifying only the gDNA of their cognate template but not any of the seven other templates (**Table 2.1**). SmaRT-LAMP can distinguish between *ST* and *SE*, which are serovars of the same *Salmonella* subspecies (*S. enterica* subsp. enterica) that are 99% identical at the DNA sequence level (*98*). It should be noted that the reduced primer sensitivity for *ST* relative to the other pathogens tested is not indicative of a failure of the reaction but rather the limited number of sequences available to design LAMP primer sets that distinguish *Salmonella* subsp. that are closely related at the DNA level (e.g., *ST* vs. *SE*).

2.2.3. Pathogen detection using whole bacterial cells

We next assessed whether our lysis protocol enables quantitative pathogen detection using whole bacterial cells, and if smaRT-LAMP can match the sensitivity of an equivalent LAMP assay performed in an qPCR instrument. *ST* cells were serially diluted into buffer at concentrations ranging from 10^1 to 10^5 CFU/mL. One mL of each dilution sample was then reduced to 2 µL via sequential centrifugation and subjected to the LAMP protocol. We derived a standard curve through a linear regression fit of Tt vs. $\log_{10}$[CFU] (**Figure 2.2a–d**); see Methods). The resultant limit of detection (LOD) was ≤ 10 CFU/mL for both smaRT-LAMP and qPCR. We also observed excellent reaction efficiency in terms of the percent of samples that were successfully amplified at 10 CFU/mL (70 and 90%, respectively; (**Figure 2.2e, f**). Such a low LOD (≤10 CFU/mL) obtained from sequential centrifugation may have clinical utility for swabbing infection sites, medical devices and other potentially contaminated surfaces.

We then tested whether our lysis procedure works with Gram-positive and -negative pathogens that have large differences in cell envelope structure. Using the same lysis protocol, we assessed the performance of both amplification platforms against Gram-positive *SPN* and *SA*, as well as Gram-negative *SE*, *EC* and *YP*. Briefly, 2 µL of spiked buffer samples containing 5×10^3 –5×10^7 CFU/mL of bacteria were processed and assessed in the smaRT-LAMP and qPCR instruments as described above. Both platforms showed strong performance against all five pathogens, with a LOD of 5×10^3 –1×10^5 CFU/mL (equivalent to 2–100 CFU/reaction), clear Tt dose dependency, and strong reaction efficiency (**Figure 2.9**). These data indicate that the smaRT-LAMP system is compatible with a diverse array of pathogens.

2.2.4. Pathogen detection in spiked murine whole blood, urine, and feces

Next, we examined the performance of smaRT-LAMP and qPCR-LAMP in diverse biological specimens and tested whether bacterial detection can be achieved at clinically-relevant concentrations. Briefly, *ST* was serially diluted in murine whole blood, urine, and feces over a range of 5×10^3 – 5×10^7 CFU/mL. After collecting and processing 2 µL aliquots from these samples, half of each lysate reaction was subjected to LAMP in both the smaRT-LAMP and qPCR platforms.

Direct specimen testing in whole blood is problematic due to the low bacterial load typically observed in circulation of sepsis patients (1–100 CFU/mL) (*63*). As a result, clinical detection methods require samples to first be incubated in blood culture bottles, resulting in a total time of ~10–48 h from inoculation to time to

pathogen ID (*68-71*). Both smaRT-LAMP and qPCR instruments were able to achieve this level of detection sensitivity of *ST* from whole blood, with an LOD of 5 × 10^3 CFU/mL (**Figure 2.3a, b**) – equivalent to just 2 CFU/reaction – with clear Tt dose dependency and strong reaction efficiency (**Figure 2.3i, j**).

Importantly, smaRT-LAMP offers the potential to achieve rapid direct detection of clinically-relevant signatures of bacterial infection in urine. Urine can offer an early readout of patients with UTIs, and potentially in cases of sepsis– particularly those that have a suspected urinary source– since infected urine is associated with a much higher bacterial load than blood (≥ 10^5 CFU/mL) (*37, 72*). However, there is currently no direct specimen testing method approved for urine, principally due to the challenges of microbial contamination at the point of collection (*72, 75*). Thus, the gold standard of care entails a bacterial culture step, delaying identification for at least 16 h (*75, 99, 100*). Once again, we demonstrated that smaRT-LAMP could match the performance of the more sophisticated and costly qPCR instrument, achieving a clinically-relevant LOD of 1–2 × 10^4 CFU/mL (**Figure 2.3c, d**), which is within the range needed to demonstrate the clinically relevant break point defining a positive clinical culture result for UTIs (10^5 CFU/mL) (*37, 72*). Notably, the scattered distribution observed at lower concentrations is a statistical byproduct of the extremely small number of bacteria per sample, with samples at the lowest concentrations containing on average two or fewer CFU each. We also demonstrated that our assay could achieve equally sensitive performance in testing fecal samples (**Figure 2.3e, f**). As with the blood specimens, we observed excellent reaction efficiency for both urine and fecal samples (**Figure 2.3g–j**). The LOD of

smaRT-LAMP is comparable to that of currently used clinical diagnostic technologies for urine and feces, but our system's capacity for direct specimen testing and minimal sample preparation offers a major advantage in terms of time to treatment.

Finally, we confirmed that smaRT-LAMP direct specimen testing works with diverse pathogens in a variety of specimen types. Specifically, we assessed the performance of smaRT-LAMP with *SPN*, *SA*, *SE*, *EC* and *YP* spiked into murine blood, and with *EC* spiked into donor human urine. SmaRT-LAMP showed strong performance with all of these pathogen-specimen combinations, achieving LODs in the range of 5×10^3 –1×10^5 CFU/mL (2–40 CFU/reaction) (**Figure 2.4**), which were again comparable with results from qPCR (**Figure 2.10**). These data indicate that the smaRT-LAMP platform is compatible with a diverse array of pathogens and biological specimens.

2.2.5. Pathogen detection in murine models of sepsis

We assessed whether the smaRT-LAMP system was compatible with several murine models of sepsis. Mice were orally infected with *ST* and whole blood was sampled at day 6 (pre-sepsis); day 8 (sepsis), and day 10 post-infection (severe sepsis). SmaRT-LAMP enabled pathogen detection via direct specimen testing of whole blood at the 3 infection time points, with an LOD of 10^4 CFU/mL, equivalent to 4 CFU/reaction (**Figure 2.5a–c**). Similarly, pathogen detection was observed in several other murine models of sepsis (*SPN*, *SA*, *SE*, *YP*, *EC*) (**Figure 2.11**). However, the CFUs in circulation for all sepsis models tested (10^4 –10^6 CFU/mL) were well-above the range needed for clinical utility in humans (1–100 CFU)/mL)

(*63*). It should be noted that the relatively high LOD in circulation is not indicative of a failure of the reaction but rather a physical limitation of the 2 µL sample volume, resulting in a ~40 µL reaction volume that is near the maximum allowable with the current platform (see Methods). Thus, we redirected subsequent efforts on pathogen detection in urine with an LOD of 5×10^3 CFU/mL, which is well within the range needed to demonstrate the clinically relevant break point defining a positive clinical culture result for UTI patients ($\geq 10^5$ CFU/mL) (*37, 72*).

2.2.6. Quantitative pathogen diagnosis in urine of human sepsis patients

Based on its strong performance with spiked murine urine samples, we assessed whether smaRT-LAMP may have immediate clinical utility for the POC analysis of urine specimens from human patients. We selected patients who met the clinical criteria for sepsis based on fever, increased heart rate, and/or elevated white blood cell count, and had a suspected urinary source of their severe infection. Some of these patients had severe sepsis, with evidence of end-organ dysfunction or septic shock. Briefly, upon presentation at the hospital, urine and blood specimens were collected from patients before antibiotic administration. A comparative urine bacterial analysis was performed between smaRT-LAMP and clinical diagnostics carried out by the hospital managing patient care. Pathogen ID in the urine and blood of sepsis patients was determined by the hospital microbiology laboratory. The bacterial load in urine of ten patient specimens was assessed by both direct colony count, and smaRT-LAMP utilizing primer sets directed against the urine pathogen identified in the clinical setting. SmaRT-LAMP achieved rapid and accurate detection

of *EC*, *KPN*, and *PA* in urine specimens of sepsis patients (10^5 –10^8 CFUs), matching that of the more cumbersome and expensive qPCR analysis (**Table 2.2**). Importantly, both smaRT-LAMP and qPCR-LAMP systems achieved a diagnosis in ~1 h, a fraction of the time required for clinical diagnostics by the hospital microbiology laboratory (18–28 h). Moreover, since false positive results are a primary concern due to contamination at collection (*72*), the bacterial load in urine of sepsis patients with clinically negative urine cultures was determined by the hospital microbiology laboratory (clinical culture) versus an academic laboratory examining CFU by direct colony count, qPCR-LAMP, and smaRT-LAMP. The bacterial load discerned by qPCR-LAMP and smaRT-LAMP direct specimen testing matched the low– or non-detectable– bacterial load obtained by clinical culture or direct colony count in all five cases (**Table 2.5**). These data demonstrate the feasibility of improving time to detection and quantitation in clinical settings and at the POC. Further, in the six patients who had bacteremic complications (defined as positive blood cultures) of their urinary sepsis, the pathogen ID from the urine matched that of the blood in all six cases (patient 002, 006, 010, 012, 015, 019). This concordance demonstrates the applicability of smaRT-LAMP to even the most severe cases of sepsis, with the advantage of accurate and rapid diagnosis at the POC in these cases, and the potential to greatly accelerate directed therapy for urinary tract infections. Notably, time to treatment was the significant factor associated with positive patient outcomes in emergency care for sepsis (*76*). SmaRT-LAMP thus offers the potential to deliver rapid diagnosis and treatment of urinary tract infections and urinary sepsis.

2.3. DISCUSSION

Efforts to improve global public health will benefit immensely from accurate, rapid, affordable and user-friendly methods for detecting microbial pathogens at the POC. Toward this goal, we have developed smaRT-LAMP, a rapid, portable diagnostic platform that can achieve sensitive and accurate bacterial detection with performance comparable to gold-standard clinical methodologies based on costly, specialized instrumentation. We have demonstrated that smaRT-LAMP can quantitatively detect diverse pathogens in blood, urine and feces, with an LOD that matches what can be achieved with an qPCR instrument based assay. Perhaps most importantly, we demonstrated that our platform can achieve robust detection of different bacterial pathogens in urine specimens collected from sepsis patients, matching the hospital diagnosis but in a much shorter time-frame (~1 h vs. 18–28 h). These results highlight the clear clinical potential of the smaRT-LAMP assay as a diagnostic tool for UTIs, particularly in the context of resource-limited settings that may lack sophisticated instrumentation or expert clinical diagnosticians.

SmaRT-LAMP requires little more than a smartphone, hot plate, LED lights, low force mini-centrifuge, and a cardboard box, making our approach highly affordable and accessible. Indeed, the entire detection system can be fabricated for less than $100 US (in addition to the smartphone), and can readily be configured for the simultaneous detection of multiple pathogens. SmaRT-LAMP thus offers the potential to leverage a widely available consumer technology to affordably deliver state-of-the-art nucleic acid diagnostics technology for accurate, quantitative pathogen detection at the POC.

Early diagnosis and intervention enabled by smaRT-LAMP direct urine testing could prove highly advantageous in a number of clinical contexts. These include cases with clinical manifestations indicating UTI (among the most common types of infection) (*73, 74*) and potentially fatal conditions arising from septicemia (e.g., pyelonephritis) (*37, 76*). Such an assay could also prove useful for monitoring pregnant women with asymptomatic bacteriuria that receive antibiotics to reduce the of risk of acute cystitis, pyelonephritis and/or miscarriage (*101*). Early intervention is also essential for accelerating directed therapy and encouraging the judicious use of antibiotics to minimize the emergence of multidrug-resistant strains that have limited treatment options (e.g., MRSA, extended-spectrum β-lactamase–producing (ESBL) and carbapenem- resistant (CRE) *Enterobacteriaceae*, and multidrug-resistant *PA* and *Acinetobacter* sp. (*102-104*). SmaRT-LAMP may complement clinical UTI diagnostic practices such as colorimetric dipstick assays, microscopy, lateral flow assays (approved for veterinary use) that are rapid (1– 2 h) but do not identify the pathogen, and MALDI-TOF mass spectrometry that rapidly identifies the pathogen but requires bacterial culture (~18–28 h) and expensive instrumentation (*75*).

There are numerous opportunities to further extend the utility of the smart-LAMP platform in the future. First, the LOD in diverse biological specimens could be improved simply by increasing the sample volume used in the assay (e.g., from 2 μL to ≥ 1mL). Although this will increase the cost of reagents and the size of the peripheral apparatus, the LOD will scale linearly with sample volume, potentially making it possible to detect 1–100 CFU from a 1 mL blood specimen. Such sensitivity could enable extremely early-stage diagnosis and intervention, particularly

in the context of multidrug-resistant pathogens for which treatment options are highly limited. Second, multiplexed detection of pathogens could be readily achieved with appropriate LAMP primers that can be designed from whole-genome databases (*105, 106*). Finally, the utility of our system for field applications could be further improved with lyophilized reagents, which will be especially useful in resource limited areas where refrigeration is impractical (*107, 108*). We therefore believe that smaRT-LAMP holds exciting potential to bring state-of-the art nucleic acid diagnostics technology within easy reach of non-expert smartphone users.

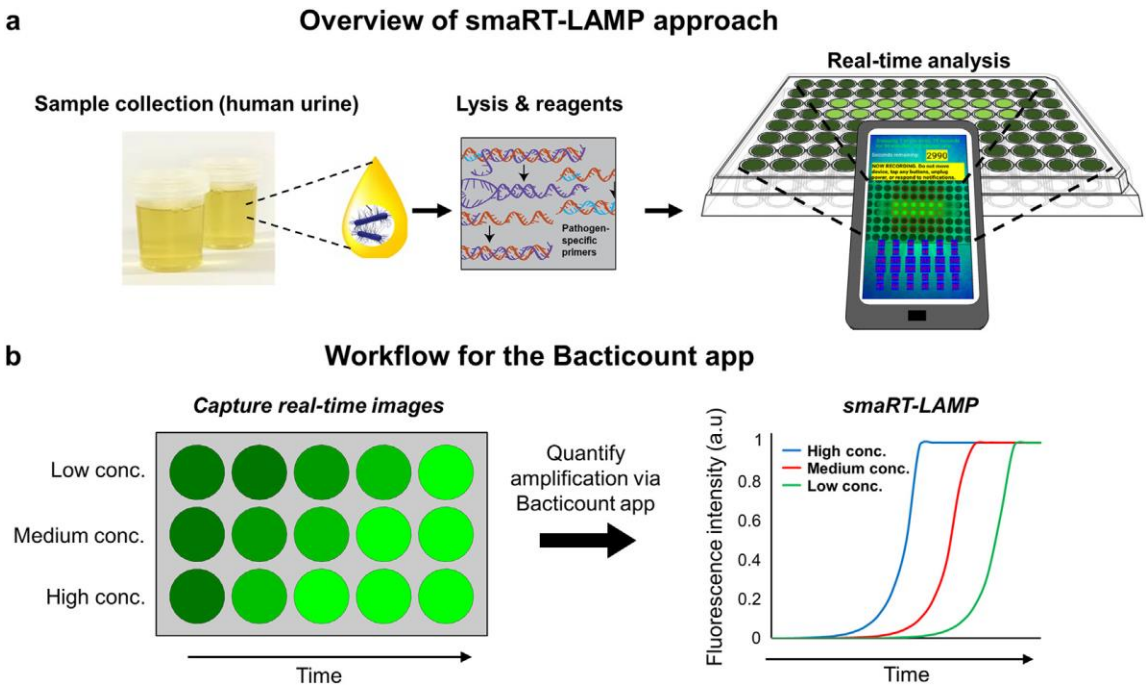

Figure 2.1. SmaRT-LAMP direct specimen testing of urine from sepsis patients. (**a**) Assay schematic for smaRT-LAMP, which entails sample collection, bacterial cell lysis/reagent addition, and real-time analysis via the smartphone. (**b**) Schematic of workflow for the Bacticount app, which analyzes fluorescence data collected continuously from multiple samples through the phone's camera (left panel), and then uses these data to automatically determine the genome copy-number of bacterial pathogens in real time (right panel).

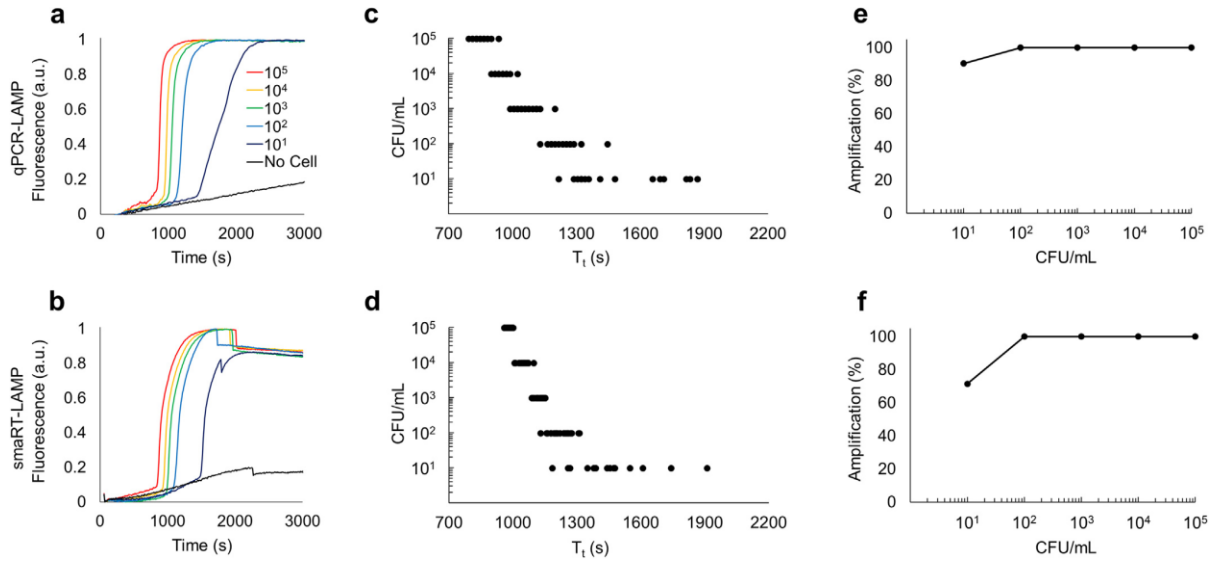

Figure 2.2. SmaRT-LAMP quantification of *ST* with performance equivalent to a benchtop laboratory qPCR instrument. (**a–d**) Normalized representative traces and Tt values of *ST* CFU in buffer at concentrations of 10^1–10^5 CFU/mL using qPCR-LAMP and smaRT-LAMP; (**e, f**), Percentage of total samples amplified at each concentration using qPCR-LAMP or smaRT-LAMP (21 samples/concentration).

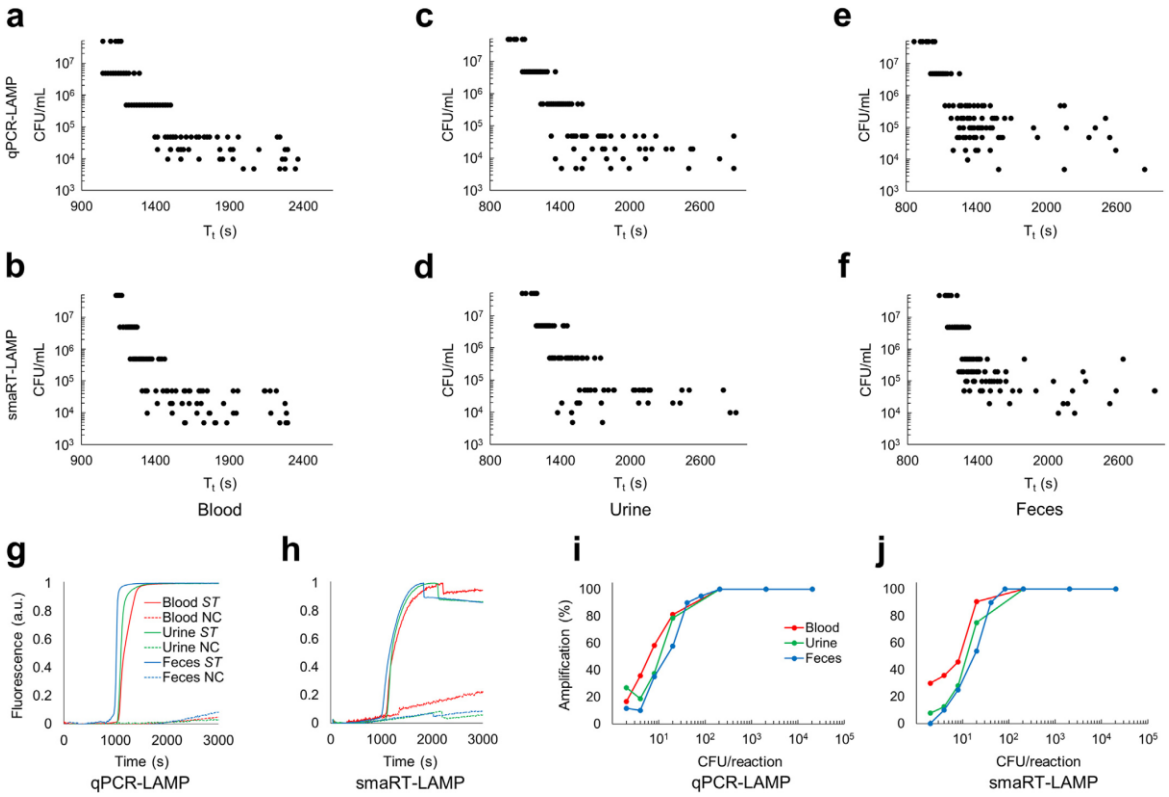

Figure 2.3. SmaRT-LAMP quantification of *ST* in spiked diverse biological specimens. (**a–f**) Tt values for *ST* CFU in murine blood, urine, and feces using qPCR-LAMP and smaRT-LAMP. (**g,h**) corresponding representative traces (2–2 × 10^4 CFU/reaction); NC, no cell. (**i, j**) Percentage of total pathogen samples amplifying at each concentration using smaRT-LAMP.

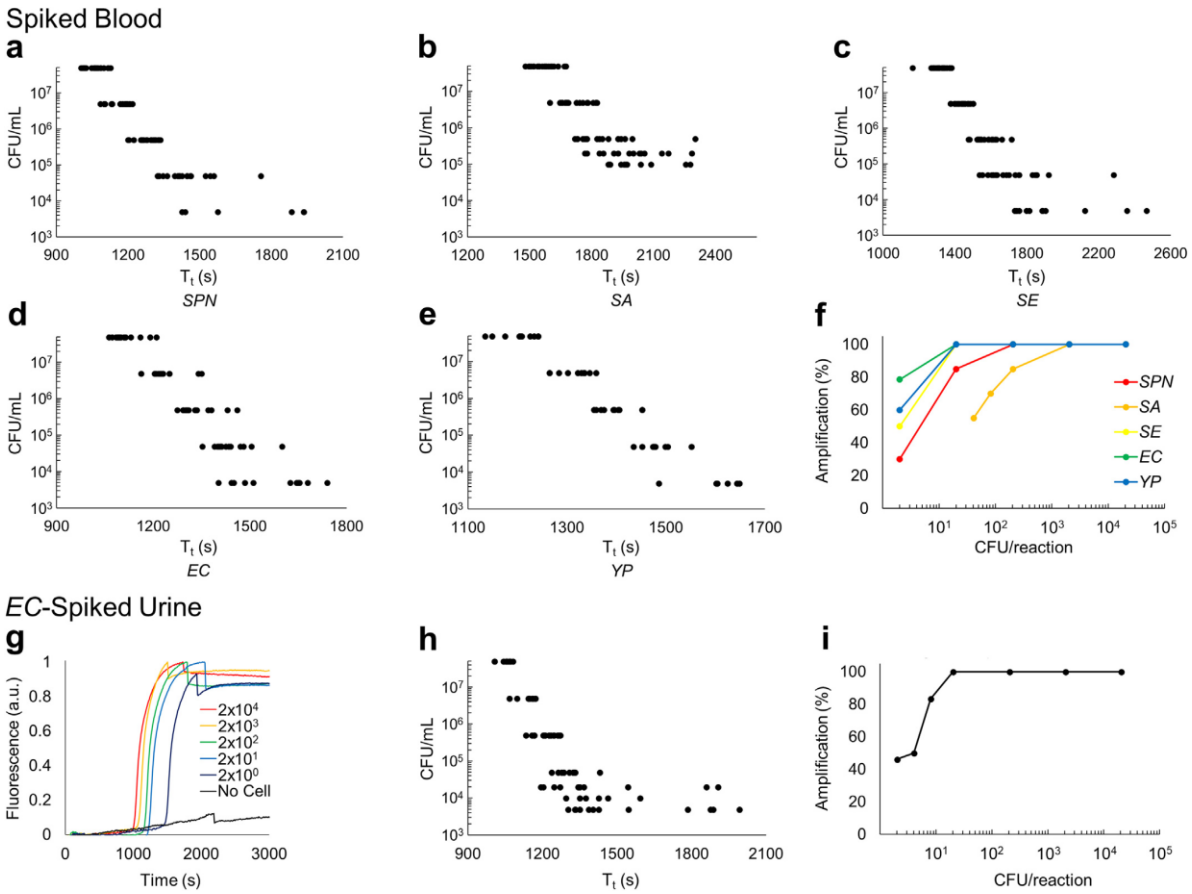

Figure 2.4. SmaRT-LAMP quantitation of diverse pathogens in spiked murine whole blood and human donor urine. (**a–e**) Tt values for *SPN*, *SE*, *EC*, *YP* (2–2 × 10^4 CFU/reaction); *SA* (4 × 10^1 –2 × 10^4 CFU/reaction). (**f**) Percentage of total pathogen samples amplifying at each concentration in smaRT-LAMP. (**g, h**) Representative traces and Tt values for *EC* in spiked human donor urine (2–2 × 10^4 CFU/reaction). (**i**) Percentage of total *EC* samples amplifying at each concentration in smaRT-LAMP (≥ 10 samples/concentration).

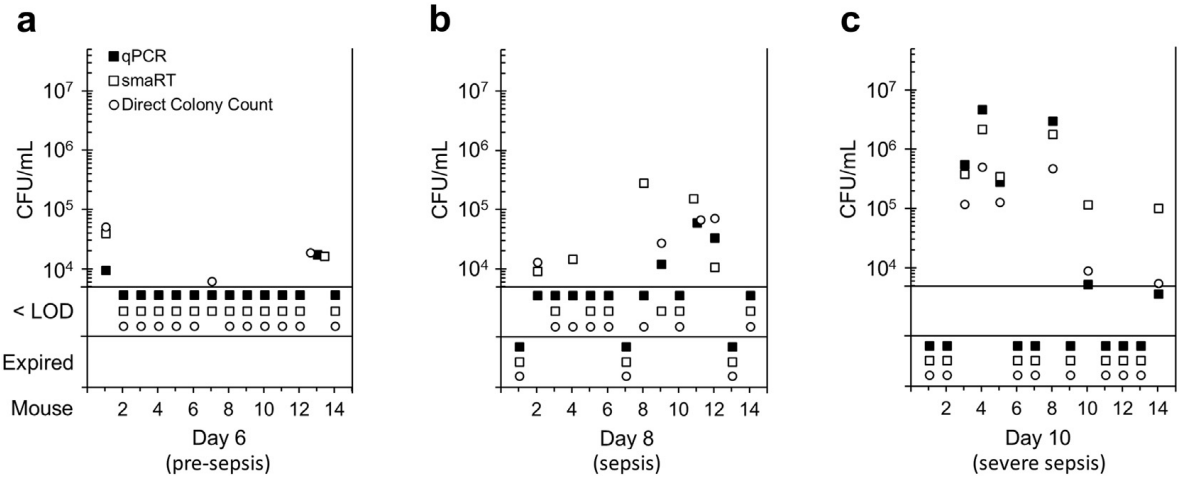

Figure 2.5. SmaRT-LAMP detection and quantitation of *Salmonella* in whole blood of septic mice. (**a–c**). Mice were orally infected with ST via gastric intubation at a dose of 2×10^7 cells and whole blood was sampled at days 6 (pre-sepsis), 8 (sepsis), and 10 (severe sepsis) post-infection. CFU were determined by qPCR-LAMP (closed boxes), smaRT-LAMP (open boxes), and direct colony count (circles). n = 14 mice.

Table 2.1. SmaRT-LAMP intra- and interspecies specificity.

Primer	gDNA template							
	ST	*SE*	*EC*	*YP*	*KPN*	*PA*	*SPN*	*SA*
ST	+	–	–	–	–	–	–	–
SE	–	+++	–	–	–	–	–	–
EC	–	–	+++	–	–	–	–	–
YP	–	–	–	+++	–	–	–	–
KPN	–	–	–	–	+++	–	–	–
PA	–	–	–	–	–	+++	–	–
SPN	–	–	–	–	–	–	+++	–
SA	–	–	–	–	–	–	–	+++

"+++" denotes amplification of cognate primer-gDNA pairs (10^3 gDNA copies) without amplification of non-cognate primer-gDNA pairs (10^5 gDNA copies). "+" denotes amplification of cognate primer-gDNA pairs (10^5 gDNA copies) without amplification of non-cognate primer-gDNA pairs (10^5 gDNA copies). "–" represents no amplification.

Table 2.2. Comparative bacterial analysis of urine from sepsis patients using smaRT-LAMP versus standard clinical diagnostics.

	Pathogen ID		Urine CFU/mL		
Patient	Urine	Blood	qPCR-LAMP	smaRT-LAMP	Colony Count
002	*PA*	*PA*	2.8×10^6	5.0×10^6	3.0×10^5
006	*KPN*	*KPN*	2.9×10^7	1.2×10^7	1.0×10^7
009	*EC*	–	1.8×10^7	4.4×10^7	8.0×10^6
010	*EC*	*EC*	1.5×10^4	8.3×10^5	9.4×10^5
011	*EC*	–	1.2×10^5	2.5×10^5	1.0×10^7
012	*EC*	*EC*	1.5×10^8	6.4×10^8	1.9×10^8
013	*EC*	–	2.2×10^4	6.6×10^4	4.3×10^7
014	*EC*	–	1.5×10^5	1.1×10^6	8.5×10^7
015	*EC*	*EC*	7.2×10^4	1.4×10^5	4.8×10^8
019	*EC*	*EC*	6.2×10^7	2.2×10^8	1.3×10^7

Pathogen ID in the urine and blood of sepsis patients was determined by the hospital microbiology laboratory. The bacterial load in urine specimens was determined by direct colony count, and by direct specimen testing via qPCR-LAMP and smaRT-LAMP utilizing primer sets directed against the urine pathogen identified in the clinical setting. A linear fit of standard curves with a clinically relevant bacterial burden (5×10^4 – 5×10^7 CFU/mL) was used to determine LAMP-based CFUs. " – " denotes no pathogen was isolated from blood cultures. qPCR-LAMP and smaRT-LAMP values depict an average of a minimum of 3 determinations from each specimen.

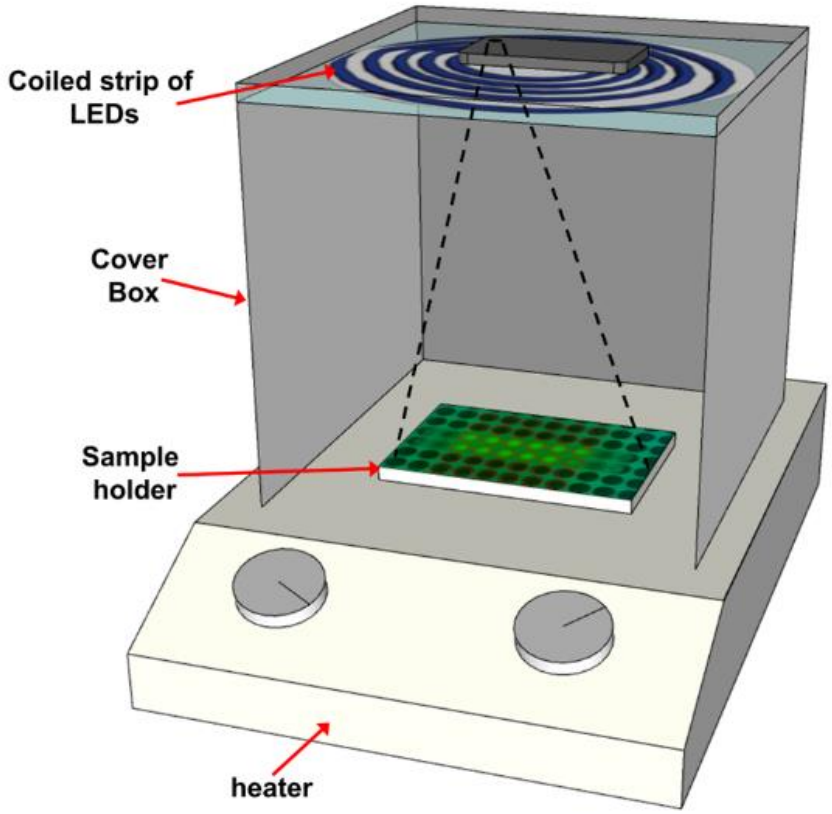

Figure 2.6. Minimal instrumentation is required for smaRT-LAMP. The system is closed off from background light with a cardboard box that is painted black (30 x 30 x 30 cm). The viewing aperture for the phone camera is located in the center of the top face (diameter 1.5 cm.) A coiled strip of LEDs on the inside of the box illuminates the samples, which give off a fluorescent signal detected by a smartphone camera outfitted with a green filter. Once the samples, LEDs, and phone lens have been aligned, the user will be guided through the details of starting a test through a tutorial provided on the Bacticount app.

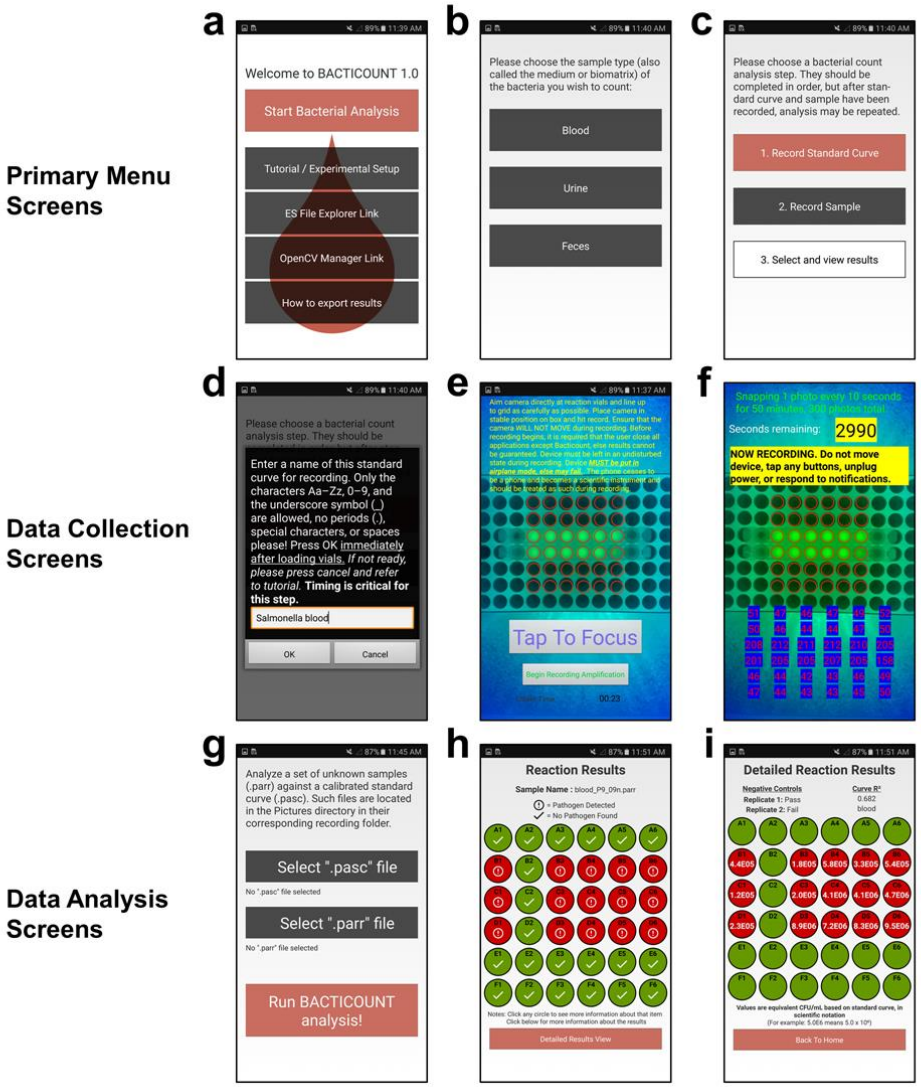

Figure 2.7. Screenshot overview of the operations carried out by users of the Bacticount app. (**a, b**) In the home screen, the user selects “Start Bacterial Analysis” and is given a choice of analyzing blood, urine, or feces samples. (**c**) The user can then either collect data (“1. Record Standard Curve” or “2. Record Sample)” or analyze data (“3. Select and view results”). (**d–f**) During data collection, the user names the sample, positions the app to collect data for up to 36 samples, and records amplification with live fluorescence images and sample intensity. (**g**) Finally, the user can analyze the data by selecting a standard curve “.pasc” file and a sample “.parr” file from a previous run. (**h, i**) After pressing “Run BACTICOUNT analysis”, an analysis summary of each 36 sample positions is shown, which can be viewed in detail for CFU quantitation. All traces are stored within “.pasc” and “.parr” files and can be used for further analysis. A detailed, step-by-step tutorial is available online at bacticount.com.

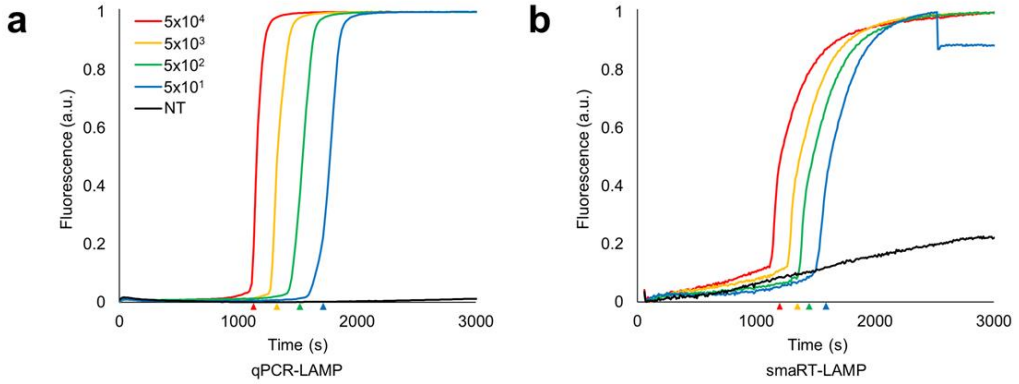

Figure 2.8. SmaRT-LAMP and qPCR instruments showed equivalent performance in measuring pathogen gDNA copy number. (**a, b**) Normalized representative *ST* gDNA traces and Tt values using qPCR-LAMP and smaRT-LAMP (5×10^1 – 5×10^4 genomes/reaction or no template (NT). The drop in smaRT-LAMP signal at later time points is due to water condensation on the tube cap that is avoided in qPCR instrument by the use of a heated lid. Colored triangles on horizontal axes indicate threshold times (Tt).

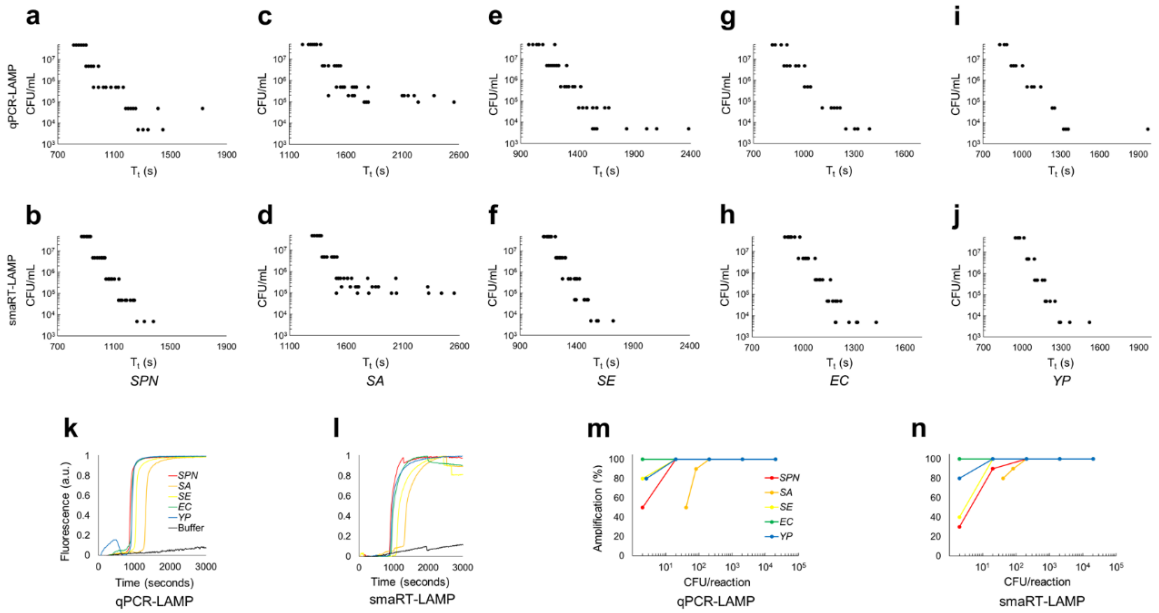

Figure 2.9. qPCR-LAMP and smaRT-LAMP quantification of diverse pathogens in spiked buffer. (**a–j**) Tt values for *SPN*, *SE*, *EC*, *YP* (2 – 2 x 10^4 CFU/reaction); *SA* (4 x10^1 – 2 x 10^4 CFU/reaction). (**k, l**) Representative traces of pathogens in spiked buffer using qPCR-LAMP and smaRT-LAMP (2 x 10^4 CFU/reaction). (**m, n**) Percentage of total samples amplifying at each concentration in qPCR-LAMP and smaRT-LAMP (5–10 samples/concentration).

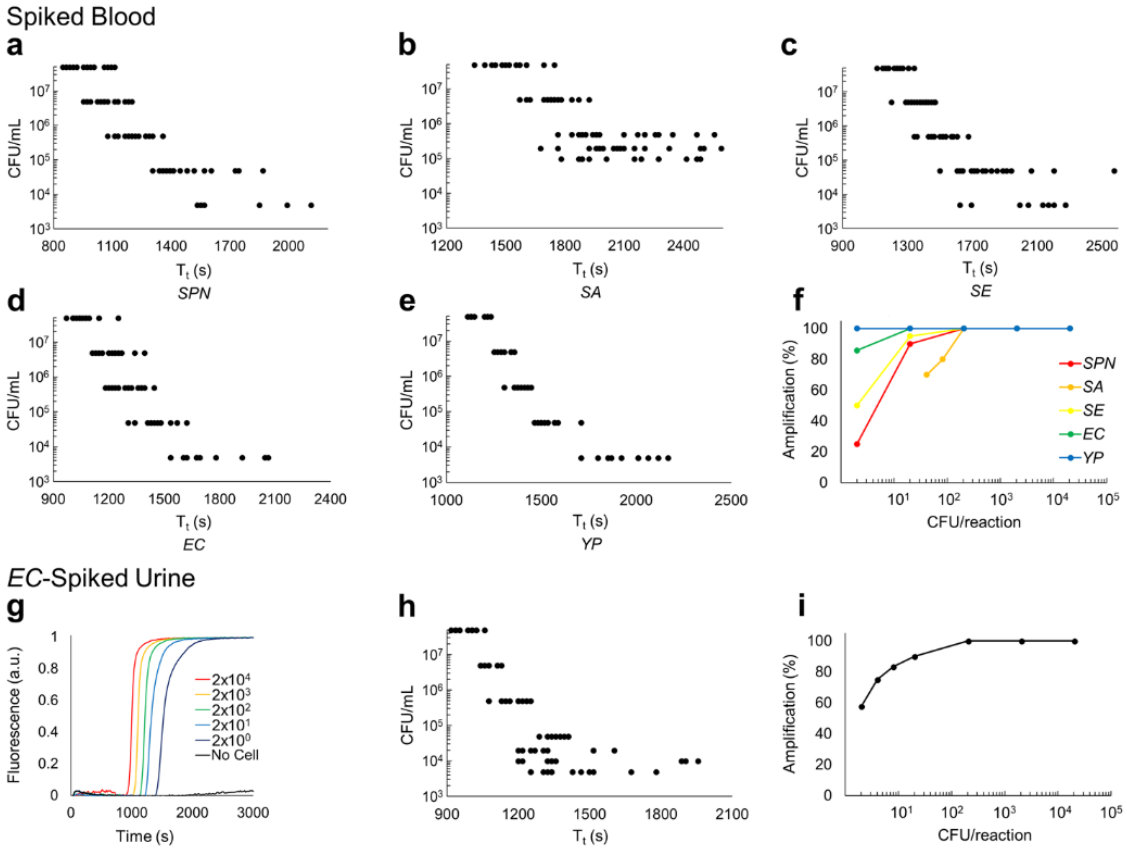

Figure 2.10. qPCR-LAMP quantitation of diverse pathogens in spiked murine whole blood and human donor urine. (**a–e**) Tt values for *SPN*, *SE*, *EC*, *YP* (2 – 2 x 10^4 CFU/reaction); *SA* (4 x10^1 – 2 x 10^4 CFU/reaction). (**f**) Percentage of total pathogen samples amplifying at each concentration in qPCR-LAMP. (**g, h**) Representative traces and Tt values for *EC* in spiked human donor urine (2 – 2 x 10^4 CFU/reaction). (**i**) Percentage of total *EC* samples amplifying at each concentration in qPCR-LAMP (> 10 samples/concentration).

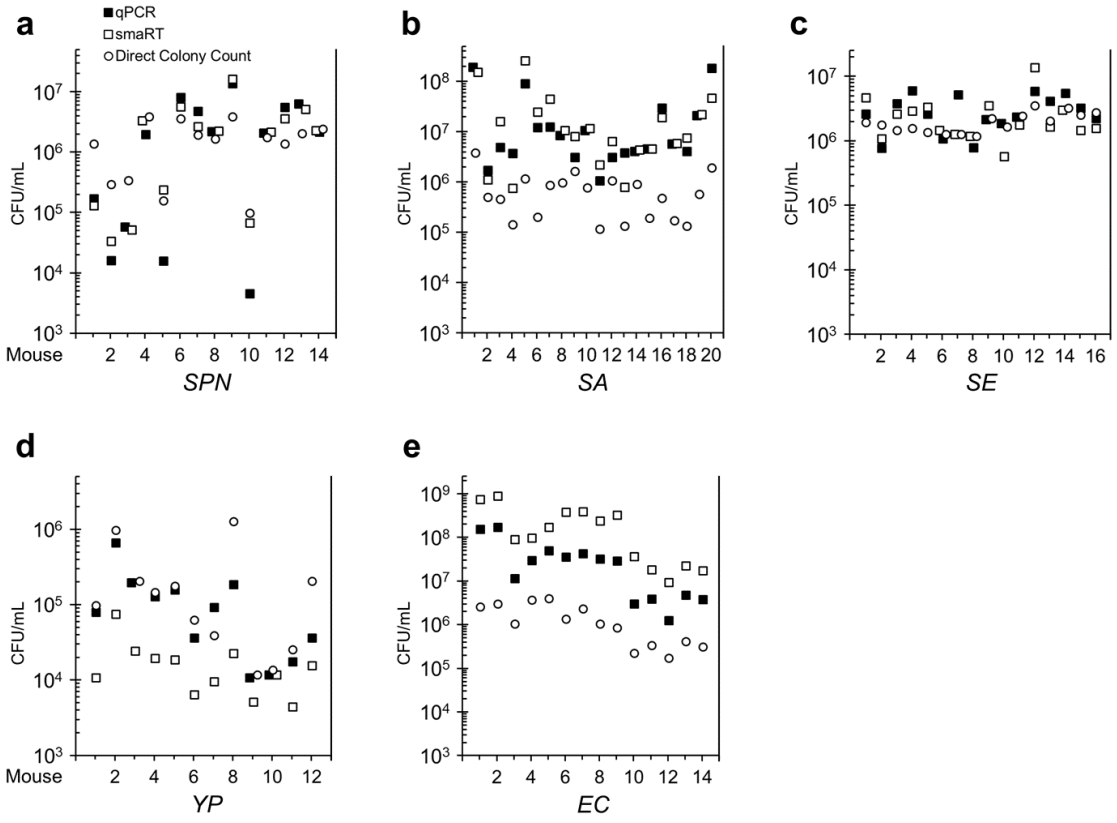

Figure 2.11. qPCR-LAMP and smaRT-LAMP detection and quantification of diverse pathogens in whole blood of septic mice. (**a–e**) Mice were infected with *SPN*, *SA*, *SE*, *YP* or *EC* and blood was collected from septic mice (see Methods for dose, route of administration, and day of sampling). CFU were determined by qPCR-LAMP (closed boxes), smaRT-LAMP (open boxes), and direct colony count (circles). n = 12–20 mice.

Table 2.3. Comparison of commercial and in-house costs of performing RT-LAMP.

	Fixed Costs (USD)		
Component	qPCR	smaRT-LAMP	Vendor
Galaxy S7 smartphone	NA	359.90	Samsung
Sample holder	NA	60.00	Universal Medical
Blue LEDs	NA	5.99	Deal eXtreme
12-V battery	NA	1.05	Walmart
Green light filter	NA	3.75	Battery Junction
Hot plate	NA	14.90	Walmart
Real-time thermal cycler	36,000.00	NA	Bio-Rad
Total apparatus cost	36,000.00	85.69 + phone	
	Marginal Costs (USD)		
Component	Purchase price	Cost / rxn	Vendor
Polymerase	300.00	0.44	New England Biolabs
Primers	126.75	0.04	IDT
Reaction buffer	1,797.79	0.48	In house
Fluorescence detection reagent	232.45	< 0.01	In house
Lysis buffer	177.95	0.01	In house
Sample tube	113.00	0.12	Bio-Rad
Sample lid	40.00	0.04	Bio-Rad
Total cost per 38 µL reaction		1.13	

Note that prices can vary according to vendor and purchaser. Tally represents necessary consumables and reagents but does not account for labor. NA = Not applicable

Table 2.4. Nucleotide primer sequences.

Gene	Pathogen	Primer Sequences	Ref.
glxK	*E. coli*	F3: 5'-GGCGAATGCCGTTATCCAG-3' B3: 5'-CGTGACGCTTGAAGTCTGC-3' FIP: 5'-CGCGCCTGAAAAGCGTAATCCCGCATGACGAATCAGCTCTC-3' BIP: 5'-CAATCACCGCCGTTTTCCCGTCGATGGGCGAAACAGTGAAT-3' LF: 5'-TGCTGGCGTCAAGTTTTGG-3' LB: 5'-CGCCGGTAAGGCCATAAAAA-3'	(*109*)
fimD	*K. pneumoniae*	F3: 5'-CGCCACTATCGACAGTCAG-3' B3: 5'-TGCAGACCGGTAAAACTCAA-3' FIP: 5'-ATCGCTGTGGCTATAGGTGCTGAGCCTGGGCTGAATCTGG-3' BIP: 5'-TCTTGCCCGCGATATTCACACCCGAAAATGCCGGAAGAGGTA-3' LF: 5'-GCAGGCGCCATGGTC-3' LB: 5'-AGCCAGCTGGTGGTCG-3'	(*110*)
oprI	*P. aeruginosa*	F3: 5'-CTGGATATTTTTTGAACAAACGA-3' B3: 5'-GTTCATCGTGTTCCCCTTA-3' FIP: 5'-TAAACTGACCAAGCGCAAGCCCAACTACTGCTAAAGTCGG-3' BIP: 5'-ACAAGTAATGGGTAGTATGTAGCCGGGACATTTCCATAACAGCAATC-3' LF: 5'-AGCAACTTTTTTTTTAGTCCCC-3' LB: 5'-GCTAATTTCCCCGGCTG-3'	(*110*)
recF	*Salmonella* sp.	F3: 5'-GCCGCGTGATTCGTCATG-3' B3: 5'-CCTCCGGCGTAATCAACTG-3' FIP: 5'-GATAAGCAGGGCGACAGCAACAGCTCCGCGATCTTGTG-3' BIP: 5'-AGCCAATCGACGTCTCACGCAGCAGGAAGCGTTTGTTCTT-3' LF*: 5'-GGTCCGTATCGACGGTACCGACGGT-3' LB*: 5'-CTTCGCTCTGTAATCGCCCGTG-3'	(*96*)
Sdf I	*S.* Enteritidis	F3: 5'-GGGAGGAGCTTTAGCCAA-3' B3: 5'-ATGGTGAGCAGACAACAG-3' FIP: 5'-CATGCTCGCTGCACAAAAGCGAGAGGCGGTTTGATGTG-3' BIP: 5'-CTGGAAAGCCTCTTTATATAGCTCATGATATACTCCCTGAATCTGAGA-3' LF: 5'-GCCTAAAAAATCAGTGACGAACCAA-3' LB: 5'-CTGACCTCTAAGCCGGTCAATG-3'	(*111*)
rfbJ	*S.* Typhimurium	F3: 5'-CGAAGCGCTAAAAAAATCGG-3' B3: 5'-CCCAATTTCATCAAAGTGTCT-3' FIP: 5'-GCAGAATCAATTGATAACTCCTCGAGGATTTCAGTTGTCGCAATC-3' BIP: 5'-AACCATTAAAGCTTCTTGATTTGGCATATAAGGCCGCATATGTTGA-3' LF: 5'-ATTATCCCAACTGCACCATCTAACA-3' LB: 5'-TCGGGCGGATATCTTTTTAAATACA-3'	(*112*)
16S	*S. aureus*	F3: 5'-CGTGGGGATCAAACAGGATT-3' B3: 5'-CATGCTCCACCGCTTGTG-3' FIP: 5'-TAGCTGCAGCACTAAGGGGCCCACGCCGTAAACGATGAG-3' BIP: 5'-ACGCATTAAGCACTCCGCCTGGGTCCCCGTCAATTCCT-3' LF: 5'-GGAAACCCCCTAACACT-3' LB: 5'-GGGGAGTACGACCGCAAGGT-3'	(*113*)
lytA	*S. pneumoniae*	F3: 5'-GCGTGCAACCATATAGGCAA-3' B3: 5'-AGCATTCCAACCGCC-3' FIP: 5'-CCGCCAGTGATAATCCGCTTCACACTCAACTGGGAATCCGC-3' BIP: 5'-TCTCGCACATTGTTGGGAACGGCCAGGCACCATTATCAACAGG-3' LF*: 5'-TTCTGTACGGTTGAAT-3' LB: 5'-TGCATCATGCAGGTAGGA-3'	(*114*)
inv	*Y. pseudotuberculosis*	F3: 5'-CTCGTCGCGTGATTTCTCC-3' B3: 5'-GATCTACCCCGACAGTGAGT-3' FIP: 5'-CCAGTTGTGGGAGTGCAGGTAACTATAAAGAGCGCCCAGCC-3' BIP: 5'-CACCGGTGAGCGTGTTGCTTTGTGTAATTGATCCCGGCAGT-3' LF: 5'-CATTCGCGCGCAAATCC-3' LB: 5'-GCAACGCAACCCTTATGC-3'	(*115*)

*loop primers developed for this study

Table 2.5. Comparative bacterial analysis of urine from sepsis patients with clinically negative urine cultures.

	CFU/mL			
Patient	Clinical Culture	qPCR-LAMP	smaRT-LAMP	Colony Count
1	No growth	–	–	< 10
2	No growth	–	–	< 10
3	No growth	–	–	9.7×10^1
4	No growth	–	–	< 10
5	$< 10^4$	5.4×10^3	1.6×10^4	4.2×10^4

The bacterial load in urine of human sepsis patients with clinically negative urine cultures (below the standard threshold for infection of 10^5 CFU) (*37, 72*) was determined by the hospital microbiology laboratory (clinical culture) versus an academic laboratory examining CFU by direct colony count, qPCR-LAMP, and smaRT-LAMP, utilizing *E. coli* primer sets. A linear fit of standard curves with a clinically relevant bacterial burden ($5 \times 10^4 – 5 \times 10^7$ CFU/mL) was used to determine LAMP-based CFUs. " – " denotes no pathogen detected. qPCR-LAMP and smaRT-LAMP values depict an average of 6 determinations from each specimen.

Chapter 3

Transforming the Smartphone into a Stand-alone Point-of-Care Diagnostic for SARS-CoV-2 and Influenza†

†This chapter contains excerpts, from Heithoff DM, Barnes L, Mahan SP, Fox GN, Arn KE, Ettinger S, Bishop AM, Fitzgibbons LN, Fried JC, Low DA, Samuel CE, and Mahan MJ (2021). Transforming the Smartphone into a Stand-alone Point-of-Care Diagnostic for SARS-CoV-2 and Influenza. *In Preparation.*

ABSTRACT

BACKGROUND**:** Pandemics including COVID-19 pose increasingly severe threats to public health. Of global concern is the lack of rapid, sensitive, affordable and scalable diagnostics at the point-of-care (POC). Here we leveraged the sensitivity of loop-mediated isothermal amplification (LAMP) with the computational power and connectivity of the smartphone to transform it into a stand-alone diagnostic for SARS-CoV-2 and influenza viruses at the POC.

METHODS: A smartphone-based real-time LAMP (smaRT-LAMP) system was developed that uses a free, custom-built mobile phone app that enables the phone to serve as an advanced diagnostic for microbial pathogens. The detection system, consisting of a hot plate, cardboard box, and LED lights, is portable and can be fabricated for less than $100 USD. Human saliva samples spiked with SARS-CoV-2 or influenza viruses were analyzed in comparison to gold-standard RT-qPCR. These analyses were used as the basis for detection of SARS-CoV-2 from self-collected clinical samples obtained from patients with COVID-19.

RESULTS: A comparative analysis of human patient saliva samples clinically evaluated for SARS-CoV-2 sensitivity and viral load revealed that smaRT-LAMP exhibited 100% concordance with gold-standard RT-qPCR. Similar performance was demonstrated with SARS-CoV-2 variants and influenza A and B viruses. SmaRT-LAMP had a limit of detection (LOD) of 1000 copies/mL, turn-around-time of 25 min, scalability (96 samples/run/phone), and was compatible with room temperature sample storage and reaction assembly – for less than $7 USD/test.

CONCLUSIONS: SmaRT-LAMP integrates state-of-the-art diagnostics with the extensive features of the smartphone to provide low-cost, advanced health care at the POC. The broad applicability of this platform was demonstrated by detection and differentiation between clinically similar respiratory viruses, SARS-CoV-2 and influenza. Moreover, as new variants of SARS-CoV-2 emerge in the developing world, testing and detection remain at the forefront of pandemic control efforts. SmaRT-LAMP thus offers the potential to provide underserved and vulnerable populations with a critical tool for the next stage in the pandemic.

3.1. INTRODUCTION

The SARS-CoV-2 virus responsible for the COVID-19 pandemic has to date infected over 155 million people worldwide, including many in countries lacking technical and financial resources to effectively monitor and respond to this pandemic (*116*). Accordingly, there is an urgent need for simple, accurate and low-cost testing at the point-of-care that can be used by healthcare providers and other authorities in remote and resource-limited settings around the world (*117*). Numerous methods for the detection of SARS-CoV-2, including molecular, antigen, and serology tests, are currently in use (*118-120*). Although molecular methods such as PCR are rapid and sensitive, they generally require access to specialized and costly laboratory instrumentation, reagents and highly-trained personnel, and are technologically complex for POC or resource-limited settings. While antigen and serology tests are simple to use, cost-effective and portable, they can be unreliable with high false positive/negative rates due to their lack of sensitivity. Loop-mediated isothermal amplification (LAMP) diagnostics have gained attention for pathogen detection because they do not require sophisticated, expensive instrumentation or highly trained personnel for operation (*42, 121*). The high sensitivity and utility of LAMP-based diagnostics have been offset by a propensity for primer-dimer self-amplification due to the requirement of six primers per target gene, increasing the incidence of false-positives (*122-124*). We addressed this problem by determining experimental conditions which effectively eliminate primer-dimer amplification, thereby permitting the development of an effective LAMP-based, point-of-care test for SARS-CoV-2 and influenza A and B viruses. Indeed, the highly-similar clinical

syndromes of SARS-CoV-2 and influenza has prompted CDC recommendations for combination diagnostics when both pathogens are circulating (*125*). Further, the imminent lifting of pandemic restrictions exacerbates the potential for a double epidemic of COVID-19 and influenza, termed a “perfect storm”, due to a potential increase in severe illness, transmission, and misdiagnosis resulting from symptom overlap (*126-129*).

Smartphones are an ideal choice for meeting the global demand for rapid, accurate, and cost-effective POC devices that are accessible even in the most remote and resource-limited settings (*130-134*). Their potential use as clinical diagnostics is bolstered by their high-resolution cameras, computer processors, software applications, touchscreen interface, wireless connectivity, portability, integral role in telemedicine and global use by nearly half the world’s population (*135*). Here, we leverage the features of the smartphone with those of LAMP to develop a smartphone-based clinical diagnostic with the capacity to rapidly and affordably for the SARS-CoV2 virus at the POC.

3.2. RESULTS

3.2.1. SmaRT-LAMP sensitivity and specificity

Study Design. A head-to-head comparison of smaRT-LAMP and gold-standard RT-qPCR methodologies was performed on human saliva samples spiked with SARS-CoV-2 or influenza viruses. These analyses were used as the basis for smaRT-LAMP detection of SARS-CoV-2 from self-collected clinical samples obtained from patients with COVID-19. Sensitivity and specificity tests using spiked saliva specimens were performed as per FDA EUA guidelines as described in the Methods and supplement (*136*).

SARS-CoV-2 sensitivity (Limit Of Detection, LOD). A comparative LOD analysis of the smaRT-LAMP platform versus the clinical gold standard CDC 2019-nCoV RT-qPCR diagnostic (*137*) was evaluated using spiked saliva samples analyzed in parallel (**Figure 3.1a**). The LOD of smaRT-LAMP for SARS-CoV-2 was 10^3 copies/mL, matching that of the CDC 2019-nCoV RT-qPCR diagnostic test (20/20 and 19/20 biological replicates, respectively), whereas saliva samples from virus-negative donors, when not spiked, gave no amplification (0/20 biological replicates; $P < 0.001$).

SARS-CoV-2 specificity (cross-reactivity). SmaRT-LAMP specificity for SARS-CoV-2 was evaluated by measuring cross-reactivity against several viral and bacterial respiratory pathogens (**Figure 3.1b**). SmaRT-LAMP (using SARS-CoV-2 primers) amplified two SARS-CoV-2 isolates tested (USA-WA and Hong Kong) (20/20 biological replicates), whereas no amplification was observed for any of the other six coronaviruses tested (SARS-CoV-1, MERS-CoV, HCoV-OC43, HCoV-

229E, HCoV-NL63, and HCoV-HKU1), nor for the four bacterial respiratory pathogens tested (*S. pneumonia*, *S. aureus, P. aeruginosa* and *K. pneumonia*) (0/20 biological replicates; $P < 0.001$).

SARS-CoV-2 variants. SARS-CoV-2 "variants of concern" continue to surge throughout the world and thus it is critical that molecular diagnostics can accurately detect them (**Figure 3.1b**) (*138*). SmaRT-LAMP detected genomic RNA isolated from 5 of 5 major SARS-CoV-2 variants tested: B.1.1.7 (UK), P.1 (Brazil, B.1.1.28.1), B.1.526 (NY), B.1.429 (CAL.20C) and B.1.617.2 (India) (10/10 biological replicates; $P < 0.001$). None of the mutations present in these variants overlap with any of the smaRT-LAMP primer sets and thus it was not unexpected that the mutations did not affect smaRT-LAMP detection of the variants (**Table 3.3**).

Influenza A and B sensitivity (LOD). A comparative LOD analysis of the smaRT-LAMP platform versus the clinical gold standard CDC influenza SARS-CoV-2 (Flu SC2) RT-qPCR multiplex assay (*139*) was evaluated using spiked saliva samples and either influenza A or influenza B primers (**Figure 3.1c**). The LOD of smaRT-LAMP matched that of Flu SC2 RT-qPCR test for influenza A (2.8×10^2 $TCID_{50}$/mL) and exceeded that for influenza B (0.8 vs. 40 $TCID_{50}$/mL) (19/20 biological replicate each), whereas unspiked saliva samples from virus-negative donors gave no amplification with either influenza A or B primers (0/20 biological replicates; $P < 0.001$).

Influenza A and B specificity (cross-reactivity). SmaRT-LAMP specificity for influenza A or B was evaluated as above using influenza A or B primers with spiked saliva samples (**Figure 3.1d**). SmaRT-LAMP amplified influenza A or B viruses

when using cognate Flu A or B primers (20/20 biological replicates), whereas no amplification was observed with any of the other eight coronaviruses or four bacterial pathogens tested (0/20 biological replicates; $P < 0.001$).

3.2.2. Clinical evaluation

Patient samples were clinically evaluated for SARS-CoV-2 sensitivity and for quantitative detection of viral load using smaRT-LAMP or CDC 2019-nCoV RT-qPCR assays. Fifty patient saliva specimens were split into equal volumes and a head-to-head comparison was performed using the two methodologies. Sensitivity was determined by the presence or absence of sample signal (binary +/- call); viral load was determined by comparison of sample signal with that of standard curves established from serial dilution of spiked saliva samples amplified with smaRT-LAMP or RT-qPCR assays. SmaRT-LAMP showed 100% concordance (50/50 patient samples) with the RT-qPCR diagnostic test for SARS-CoV-2 sensitivity (20/20 positive and 30/30 negative) and for quantitative detection of viral loads (copies/mL) (**Fig. 3.2**).

3.2.3. Storage conditions for patient saliva specimens

SmaRT-LAMP compatibility with SARS-CoV-2 room temperature saliva specimen storage and reaction mix assembly was evaluated to determine suitability for resource-limited settings wherein refrigeration may not be available. Viral concentration was determined as a function of storage time and temperature by smaRT-LAMP, using reaction mixes assembled at room temperature. The smaRT-LAMP protocol amplified SARS-CoV-2 contrived samples without significant loss of sensitivity after sample storage for $\leq$ 4 h at room temperature and < 10-fold loss in

sensitivity after sample storage for up to at least one week in a refrigerator (4 ^{o}C) (**Figure 3.3**).

3.3. DISCUSSION

At the forefront of COVID-19 pandemic control efforts is accurate, accessible diagnostic testing, which can be employed universally in underserved settings, and is robust against the circulating variants of SARS-CoV-2 virus. As a step toward achieving this goal, we developed smaRT-LAMP, a phone-based molecular diagnostic: a simple test that is rapid, sensitive, affordable and scalable. We have demonstrated the smaRT-LAMP platform evaluation of SARS-CoV-2 sensitivity and quantitative detection of viral load matched the performance of a clinical gold-standard RT-qPCR diagnostic test. Using the smaRT-LAMP protocol, we also demonstrated that false positives seen in other LAMP assays due to dimerization of primers was successfully eliminated. SmaRT-LAMP performed well under room temperature conditions, circumvents the need for expensive fluorescent probes, and is anticipated to be particularly useful in the context of resource-limited settings that may otherwise lack sophisticated instrumentation, specialized reagents or suitably-trained technical staff.

The smaRT-LAMP detection system consists of a hot plate, cardboard box, and LED lights is inexpensive and portable and, can be fabricated for less than $100 USD (in addition to the smartphone). The system is designed for rapid and frequent testing of large populations (96 samples/run/phone) at a cost of < $7 USD/ test, enabling low-cost, advanced diagnostics at the POC. As reported by others, SARS-CoV-2 can be detected in saliva samples that have numerous advantages relative to nasopharyngeal swabs including: cost, ease of use (self-collection vs. trained personnel and PPE for sample collection), availability, and utility in resource poor

countries (*140, 141*). The saliva sample collection for smaRT-LAMP diagnostic analysis is far less intrusive than swab sample collection by healthcare workers. Furthermore, saliva sampling circumvents the need for specialized swabs and reagents, which are vulnerable to supply-chain disruptions and resource limitations.

There are numerous opportunities to adapt the protocol from a lab test to a field test and reduce the cost of smaRT-LAMP-based clinical diagnostics as a powerful tool to combat widespread disease and future pandemics. First, since ~90% of the cost per test comes from commercially-available enzymes, bulk enzyme purification would be a significant improvement. Second, field-test applicability could conceivably be achieved with the use of lyophilized reagents, ideal for areas that lack refrigeration (*107, 108*). The use of lyophilized reagents can further streamline smaRT-LAMP by enabling the simple addition of specimen to a pre-assembled master mix, thereby minimizing sample handling, preparation time and user error, while enhancing user biosafety.

Integration of smaRT-LAMP with telemedicine has the potential to deliver advanced health care to vulnerable populations, while markedly broadening the scope of personalized medicine (*142, 143*). The capacity to rapidly and accurately test vulnerable populations, particularly in developing nations struggling with adequate vaccine and testing access amidst a landscape of new, and more highly transmissible variants is critically important. To this end, smaRT-LAMP detected 5 of 5 major SARS-CoV-2 variants, and through primer changes, smart-LAMP can be further adjusted if new, as yet unseen, variants evolve. The broad applicability of smaRT-LAMP has been established with many microbial pathogens and body fluids

(blood, urine, stool) (*144*). Taken together, smaRT-LAMP integrates advanced diagnostic techniques with the connectivity and computational power of the smartphone, offering the potential to provide fair and equal access to precision diagnostic medicine.

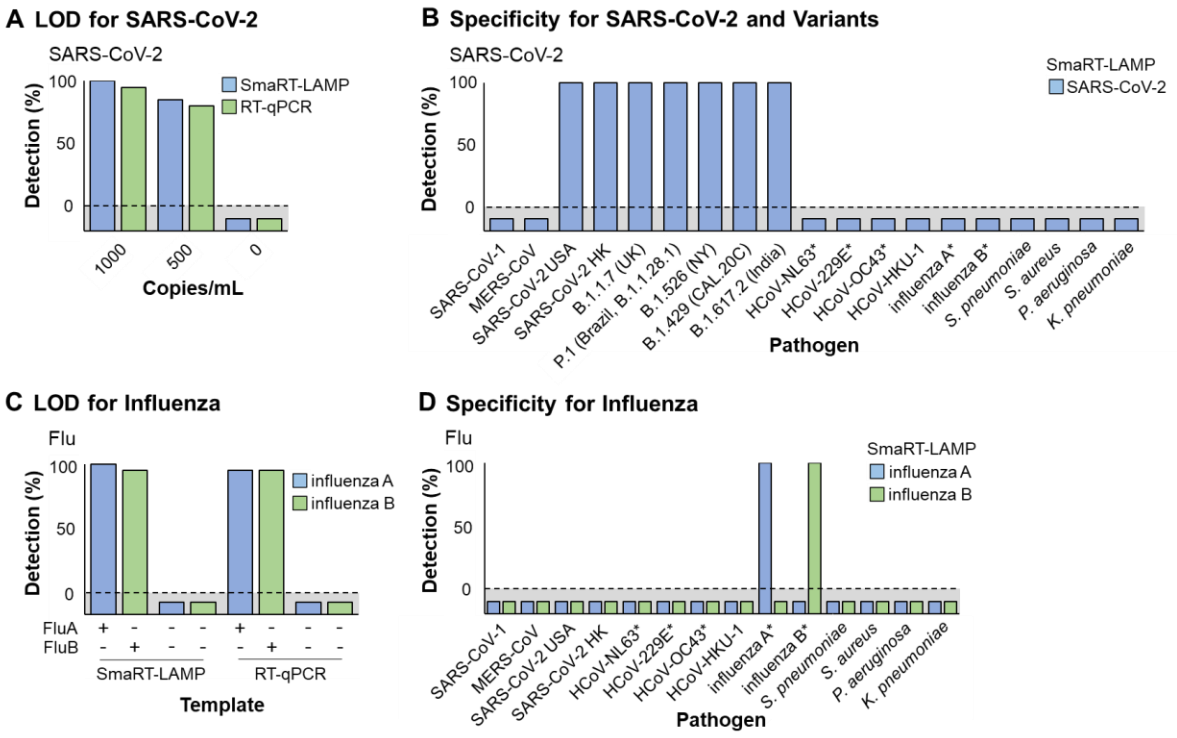

Figure 3.1. SmaRT-LAMP Sensitivity and Specificity for SARS-CoV-2 and Influenza Viruses. (**a**) Limit of detection (LOD) for SARS-CoV-2 measured by smaRT-LAMP vs. CDC 2019-nCoV RT-qPCR, using SARS-CoV-2 primers, was determined by the largest serial dilution of SARS-CoV-2 USA viral stock giving a signal in $\geq$ 19/20 biological replicates. (**b**) Specificity (cross-reactivity) of smaRT-LAMP for SARS-Cov-2, CoV-2 variants, and other viral and bacterial respiratory pathogens, using SARS-CoV-2 primers was determined by the presence or absence of signal (binary + or - call) (see Methods and supplement). (**c**) LOD for influenza A and B measured by smaRT-LAMP vs. CDC Flu SC2 RT-qPCR was determined as in (**a**) using influenza A or B primers. (**d**) Specificity was evaluated as in (**b**) using influenza A and B primers. *designates quantitation by $TCID_{50}$. n = 10 biological replicates for SARS-CoV-2 variants; n = 20 biological replicates for all other pathogens.

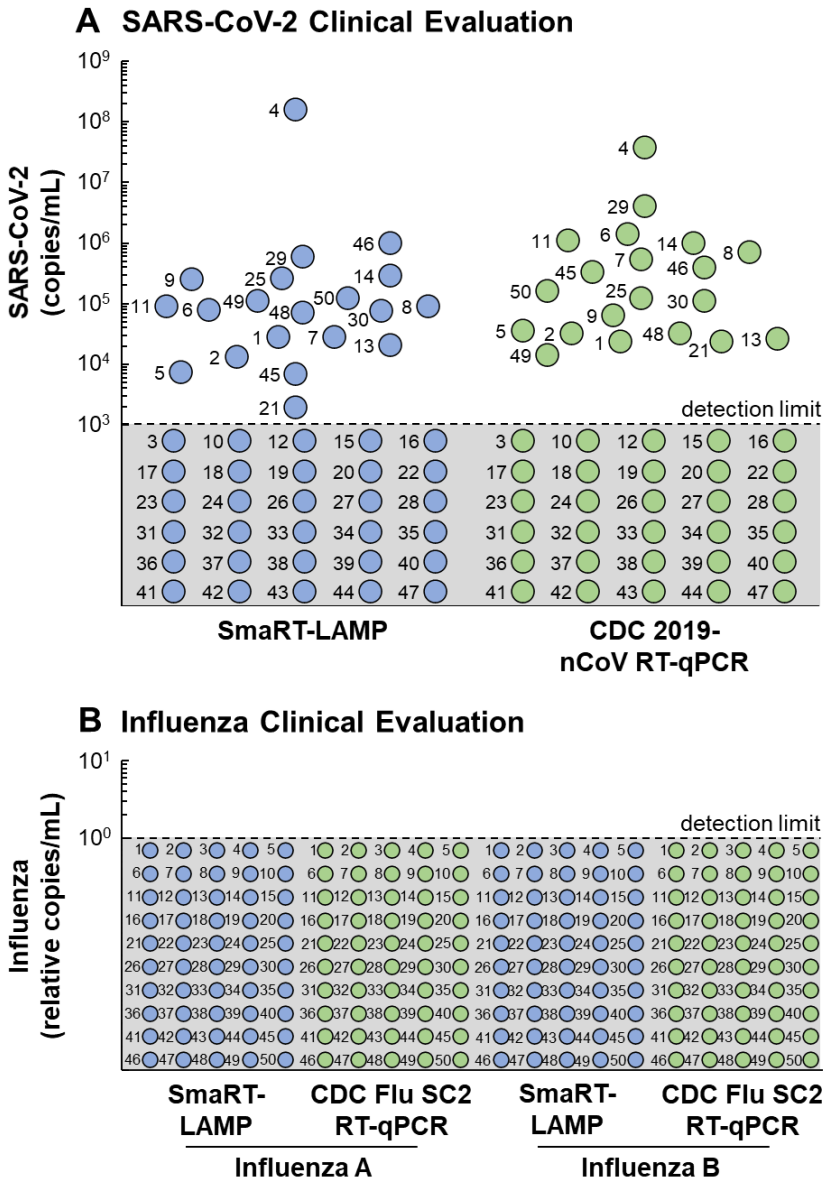

Figure 3.2. Clinical Evaluation of SARS-CoV-2 Patient Saliva Specimens. Fifty patient saliva specimens were split into equal volumes and a comparative analysis was performed using smaRT-LAMP or CDC 2019-nCoV RT-qPCR assays (see supplement). Sensitivity was determined by the presence or absence of sample signal (binary +/- call); quantitative detection of viral load was determined by comparison of sample signal with that of standard curves established from serial dilution of spiked saliva samples amplified with smaRT-LAMP or CDC 2019-nCoV RT-qPCR assays.

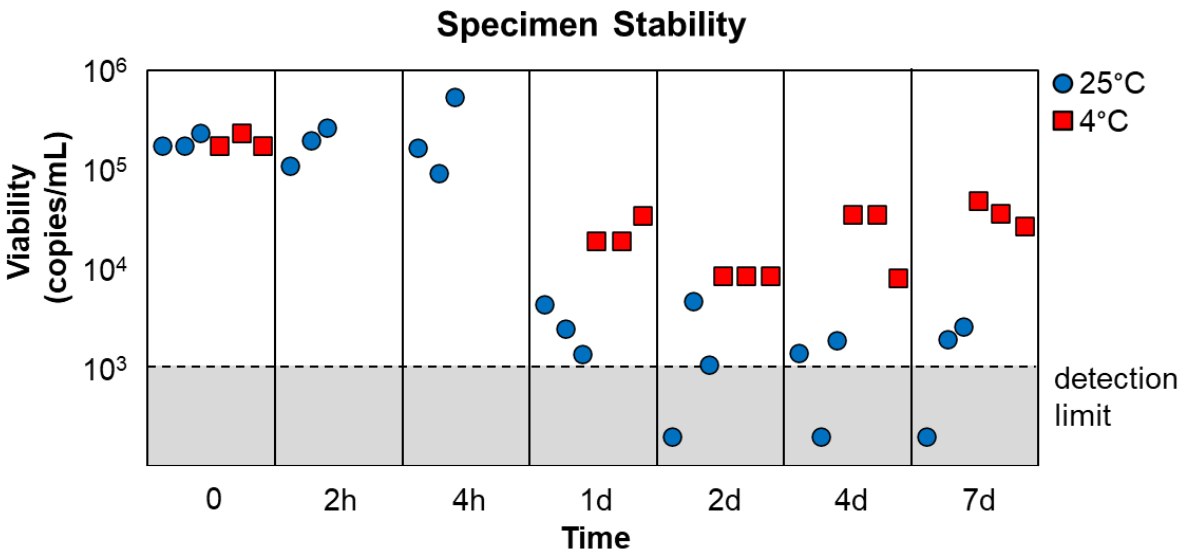

Figure 3.3. SmaRT-LAMP Compatibility with Room Temperature Specimen Storage and Reaction Assembly. Spiked saliva samples (2.5 x 10^5 copies/mL) were prepared in fresh saliva from virus-negative donors. The viral concentration (copies/ml) as a function of time and temperature was evaluated by smaRT-LAMP using a reaction mix assembled at room temperature. Quantitative detection of viral load was determined by comparison of sample signal with that of a standard curve established from serial dilution of spiked saliva samples amplified with smaRT-LAMP assays. n = 3 biological replicates for each condition.

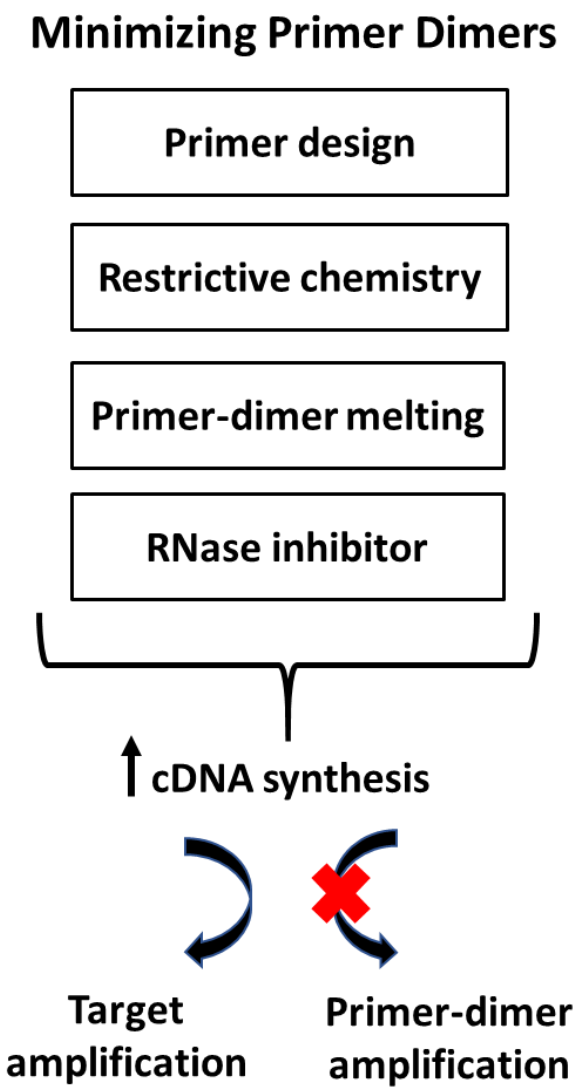

Figure 3.4. Minimizing LAMP primer-dimer amplification. The smaRT-LAMP protocol, optimizing primer design and reaction conditions, favors viral RNA stability and cDNA synthesis while effectively eliminating LAMP primer-dimer amplification (false positives). Parameters include: (i) optimal primer design to reduce the probability of primer-dimer formation; (ii) optimal reaction chemistry favoring primer binding to viral nucleic acids; (iii) primer melting at 70 ^{o}C before addition to master mix; and (iv) addition of RNase inhibitor to stabilize viral RNA in saliva specimens. The order of assembly of LAMP reagents is critical to improve LAMP performance and reduce primer-dimer self-amplification (false positives) as described in the supplement.

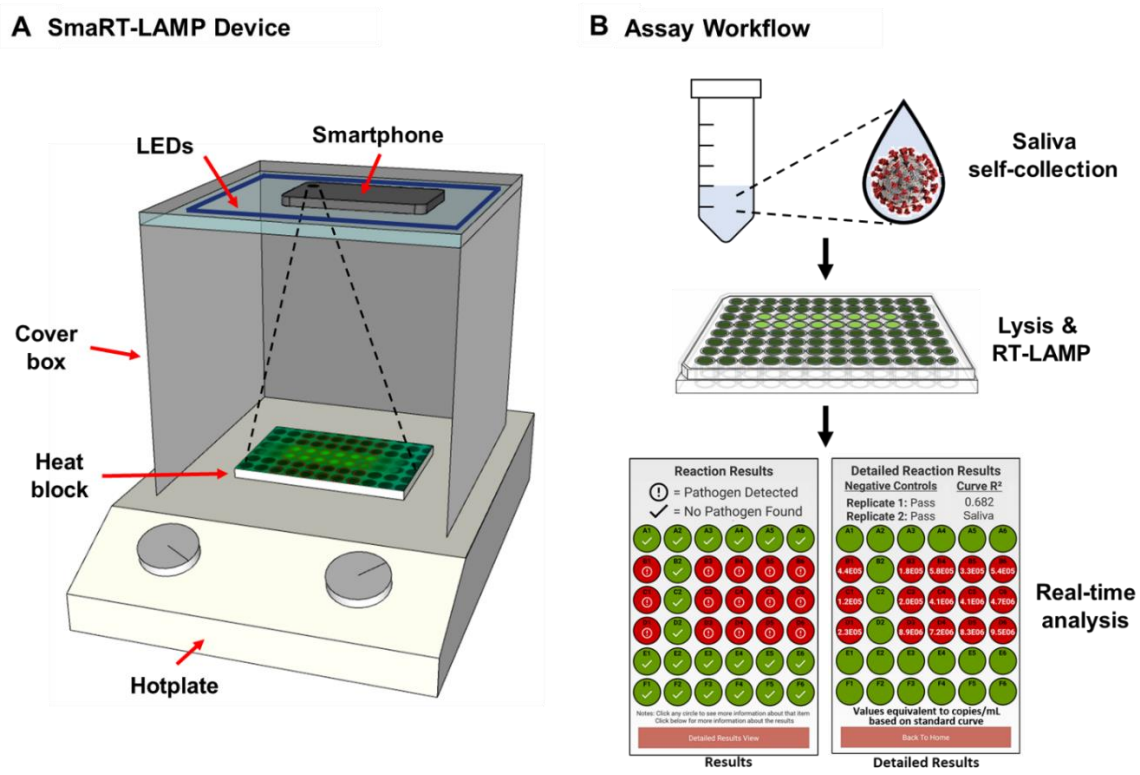

Figure 3.5. Overview of SmaRT-LAMP instrumentation and workflow. (**a**) Device: LEDs are affixed to the inside top of a cardboard box that covers a heat block resting on a hotplate. A smartphone camera is directed towards the samples through a box aperture. (**b**) Workflow: The smaRT-LAMP reaction mix, containing "sample mix" (saliva specimen with RNA stabilizers) and "master mix" (lysis reagents, primers and polymerase enzymes), is assembled at room temperature and loaded onto a 70 ^{o}C heat block, which initiates both the reverse transcription and LAMP reactions. The mobile phone app displays the sample results in a binary manner as follows: "Pathogen Detected" - designated as red circle; or, "No Pathogen Found" - designated as green circle on the "Reaction Results" screen. Clicking on the red circle results in the app displaying the viral load in copies/mL on the "Detailed Reaction Results" screen.

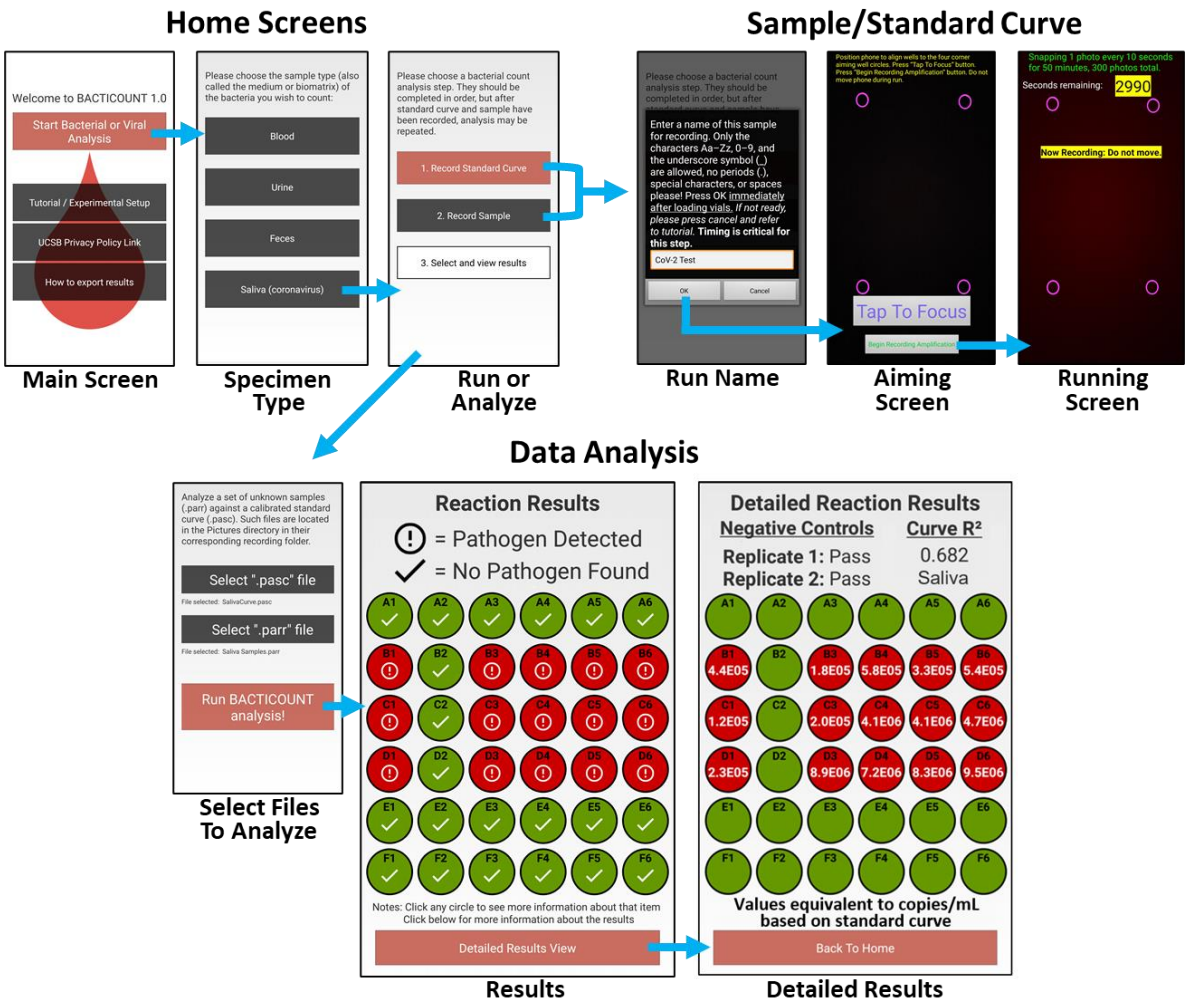

Figure 3.6. Workflow of the Bacticount smaRT-LAMP mobile phone app. The user is prompted to pick the sample type (saliva) followed by a three-step procedure: 1) Record Standard Curve for a pathogen of interest in contrived (spiked) samples (e.g., SARS-CoV-2; influenza); 2) Record Sample; and 3) Select and view results where the app displays the sample results in a binary manner as follows: “Pathogen Detected” - designated as red circle; or, “No Pathogen Found” - designated as green circle on the “Reaction Results” screen. By clicking on the red circle that appears if a pathogen is detected, the app displays the viral load in copies/mL on the “Detailed Reaction Results” screen. Blue arrows represent connecting app screenshots.

Table 3.1. Oligonucleotide primer sequences.

Gene	Pathogen	Primer Set	Primer Sequences	Ref.
N	SARS-CoV-2	3	F3: 5′-AACACAAGCTTTCGGCAG-3′ B3: 5′-GAAATTTGGATCTTTGTCATCC-3′ FIP: 5′-TGCGGCCAATGTTTGTAATCAG-CCAAGGAAATTTTGGGGAC-3′ BIP: 5′-CGCATTGGCATGGAAGTCAC-TTTGATGGCACCTGTGTAG-3′ FL: 5′-TTCCTTGTCTGATTAGTTC-3′ BL: 5′-ACCTTCGGGAACGTGGTT-3′	(*145*)
N	SARS-CoV-2	16	F3: 5′-TGGCTACTACCGAAGAGCT-3′ B3: 5′-TGCAGCATTGTTAGCAGGAT-3′ FIP: 5′-TCTGGCCCAGTTCCTAGGTAGT-CCAGACGAATTCGTGGTGG-3′ BIP: 5′-AGACGGCATCATATGGGTTGCA-CGGGTGCCAATGTGATCT-3′ FL: 5′-GGACTGAGATCTTTCATTTTACCGT-3′ BL: 5′-ACTGAGGGAGCCTTGAATACA-3′	(*146*)
ORF1ab	SARS-CoV-2	9	F3: 5′-TCGGTGGACAAATTGTCAC-3′ B3: 5′-GTAGGCCAGTTTCTTCTCTG-3′ FIP: 5′-GAGTCAGCACACAAAGCCAAAAAT-CTGTGCAAAGGAAATTAAGGAG-3′ BIP: 5′-TGGTGGAGCTAAACTTAAAGCCT-CACACTTTCTGTACAATCCCTT-3′ FL: 5′-ACAAGCTTAAAGAATGTCTGAACAC-3′ BL: 5′-TTAGGTGAAACATTTGTCACGC-3′	This study
ORF1ab	SARS-CoV-2	15	F3: 5′-CGGTGGACAAATTGTCAC-3′ B3: 5′-CTTCTCTGGATTTAACACACTT-3′ FIP: 5′-TCAGCACACAAAGCCAAAAATTTAT-CTGTGCAAAGGAAATTAAGGAG-3′ BIP: 5′-TATTGGTGGAGCTAAACTTAAAGCC-CTGTACAATCCCTTTGAGTG-3′ FL: 5′-ACAAGCTTAAAGAATGTCTGAACAC-3′ BL: 5′-GAATTTAGGTGAAACATTTGTCACG-3′	*Adapted from (*147*)
M1	Influenza A H1N1, H3N2	A6	F3: 5′-TGGTGCACTTGCCAGTTG-3′ B3: 5′-CCAGCCATCTGTTCCATAGC-3′ FIP: 5′-TGCTGTGAATCAGCAATCTGTT-ACAGGATGGGAACAGTGACC-3′ BIP: 5′-AGACAGATGGCTACTACCACC-CGTAGTGCTAGCCAGCACC-3′ FL: 5′-GCACACACTAGACCAAAAGCAGCTT-3′ BL: 5′-TCCACTAATCAGGCATGAAAACAG-3′	*Adapted from (*148*)
PB1	Influenza A H1N1, H3N2	A5a	F3: 5′-ACCAAGACAACATACTGGTG-3′ B3: 5′-GCCACAAATCCATAGCGATA-3′ FIP: 5′-TCCACTCCTGCTTGTATTCCCT-TCCAATCATCCGACGATT-3′ BIP: 5′-AGGACCTGCAAGTTAGTGGGA-GTGAATTCAAATGTCCCTGT-3′ FL: 5′-GGTTTGGTGCATTCACTATGAGAGC-3′ BL: 5′-ATCAACATGAGCAAAAAGAAGTCCT-3′	This study
M1	Influenza B Yamagata	B5	F3: 5′-TGAAAGCTCAGCGCTACT-3′ B3: 5′-TGTTCATAGCTGAGACCATC-3′ FIP: 5′-TCGCACAAAGCACAGAGCGTT-CATGTACCTGAATCCTGGAA-3′ BIP: 5′-AGCATCACATTCACACAGGGCT-GCATTTCTCGTCTCACTCC-3′ FL: 5′-CCTAGTTTTACTTGCATTGA-3′ BL: 5′-AGCAGAGCAGCGAGATCTTC-3′	This study
NS1	Influenza B Yamagata	B7	F3: 5′-AAGTCCTTATCAACTCTGCA-3′ B3: 5′-GTGCTCTTGACCAAATTGG-3′ FIP: 5′-CGATGGCCATCTTCTTCATCCT-ACCAGAGTGGAAGGCTTGT-3′ BIP: 5′-CTCAATTCACTCTTCGAGCGTC-ATAAGACTCCCACCGCAG-3′ FL: 5′-CACTGTAAGATCATCAGTAGCAACA-3′ BL: 5′-TTAATGAAGGACATTCAAAGCC-3′	This study

*Loop primers were designed for SARS-CoV-2 primer set 15.(*147*) Influenza A primer set A6 was modified from (*148*) by designing loop primers, and by using consensus sequences to redesign primers.

Table 3.2. SmaRT-LAMP test expenditures, equipment and scale-up protocol for reaction mix.

(a) Chemical Reagents	Volume/ reaction (µL)	Vendor	Part no.	Item Price (USD)	Price/mL (USD)	Price/ Reaction (USD)	Website link
NEB 10X isothermal amplification buffer	5	NEB	M0538M	Comes with Bst			
NEB $MgSO_4$ (100 µM)	1.85	NEB	M0538M	Comes with Bst			
NEB dNTP mix (10 mM)	7	NEB	N0447L	5 vials of 800 µL, 10 mM each nt, $204.00	0.051	0.357	https://www.neb.com/products/n0447-deoxynucleotide-dntp-solution-mix#Product%20Information
FIP/BIP primers (300 µM) for 2 targets	0.261 x 4	IDT	Custom	$0.149314657/µL	0.149314657	0.155884502	
F3/B3 primers (30 µM) for 2 targets	0.34 x 4	IDT	Custom	$0.007475021/µL	0.007475021	0.010166028	
FL/BL primers (30 µM) for 2 targets	1.32 x 4	IDT	Custom	$0.0100047/µL	0.0100047	0.052824818	
NEB Bst 2.0 WarmStart DNA polymerase (120 U/mL)	0.266	NEB	M0538M	8,000 U at 120,000 U/mL, $255.20	3.828	1.018248	https://www.neb.com/products/m0538-bst-20-warmstart-dna-polymerase
NEB RTx WarmStart reverse transcriptase (15 U/µL)	2	NEB	M0380L	15,000 U/mL, 250 rxns (0.5 µL/rxn), $221.60	1.7728	3.5456	https://www.neb.com/products/m0380-warmstart-rtx-reverse-transcriptase#Product%20Information
Fluorescence Detection Reagent (FDR): 0.5 mM calcein, 10 mM $MnCl_2$ in H_2O	2	In house			5.53237E-05	0.000110647	
RNase Inhibitor, Murine	1.25	NEB	M0314L	40,000 U/mL, 15,000 Units, $233.60	0.622933333	0.778666667	https://www.neb.com/products/m0314-rnase-inhibitor-murine#Product%20Information
40% Tween 20	0.5	In house			0.0000446	0.0000223	
40 mM Tris	25	In house			2.3024E-06	0.00005756	
Nuclease-free H_2O	5	Ambion (Thermo)	AM9938	100 mL, $36.03	0.0003603	0.0018015	https://www.thermofisher.com/order/catalog/product/AM9938#/AM9938
Total Price of Chemical Reagents:						**5.92**	
(b) Consumables							

96-well PCR plate	1 of 96 tubes	Thermo (Fisher)	AB0700	25 plates, $27.70	NA	0.011541667	https://www.thermofisher.com/order/catalog/product/AB0700#/AB0700
Optically clear strips	1 of 96 lids	Bio-Rad	TCS0803	128, 8-cap strips, $27.52	NA	0.026875	https://www.bio-rad.com/en-us/sku/tcs0803-0-2-ml-flat-pcr-tube-8-cap-strips-optical-ultraclear?ID=tcs0803
10 µL pipette tips	1 tip	Eppendorf	30078519	960 tips, $131.17	NA	0.136635417	
100 µL pipette tips	1 tip	Eppendorf	30078551	960 tips, $123.88	NA	0.129041667	
50 mL Falcon Tubes	1 tube	Corning	1495949A	500 tubes, $87.98	NA	0.17596	https://www.fishersci.com/shop/products/falcon-50ml-conical-centrifuge-tubes-25-rack/1495949a
RNase Away	Variable	Thermo	2123621	$21.21 each bottle	NA		https://www.fishersci.com/shop/products/molecular-bioproducts-rnase-away-surface-decontaminant-surface-decontaminant-8-5-oz-bottle-0-25l/2123621
Total Price of Consumables:						**0.48**	

(c) Other calculations

Calcein powder (for 50 mM Calcein stock)	Sigma	C0875	5 g, $107.64	0.000670167		https://www.sigmaaldrich.com/catalog/product/sigma/c0875?lang=en&region=US
DMSO (for 100 µL working FDR stock)	Thermo Fisher	TS-20684	50 mL, $72.31	0.0014462		https://www.fishersci.com/shop/products/thermo-scientific-silylation-grade-solvents-dimethylsulfoxide-dmso-50ml/pi20684
$MnCl_2$ (for 100 µL working FDR stock)	Sigma	M1787	10 mL, 1M, $34.16	0.003416		https://www.sigmaaldrich.com/catalog/product/sigma/m1787?lang=en&region=US
Calcein stock (50 mM = 31.13 mg/mL DMSO)	In house			0.005532367		
Fluorescence Detection Reagent cost	In house		0.01 for 100 µL FDR	5.53237E-05		
Tween 20 (40% stock)	Fisher	BP337	$11.15/100 mL at 100% stock	0.0000446		https://www.fishersci.com/shop/products/tween-20-fisher-bioreagents-2/BP337100
Tris-HCl 1M, pH 7.5	Invitrogen (Thermo)	15567027	$57.56/L at 1 M	0.0000575 6		https://www.thermofisher.com/order/catalog/product/15567027?us&en#/15567027?us&en

Price per reaction: 20 µL saliva into 50 µL rxn, 2x Bst, 2x RTx, 1x RI			**6.40**	

(d) Equipment: Validated Platform

Digital Hot Plate	Torrey Pines Scientific	HP30A	1,260.00	https://www.torreypinesscientific.com/product/digital-standard-hot-plate/
Cardboard Display Board (For Box Construction)	Walmart	730318	3.18	https://www.walmart.com/ip/Elmer-s-Tri-Fold-Self-Standing-Project-Display-Board-36-X-48-Black-1-count/16817689
DC Power Supply	Keysight (previously Agilent)	U8001A	466.00	https://www.keysight.com/us/en/products/dc-power-supplies/bench-power-supplies/u8000-series-bench-power-supply-90-150w.html
480 nm LED lights	Shopmadeinchina (previously DealExtreme)	180563	10.53	http://www.shopmadeinchina.com/product/96W-480nm-672lm-96-LED-Blue-Light-Car-Chassis_14238925.shtml
520 nm green light filter	Edmund Optics	65-699	135.00	https://www.edmundoptics.com/p/520nm-cwl-10nm-fwhm-25mm-mounted-diameter/20217/
96-Well Aluminum Block Sample Holder	LightLabs	A-7079	69.90	https://www.lightlabsusa.com/96-Well-Aluminum-Block.html
Total Price of Validated Platform:		**1944.61**		

(e) Equipment: Low-Cost Alternative Platform

Hot Plate (electric single burner with temperature knob)	Amazon	GAU-80305	11.99	https://www.amazon.com/GAU-80305-Electric-Single-Burner-1100-Watts/dp/B005T0SN0K
Cardboard Display Board (for box construction)	Walmart	730318	3.18	https://www.walmart.com/ip/Elmer-s-Tri-Fold-Self-Standing-Project-Display-Board-36-X-48-Black-1-count/16817689

DC Power Supply (9V battery)	BatteryJunction	1222	0.72	https://www.batteryjunction.com/energizer-1222.html
480 nm LED lights	Shopmadeinchina (previously DealExtreme)	180563	10.53	http://www.shopmadeinchina.com/product/96W-480nm-672lm-96-LED-Blue-Light-Car-Chassis_14238925.shtml
520 nm green light filter	AliExpress	SLB520	3.51	https://www.aliexpress.com/item/32900291133.html?aff_platform=portals-tool&sk=_dZqrWKC&aff_trace_key=3b742b01a6d64307a781b867799dbabb-1607110278738-03064-_dZqrWKC&dp=_dZqrWKC-32900291133&terminal_id=d0068eb438984ed581059c768e27a5da&tmLog=new_Detail
96-Well Aluminum Block Sample Holder	LightLabs	A-7079	69.90	https://www.lightlabsusa.com/96-Well-Aluminum-Block.html
Total Price of Low-Cost Alternative Platform		**99.83**		

(f) Scale-up Protocol for Reaction Mix (96 reactions)*

	Volume/1 reaction (µL)	Volume/96 reactions (µL)
Master mix components		
NEB 10X isothermal amplification buffer	5	530
NEB $MgSO_4$ (100 µM)	1.85	196.1
NEB dNTP mix (10 mM)	7	742
FIP/BIP primers (300 µM) for 2 targets	0.26 x 4	27.6 x 4
F3/B3 primers (30 µM) for 2 targets	0.34 x 4	36.0 x 4
FL/BL primers (30 µM) for 2 targets	1.32 x 4	139.9 x 4

NEB Bst 2.0 WarmStart DNA polymerase (120 U/µL)	0.27	28.6
NEB RTx WarmStart reverse transcriptase (15 U/µL)	2	212
Fluorescence Detection Reagent (0.5 mM calcein, 10 mM $MnCl_2$ in H_2O)	2	212
40% Tween 20	0.5	53.0
<u>Sample mix components</u>		
Saliva specimen	20	20 x 96
Tris-HCl pH 7.5 (400 mM)	2.5	265
NEB RNase Inhibitor, Murine (40 U/µL)	1.25	132.5
Nuclease-free water	1.25	132.5

*10% additional reagents

Table 3.3. Evaluation of LAMP primer sequences for nucleotide mutations present in SARS-CoV-2 variants.

Variant*	Alpha B.1.1.7 (UK)		Beta B.1.351 (S. Africa)		Gamma P.1 (Brazil, B.1.1.28)		Delta B.1.617.2 (India)		Epsilon B.1.429 (CAL.20C)		Iota B.1.526 (NY)		**LAMP Primers
Gene	Nucleotide(*149*)	Amino acid(*150*)	Nucleotide(*151*)	Amino acid(*150*)	Nucleotide(*152*)	Amino acid(*150*)	Nucleotide	Amino acid(*150*)	Nucleotide(*153*)	Amino acid(*153*)	Nucleotide(*154*)	Amino acid(*154*)	
5' UTR											C241T		Not present
ORF1ab	C3267T C5388A T6954C 11288-11296 (deletion)	T1001I A1708D I2230T SGF 3675-3677 (deletion)	G5230T	K1655N	C3828T A5648C	S1188L K1795Q 11288-11296 (deletion)			C241T C1059T T2597C G3037T A12878G C14408T G17014T	T265I I4205V P314L D1183Y	C1059T C3037T T9867C 11288-11297 (deletion) C14408T A16500C A20262G	T851I L438P S106del G107del F108del P323L Q88H	Not present
Spike	21765-21770 (deletion) 21991-21993 (deletion) A23063T C23271A C23604A C23709T T24506G G24914C	HV 69-70 (deletion) Y144 (deletion) N501Y A570D P681H T716I S982A D1118H	A21801C A22206G G22813T C23664T A23063T G23012A	D80A D215G K417N A701V N501Y E484K	C21614T C21621A C21638T G21974T G22132T A22812C G23012A A23063T C23525T C24642T	L18F T20N P26S D138Y R190S K417T E484K N501Y H655Y T1027I	C21618G T22917G C22995A C23604G G24410A	T19R L452R T478K P681R D950N	G21600T G22018T T22917G A23403G T24349C	S13I W152C L452R D614G	C21575T C21846T A22320G G23012A A23403G C23664T	L5F T95I D253G E484K D614G A701V	Not present
ORF3a						G174C	C25469T	S26L	G25563T	O57H	C25517T G25563T	P42L Q57H	Not present
E			C26456T	P71L									Not present
M							T26767C	I82T	C26681T				Not present
ORF7a							T27638C C27752T	V82A T120I					Not present
ORF8	C27972T G28048T A28111G	Q27stop R52I Y73C			G28167A	E92K			G27890T (intergenic)		C27925T	T11I	Not present
N	28280 GAT -> CTA C28977T	D3L S235F	C28887T	T205I	C28512G	P80R	A28461G G28881T G29402T	D63G R203M D377Y	A28272T (intergenic) C28887T	T205I	28274del C28869T G28975A	P199L M234I	Not present
Stem Loop											G29764T		Not present

*Variant WHO designation: Alpha, B.1.1.7 (UK); Beta, B.1.351 (S. Africa); Gamma, P.1 (Brazil); Delta, B.1.617.2 (India); Epsilon, B.1.429 (CAL20C); and Iota, B.1.526 (NY).(*155*)

**Primer set 3 (N; nt 29083 to 29311), set 9 (ORF1ab; nt 2244 to 2453), set 15 (ORF1ab; nt 2245-2441), and set 16 (N; nt 28525 to 28741).

Chapter 4

Correcting a Fundamental Flaw in the Paradigm for Antimicrobial Susceptibility Testing†

†This chapter contains excerpts, reproduced with permission, from Ersoy SC, Heithoff DM, Barnes L, Tripp GK, House JK, Marth JD, Smith JW, and Mahan MJ. (2017). Correcting a fundamental flaw in the paradigm for antimicrobial susceptibility testing. *EBioMedicine*. 20(2017) 173-181.

ABSTRACT

The emergence and prevalence of antibiotic-resistant bacteria are an increasing cause of death worldwide, resulting in a global ‘call to action’ to avoid receding into an era lacking effective antibiotics. Despite the urgency, the healthcare industry still relies on a single in vitro bioassay to determine antibiotic efficacy. This assay fails to incorporate environmental factors normally present during host-pathogen interactions in vivo that significantly impact antibiotic efficacy. Here we report that standard antimicrobial susceptibility testing (AST) failed to detect antibiotics that are in fact effective in vivo; and frequently identified antibiotics that were instead ineffective as further confirmed in mouse models of infection and sepsis. Notably, AST performed in media mimicking host environments succeeded in identifying specific antibiotics that were effective in bacterial clearance and host survival, even though these same antibiotics failed in results using standard test media. Similarly, our revised media further identified antibiotics that were ineffective in vivo despite passing the AST standard for clinical use. Supplementation of AST medium with sodium bicarbonate, an abundant in vivo molecule that stimulates global changes in bacterial structure and gene expression, was found to be an important factor improving the predictive value of AST in the assignment of appropriate therapy. These findings have the potential to improve the means by which antibiotics are developed, tested, and prescribed.

4.1. INTRODUCTION

Multidrug-resistant bacteria are a leading cause of death worldwide and undermine advances in medical and surgical management of multiple diseases (*156, 157*). Despite this urgent threat (*158, 159*), the healthcare industry continues to rely on a single bioassay standardized in 1961 by the World Health Organization to determine antibiotic efficacy (*160*). Although this bioassay has been immensely valuable for several decades, it is fundamentally flawed because it is based largely on in vitro efficacy, and often fails to correlate with patient outcome (*54*). Reliance on this bioassay may have inadvertently contributed to the rise in multidrug-resistant bacteria because it disqualifies efficacious compounds (*161*).

A key parameter that guides decisions regarding antimicrobial therapy is the clinical breakpoint: the antimicrobial concentrations that are used to define isolates as susceptible (“S”), intermediate (“I”), or resistant (“R”) (*162, 163*). Clinical breakpoints are established by a sequential procedure. (1) In vitro efficacy is assessed by standard antimicrobial susceptibility testing (AST), which determines the minimum inhibitory concentration (“MIC”) of antibiotics to which a pathogen is sensitive. (2) Pharmacokinetic/pharmacodynamic (PK/PD) parameters are measured in animals (dosing, distribution, localization). (3) Efficacy/toxicity is established in animals for a limited number of model pathogens. (4) Dosing protocols are validated with limited patient clinical data. Unfortunately, this testing pipeline is fundamentally unsound because the first step, AST, is performed on Mueller-Hinton Broth (MHB), a rich laboratory medium that fails to recapitulate most aspects of host environments. So, the

fact that clinical breakpoints are based on a foundational assay performed in vitro raises questions as to how relevant they are to patient outcome.

Supporting this notion, several reports suggest that the clinical predictive value of AST in the assignment of appropriate therapy is limited. (1) Clinical observations have given rise to the “90–60” rule: “susceptible” infections respond well to appropriate therapy in 90% of cases, whereas “resistant” infections respond well to these antibiotics in 60% of cases (*49, 50*). (2) Pneumococcal patients treated with antibiotics that failed standard tests (discordant therapy) had similar treatment outcomes as those that passed standard tests (concordant therapy) (*164*). (3) AST-recommended antibiotics failed to clear *Salmonella enterica* Typhimurium and *Enterobacter cloacae* in murine models of sepsis (*54, 165*). (4) An AST disqualified antibiotic cleared multidrug-resistant Gram-negative pathogens in murine pulmonary models of infection (*166*). Here we propose that the antimicrobial testing assay should be revamped to account for pathogen conditions in the host, and show several circumstances in which susceptibility testing in host-mimicking media is more accurate than standard AST in predicting antibiotic efficacy in vivo. We have termed this behavior in vivo altered susceptibility (IVAS), providing insight into why some patients fail to respond to certain antibiotics despite passing standard tests for clinical use.

4.2. RESULTS

4.2.1. Antibiotic MICs Are Markedly Different When Derived From Host-mimicking Media vs. Standard MHB Medium

A collection of human and veterinary clinical isolates was subjected to antimicrobial susceptibility testing in host-mimicking media vs. standard MHB medium. Four host-mimicking media were examined including (i) Dulbecco's Modified Eagle Medium (DMEM), a tissue culture medium supporting mammalian cell growth (*167*); (ii) Lacks medium, supporting pneumococcal growth (*168, 169*); (iii) modified Lacks medium (MLM), simulating the nasopharynx for invasive pneumococcal carriage (*170*); and (iv) low-phosphate, low-magnesium medium (LPM pH 5.5), simulating the macrophage phagosome in which many intracellular pathogens reside/replicate (*53, 171*). Emphasis was placed on the identification of pathogen-antibiotic combinations that exhibited altered MICs from host-mimicking media relative to standard MHB medium; and whose MICs crossed clinical breakpoint designations that are used to define isolates as susceptible (“S”), intermediate (“I”), or resistant (“R”), and can impact clinical decision making on appropriate antibiotic therapy.

Thus, we sought to identify antibiotics for which a given pathogen is classified as “S” in MHB medium but “R” in host-mimicking media (S to R); and antibiotics for which a given pathogen is classified as “R” in MHB medium but “S” in host-mimicking media (R to S).

Staphylococcus (MRSA; MSSA; CoNS). A panel of antibiotics used in human and veterinary medicine was tested for efficacy against clinical isolates of methicillin-resistant and -sensitive *S. aureus* (MRSA/MSSA), and coagulase negative

Staphylococcus (CoNS) (**Figure 4.1**). Growth of *Staphylococcus* in tissue culture medium and modified Lacks medium conferred increased susceptibility to azithromycin, erythromycin, and streptomycin relative to MHB medium (4 to 256-fold; **Figure 4.1a**). Conversely, *Staphylococcus* exhibited increased resistance to daptomycin and rifampin in modified Lacks medium, and to tetracycline in tissue culture medium, relative to MHB medium (4 to 16-fold). **Table 4.1** lists pathogen-antibiotic combinations that exhibited at least an 8-fold change in MIC when derived in host-mimicking media vs. standard MHB medium and whose altered MICs crossed clinical breakpoint designations that advise on patient therapy. For example, 1 antibiotics for which MRSA was classified as “R” in MHB medium, but classified as “S” in tissue culture medium (cephalothin); and antibiotics for which MSSA was classified as “I” in MHB medium, but classified as “S” in tissue culture medium (erythromycin) (**Table 4.2a**). Notably, although many pathogen-antibiotic combinations have significant changes in MIC in host-mimicking media, many do not cross breakpoint designations (R to S; S to R) and would not alter physician making on appropriate therapy. For example, 3/3 MRSA isolates exhibited a 4- to 32-fold increased susceptibility to oxacillin in tissue culture medium, but the “altered MICs” of two MRSA isolates did not cross clinical breakpoints. Thus, they remain “Resistant” to oxacillin as defined by AST standards for clinical use.

S. pneumoniae. Altered MICs were also examined for *S. pneumoniae* clinical isolates tested in host-mimicking media vs. standard MHB medium. Most *S. pneumoniae* strains tested showed increased susceptibility to azithromycin in tissue culture medium and modified Lacks medium relative to MHB medium; and increased resistance to daptomycin and trimethoprim in modified Lacks medium (4 to 32-fold;

Figure 4.1b). Many *S. pneumoniae* MICs derived in host-mimicking media crossed clinical breakpoint designations (listed in **Table 4.1**); e.g., antibiotics for which *S. pneumoniae* was classified as “S” in MHB medium, but classified as “R” in modified Lacks medium (trimethoprim); and those for which *S. pneumoniae* classified was “R” in MHB medium, but classified as “S” in modified Lacks medium (azithromycin) (**Table 4.2b**).

Gram-negative Bacteria. Antibiotic efficacy was also examined for Gram-negative bacterial isolates tested in host-mimicking media vs. standard MHB medium. A subset of these antibiotics (10 of 20), which were not subject to acute pH and/or media composition effects under LPM pH 5.5 conditions (*54*), were also interrogated. Several Gram-negative bacteria were associated with increased resistance to colistin or polymyxin B in tissue culture medium and LPM pH 5.5 conditions relative to MHB medium (4 to 512-fold) (**Figure 4.1c**). Growth of *Yersinia* spp. (4 of 4 isolates) was associated with increased susceptibility to trimethoprim and co-trimoxazole in tissue culture medium relative to MHB medium (8 to 64-fold). Many Gram-negative bacteria MICs derived in host-mimicking media crossed clinical breakpoint designations (listed in **Table 4.1**); e.g., *Salmonella* Typhimurium (*ST*) susceptibility to colistin was classified as “S” in MHB medium but “R” in tissue culture medium (**Table 4.2c–f**).

Comparison Summary of MICs Derived From Host-mimicking Media vs. Standard MHB Medium. We evaluated the percentage of pathogen-antibiotic combinations that resulted in altered MICs when derived from host-mimicking media vs. standard MHB medium (**Figure 4.2a**). Although the MICs obtained from host-mimicking

media were comparable to those from MHB medium for approximately two-thirds of cases tested (852/1311), one third of these cases exhibited at least a 4-fold change in MIC, which may signal altered antibiotic susceptibility in vivo. Further, 8.2% (107/1311) of altered MICs derived from the host-mimicking media tested resulted in a change in clinical breakpoint designation, which may impact physician decision making (**Figure 4.2b**). Taken together, these data suggest that inclusion of environmental factors normally present during host-pathogen interactions may improve the predictive value of standard AST in identifying effective antibiotics to treat microbial infections.

4.2.2. Drug Testing in Host-mimicking Media Improves the Assignment of Appropriate Antibiotic Therapy

Several pathogen-antibiotic combinations that exhibited altered MICs in host-mimicking media were tested for efficacy in murine models of sepsis. We focused on antibiotics whose MICs exhibited at least an 8-fold altered susceptibility in host-mimicking media relative to standard MHB medium, and whose MICs crossed clinical breakpoint designations. This analysis was limited to human and veterinary clinical isolates that also infect mice.

MRSA, MSSA. All mice (10/10) survived infection with MRSA (USA300) following treatment with cephalothin or ceftriaxone (**Figure 4.3a**; $P < 0.001$), identified as efficacious in tissue culture medium even though these agents failed standard testing in MHB medium (R to S; R to I; **Table 4.2a**). Similarly, nearly all mice (8/10) survived MSSA (MT3307) infection following treatment with erythromycin ($P < 0.001$), identified as bioactive in tissue culture medium but relatively ineffective by standard testing (I to

S). Treatment with co-trimoxazole, often used clinically (*172*), failed to improve survivorship (1/10; P = 1.0), as predicted by testing in tissue culture medium but not MHB medium (S to R).

Further analysis was done using a MRSA isolate (MT3302) linked to a fatal case of human sepsis. AST in host-mimicking media was evaluated in an effort to retroactively identify alternative therapeutic options. Treatment with cephalosporins (ceftriaxone or ceftiofur) resulted in high efficacy in murine models of MRSA sepsis (8/10; 7/10; P < 0.001; P < 0.01). Both of these antibiotics were identified as efficacious in tissue culture medium even though they were rejected by standard testing (R to I). Further, all mice (10/10) survived treatment with daptomycin and ciprofloxacin (Fig. 3a; P < 0.001), as predicted by testing of daptomycin in standard MHB medium and tissue culture medium; and of ciprofloxacin in all media examined (**Table 4.2a**). Notably, testing of daptomycin in modified Lacks medium predicted resistance (S to R), indicating that this drug may be effective against certain types of infections but not others (e.g., systemic vs. localized).

S. pneumoniae. Despite passing standard testing in MHB medium, trimethoprim failed to protect mice (0/10) from *SPN* infection (strain Daw 25) (**Figure 4.3b**; P = 1.0), as predicted by testing in modified Lacks medium (S to R; **Table 4.2b**). Further, all mice (10/10) survived following treatment with ceftriaxone (P < 0.001), for which susceptibility was indicated in all media tested.

Gram-negative Bacteria. Colistin, a drug of last resort (*173*), failed to protect mice (1/10) from infection with *S.* Typhimurium (*ST* 14028) (**Figure 4.3c**; P = 1.0), as predicted by testing in tissue culture medium (S to R; **Table 4.2c**). Conversely, all mice

(10/10) survived treatment with ciprofloxacin ($P < 0.001$), for which susceptibility was indicated in all media tested. Additionally, most mice (8/10) survived infection with *K. pneumoniae* following treatment with tetracycline ($P < 0.001$). Such efficacy was predicted by standard testing in MHB and LPM pH 5.5 media (S to S), which mimics the macrophage phagosome wherein *K. pneumoniae* resides and replicates during infection (*174*) (**Table 4.2f**). Such efficacy was comparable to treatment with ciprofloxacin (8/10; $P < 0.001$) that has established activity against intracellular pathogens (*175*). Notably, testing of tetracycline in tissue culture medium predicted resistance (S to R), suggesting that testing in media that reflect the intracellular lifestyle of *K. pneumoniae* is a more accurate predictor of treatment outcome for this pathogen.

Bacterial Clearance. Bacterial clearance from circulation in the blood was investigated following treatment with antibiotics predicted as highly efficacious by testing in standard MHB medium (co-trimoxazole) or tissue culture medium (azithromycin), respectively (**Table 4.2a**). Treatment with the AST-recommended antibiotic, co-trimoxazole, was ineffective in MSSA (MT3307) clearance as predicted by testing in host-mimicking media (S to R) (**Figure 4.3d**). This treated cohort exhibited a progressive bacteremia (up to 2.5×10^5 colony forming units (CFU)/ml blood by day 6), with all mice (10/10) succumbing to infection by day 10 (open boxes). Such efficacy was comparable to that of untreated animals (open circles). Conversely, as predicted by testing in tissue culture medium, azithromycin was able to clear MSSA from circulation, with all mice (10/10) surviving the infection and harboring $\leq 2 \times 10^3$ CFU/ml in the blood at day 10 (closed boxes; $P < 0.001$). These data suggest that drug testing in host-

mimicking media improves the predictive value of standard AST in the assignment of appropriate therapy.

4.2.3. Addition of $NaHCO_3$ to Standard MHB Medium Improves the Accuracy of Antibiotic Efficacy In Vivo

We suspected that sodium bicarbonate ($NaHCO_3$) may be a key in vivo molecule contributing to antibiotic susceptibility for a number of pathogens for the following reasons. $NaHCO_3$ serves as an abundant ionic factor present in mammalian tissues that stimulates global changes in bacterial structure, gene expression, and membrane permeability that correspond to increased susceptibility to human cationic antimicrobial peptides (*55*). $NaHCO_3$ is present in nearly all host-mimicking media examined that resulted in altered antibiotic susceptibility relative to MHB medium. Thus, we evaluated whether supplementation of standard MHB medium with physiological levels of $NaHCO_3$ improved the predictive value of the AST standard for clinical use. This analysis was initially focused on *Staphylococcus*-antibiotic combinations that exhibited at least an 8-fold change in MIC in tissue culture medium vs. MHB medium, representing 13.5% (31/230) of combinations examined (**Figure 4.1a, top panel**).

We investigated the fold-change between MICs derived in MHB medium in the presence/absence of $NaHCO_3$ (test/standard condition; left of slash); and in tissue culture medium in the absence/presence of $NaHCO_3$ (test/standard condition; right of slash) (**Figure 4.4a**; **Table 4.3a**). Increased susceptibility is depicted in blue; increased resistance is depicted in red. Four phenotypic classes were identified.

Class 1 (21/31). Addition of $NaHCO_3$ to MHB medium resulted in MICs

similar to tissue culture medium; its removal from tissue culture medium resulted in MICs similar to MHB medium (azithromycin, erythromycin, tetracycline).

Class 2 (5/31). Addition of $NaHCO_3$ to MHB medium resulted in MICs similar to tissue culture medium; its removal from tissue culture medium had no effect on the MIC (ceftriaxone, ceftiofur).

Class 3 (2/31). Addition of $NaHCO_3$ addition to MHB medium had no MIC effect; its removal from tissue culture medium resulted in MICs similar to MHB medium (oxacillin).

Class 4 (3/31). Addition/removal of $NaHCO_3$ had no effect on MICs in MHB medium or tissue culture medium (trimethoprim). These data indicate that addition of $NaHCO_3$ to MHB medium restored the altered susceptibility observed in tissue culture medium in 83.9% (26 of 31) of cases tested.

Next, we examined whether physiological levels of $NaHCO_3$ in MHB medium were required to stimulate the altered susceptibility observed in tissue culture medium. A dose response analysis of MRSA (USA300; MT3302) and MSSA (MT3307) strains revealed that physiological levels of $NaHCO_3$ (~25 mM) (*176*) were necessary to induce altered antibiotic susceptibility in MHB medium (**Figure 4.4b**). These data suggest that $NaHCO_3$ may be a key in vivo component contributing to antibiotic susceptibility for a number of pathogens. Supporting this suggestion, supplementation of MHB medium with physiological levels of $NaHCO_3$ also resulted in altered drug susceptibilities in *S. pneumoniae* and *Salmonella* spp. isolates (**Figure 4.4c**; **Table 4.3b, c**). Further, many

altered MICs crossed clinical breakpoint designations (listed in **Table 4.1**), and such predicted changes in antibiotic efficacy were confirmed in mouse models of infection and sepsis (**Figure 4.2a**); e.g., MRSA (cephalothin [R to S]; ceftriaxone [R to I]); and MSSA (erythromycin [I to S]); (**Table 4.3a**). These findings suggest that supplementation of standard MHB medium with physiological levels of $NaHCO_3$ improved the predictive value of AST in the assignment of appropriate antibiotics for therapeutic intervention.

4.3. DISCUSSION

Multidrug-resistant bacteria are a significant cause of sepsis, the most common cause of death in hospitalized patients, with an annual incidence of 1 million cases and 200,000 deaths in the U.S. alone (*177*). This dire perspective reflects the failed efforts to fully contain bacteria with the misuse of antibiotics, and the legal, financial, and scientific hurdles to discovering new ones. We demonstrate that one viable approach to address this alarming threat is to incorporate host-mimicking media in standard AST methods for clinical use. Validation of the improved predictive value of AST in the assignment of appropriate antibiotic therapy was provided in several Gram-positive and -negative animal models of infection and sepsis. Our findings suggest that standard AST may be hindering optimal patient treatment, and slowing the process of discovery of new, effective, and safe antibiotics because it disqualifies efficacious compounds. Susceptibility testing that accounts for the biology of a pathogen in the context of its host may enable the re-purposing of omitted antibiotics while aiding the discovery of new ones by screening compounds under conditions that more accurately reflect the host milieu.

Altered drug susceptibility in vivo provides insight as to why some patients fail to respond to certain antibiotics despite passing standard susceptibility tests. Our findings with a MRSA isolate from a deceased patient provide a clear example as antibiotics omitted by standard AST were highly efficacious in bacterial clearance. If these alternative therapeutic options had been made available to clinicians managing this case, it may have changed the patient outcome. Additionally, we show that supplementation of standard MHB medium with physiological levels of sodium

bicarbonate improved the predictive value of AST in the assignment of appropriate therapy. The molecular basis likely involves the role of $NaHCO_3$ as an abundant ionic factor that stimulates global changes in bacterial structure and gene expression, leading to alterations in bacterial cell wall thickness and membrane permeability that correspond with increased susceptibility to human cationic antimicrobial peptides (*55*). Two potential alternative mechanisms include the role of bicarbonate in the maintenance of blood pH (*178, 179*); and/or the inhibition of growth and viability of periodontal pathogens (*180*). However, these mechanisms are unlikely to play a role in the improved predictive value of AST due to the inclusion of Tris buffer in the test media to preclude bicarbonate-mediated pH fluctuations that can affect antibiotic potency and bacterial cell viability.

Standard AST in clinical use has likely contributed to the alarming rise of multidrug-resistant bacteria in hospitals because high doses of ineffective antibiotics are given to infected patients without the knowledge that the host environment may render bacteria inherently resistant to the antibiotics prescribed to kill them. Based on the findings of this study, rather than extending the dose/duration of an antibiotic that is not effective, physicians might consider that the more appropriate approach is to prescribe a totally different antibiotic. Standard AST in combination with host-mimicking media may serve as a valuable tool in advising clinicians on appropriate antibiotic therapy. Antibiotics identified by both approaches were efficacious in every animal model examined; thus, such cases should bestow high confidence in clinical decision making on appropriate therapy. Conversely, physicians should exercise caution in cases where marked MIC disparities occur between testing in host-mimicking media vs. standard MHB medium. Further, predicted drug failure in a particular host-

mimicking media may indicate that certain drugs may be effective against certain types of infections but not others (e.g., systemic vs. localized). Supporting this suggestion, MRSA inactivates daptomycin by releasing membrane phospholipids under certain experimental conditions (*181*); and herein we show that a MRSA isolate was susceptible to daptomycin in tissue culture medium and in a murine model of sepsis, but displayed resistance in other host-mimicking media examined (minimal Lacks medium).

Future considerations must be given to host-pathogen interactions that can also influence drug susceptibility. (1) Animals, including primates, often tolerate drugs differently than humans (pharmacokinetic parameters such as drug clearance, volume of distribution, and half-life can result in unanticipated changes in antimicrobial efficacy) (*182, 183*). (2) Bacterial community composition can compromise antibiotic efficacy (antibiotic deactivation or biofilm production provides passive resistance for all microbes within a polymicrobial environment) (*184, 185*). (3) Antimicrobial selection is based on drug concentrations achieved in plasma, but concentrations achieved in different tissues and sites of infection may be greater or less depending on the drug's properties (pH at the infection site or within an organelle can dictate lipid solubility of the drug or its distribution in cells and tissues) (*186*). (4) Antibiotic resistance may be inadvertently triggered by diet, underlying conditions in the patient, or by clinical interventions that may disrupt drug efficacy (ascorbic acid treatment of urinary tract infections to lower urine pH) (*187*). (5) Many patients that develop multidrug-resistant infections have comorbidities, immunosuppressive therapy and/or the presence of invasive medical devices that impact susceptibility to indicated pathogens (*188*).

Our findings suggest that the susceptibility testing in media that reflect the host milieu will not only improve the predictive value of AST in the assignment of appropriate antibiotic therapy, but also provides a new paradigm for drug discovery and therapeutic intervention for infectious diseases. However, such testing will always be open to further improvement, especially as we learn more about the subtle nuances of host-pathogen interactions in natural environments that influence the impact of antibiotics on bacterial clearance (e.g., virulence factors, ecological factors, and cell physiological parameters).

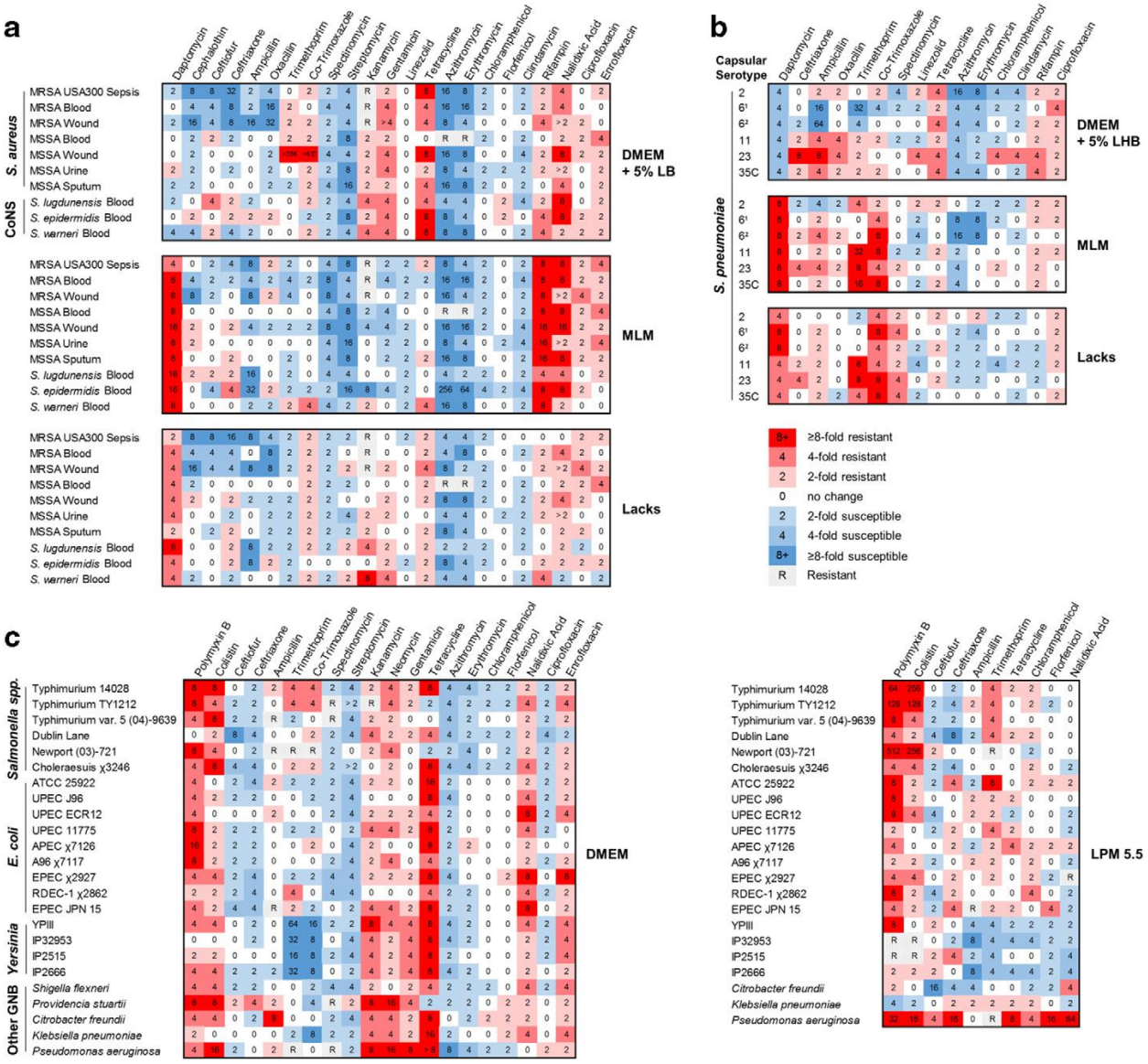

Figure 4.1. Comparison of pathogen-antibiotic combinations that exhibited altered MICs derived from host-mimicking media relative to standard MHB medium. A panel of antibiotics was screened for altered MICs against (**a**) *Staphylococcus* spp., (**b**) *S. pneumoniae*, and (**c**) Gram-negative bacteria when tested in Dulbecco's Modified Eagle Medium (DMEM), Lacks medium, modified Lacks medium (MLM), low-phosphate, low-magnesium medium (LPM pH 5.5) relative to standard MHB medium, according to CLSI guidelines (*47, 162*). Values depict the fold-change in MICs when derived in host-mimicking media relative to standard MHB medium (test/standard condition). Increased susceptibility depicted in blue; increased resistance depicted in red. MIC values were obtained from at least 6 independent determinations.

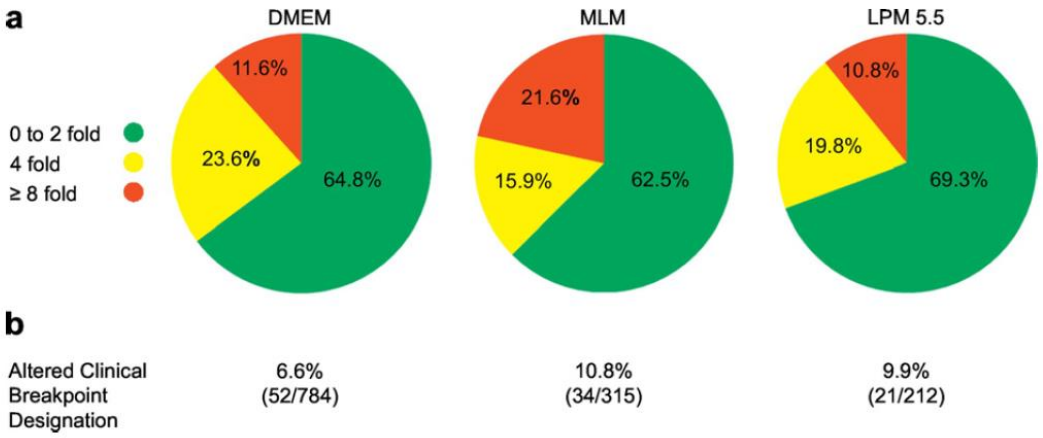

Figure 4.2. Comparison summary of MICs derived from host-mimicking media versus standard MHB medium. (**a**) Colored regions depict the fraction of pathogen-antibiotic combinations tested that exhibited a fold-change in MICs (increased susceptibility or resistance) when derived in host-mimicking media (DMEM, MLM, LPM pH 5.5) relative to standard MHB medium (test/standard condition); ≤ 2-fold (green), 4-fold (yellow), ≥ 8-fold (red). (**b**) Depicted are percentages of pathogen-antibiotic combinations that resulted in altered MICs that crossed clinical breakpoint designations, used to define isolates as susceptible (“S”), intermediate (“I”), or resistant (“R”), that can impact clinical decision making on appropriate antibiotic therapy (*162, 163*).

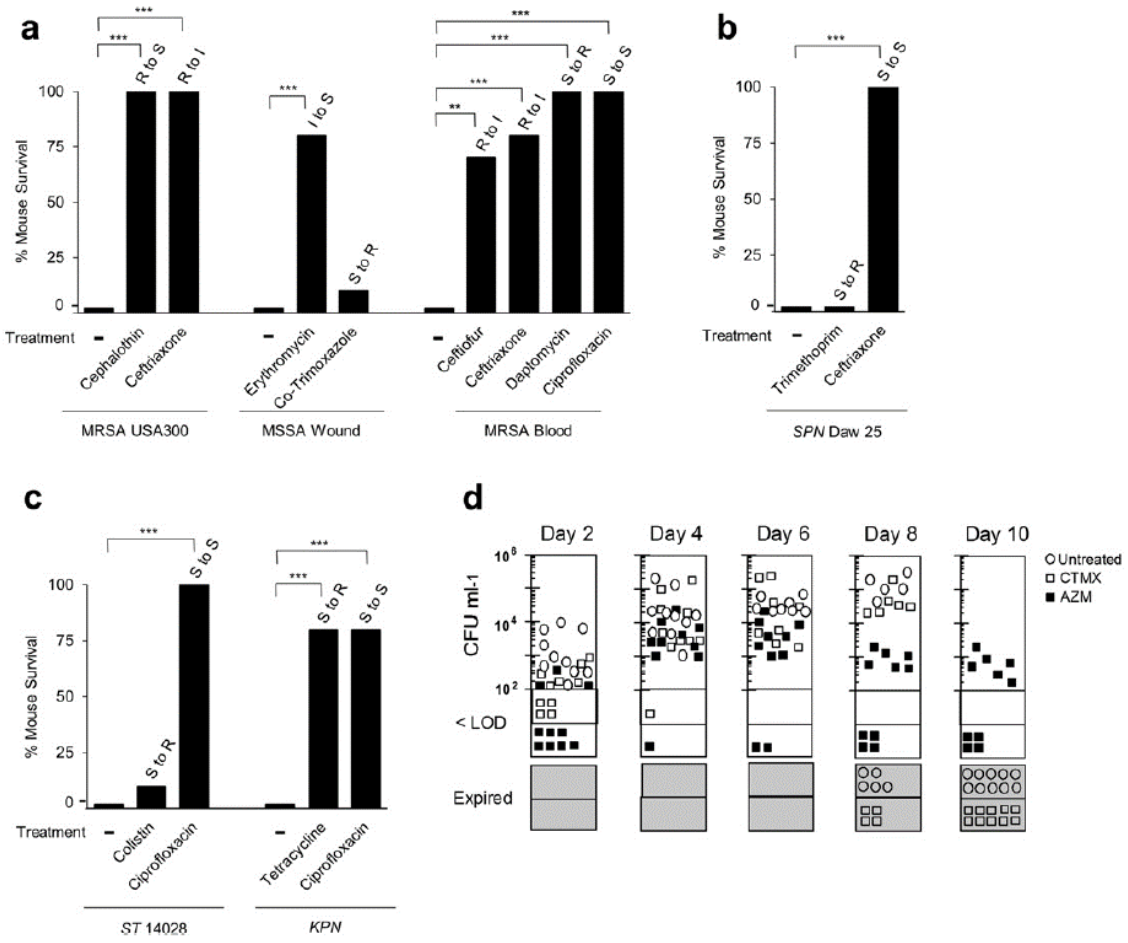

Fig. 4.3. Antibiotic susceptibility testing in host-mimicking media improves the predictive value of AST in the assignment of appropriate antibiotic therapy in murine models of sepsis. Pathogen-antibiotic combinations that exhibited altered MICs in host-mimicking media relative to standard MHB medium and whose MICs crossed clinical breakpoint designations were evaluated in murine sepsis models of (**a**) *S. aureus* (MRSA [USA300]; MSSA Wound [MT3307]; MRSA Blood [MT3302]); (**b**) *S. pneumoniae* (*SPN* Daw 25); and (**c**) *S.* Typhimurium (*ST* 14028) and *K. pneumoniae* (*KPN* ATCC13883). (**d**) MSSA (MT3307) clearance from blood circulation was examined following treatment with antibiotics predicted as highly effective via testing in standard MHB medium (co-trimoxazole, open boxes) or tissue culture medium (DMEM) (azithromycin, closed boxes), respectively. Untreated mice (open circles); expired mice (gray region); Colony Forming Units (CFU); Limit of Detection (LOD) = 100 CFU/ml (*96*). Ten mice were evaluated per cohort. ***P < 0.001, **P < 0.01, or *P < 0.05.

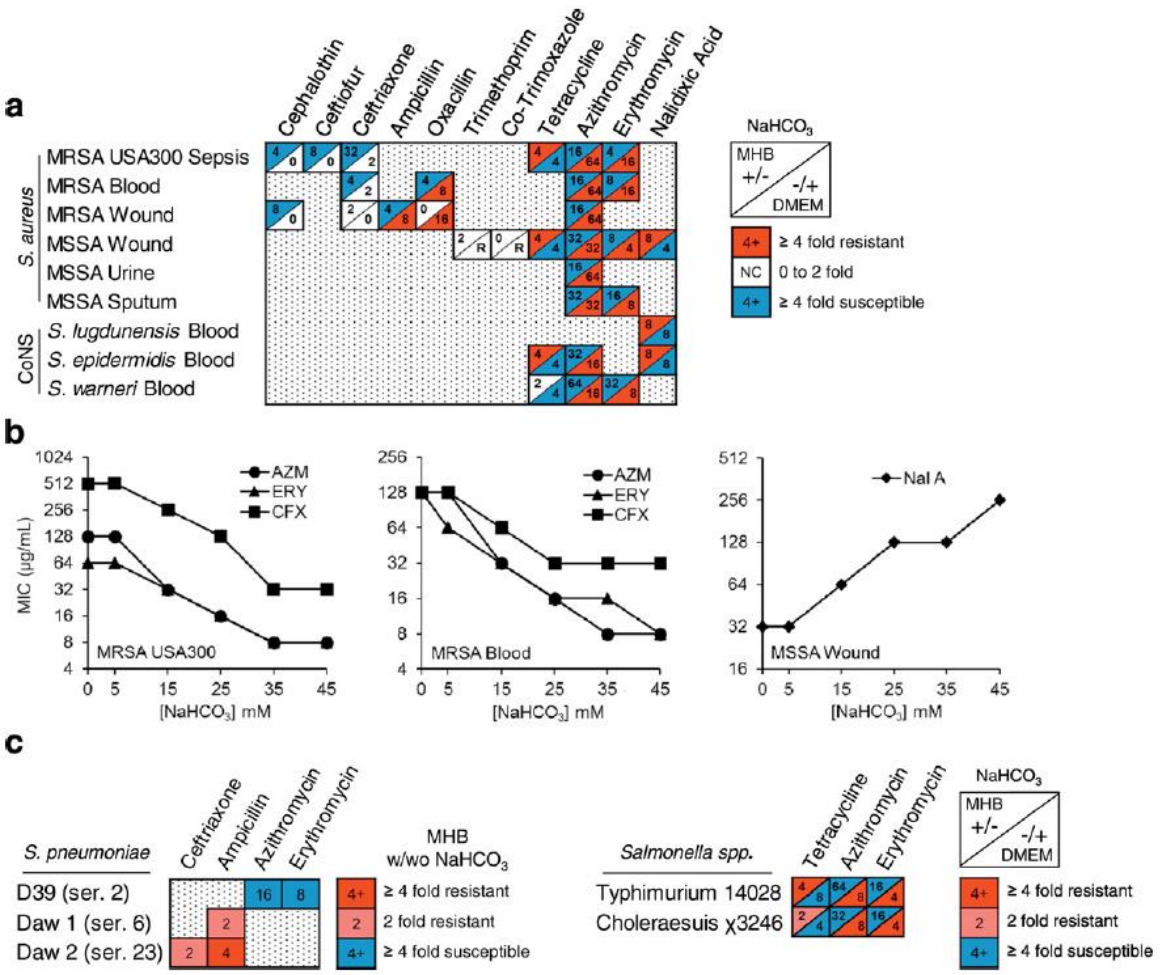

Fig. 4.4. Supplementation of standard MHB medium with physiological levels of $NaHCO_3$ improves the predictive value of AST in the assignment of appropriate antibiotics for therapeutic intervention. (**a**) *S. aureus* exhibiting at least an 8-fold change in MIC in tissue culture medium (DMEM) vs. MHB medium were subjected to susceptibility tests in the presence and absence of physiological levels of $NaHCO_3$. Values represent MIC fold-change when derived in MHB medium in the presence/absence of $NaHCO_3$ (test/standard condition; left of slash); and in DMEM medium in the absence/presence of $NaHCO_3$ (test/standard condition; right of slash). Increased susceptibility is depicted in blue; increased resistance is depicted in red. Stippled boxes represent those that exhibited < 8-fold altered susceptibility between MHB and DMEM media. To control for pH and buffer considerations, strains were grown in MHB pH 7.2; MHB adjusted to pH 7.2 w/100 mM Tris; and DMEM liquid pH 7.4 (containing 44 mM $NaHCO_3$); all other media conditions were adjusted to pH 7.4 with 100 mM Tris including: MHB w/$NaHCO_3$; and $NaHCO_3$-free powdered DMEM w/wo $NaHCO_3$ (Supplementary Table 2a). (**b**) Dose response analysis of MRSA (USA300; MT3302) and MSSA (MT3307) antibiotic susceptibility following exposure to increasing concentrations of $NaHCO_3$ in standard MHB medium. AZM (azithromycin); ERY

(erythromycin); CFX (ceftriaxone). (**c**) Susceptibility of *S. pneumoniae* and *Salmonella* spp. in the presence/absence of physiological levels of $NaHCO_3$ in MHB and/or DMEM media. For *S. pneumoniae*, values represent fold-change between MICs derived in MHB medium in the presence/absence of $NaHCO_3$ (test/standard condition). For *Salmonella* spp. values represent fold-change between MICs derived in MHB medium in the presence/absence of $NaHCO_3$ (test/standard condition; left of slash); and DMEM in the absence/presence of $NaHCO_3$ (test/standard condition; right of slash). No change (NC), Resistant (R). MICs were a consensus of at least 6 independent isolates.

Table 4.1. AST in host-mimicking media identifies MICs that cross clinical breakpoint designations which advise on patient therapy.

Drug	Target	Pathogen	Host-Mimicking Media	Clinical Breakpoint
Increased Susceptibility				
Cephalothin	Cell Wall	MRSA[1]	DMEM / MHB + $NaHCO_3$	R to S
Ceftriaxone	Cell Wall	MRSA[1-3]	DMEM / MHB + $NaHCO_3$	R to S, I
Oxacillin	Cell Wall	MRSA[3]	DMEM	R to S
Ampicillin	Cell Wall	CoNS[1]; *SPN*[1,2]	MLM / DMEM	R, I to S
Trimethoprim	Folate	*SPN*[2]	DMEM	R to S
Azithromycin	Protein	CoNS[1,3]; *SPN*[1,2]	MLM / MHB + $NaHCO_3$	R to S, I
Erythromycin	Protein	MSSA[1,2]; CoNS[1]	DMEM / MLM / MHB + $NaHCO_3$	R, I to I, S
Streptomycin	Protein	MRSA[1]; MSSA[1-4]	DMEM / MLM	R, I to S
Decreased Susceptibility				
Colistin	Membrane	*ST*; *PA*	DMEM	S to R
Daptomycin	Membrane	MRSA[2,3]; MSSA[1-4]; CoNS[1-3]	MLM	S to R
Ceftriaxone	Cell Wall	*SPN*[3]	DMEM	S to R
Ampicillin	Cell Wall	*SPN*[3]; CF	DMEM / MHB + $NaHCO_3$	S, I to R, I
Trimethoprim	Folate	MSSA[1]; *SPN*[4, 5]	DMEM / MLM	S to R
Co-Trimoxazole	Folate	MSSA[1]; *SPN*[4, 5]	DMEM / MLM	S to R, I
Gentamicin	Protein	*PA*	DMEM	S to R
Tetracycline	Protein	*KPN; CF*; *ST*; *SC*; *EC*[1-3]; *YP*[1-4]	DMEM / MHB + $NaHCO_3$	S to R, I
Enrofloxacin	DNA	*EC*[4]	DMEM	S to R

Depicted are clinical breakpoint designations derived from MICs obtained in standard MHB vs. host-mimicking media, which exhibited an $\geq$ 8-fold altered susceptibility. Clinical breakpoints define isolates as susceptible (S), intermediate (I), or resistant (R). R to S refers to an R classification when tested for susceptibility in MHB but an S classification in host-mimicking media. MRSA[1-3] (USA 300; Blood; Wound); CoNS[1-3] (*S*. *epidermidis*; *S. lugdunensis*; *S*. *warneri*); *SPN*[1-5] (serotype 6; 6; 23; 11; 35C); MSSA[1-4] (Wound; Sputum; Urine; Blood); *ST* (*S.* Typhimurium); *PA* (*P. aeruginosa*); *CF* (*C. freundii*); *KPN* (*K. pneumoniae*); *SC* (*S*. Choleraesuis); *EC*[1-4] (*E. coli* ATCC 25922; UPEC J96; UPEC ATCC 11775; EPEC χ2927); *YP*[1-4] (YPIII; IP32953; IP2515; IP2666). Clinical breakpoint concentrations for listed drugs (*189-195*).

Table 4.2a. Antimicrobial susceptibility testing in host-mimicking media (*Staphylococcus*).

"Susceptible" MIC
"Intermediate" MIC
"Resistant" MIC

Strain #	Strain Name	Daptomycin MIC (µg/mL)				Cephalothin MIC (µg/mL)				Ceftiofur MIC (µg/mL)				Ceftriaxone MIC (µg/mL)			
Clinical Breakpoints[a]:		S ≤ 1; NS ≥ 2				S ≤ 8; I = 16; R ≥ 32[190]				S ≤ 2; I = 4; R ≥ 8[191]				S ≤ 8; I =16-32; R ≥ 64[190]			
		Ca-MHB	DMEM + 5% LB	MLM	Lacks Medium	Ca-MHB	DMEM + 5% LB	MLM	Lacks Medium	Ca-MHB	DMEM + 5% LB	MLM	Lacks Medium	Ca-MHB	DMEM + 5% LB	MLM	Lacks Medium
MT3322	MRSA USA300	1	0.5	4	2	32	4	32	4	64	8	32	8	512	16	128	32
MT3302	MRSA Blood	0.5	0.5	4	2	8	2	2	2	16	4	8	4	128	16	64	32
MT3315	MRSA Wound	0.5	0.25	4	2	8	0.5	1	0.5	16	4	8	4	64	8	64	16
MT3305	MSSA Blood	0.5	0.5	4	2	0.5	0.25	0.5	0.25	1	2	1	1	4	2	4	4
MT3307	MSSA Wound	0.5	0.5	8	2	0.125	0.0625	0.25	0.25	1	1	1	1	2	2	4	4
MT3309	MSSA Urine	0.5	1	4	2	0.25	0.125	0.5	0.25	1	1	1	1	4	2	4	2
MT3314	MSSA Sputum	1	0.5	8	2	0.25	0.125	0.25	0.25	1	1	1	0.5	2	2	4	4
MT3317	CoN S. lugdunensis	0.25	0.125	4	2	0.5	0.5	1	0.5	0.5	2	1	0.5	2	4	4	4
MT3320	CoN S. epidermidis	0.5	0.5	8	2	0.125	0.25	0.125	0.125	0.5	0.5	0.125	0.5	1	2	4	2
MT3321	CoN S. warneri	0.5	0.125	4	2	0.125	0.03125	0.125	0.0625	0.25	0.5	0.25	0.25	2	0.5	2	1

Strain #	Strain Name	Ampicillin MIC (µg/mL)				Oxacillin MIC (µg/mL)				Trimethoprim MIC (µg/mL)				Co-Trimoxazole MIC (µg/mL)			
Clinical Breakpoints[a]:		S ≤ 0.25; R ≥ 0.5[190]				S ≤ 2; R ≥ 4				S ≤ 8; R ≥ 16				S ≤ 2/38; R ≥ 4/76			
		Ca-MHB	DMEM + 5% LB	MLM	Lacks Medium	Ca-MHB	DMEM + 5% LB	MLM	Lacks Medium	Ca-MHB	DMEM + 5% LB	MLM	Lacks Medium	Ca-MHB	DMEM + 5% LB	MLM	Lacks Medium
MT3322	MRSA USA300	512	256	64	64	64	16	128	16	2	2	1	1	0.0625/1.2	0.125/2.4	0.0625/1.2	0.125/2.4
MT3302	MRSA Blood	256	128	64	256	64	4	32	8	2	4	0.5	1	0.125/2.4	0.125/2.4	0.0625/1.2	0.25/4.8
MT3315	MRSA Wound	8	0.5	1	1	32	1	64	4	2	4	0.5	1	0.0625/1.2	0.125/2.4	0.0625/1.2	0.125/2.4
MT3305	MSSA Blood	2	2	2	2	0.25	0.25	0.25	0.25	1	2	1	1	0.0625/1.2	0.125/2.4	0.0625/1.2	0.125/2.4
MT3307	MSSA Wound	0.125	0.125	0.03125	0.0625	0.25	0.125	0.125	0.125	2	>512	1	1	0.125/2.4	>64/1216	0.0625/1.2	0.25/4.8
MT3309	MSSA Urine	0.125	0.125	0.125	0.125	0.25	0.125	0.25	0.125	1	1	1	0.5	0.0625/1.2	0.125/2.4	0.0625/1.2	0.125/2.4
MT3314	MSSA Sputum	0.125	0.125	0.125	0.125	0.25	0.125	0.25	0.125	2	1	1	1	0.0625/1.2	0.125/2.4	0.0625/1.2	0.125/2.4
MT3317	CoN S. lugdunensis	128	64	8	16	0.5	0.5	0.5	0.25	16	16	8	8	0.25/4.8	0.5/9.5	0.25/4.8	0.5/9.5
						Clinical Breakpoints: S ≤ 0.25; R ≥ 0.5											
MT3320	CoN S. epidermidis	8	16	0.25	1	0.125	0.25	0.25	0.25	1	1	0.5	0.5	0.25/4.8	0.125/2.4	0.125/2.4	0.25/4.8
MT3321	CoN S. warneri	0.03125	0.0156	0.0156	0.03125	0.125	0.125	0.0625	0.125	2	2	4	1	0.0625/1.2	0.125/2.4	0.25/4.8	0.125/2.4

Strain #	Strain Name	Spectinomycin MIC (µg/mL)				Streptomycin MIC (µg/mL)				Kanamycin MIC (µg/mL)				Gentamicin MIC (µg/mL)			
Clinical Breakpoints:						S ≤ 8; I = 16; R ≥ 32[189]				S ≤ 16; I = 32; R ≥ 64				S ≤ 4; I = 8; R ≥ 16			
		Ca-MHB	DMEM + 5% LB	MLM	Lacks Medium	Ca-MHB	DMEM + 5% LB	MLM	Lacks Medium	Ca-MHB	DMEM + 5% LB	MLM	Lacks Medium	Ca-MHB	DMEM + 5% LB	MLM	Lacks Medium
MT3322	MRSA USA300	128	64	32	64	16	4	2	8	> 512	> 512	> 512	> 512	1	2	0.5	1
MT3302	MRSA Blood	128	32	16	64	8	2	2	8	> 512	> 512	> 512	> 512	1	4	0.25	1
MT3315	MRSA Wound	128	64	16	64	4	1	1	8	> 512	> 512	512	> 512	128	>512	128	256
MT3305	MSSA Blood	128	64	32	64	16	2	2	8	8	16	4	8	1	2	0.25	1
MT3307	MSSA Wound	256	64	32	128	16	4	2	16	8	16	2	8	1	4	0.25	2
MT3309	MSSA Urine	128	64	32	64	32	4	2	8	4	8	4	8	0.5	2	0.25	1
MT3314	MSSA Sputum	256	64	64	128	32	2	4	16	4	8	4	8	1	2	0.5	1
MT3317	CoN S. lugdunensis	64	32	16	32	4	1	1	8	1	4	1	4	0.125	0.5	0.125	0.25
MT3320	CoN S. epidermidis	128	64	64	128	4	0.5	0.25	4	4	8	0.5	4	0.125	0.5	0.03125	0.25
MT3321	CoN S. warneri	64	32	16	32	4	1	2	8	1	4	2	8	0.125	0.5	0.125	0.5

Strain #	Strain Name	Linezolid MIC (µg/mL)				Tetracycline MIC (µg/mL)				Azithromycin MIC (µg/mL)				Erythromycin MIC (µg/mL)			
Clinical Breakpoints:		S ≤ 4; R ≥ 8				S ≤ 4; I = 8; R ≥ 16				S ≤ 2; I = 4; R ≥ 8				S ≤ 0.5; I = 1 - 4; R ≥ 8			
		Ca-MHB	DMEM + 5% LB	MLM	Lacks Medium	Ca-MHB	DMEM + 5% LB	MLM	Lacks Medium	Ca-MHB	DMEM + 5% LB	MLM	Lacks Medium	Ca-MHB	DMEM + 5% LB	MLM	Lacks Medium
MT3322	MRSA USA300	4	4	2	2	0.5	4	1	1	128	8	16	32	64	8	16	16
MT3302	MRSA Blood	2	2	1	2	0.5	2	0.25	1	128	8	8	32	128	8	8	16
MT3315	MRSA Wound	2	2	1	2	0.25	1	0.25	1	1	0.125	0.0625	0.125	0.25	0.0625	0.0625	0.125
MT3305	MSSA Blood	2	2	2	2	0.5	0.5	0.5	1	>512	>512	>512	>512	>512	>512	>512	>512
MT3307	MSSA Wound	2	2	1	2	0.5	4	0.5	1	2	0.125	0.125	0.25	1	0.125	0.0625	0.125
MT3309	MSSA Urine	2	2	1	2	4	8	4	4	1	0.125	0.125	0.25	0.5	0.125	0.125	0.125
MT3314	MSSA Sputum	2	2	1	2	0.5	2	1	1	2	0.125	0.125	0.25	1	0.125	0.125	0.25
MT3317	CoN S. lugdunensis	1	1	0.5	1	0.25	1	0.25	0.5	0.25	0.0625	0.0625	0.125	0.125	0.03125	0.0625	0.0625
MT3320	CoN S. epidermidis	2	2	1	1	0.5	4	0.5	1	256	32		32	128	32	2	32
MT3321	CoN S. warneri	2	2	1	2	0.5	4	2	1	256	32	16	64	256	32	32	64

Strain #	Strain Name	Chloramphenicol MIC (µg/mL)				Florfenicol MIC (µg/mL)				Clindamycin MIC (µg/mL)				Rifampin MIC (µg/mL)			
Clinical Breakpoints:		S ≤ 8; I = 16; R ≥ 32								S ≤ 0.5; I = 1 - 2; R ≥ 4				S ≤ 1; I = 2; R ≥ 4			
		Ca-MHB	DMEM + 5% LB	MLM	Lacks Medium	Ca-MHB	DMEM + 5% LB	MLM	Lacks Medium	Ca-MHB	DMEM + 5% LB	MLM	Lacks Medium	Ca-MHB	DMEM + 5% LB	MLM	Lacks Medium
MT3322	MRSA USA300	16	8	8	8	4	4	4	4	0.125	0.0625	0.0625	0.125	0.0078	0.0156	0.0625	0.0078
MT3302	MRSA Blood	8	4	4	8	4	4	4	4	0.25	0.125	0.0625	0.125	0.0078	0.0156	0.0625	0.0156
MT3315	MRSA Wound	8	8	4	4	4	4	4	4	0.125	0.125	0.0625	0.125	0.0078	0.03125	0.0625	0.0156
MT3305	MSSA Blood	16	8	8	8	4	4	4	4	0.25	0.125	0.125	0.125	0.0156	0.0156	0.125	0.0156
MT3307	MSSA Wound	16	16	8	8	4	4	4	4	0.25	0.0625	0.0625	0.125	0.0078	0.0156	0.125	0.0156
MT3309	MSSA Urine	8	4	8	8	8	4	4	4	0.25	0.125	0.0625	0.125	0.0078	0.0156	0.125	0.0156
MT3314	MSSA Sputum	8	4	8	8	4	4	4	4	0.25	0.125	0.125	0.125	0.0156	0.0156	0.25	0.0156
MT3317	CoN S. lugdunensis	8	8	4	4	2	4	2	2	0.125	0.03125	0.0625	0.0625	0.0078	0.0156	0.03125	0.0078
MT3320	CoN S. epidermidis	8	8	2	4	4	8	2	4	0.125	0.125	0.03125	0.125	0.0078	0.03125	0.0625	0.0156
MT3321	CoN S. warneri	8	8	8	8	4	4	4	4	0.125	0.0625	0.0625	0.0625	0.002	0.0078	0.0156	0.0078

Strain #	Strain Name	Nalidixic Acid MIC (µg/mL)				Ciprofloxacin MIC (µg/mL)				Enrofloxacin MIC (µg/mL)			
Clinical Breakpoints:						S ≤ 1; I = 2; R ≥ 4							
		Ca-MHB	DMEM + 5% LB	MLM	Lacks Medium	Ca-MHB	DMEM + 5% LB	MLM	Lacks Medium	Ca-MHB	DMEM + 5% LB	MLM	Lacks Medium
MT3322	MRSA USA300	64	256	512	64	0.5	0.5	1	1	0.125	0.25	0.5	0.25
MT3302	MRSA Blood	64	256	512	256	0.25	0.25	0.5	0.5	0.25	0.25	0.5	0.25
MT3315	MRSA Wound	256	>512	>512	>512	8	16	32	32	4	4	8	8
MT3305	MSSA Blood	64	128	512	128	0.125	0.25	0.25	0.25	0.0625	0.25	0.25	0.25
MT3307	MSSA Wound	32	256	512	128	0.25	0.5	0.5	0.5	0.125	0.25	0.25	0.125
MT3309	MSSA Urine	256	>512	>512	>512	16	16	32	16	4	8	16	4
MT3314	MSSA Sputum	32	128	256	64	0.25	0.25	0.5	0.5	0.125	0.25	0.25	0.125
MT3317	CoN S. lugdunensis	64	512	256	128	0.25	0.25	0.25	0.125	0.125	0.25	0.25	0.125
MT3320	CoN S. epidermidis	32	256	256	64	0.125	0.25	0.25	0.25	0.125	0.25	0.125	0.25
MT3321	CoN S. warneri	256	512	512	128	0.25	0.5	0.25	0.25	0.25	0.5	0.25	0.125

MHB, DMEM, MLM and Lacks Medium MICs were determined by broth microdilution in accordance with CLSI guidelines. DMEM MICs were incubated in a 5% CO2 incubator. S = Susceptible, NS = Non-Susceptible, I = Intermediate, R = Resistant
[a]All Clinical Breakpoints are referenced from the CLSI 2014 twenty-fourth informational supplement (*192*) unless otherwise indicated.

Table 4.2b. Antimicrobial susceptibility testing in host-mimicking media (*Streptococcus pneumoniae*).

Supplementary Table 1B. *Streptococcus pneumoniae*

		Daptomycin MIC (µg/mL)			
Clinical Breakpoints[a]:		S ≤ 2; NS ≥4[192]			
Strain	Capsular Serotype	Ca-MHB + 5% LHB	DMEM + 5% LHB	MLM	Lacks Medium
D39	2	0.25	0.0625	2	1
Daw 1	6	0.25	0.0625	2	2
Daw 19	6	0.25	0.0625	2	2
Daw 20	11	0.25	0.0625	2	1
Daw 2	23	0.25	0.0625	2	1
Daw 25	35C	0.25	0.0625	2	1

		Ceftriaxone MIC (µg/mL)			
		S ≤ 1; I = 2; R ≥ 4			
Strain	Capsular Serotype	Ca-MHB + 5% LHB	DMEM + 5% LHB	MLM	Lacks Medium
D39	2	0.0156	0.0156	0.0078	0.0156
Daw 1	6	0.5	0.5	0.5	0.5
Daw 19	6	1	0.5	2	1
Daw 20	11	0.0156	0.03125	0.0156	0.03125
Daw 2	23	0.5	4	2	2
Daw 25	35C	0.0156	0.03125	0.0156	0.0156

		Ampicillin MIC (µg/mL)			
		S ≤ 0.5; I = 1-2; R ≥ 4[197]			
Strain	Capsular Serotype	Ca-MHB + 5% LHB	DMEM + 5% LHB	MLM	Lacks Medium
D39	2	0.0156	0.03125	0.0039	0.0156
Daw 1	6	1	0.0625	2	2
Daw 19	6	4	0.0625	16	8
Daw 20	11	0.0156	0.0625	0.03125	0.03125
Daw 2	23	0.5	4	2	1
Daw 25	35C	0.0156	0.0625	0.03125	0.03125

		Oxacillin MIC (µg/mL)			
Strain	Capsular Serotype	Ca-MHB + 5% LHB	DMEM + 5% LHB	MLM	Lacks Medium
D39	2	0.0625	0.125	0.03125	0.0625
Daw 1	6	8	8	8	8
Daw 19	6	8	8	16	8
Daw 20	11	0.0625	0.25	0.0625	0.0625
Daw 2	23	2	8	4	2
Daw 25	35C	0.0625	0.125	0.0625	0.03125

		Trimethoprim MIC (µg/mL)			
Clinical Breakpoints:		S ≤ 2; R ≥ 4[194]			
Strain	Capsular Serotype	Ca-MHB + 5% LHB	DMEM + 5% LHB	MLM	Lacks Medium
D39	2	0.5	0.5	2	0.25
Daw 1	6	64	2	64	64
Daw 19	6	64	16	64	64
Daw 20	11	1	2	32	8
Daw 2	23	4	8	32	32
Daw 25	35C	1	2	16	4

		Co-Trimoxazole MIC (µg/mL)			
		S ≤ 0.5/9.5; I = 1/19 - 2/38; R ≥ 4/76			
Strain	Capsular Serotype	Ca-MHB + 5% LHB	DMEM + 5% LHB	MLM	Lacks Medium
D39	2	0.0625/1.2	0.125/2.4	0.125/2.4	0.25/4.8
Daw 1	6	4/76	1/19	16/304	32/608
Daw 19	6	4/76	4/76	32/604	16/304
Daw 20	11	0.25/4.8	0.5/9.5	2/38	1/19
Daw 2	23	2/38	2/38	8/152	16/304
Daw 25	35C	0.125/2.4	0.25/4.8	1/19	1/19

		Spectinomycin MIC (µg/mL)			
Strain	Capsular Serotype	Ca-MHB + 5% LHB	DMEM + 5% LHB	MLM	Lacks Medium
D39	2	32	8	32	64
Daw 1	6	16	8	16	64
Daw 19	6	16	16	16	32
Daw 20	11	32	16	16	64
Daw 2	23	16	16	32	64
Daw 25	35C	16	16	16	64

		Linezolid MIC (µg/mL)			
		S ≤ 2; NS ≥ 4			
Strain	Capsular Serotype	Ca-MHB + 5% LHB	DMEM + 5% LHB	MLM	Lacks Medium
D39	2	0.5	1	1	0.5
Daw 1	6	1	0.5	0.5	1
Daw 19	6	2	2	0.5	1
Daw 20	11	2	1	1	0.5
Daw 2	23	0.5	2	0.5	0.5
Daw 25	35C	1	1	0.5	0.5

		Tetracycline MIC (µg/mL)			
Clinical Breakpoints:		S ≤ 1; I = 2; R ≥ 4			
Strain	Capsular Serotype	Ca-MHB + 5% LHB	DMEM + 5% LHB	MLM	Lacks Medium
D39	2	0.125	0.5	0.25	0.25
Daw 1	6	0.5	1	0.5	0.5
Daw 19	6	0.25	1	0.25	0.5
Daw 20	11	0.25	0.5	0.5	0.25
Daw 2	23	0.125	0.5	0.125	0.25
Daw 25	35C	0.125	0.5	0.25	0.125

		Azithromycin MIC (µg/mL)			
		S ≤ 0.5; I = 1; R ≥ 2			
Strain	Capsular Serotype	Ca-MHB + 5% LHB	DMEM + 5% LHB	MLM	Lacks Medium
D39	2	0.0625	0.0039	0.0625	0.0625
Daw 1	6	8	2	1	4
Daw 19	6	8	2	0.5	4
Daw 20	11	0.0625	0.0156	0.03125	0.03125
Daw 2	23	0.0625	0.0156	0.0156	0.03125
Daw 25	35C	0.0625	0.0156	0.0156	0.0625

		Erythromycin MIC (µg/mL)			
		S ≤ 0.25; I = 0.5; R ≥ 1			
Strain	Capsular Serotype	Ca-MHB + 5% LHB	DMEM + 5% LHB	MLM	Lacks Medium
D39	2	0.03125	0.0039	0.0156	0.0625
Daw 1	6	8	2	1	2
Daw 19	6	8	2	1	4
Daw 20	11	0.03125	0.0156	0.03125	0.0156
Daw 2	23	0.03125	0.0156	0.03125	0.0156
Daw 25	35C	0.03125	0.0078	0.03125	0.03125

		Chloramphenicol MIC (µg/mL)			
		S ≤ 4; R ≥ 8			
Strain	Capsular Serotype	Ca-MHB + 5% LHB	DMEM + 5% LHB	MLM	Lacks Medium
D39	2	4	1	2	2
Daw 1	6	4	2	2	4
Daw 19	6	2	2	2	2
Daw 20	11	4	2	4	1
Daw 2	23	1	4	2	1
Daw 25	35C	2	2	2	2

		Clindamycin MIC (µg/mL)			
Clinical Breakpoints:		S ≤ 0.25; I = 0.5; R ≥ 1			
Strain	Capsular Serotype	Ca-MHB + 5% LHB	DMEM + 5% LHB	MLM	Lacks Medium
D39	2	0.03125	0.0078	0.0156	0.0156
Daw 1	6	0.0625	0.03125	0.0625	0.0625
Daw 19	6	0.0625	0.03125	0.03125	0.03125
Daw 20	11	0.0625	0.0625	0.0625	0.03125
Daw 2	23	0.0156	0.0625	0.0156	0.0156
Daw 25	35C	0.0625	0.03125	0.0625	0.03125

		Rifampin MIC (µg/mL)			
		S ≤ 1; I = 2; R ≥ 4			
Strain	Capsular Serotype	Ca-MHB + 5% LHB	DMEM + 5% LHB	MLM	Lacks Medium
D39	2	0.0156	0.03125	0.03125	0.0156
Daw 1	6	0.0156	0.0156	0.03125	0.0156
Daw 19	6	0.0156	0.03125	0.0156	0.0078
Daw 20	11	0.03125	0.0625	0.0625	0.0156
Daw 2	23	0.0156	0.0625	0.03125	0.0078
Daw 25	35C	0.0156	0.0625	0.03125	0.0156

		Ciprofloxacin MIC (µg/mL)			
		S ≤ 0.125; I = 0.25-2; R ≥ 4[197]			
Strain	Capsular Serotype	Ca-MHB + 5% LHB	DMEM + 5% LHB	MLM	Lacks Medium
D39	2	0.5	1	1	1
Daw 1	6	0.5	2	1	1
Daw 19	6	0.5	1	0.5	1
Daw 20	11	1	2	2	2
Daw 2	23	1	2	1	1
Daw 25	35C	0.5	1	0.5	1

MHB, DMEM, MLM and Lacks Medium MICs were determined by broth microdilution in accordance with CLSI guidelines. DMEM MICs were incubated in a 5% CO2 incubator. S = Susceptible, NS = Non-Susceptible, I = Intermediate, R = Resistant

[a]All Clinical Breakpoints are referenced from the CLSI 2014 twenty-fourth informational supplement (*192*) unless otherwise indicated.

Table 4.2c. Antimicrobial susceptibility testing in host-mimicking media (*Salmonella*).

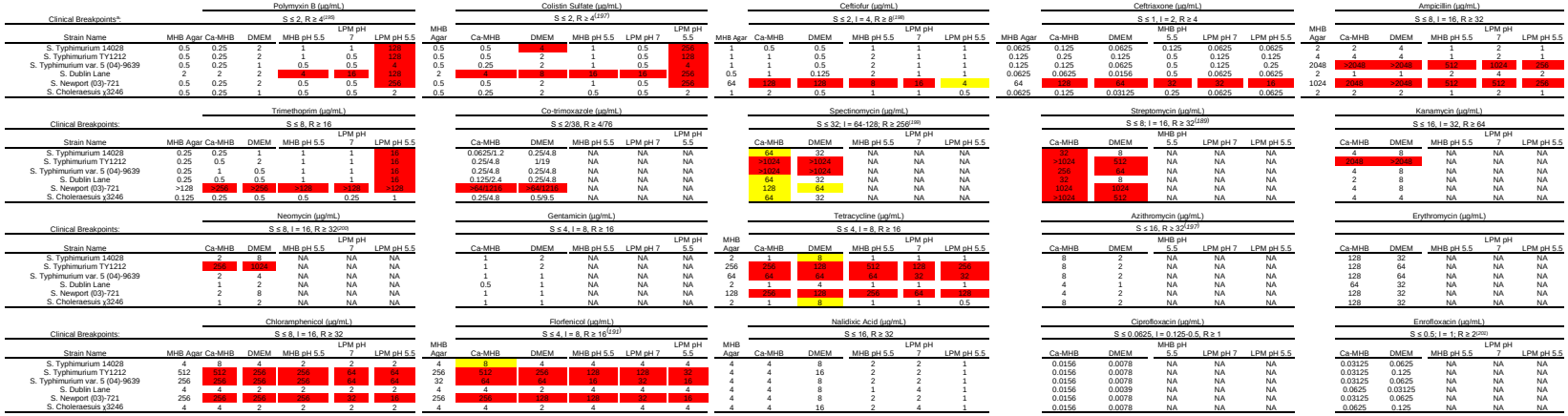

Polymyxin B (µg/mL)						Colistin Sulfate (µg/mL)						Ceftiofur (µg/mL)						Ceftriaxone (µg/mL)						Ampicillin (µg/mL)					
Clinical Breakpoints[a]:	S ≤ 2, R ≥ 4[(195)]					S ≤ 2, R ≥ 4[(197)]						S ≤ 2, I = 4, R ≥ 8[(198)]						S ≤ 1, I = 2, R ≥ 4						S ≤ 8, I = 16, R ≥ 32					
Strain Name	MHB Agar	Ca-MHB	DMEM	MHB pH 5.5	LPM pH 7	LPM pH 5.5	MHB Agar	Ca-MHB	DMEM	MHB pH 5.5	LPM pH 7	LPM pH 5.5	MHB Agar	Ca-MHB	DMEM	MHB pH 5.5	LPM pH 7	LPM pH 5.5	MHB Agar	Ca-MHB	DMEM	MHB pH 5.5	LPM pH 7	LPM pH 5.5	MHB Agar	Ca-MHB	DMEM	MHB pH 5.5	LPM pH 7	LPM pH 5.5
S. Typhimurium 14028	0.5	0.25	2	1	1	128	0.5	0.5	4	1	0.5	256	1	0.5	0.5	1	1	1	0.0625	0.125	0.0625	0.125	0.0625	0.0625	2	2	4	1	2	1
S. Typhimurium TY1212	0.5	0.25	2	1	0.5	128	0.5	0.5	2	1	0.5	128	1	1	0.5	2	1	1	0.125	0.25	0.125	0.5	0.125	0.125	4	4	4	1	2	1
S. Typhimurium var. 5 (04)-9639	0.5	0.25	1	0.5	0.5	4	0.5	0.25	2	1	0.5	4	1	1	0.5	2	1	1	0.125	0.125	0.0625	0.5	0.125	0.25	2048	>2048	>2048	512	1024	256
S. Dublin Lane	2	2	2	4	16	128	2	4	8	16	16	256	0.5	1	0.125	2	1	1	0.0625	0.0625	0.0156	0.5	0.0625	0.0625	2	1	1	2	4	2
S. Newport (03)-721	0.5	0.25	2	0.5	0.5	256	0.5	0.5	2	1	0.5	256	64	128	128	8	16	4	64	128	64	32	32	16	1024	2048	>2048	512	512	256
S. Choleraesuis χ3246	0.5	0.25	1	0.5	0.5	2	0.5	0.25	2	0.5	0.5	2	1	2	0.5	1	1	0.5	0.0625	0.125	0.03125	0.25	0.0625	0.0625	2	2	2	1	2	1

Trimethoprim (µg/mL)						Co-trimoxazole (µg/mL)					Spectinomycin (µg/mL)					Streptomycin (µg/mL)					Kanamycin (µg/mL)				
Clinical Breakpoints:	S ≤ 8, R ≥ 16					S ≤ 2/38, R ≥ 4/76					S ≤ 32, I = 64-128, R ≥ 256[(228)]					S ≤ 8, I = 16, R ≥ 32[(189)]					S ≤ 16, I = 32, R ≥ 64				
Strain Name	MHB Agar	Ca-MHB	DMEM	MHB pH 5.5	LPM pH 7	LPM pH 5.5	Ca-MHB	DMEM	MHB pH 5.5	LPM pH 7	LPM pH 5.5	Ca-MHB	DMEM	MHB pH 5.5	7	LPM pH 5.5	Ca-MHB	DMEM	MHB pH 5.5	LPM pH 7	LPM pH 5.5	Ca-MHB	DMEM	MHB pH 5.5	LPM pH 7	LPM pH 5.5
S. Typhimurium 14028	0.25	0.25	1	1	1	16	0.0625/1.2	0.25/4.8	NA	NA	NA	64	32	NA	NA	NA	32	8	NA	NA	NA	4	8	NA	NA	NA
S. Typhimurium TY1212	0.25	0.5	2	1	1	16	0.25/4.8	1/19	NA	NA	NA	>1024	>1024	NA	NA	NA	>1024	512	NA	NA	NA	2048	>2048	NA	NA	NA
S. Typhimurium var. 5 (04)-9639	0.25	1	0.5	1	1	16	0.25/4.8	0.25/4.8	NA	NA	NA	>1024	>1024	NA	NA	NA	256	64	NA	NA	NA	4	8	NA	NA	NA
S. Dublin Lane	0.25	0.5	0.5	1	1	16	0.125/2.4	0.25/4.8	NA	NA	NA	64	32	NA	NA	NA	32	8	NA	NA	NA	2	8	NA	NA	NA
S. Newport (03)-721	>128	>256	>256	>128	>128	>128	>64/1216	>64/1216	NA	NA	NA	128	64	NA	NA	NA	1024	1024	NA	NA	NA	4	8	NA	NA	NA
S. Choleraesuis χ3246	0.125	0.25	0.5	0.5	0.25	1	0.25/4.8	0.5/9.5	NA	NA	NA	64	32	NA	NA	NA	>1024	512	NA	NA	NA	4	4	NA	NA	NA

Neomycin (µg/mL)						Gentamicin (µg/mL)					Tetracycline (µg/mL)					Azithromycin (µg/mL)					Erythromycin (µg/mL)				
Clinical Breakpoints:	S ≤ 8, I = 16, R ≥ 32[(209)]					S ≤ 4, I = 8, R ≥ 16					S ≤ 4, I = 8, R ≥ 16					S ≤ 16, R ≥ 32[(197)]									
Strain Name		Ca-MHB	DMEM	MHB pH 5.5	LPM pH 7	LPM pH 5.5	Ca-MHB	DMEM	MHB pH 5.5	LPM pH 7	LPM pH 5.5	MHB Agar	Ca-MHB	DMEM	MHB pH 5.5	7	LPM pH 5.5	Ca-MHB	DMEM	MHB pH 5.5	LPM pH 7	LPM pH 5.5	Ca-MHB	DMEM	MHB pH 5.5	LPM pH 7	LPM pH 5.5
S. Typhimurium 14028		2	8	NA	NA	NA	1	2	NA	NA	NA	2	1	8	1	1	1	8	2	NA	NA	NA	128	32	NA	NA	NA
S. Typhimurium TY1212		256	1024	NA	NA	NA	1	2	NA	NA	NA	256	256	128	512	128	256	8	2	NA	NA	NA	128	64	NA	NA	NA
S. Typhimurium var. 5 (04)-9639		2	4	NA	NA	NA	1	1	NA	NA	NA	64	64	64	64	32	32	8	2	NA	NA	NA	128	64	NA	NA	NA
S. Dublin Lane		1	2	NA	NA	NA	0.5	1	NA	NA	NA	2	1	4	1	1	1	4	1	NA	NA	NA	64	32	NA	NA	NA
S. Newport (03)-721		2	8	NA	NA	NA	1	1	NA	NA	NA	128	256	128	256	64	128	4	2	NA	NA	NA	128	32	NA	NA	NA
S. Choleraesuis χ3246		1	2	NA	NA	NA	1	1	NA	NA	NA	2	1	8	1	1	0.5	8	2	NA	NA	NA	128	32	NA	NA	NA

Chloramphenicol (µg/mL)						Florfenicol (µg/mL)					Nalidixic Acid (µg/mL)					Ciprofloxacin (µg/mL)					Enrofloxacin (µg/mL)				
Clinical Breakpoints:	S ≤ 8, I = 16, R ≥ 32					S ≤ 4, I = 8, R ≥ 16[(192)]					S ≤ 16, R ≥ 32					S ≤ 0.0625, I = 0.125-0.5, R ≥ 1					S ≤ 0.5; I = 1; R ≥ 2[(228)]				
Strain Name	MHB Agar	Ca-MHB	DMEM	MHB pH 5.5	LPM pH 7	LPM pH 5.5	MHB Agar	Ca-MHB	DMEM	MHB pH 5.5	LPM pH 7	LPM pH 5.5	MHB Agar	Ca-MHB	DMEM	MHB pH 5.5	7	LPM pH 5.5	Ca-MHB	DMEM	MHB pH 5.5	LPM pH 7	LPM pH 5.5	Ca-MHB	DMEM	MHB pH 5.5	LPM pH 7	LPM pH 5.5
S. Typhimurium 14028	4	8	4	2	2	2	4	8	4	4	4	4	4	4	8	2	2	1	0.0156	0.0078	NA	NA	NA	0.03125	0.0625	NA	NA	NA
S. Typhimurium TY1212	512	512	256	256	64	64	256	512	256	128	128	32	4	4	16	2	2	1	0.0156	0.0078	NA	NA	NA	0.03125	0.125	NA	NA	NA
S. Typhimurium var. 5 (04)-9639	256	256	256	256	64	64	32	64	64	16	32	16	4	4	8	2	2	1	0.0156	0.0078	NA	NA	NA	0.03125	0.0625	NA	NA	NA
S. Dublin Lane	4	4	2	2	2	2	4	4	2	4	4	4	4	4	8	1	4	1	0.0156	0.0039	NA	NA	NA	0.0625	0.03125	NA	NA	NA
S. Newport (03)-721	256	256	256	256	32	16	256	256	128	128	32	16	4	4	8	2	2	1	0.0156	0.0078	NA	NA	NA	0.03125	0.0625	NA	NA	NA
S. Choleraesuis χ3246	4	4	2	2	2	2	4	4	2	4	4	4	4	4	16	2	4	1	0.0156	0.0078	NA	NA	NA	0.0625	0.125	NA	NA	NA

MHB and DMEM MICs were determined by broth microdilution in accordance with CLSI guidelines. DMEM MICs were incubated in a 5% CO2 incubator. S = Susceptible, NS = Non-Susceptible, I = Intermediate, R = Resistant.

[a]All Clinical Breakpoints are referenced from the CLSI 2014 twenty-fourth informational supplement (*192*) unless otherwise indicated.

Table 4.2d. Antimicrobial susceptibility testing in host-mimicking media (*Escherichia coli*).

Clinical Breakpoints[a]:	Polymyxin B (μg/mL) S ≤ 2, R ≥ 4 (195)					
Strain Name	MHB Agar	Ca-MHB	DMEM	MHB pH 5.5	LPM pH 7	LPM pH 5.5
Seattle 1946; O6 biotype 1 ATCC 25922	0.5	0.25	1	0.5	0.5	1
UPEC J96	0.5	0.25	1	0.25	0.5	2
UPEC ECR12	1	0.25	1	0.25	0.5	1
UPEC ATCC 11775	0.5	0.125	1	0.5	1	2
APEC χ7126	0.5	0.125	2	0.5	0.5	2
A96 χ7117	0.5	0.125	1	0.5	0.5	1
EPEC χ2927	0.5	0.25	1	0.25	0.5	1
RDEC-1 χ2862	0.5	0.25	0.5	0.125	0.5	1
EPEC JPN 15	0.5	0.25	1	0.25	0.5	1

	Colistin Sulfate (μg/mL) S ≤ 2, R ≥ 4 (197)				
	Ca-MHB	DMEM	MHB pH 5.5	LPM pH 7	LPM pH 5.5
Seattle 1946; O6 biotype 1 ATCC 25922	1	1	4	4	32
UPEC J96	0.5	1	2	4	32
UPEC ECR12	1	1	2	4	32
UPEC ATCC 11775	0.5	1	2	4	16
APEC χ7126	0.5	1	2	4	16
A96 χ7117	0.5	1	1	4	16
EPEC χ2927	0.25	1	0.25	1	4
RDEC-1 χ2862	0.5	1	1	4	16
EPEC JPN 15	0.5	1	1	1	4

	Ceftiofur (μg/mL) S ≤ 2, I = 4, R ≥ 8 (198)					
	MHB Agar	Ca-MHB	DMEM	MHB pH 5.5	LPM pH 7	LPM pH 5.5
Seattle 1946; O6 biotype 1 ATCC 25922	0.5	0.5	0.25	2	0.25	0.5
UPEC J96	0.5	0.5	0.25	1	0.25	0.5
UPEC ECR12	0.25	0.5	0.5	1	0.5	0.5
UPEC ATCC 11775	0.25	0.5	0.25	1	0.25	0.5
APEC χ7126	0.25	0.25	0.125	0.5	0.125	0.25
A96 χ7117	0.25	0.25	0.125	1	0.25	0.5
EPEC χ2927	0.5	0.5	0.25	1	0.25	0.5
RDEC-1 χ2862	0.25	0.5	0.25	1	0.25	0.25
EPEC JPN 15	0.5	2	0.5	1	0.5	0.5

	Ceftriaxone (μg/mL) S ≤ 1, I = 2, R ≥ 4				
	Ca-MHB	DMEM	MHB pH 5.5	LPM pH 7	LPM pH 5.5
Seattle 1946; O6 biotype 1 ATCC 25922	0.125	0.03125	0.125	0.015625	0.0625
UPEC J96	0.0625	0.03125	0.125	0.015625	0.03125
UPEC ECR12	0.0625	0.0625	0.125	0.015625	0.03125
UPEC ATCC 11775	0.0625	0.03125	0.125	0.0078125	0.03125
APEC χ7126	0.03125	0.0156	0.0625	0.0078125	0.03125
A96 χ7117	0.0625	0.03125	0.0625	0.015625	0.015625
EPEC χ2927	0.0625	0.0156	0.0625	0.0078125	0.015625
RDEC-1 χ2862	0.125	0.03125	0.125	0.0078125	0.015625
EPEC JPN 15	0.125	0.03125	0.125	0.015625	0.0625

	Ampicillin (μg/mL) S ≤ 8, I = 16, R ≥ 32				
	Ca-MHB	DMEM	MHB pH 5.5	LPM pH 7	LPM pH 5.5
Seattle 1946; O6 biotype 1 ATCC 25922	4	8	4	2	1
UPEC J96	4	4	2	1	1
UPEC ECR12	4	8	2	1	1
UPEC ATCC 11775	4	4	2	1	0.5
APEC χ7126	2	2	2	1	0.5
A96 χ7117	4	4	2	1	1
EPEC χ2927	4	4	2	1	0.5
RDEC-1 χ2862	8	8	4	1	0.5
EPEC JPN 15	>2048	>2048	>2048	>2048	>2048

Clinical Breakpoints:	Trimethoprim (μg/mL) S ≤ 8, R ≥ 16				
Strain Name	MHB Agar	Ca-MHB	DMEM	MHB pH 5.5	LPM pH 7	LPM pH 5.5
Seattle 1946; O6 biotype 1 ATCC 25922	0.5	1	0.5	4	0.5	16
UPEC J96	0.5	0.5	0.5	4	1	16
UPEC ECR12	0.25	0.5	0.5	4	1	16
UPEC ATCC 11775	0.5	1	0.5	4	1	16
APEC χ7126	0.125	0.25	0.25	2	1	16
A96 χ7117	0.125	0.25	0.25	4	0.5	16
EPEC χ2927	0.125	0.25	0.125	4	0.5	16
RDEC-1 χ2862	0.125	0.25	1	4	1	16
EPEC JPN 15	0.25	0.25	0.5	4	0.5	16

	Co-trimoxazole (μg/mL) S ≤ 2/38, R ≥ 4/76				
	Ca-MHB	DMEM	MHB pH 5.5	LPM pH 7	LPM pH 5.5
Seattle 1946; O6 biotype 1 ATCC 25922	0.0625/1.2	0.03125/0.6	NA	NA	NA
UPEC J96	0.0625/1.2	0.03125/0.6	NA	NA	NA
UPEC ECR12	0.0625/1.2	0.0625/1.2	NA	NA	NA
UPEC ATCC 11775	0.125/2.4	0.0625/1.2	NA	NA	NA
APEC χ7126	0.03125/0.6	0.0625/1.2	NA	NA	NA
A96 χ7117	0.03125/0.6	0.03125/0.6	NA	NA	NA
EPEC χ2927	0.0625/1.2	0.03125/0.6	NA	NA	NA
RDEC-1 χ2862	0.03125/0.6	0.03125/0.6	NA	NA	NA
EPEC JPN 15	0.0625/1.2	0.03125/0.6	NA	NA	NA

	Spectinomycin (μg/mL) S ≤ 32; I = 64-128; R ≥ 256 (199)				
	Ca-MHB	DMEM	MHB pH 5.5	LPM pH 7	LPM pH 5.5
Seattle 1946; O6 biotype 1 ATCC 25922	32	16	NA	NA	NA
UPEC J96	32	16	NA	NA	NA
UPEC ECR12	16	8	NA	NA	NA
UPEC ATCC 11775	16	16	NA	NA	NA
APEC χ7126	16	16	NA	NA	NA
A96 χ7117	32	16	NA	NA	NA
EPEC χ2927	32	8	NA	NA	NA
RDEC-1 χ2862	16	4	NA	NA	NA
EPEC JPN 15	16	16	NA	NA	NA

	Streptomycin (μg/mL) S ≤ 8; I = 16, R ≥ 32 (189)				
	Ca-MHB	DMEM	MHB pH 5.5	LPM pH 7	LPM pH 5.5
Seattle 1946; O6 biotype 1 ATCC 25922	8	2	NA	NA	NA
UPEC J96	4	1	NA	NA	NA
UPEC ECR12	8	2	NA	NA	NA
UPEC ATCC 11775	4	2	NA	NA	NA
APEC χ7126	8	2	NA	NA	NA
A96 χ7117	8	2	NA	NA	NA
EPEC χ2927	4	1	NA	NA	NA
RDEC-1 χ2862	4	1	NA	NA	NA
EPEC JPN 15	8	4	NA	NA	NA

	Kanamycin (μg/mL) S ≤ 16, I = 32, R ≥ 64				
	Ca-MHB	DMEM	MHB pH 5.5	LPM pH 7	LPM pH 5.5
Seattle 1946; O6 biotype 1 ATCC 25922	4	8	NA	NA	NA
UPEC J96	4	4	NA	NA	NA
UPEC ECR12	4	8	NA	NA	NA
UPEC ATCC 11775	2	8	NA	NA	NA
APEC χ7126	4	8	NA	NA	NA
A96 χ7117	4	8	NA	NA	NA
EPEC χ2927	1	2	NA	NA	NA
RDEC-1 χ2862	2	2	NA	NA	NA
EPEC JPN 15	2	8	NA	NA	NA

Clinical Breakpoints:	Neomycin (μg/mL) S ≤ 8, I = 16, R ≥ 32 (200)				
Strain Name	Ca-MHB	DMEM	MHB pH 5.5	LPM pH 7	LPM pH 5.5
Seattle 1946; O6 biotype 1 ATCC 25922	2	4	NA	NA	NA
UPEC J96	2	2	NA	NA	NA
UPEC ECR12	2	4	NA	NA	NA
UPEC ATCC 11775	1	4	NA	NA	NA
APEC χ7126	2	2	NA	NA	NA
A96 χ7117	1	4	NA	NA	NA
EPEC χ2927	0.5	1	NA	NA	NA
RDEC-1 χ2862	1	1	NA	NA	NA
EPEC JPN 15	1	4	NA	NA	NA

	Gentamicin (μg/mL) S ≤ 4, I = 8, R ≥ 16				
	Ca-MHB	DMEM	MHB pH 5.5	LPM pH 7	LPM pH 5.5
Seattle 1946; O6 biotype 1 ATCC 25922	1	1	NA	NA	NA
UPEC J96	1	1	NA	NA	NA
UPEC ECR12	0.5	1	NA	NA	NA
UPEC ATCC 11775	0.5	1	NA	NA	NA
APEC χ7126	1	1	NA	NA	NA
A96 χ7117	1	1	NA	NA	NA
EPEC χ2927	0.25	0.5	NA	NA	NA
RDEC-1 χ2862	0.5	0.5	NA	NA	NA
EPEC JPN 15	0.5	1	NA	NA	NA

	Tetracycline (μg/mL) S ≤ 4, I = 8, R ≥ 16					
	MHB Agar	Ca-MHB	DMEM	MHB pH 5.5	LPM pH 7	LPM pH 5.5
Seattle 1946; O6 biotype 1 ATCC 25922	0.5	0.5	8	0.5	0.5	0.5
UPEC J96	1	1	8	0.5	0.5	0.5
UPEC ECR12	1	2	8	1	1	0.5
UPEC ATCC 11775	1	1	8	0.5	0.5	0.5
APEC χ7126	1	0.5	4	0.5	0.25	0.5
A96 χ7117	1	1	4	1	0.5	0.5
EPEC χ2927	1	0.5	4	1	0.5	0.5
RDEC-1 χ2862	1	2	8	1	0.5	0.5
EPEC JPN 15	1	0.5	4	1	0.25	0.5

	Azithromycin (μg/mL) S ≤ 16, R ≥ 32 (197)				
	Ca-MHB	DMEM	MHB pH 5.5	LPM pH 7	LPM pH 5.5
Seattle 1946; O6 biotype 1 ATCC 25922	4	2	NA	NA	NA
UPEC J96	4	1	NA	NA	NA
UPEC ECR12	4	2	NA	NA	NA
UPEC ATCC 11775	4	2	NA	NA	NA
APEC χ7126	4	2	NA	NA	NA
A96 χ7117	4	2	NA	NA	NA
EPEC χ2927	4	1	NA	NA	NA
RDEC-1 χ2862	8	4	NA	NA	NA
EPEC JPN 15	4	2	NA	NA	NA

	Erythromycin (μg/mL)				
	Ca-MHB	DMEM	MHB pH 5.5	LPM pH 7	LPM pH 5.5
Seattle 1946; O6 biotype 1 ATCC 25922	64	64	NA	NA	NA
UPEC J96	64	64	NA	NA	NA
UPEC ECR12	64	64	NA	NA	NA
UPEC ATCC 11775	64	64	NA	NA	NA
APEC χ7126	32	64	NA	NA	NA
A96 χ7117	64	64	NA	NA	NA
EPEC χ2927	32	32	NA	NA	NA
RDEC-1 χ2862	256	128	NA	NA	NA
EPEC JPN 15	64	32	NA	NA	NA

Clinical Breakpoints:	Chloramphenicol (μg/mL) S ≤ 8, I = 16, R ≥ 32				
Strain Name	MHB Agar	Ca-MHB	DMEM	MHB pH 5.5	LPM pH 7	LPM pH 5.5
Seattle 1946; O6 biotype 1 ATCC 25922	4	4	4	2	2	2
UPEC J96	4	8	8	4	2	2
UPEC ECR12	4	8	8	4	2	2
UPEC ATCC 11775	4	4	4	4	2	2
APEC χ7126	4	4	4	2	1	1
A96 χ7117	4	4	4	2	2	2
EPEC χ2927	4	4	4	2	2	2
RDEC-1 χ2862	8	8	8	2	1	1
EPEC JPN 15	4	8	8	4	2	2

	Florfenicol (μg/mL) S ≤ 16, R ≥ 32 (202)				
	Ca-MHB	DMEM	MHB pH 5.5	LPM pH 7	LPM pH 5.5
Seattle 1946; O6 biotype 1 ATCC 25922	8	8	8	2	4
UPEC J96	8	8	8	4	4
UPEC ECR12	8	8	8	4	4
UPEC ATCC 11775	8	8	8	4	4
APEC χ7126	4	4	4	2	4
A96 χ7117	4	4	8	2	4
EPEC χ2927	4	8	8	4	4
RDEC-1 χ2862	8	8	8	2	2
EPEC JPN 15	8	8	8	2	8

	Nalidixic Acid (μg/mL) S ≤ 16, R ≥ 32				
	Ca-MHB	DMEM	MHB pH 5.5	LPM pH 7	LPM pH 5.5
Seattle 1946; O6 biotype 1 ATCC 25922	2	4	2	0.5	1
UPEC J96	128	512	128	32	32
UPEC ECR12	64	512	64	64	32
UPEC ATCC 11775	2	8	2	1	0.5
APEC χ7126	2	4	1	0.5	0.5
A96 χ7117	2	4	2	1	0.5
EPEC χ2927	256	2048	>512	256	>512
RDEC-1 χ2862	4	16	4	2	1
EPEC JPN 15	256	2048	>512	>512	>512

	Ciprofloxacin (μg/mL) S ≤ 1, I = 2, R ≥ 4				
	Ca-MHB	DMEM	MHB pH 5.5	LPM pH 7	LPM pH 5.5
Seattle 1946; O6 biotype 1 ATCC 25922	0.0078	0.0039	NA	NA	NA
UPEC J96	0.125	0.0625	NA	NA	NA
UPEC ECR12	0.125	0.0625	NA	NA	NA
UPEC ATCC 11775	0.0156	0.0078	NA	NA	NA
APEC χ7126	0.0078	0.0078	NA	NA	NA
A96 χ7117	0.0078	0.0039	NA	NA	NA
EPEC χ2927	0.25	0.25	NA	NA	NA
RDEC-1 χ2862	0.0156	0.0078	NA	NA	NA
EPEC JPN 15	0.125	0.125	NA	NA	NA

	Enrofloxacin (μg/mL) S ≤ 0.5; I = 1; R ≥ 2 (201)				
	Ca-MHB	DMEM	MHB pH 5.5	LPM pH 7	LPM pH 5.5
Seattle 1946; O6 biotype 1 ATCC 25922	0.0078	0.0156	NA	NA	NA
UPEC J96	0.25	0.5	NA	NA	NA
UPEC ECR12	0.125	0.5	NA	NA	NA
UPEC ATCC 11775	0.0156	0.0156	NA	NA	NA
APEC χ7126	0.0078	0.0078	NA	NA	NA
A96 χ7117	0.0078	0.0156	NA	NA	NA
EPEC χ2927	0.25	2	NA	NA	NA
RDEC-1 χ2862	0.0156	0.03125	NA	NA	NA
EPEC JPN 15	0.25	0.5	NA	NA	NA

MHB and DMEM MICs were determined by broth microdilution in accordance with CLSI guidelines. DMEM MICs were incubated in a 5% CO2 incubator. S = Susceptible, NS = Non-Susceptible, I = Intermediate, R = Resistant.

[a]All Clinical Breakpoints are referenced from the CLSI 2014 twenty-fourth informational supplement (*192*) unless otherwise indicated.

Table 4.2e. Antimicrobial susceptibility testing in host-mimicking media (*Yersinia pseudotuberculosis*).

Polymyxin B (μg/mL)						
Clinical Breakpoints[a]:			S ≤ 2, R ≥ 4[192]			
				MHB pH		LPM pH
Strain Name	MHB Agar	Ca-MHB	DMEM	5.5	LPM pH 7	5.5
Y. pseudotuberculosis YPIII/pIB1	0.25	0.25	1	0.25	1	8
Y. pseudotuberculosis IP32953	256	128	128	>512	512	256
Y. pseudotuberculosis IP2515	128	64	128	>512	>512	512
Y. pseudotuberculosis IP2666	0.25	0.25	1	0.25	0.5	1

Colistin Sulfate (μg/mL)						
			S ≤ 2, R ≥ 4[192]			
				MHB pH		LPM pH
MHB Agar	Ca-MHB	DMEM	5.5	LPM pH 7	5.5
0.5	0.25	1	1	2	4
256	256	256	>512	512	512
256	128	256	>512	1024	1024
0.5	0.25	1	1	0.5	2

Ceftiofur (μg/mL)					
			S ≤ 2, I = 4, R ≥ 8[193]		
			MHB pH		LPM pH
MHB Agar	Ca-MHB	DMEM	5.5	LPM pH 7	5.5
0.5	0.125	0.125	1	0.125	0.5
0.25	0.125	0.125	1	0.25	1
0.25	0.125	0.125	1	0.25	2
0.25	0.125	0.0625	1	0.125	1

Ceftriaxone (μg/mL)						
			S ≤ 1, I = 2, R ≥ 4			
				MHB pH		LPM pH
MHB Agar	Ca-MHB	DMEM	5.5	LPM pH 7	5.5
0.03125	0.03125	0.0156	0.0625	0.0156	0.03125
0.015625	0.03125	0.0156	0.0625	0.03125	0.0625
0.03125	0.0156	0.0156	0.0625	0.0156	0.125
0.015625	0.0156	0.0078	0.0625	0.0156	0.0625

Ampicillin (μg/mL)						
			S ≤ 8, I = 16, R ≥ 32			
				MHB pH	LPM pH	LPM pH
MHB Agar	Ca-MHB	DMEM	5.5	7	5.5
1	0.25	0.25	2	2	1
1	0.25	0.25	4	4	2
1	0.25	0.25	4	2	4
1	0.25	0.125	4	4	2

Trimethoprim (μg/mL)						
Clinical Breakpoints:			S ≤ 8, R ≥ 16			
				MHB pH		LPM pH
Strain Name	MHB Agar	Ca-MHB	DMEM	5.5	LPM pH 7	5.5
Y. pseudotuberculosis YPIII/pIB1	1	4	0.0625	64	0.5	8
Y. pseudotuberculosis IP32953	1	2	0.0625	64	1	16
Y. pseudotuberculosis IP2515	1	1	0.0625	64	0.5	8
Y. pseudotuberculosis IP2666	1	2	0.0625	64	2	32

Co-trimoxazole (μg/mL)					
		S ≤ 2/38, R ≥ 4/76			
			MHB pH		LPM pH
Ca-MHB	DMEM	5.5	LPM pH 7	5.5
0.25/4.8	0.0156/0.3	NA	NA	NA
0.125/2.4	0.0156/0.3	NA	NA	NA
0.125/2.4	0.0156/0.3	NA	NA	NA
0.125/2.4	0.0156/0.3	NA	NA	NA

Spectinomycin (μg/mL)					
		S ≤ 32, I = 64-128, R ≥ 256[193]			
			MHB pH		LPM pH
Ca-MHB	DMEM	5.5	LPM pH 7	5.5
16	8	NA	NA	NA
16	16	NA	NA	NA
16	8	NA	NA	NA
16	16	NA	NA	NA

Streptomycin (μg/mL)						
			S ≤ 8, I = 16, R ≥ 32[193]			
				MHB pH		LPM pH
MHB Agar	Ca-MHB	DMEM	5.5	LPM pH 7	5.5
0.5	1	0.5	NA	NA	NA
4	4	1	NA	NA	NA
2	2	0.5	NA	NA	NA
1	2	1	NA	NA	NA

Kanamycin (μg/mL)						
			S ≤ 16, I = 32, R ≥ 64			
				MHB pH	LPM pH	LPM pH
MHB Agar	Ca-MHB	DMEM	5.5	7	5.5
0.25	0.25	2	NA	NA	NA
1	1	4	NA	NA	NA
0.5	0.5	2	NA	NA	NA
0.5	1	4	NA	NA	NA

Neomycin (μg/mL)						
Clinical Breakpoints:			S ≤ 8, I = 16, R ≥ 32[193]			
				MHB pH		LPM pH
Strain Name	MHB Agar	Ca-MHB	DMEM	5.5	LPM pH 7	5.5
Y. pseudotuberculosis YPIII/pIB1	1	0.25	1	NA	NA	NA
Y. pseudotuberculosis IP32953	2	1	2	NA	NA	NA
Y. pseudotuberculosis IP2515	1	0.5	1	NA	NA	NA
Y. pseudotuberculosis IP2666	1	1	2	NA	NA	NA

Gentamicin (μg/mL)					
		S ≤ 4, I = 8, R ≥ 16			
			MHB pH		LPM pH
Ca-MHB	DMEM	5.5	LPM pH 7	5.5
0.125	0.5	NA	NA	NA
0.5	2	NA	NA	NA
0.25	1	NA	NA	NA
0.25	1	NA	NA	NA

Tetracycline (μg/mL)						
			S ≤ 4, I = 8, R ≥ 16			
				MHB pH		LPM pH
MHB Agar	Ca-MHB	DMEM	5.5	LPM pH 7	5.5
2	1	8	2	1	0.5
2	1	8	2	2	0.5
2	1	8	1	2	1
2	1	8	2	2	0.5

Azithromycin (μg/mL)						
			S ≤ 16, R ≥ 32[193]			
				MHB pH		LPM pH
Ca-MHB	DMEM	5.5	LPM pH 7	5.5
8	2	NA	NA	NA
8	2	NA	NA	NA
4	2	NA	NA	NA
8	2	NA	NA	NA

Erythromycin (μg/mL)						
				MHB pH	LPM pH	LPM pH
Ca-MHB	DMEM	5.5	7	5.5
64	32	NA	NA	NA
64	32	NA	NA	NA
64	64	NA	NA	NA
64	32	NA	NA	NA

Chloramphenicol (μg/mL)						
Clinical Breakpoints:			S ≤ 8, I = 16, R ≥ 32			
				MHB pH		LPM pH
Strain Name	MHB Agar	Ca-MHB	DMEM	5.5	LPM pH 7	5.5
Y. pseudotuberculosis YPIII/pIB1	8	8	8	8	4	2
Y. pseudotuberculosis IP32953	4	8	8	8	4	2
Y. pseudotuberculosis IP2515	8	4	4	8	8	8
Y. pseudotuberculosis IP2666	8	8	8	8	8	2

Florfenicol (μg/mL)						
				MHB pH		LPM pH
MHB Agar	Ca-MHB	DMEM	5.5	LPM pH 7	5.5
4	4	4	8	4	4
4	4	4	8	4	4
4	4	4	8	8	8
4	4	4	8	4	4

Nalidixic Acid (μg/mL)						
			S ≤ 16, R ≥ 32			
				MHB pH		LPM pH
MHB Agar	Ca-MHB	DMEM	5.5	LPM pH 7	5.5
0.5	0.5	2	0.5	0.5	0.25
0.5	1	2	0.5	0.5	0.25
0.5	1	2	1	1	0.5
0.5	1	2	0.5	1	0.25

Ciprofloxacin (μg/mL)						
			S ≤ 1, I = 2, R ≥ 4			
				MHB pH		LPM pH
MHB Agar	Ca-MHB	DMEM	5.5	LPM pH 7	5.5
0.0078	0.0078	0.0039	NA	NA	NA
0.0156	0.0156	0.0078	NA	NA	NA
0.0156	0.0156	0.0078	NA	NA	NA
0.0078	0.0078	0.0078	NA	NA	NA

Enrofloxacin (μg/mL)						
			S ≤ 0.5, I = 1, R ≥ 2[193]			
				MHB pH	LPM pH	LPM pH
MHB Agar	Ca-MHB	DMEM	5.5	7	5.5
0.0039	0.0039	0.0156	NA	NA	NA
0.03125	0.0078	0.03125	NA	NA	NA
0.0078	0.0039	0.0156	NA	NA	NA
0.0078	0.0078	0.0156	NA	NA	NA

MHB and DMEM MICs were determined by broth microdilution in accordance with CLSI guidelines. DMEM MICs were incubated in a 5% CO2 incubator. S = Susceptible, NS = Non-Susceptible, I = Intermediate, R = Resistant.
[a]All Clinical Breakpoints are referenced from the CLSI 2014 twenty-fourth informational supplement (*192*) unless otherwise indicated.

Table 4.2f. Antimicrobial susceptibility testing in host-mimicking media (Gram-negative bacteria).

		Polymyxin B (μg/mL)					Colistin Sulfate (μg/mL)					Ceftiofur (μg/mL)					Ceftriaxone (μg/mL)					Ampicillin (μg/mL)				
Clinical Breakpoints[a]		S ≤ 2, R ≥ 4[189]					S ≤ 2, R ≥ 4[197]					S ≤ 2, I = 4, R ≥ 8[189]					S ≤ 1, I = 2, R ≥ 4					S ≤ 8, I = 16, R ≥ 32				
Strain	Strain Name	Ca-MHB	DMEM	MHB pH 5.5	LPM pH 7	LPM pH 5.5	Ca-MHB	DMEM	MHB pH 5.5	LPM pH 7	LPM pH 5.5	Ca-MHB	DMEM	MHB pH 5.5	LPM pH 7	LPM pH 5.5	Ca-MHB	DMEM	MHB pH 5.5	LPM pH 7	LPM pH 5.5	Ca-MHB	DMEM	MHB pH 5.5	LPM pH 7	LPM pH 5.5
MT1942	*Shigella flexneri* ATCC 29903	0.25	1	NA	NA	NA	0.25	1	NA	NA	NA	0.25	0.125	NA	NA	NA	0.03125	0.0156	NA	NA	NA	2	2	NA	NA	NA
MT1944	*Providencia stuartii* ATCC 29914	32	256	NA	NA	NA	64	512	NA	NA	NA	0.25	0.5	NA	NA	NA	0.0156	0.0625	NA	NA	NA	32	64	NA	NA	NA
MT1946	*Citrobacter freundii* ATCC 8090	0.5	2	1	4	16	0.5	2	2	4	16	0.5	0.5	256	0.5	16	0.125	0.0625	8	0.0625	1	16	128	16	32	8
MT1947	*Klebsiella pneumoniae* ATCC 13883	8	16	128	128	512	16	16	128	128	512	1	1	2	0.5	1	0.125	0.125	0.125	0.03125	0.0625	256	256	256	128	256
Clinical Breakpoints:		S ≤ 2, I = 4, R ≥ 8					S ≤ 2, I = 4, R ≥ 8					S ≤ 2, I = 4, R ≥ 8[b]														
MT1945	*Pseudomonas aeruginosa* ATCC 10145	2	8	1	2	32	1	16	1	2	32	64	32	32	4	16	8	8	16	0.5	16	128	256	512	16	64

		Trimethoprim (μg/mL)					Co-trimoxazole (μg/mL)					Spectinomycin (μg/mL)					Streptomycin (μg/mL)					Kanamycin (μg/mL)				
Clinical Breakpoints:		S ≤ 8, R ≥ 16					S ≤ 2/38, R ≥ 4/76					S ≤ 32; I = 64-128; R ≥ 256[189]					S ≤ 8, I = 16, R ≥ 32[189]					S ≤ 16, I = 32, R ≥ 64				
Strain	Strain Name	Ca-MHB	DMEM	MHB pH 5.5	LPM pH 7	LPM pH 5.5	Ca-MHB	DMEM	MHB pH 5.5	LPM pH 7	LPM pH 5.5	Ca-MHB	DMEM	MHB pH 5.5	LPM pH 7	LPM pH 5.5	Ca-MHB	DMEM	MHB pH 5.5	LPM pH 7	LPM pH 5.5	Ca-MHB	DMEM	MHB pH 5.5	LPM pH 7	LPM pH 5.5
MT1942	*Shigella flexneri* ATCC 29903	0.25	0.25	NA	NA	NA	0.25/4.8	0.125/2.4	NA	NA	NA	64	16	NA	NA	NA	8	2	NA	NA	NA	4	8	NA	NA	NA
MT1944	*Providencia stuartii* ATCC 29914	2	2	NA	NA	NA	0.25/4.8	0.0625/1.2	NA	NA	NA	>512	>512	NA	NA	NA	64	128	NA	NA	NA	0.5	4	NA	NA	NA
MT1946	*Citrobacter freundii* ATCC 8090	1	1	32	0.5	16	0.0625/1.2	0.0625/1.2	NA	NA	NA	32	16	NA	NA	NA	4	1	NA	NA	NA	2	8	NA	NA	NA
MT1947	*Klebsiella pneumoniae* ATCC 13883	2	1	32	4	128	0.25/4.8	0.03125/0.6	NA	NA	NA	16	8	NA	NA	NA	2	1	NA	NA	NA	1	4	NA	NA	NA
Clinical Breakpoints:																										
MT1945	*Pseudomonas aeruginosa* ATCC 10145	512	>512	>512	16	256	32/608	32/608	NA	NA	NA	>512	512	NA	NA	NA	64	32	NA	NA	NA	64	512	NA	NA	NA

		Neomycin (μg/mL)					Gentamicin (μg/mL)					Tetracycline (μg/mL)					Azithromycin (μg/mL)					Erythromycin (μg/mL)				
Clinical Breakpoints:		S ≤ 8, I = 16, R ≥ 32[189]					S ≤ 4, I = 8, R ≥ 16					S ≤ 4, I = 8, R ≥ 16					S ≤ 16, R ≥ 32[193]									
Strain	Strain Name	Ca-MHB	DMEM	MHB pH 5.5	LPM pH 7	LPM pH 5.5	Ca-MHB	DMEM	MHB pH 5.5	LPM pH 7	LPM pH 5.5	Ca-MHB	DMEM	MHB pH 5.5	LPM pH 7	LPM pH 5.5	Ca-MHB	DMEM	MHB pH 5.5	LPM pH 7	LPM pH 5.5	Ca-MHB	DMEM	MHB pH 5.5	LPM pH 7	LPM pH 5.5
MT1942	*Shigella flexneri* ATCC 29903	4	4	NA	NA	NA	1	2	NA	NA	NA	1	4	NA	NA	NA	2	1	NA	NA	NA	32	16	NA	NA	NA
MT1944	*Providencia stuartii* ATCC 29914	0.5	8	NA	NA	NA	0.5	2	NA	NA	NA	128	64	NA	NA	NA	32	16	NA	NA	NA	256	128	NA	NA	NA
MT1946	*Citrobacter freundii* ATCC 8090	1	4	NA	NA	NA	0.5	1	NA	NA	NA	1	8	2	0.5	1	8	8	NA	NA	NA	256	128	NA	NA	NA
MT1947	*Klebsiella pneumoniae* ATCC 13883	0.5	2	NA	NA	NA	0.25	0.5	NA	NA	NA	1	16	2	1	4	8	4	NA	NA	NA	64	64	NA	NA	NA
Clinical Breakpoints:							S ≤ 4, I = 8, R ≥ 16																			
MT1945	*Pseudomonas aeruginosa* ATCC 10145	16	256	NA	NA	NA	4	32	NA	NA	NA	64	>512	32	1	4	256	32	NA	NA	NA	512	128	NA	NA	NA

		Chloramphenicol (μg/mL)					Florfenicol (μg/mL)					Nalidixic Acid (μg/mL)					Ciprofloxacin (μg/mL)					Enrofloxacin (μg/mL)				
Clinical Breakpoints:		S ≤ 8, I = 16, R ≥ 32										S ≤ 16, R ≥ 32					S ≤ 1, I = 2, R ≥ 4					S ≤ 0.5; I = 1; R ≥ 2[203]				
Strain	Strain Name	Ca-MHB	DMEM	MHB pH 5.5	LPM pH 7	LPM pH 5.5	Ca-MHB	DMEM	MHB pH 5.5	LPM pH 7	LPM pH 5.5	Ca-MHB	DMEM	MHB pH 5.5	LPM pH 7	LPM pH 5.5	Ca-MHB	DMEM	MHB pH 5.5	LPM pH 7	LPM pH 5.5	Ca-MHB	DMEM	MHB pH 5.5	LPM pH 7	LPM pH 5.5
MT1942	*Shigella flexneri* ATCC 29903	2	1	NA	NA	NA	1	1	NA	NA	NA	2	8	NA	NA	NA	0.0156	0.0078	NA	NA	NA	0.0156	0.0625	NA	NA	NA
MT1944	*Providencia stuartii* ATCC 29914	32	32	NA	NA	NA	4	8	NA	NA	NA	2	4	NA	NA	NA	0.0156	0.0156	NA	NA	NA	0.0625	0.125	NA	NA	NA
MT1946	*Citrobacter freundii* ATCC 8090	4	8	8	4	4	4	8	8	8	8	4	8	2	1	2	0.0039	0.0039	NA	NA	NA	0.0156	0.03125	NA	NA	NA
MT1947	*Klebsiella pneumoniae* ATCC 13883	8	8	8	8	16	4	8	8	8	16	4	16	4	16	8	0.03125	0.03125	NA	NA	NA	0.03125	0.125	NA	NA	NA
Clinical Breakpoints:																	S ≤ 1, I = 2, R ≥ 4									
MT1945	*Pseudomonas aeruginosa* ATCC 10145	256	128	256	4	16	512	256	256	8	64	256	256	64	16	256	0.125	0.25	NA	NA	NA	1	2	NA	NA	NA

MHB and DMEM MICs were determined by broth microdilution in accordance with CLSI guidelines. DMEM MICs were incubated in a 5% CO2 incubator. S = Susceptible, NS = Non-Susceptible, I = Intermediate, R = Resistant.

[a]All Clinical Breakpoints are referenced from the CLSI 2014 twenty-fourth informational supplement (*192*) unless otherwise indicated.

Table 4.3a. Antimicrobial susceptibility test in media w/ and w/o $NaHCO_3$ (*Staphylococcus*)

"Susceptible" MIC
"Intermediate" MIC
"Resistant" MIC

		Cephalothin MIC (µg/mL)					
Clinical Breakpoints[a]:		S ≤ 8; I = 16; R ≥ 32[192]					
Strain #	Strain Name	Ca-MHB pH 7.2	Ca-MHB 100 mM Tris pH 7.2	Ca-MHB 100 mM Tris 44 mM $NaHCO_3$ pH 7.4	DMEM + 5% LB pH 7.4	DMEM + 5% LB 100 mM Tris 44 mM $NaHCO_3$ pH 7.4	DMEM + 5% LB 100 mM Tris (w/o $NaHCO_3$) pH 7.4
MT3322	MRSA USA300	32	32	8	4	4	4
MT3315	MRSA Wound	8	4	1	0.5	0.5	0.5

		Ceftiofur MIC (µg/mL)					
Clinical Breakpoints:		S ≤ 2; I = 4; R ≥ 8[192]					
Strain #	Strain Name	Ca-MHB pH 7.2	Ca-MHB 100 mM Tris pH 7.2	Ca-MHB 100 mM Tris 44 mM $NaHCO_3$ pH 7.4	DMEM + 5% LB pH 7.4	DMEM + 5% LB 100 mM Tris 44 mM $NaHCO_3$ pH 7.4	DMEM + 5% LB 100 mM Tris (w/o $NaHCO_3$) pH 7.4
MT3322	MRSA USA300	64	128	8	8	4	8

		Ceftriaxone MIC (µg/mL)					
Clinical Breakpoints:		S ≤ 8; I =16-32; R ≥ 64[190]					
Strain #	Strain Name	Ca-MHB pH 7.2	Ca-MHB 100 mM Tris pH 7.2	Ca-MHB 100 mM Tris 44 mM $NaHCO_3$ pH 7.4	DMEM + 5% LB pH 7.4	DMEM + 5% LB 100 mM Tris 44 mM $NaHCO_3$ pH 7.4	DMEM + 5% LB 100 mM Tris (w/o $NaHCO_3$) pH 7.4
MT3322	MRSA USA300	512	256	16	16	16	32
MT3302	MRSA Blood	128	64	32	16	8	8
MT3315	MRSA Wound	64	64	32	8	16	8

		Ampicillin MIC (µg/mL)					
Clinical Breakpoints:		S ≤ 0.25; R ≥ 0.5[190]					
Strain #	Strain Name	Ca-MHB pH 7.2	Ca-MHB 100 mM Tris pH 7.2	Ca-MHB 100 mM Tris 44 mM $NaHCO_3$ pH 7.4	DMEM + 5% LB pH 7.4	DMEM + 5% LB 100 mM Tris 44 mM $NaHCO_3$ pH 7.4	DMEM + 5% LB 100 mM Tris (w/o $NaHCO_3$) pH 7.4
MT3315	MRSA Wound	8	8	2	0.5	1	4

		Oxacillin MIC (µg/mL)					
Clinical Breakpoints:		S ≤ 2; R ≥ 4					
Strain #	Strain Name	Ca-MHB pH 7.2	Ca-MHB 100 mM Tris pH 7.2	Ca-MHB 100 mM Tris 44 mM $NaHCO_3$ pH 7.4	DMEM + 5% LB pH 7.4	DMEM + 5% LB 100 mM Tris 44 mM $NaHCO_3$ pH 7.4	DMEM + 5% LB 100 mM Tris (w/o $NaHCO_3$) pH 7.4
MT3302	MRSA Blood	64	64	16	4	8	32
MT3315	MRSA Wound	32	64	32	1	1	16

		Trimethoprim MIC (µg/mL)					
Clinical Breakpoints:		S ≤ 8; R ≥ 16					
Strain #	Strain Name	Ca-MHB pH 7.2	Ca-MHB 100 mM Tris pH 7.2	Ca-MHB 100 mM Tris 44 mM $NaHCO_3$ pH 7.4	DMEM + 5% LB pH 7.4	DMEM + 5% LB 100 mM Tris 44 mM $NaHCO_3$ pH 7.4	DMEM + 5% LB 100 mM Tris (w/o $NaHCO_3$) pH 7.4
MT3307	MSSA Wound	2	1	1	>512	>512	>512

		Co-Trimoxazole MIC (µg/mL)					
Clinical Breakpoints:		S ≤ 2/38; R ≥ 4/76					
Strain #	Strain Name	Ca-MHB pH 7.2	Ca-MHB 100 mM Tris pH 7.2	Ca-MHB 100 mM Tris 44 mM $NaHCO_3$ pH 7.4	DMEM + 5% LB pH 7.4	DMEM + 5% LB 100 mM Tris 44 mM $NaHCO_3$ pH 7.4	DMEM + 5% LB 100 mM Tris (w/o $NaHCO_3$) pH 7.4
MT3307	MSSA Wound	0.125/2.4	0.0625/1.2	0.125/2.4	>64/1216	>64/1216	>64/1216

		Tetracycline MIC (µg/mL)					
Clinical Breakpoints:		S ≤ 4; I = 8; R ≥ 16					
Strain #	Strain Name	Ca-MHB pH 7.2	Ca-MHB 100 mM Tris pH 7.2	Ca-MHB 100 mM Tris 44 mM $NaHCO_3$ pH 7.4	DMEM + 5% LB pH 7.4	DMEM + 5% LB 100 mM Tris 44 mM $NaHCO_3$ pH 7.4	DMEM + 5% LB 100 mM Tris (w/o $NaHCO_3$) pH 7.4
MT3322	MRSA USA300	0.5	0.5	2	4	2	1
MT3307	MSSA Wound	0.5	0.5	2	4	2	1
MT3320	CoN *S. epidermidis*	0.5	0.25	2	4	2	1
MT3321	CoN *S. warneri*	0.5	0.25	1	4	2	1

		Azithromycin MIC (µg/mL)					
Clinical Breakpoints:		S ≤ 2; I = 4; R ≥ 8					
Strain #	Strain Name	Ca-MHB pH 7.2	Ca-MHB 100 mM Tris pH 7.2	Ca-MHB 100 mM Tris 44 mM $NaHCO_3$ pH 7.4	DMEM + 5% LB pH 7.4	DMEM + 5% LB 100 mM Tris 44 mM $NaHCO_3$ pH 7.4	DMEM + 5% LB 100 mM Tris (w/o $NaHCO_3$) pH 7.4
MT3322	MRSA USA300	128	128	8	8	16	512
MT3302	MRSA Blood	128	256	8	8	16	512
MT3315	MRSA Wound	1	2	0.0625	0.125	0.25	8
MT3307	MSSA Wound	2	2	0.0625	0.125	0.25	4
MT3309	MSSA Urine	1	2	0.0625	0.125	0.25	8
MT3314	MSSA Sputum	2	2	0.0625	0.125	0.25	4
MT3320	CoN *S. epidermidis*	256	256	8	32	64	512
MT3321	CoN *S. warneri*	256	128	4	32	64	512

		Erythromycin MIC (µg/mL)					
Clinical Breakpoints:		S ≤ 0.5; I = 1 - 4; R ≥ 8					
Strain #	Strain Name	Ca-MHB pH 7.2	Ca-MHB 100 mM Tris pH 7.2	Ca-MHB 100 mM Tris 44 mM $NaHCO_3$ pH 7.4	DMEM + 5% LB pH 7.4	DMEM + 5% LB 100 mM Tris 44 mM $NaHCO_3$ pH 7.4	DMEM + 5% LB 100 mM Tris (w/o $NaHCO_3$) pH 7.4
MT3322	MRSA USA300	64	64	16	8	8	128
MT3302	MRSA Blood	128	128	16	8	16	128
MT3307	MSSA Wound	1	0.5	0.125	0.125	0.25	0.5
MT3314	MSSA Sputum	1	0.5	0.0625	0.125	0.25	1
MT3321	CoN *S. warneri*	256	128	8	32	64	256

		Nalidixic Acid MIC (µg/mL)					
Clinical Breakpoints:							
Strain #	Strain Name	Ca-MHB pH 7.2	Ca-MHB 100 mM Tris pH 7.2	Ca-MHB 100 mM Tris 44 mM $NaHCO_3$ pH 7.4	DMEM + 5% LB pH 7.4	DMEM + 5% LB 100 mM Tris 44 mM $NaHCO_3$ pH 7.4	DMEM + 5% LB 100 mM Tris (w/o $NaHCO_3$) pH 7.4
MT3307	MSSA Wound	32	32	256	256	256	64
MT3317	CoN *S. lugdunensis*	64	128	512	512	512	64
MT3320	CoN *S. epidermidis*	32	64	256	256	128	32

All MICs were determined by broth microdilution in accordance with CLSI guidelines. DMEM MICs were incubated in a 5% CO2 incubator. S = Susceptible, NS = Non-Susceptible, I = Intermediate, R = Resistant. [a]All Clinical Breakpoints are referenced from the CLSI 2014 twenty-fourth informational supplement (*192*) unless otherwise indicated.

Table 4.3b. Antimicrobial susceptibility test in media w/ and w/o $NaHCO_3$ (*Streptococcus*).

		Ceftriaxone MIC (µg/mL)		
Clinical Breakpoints[a]:		S ≤ 1; I = 2; R ≥ 4		
Strain	Capsular Serotype	Ca-MHB + 5% LHB pH 7.2	Ca-MHB + 5% LHB 100 mM Tris pH 7.2	Ca-MHB + 5% LHB 100 mM Tris 44 mM $NaHCO_3$ pH 7.4
Daw 2	23	2	2	4
		Ampicillin MIC (µg/mL)		
Clinical Breakpoints:		S ≤ 0.5; I = 1-2; R ≥ 4[(197)]		
Strain	Capsular Serotype	Ca-MHB + 5% LHB pH 7.2	Ca-MHB + 5% LHB 100 mM Tris pH 7.2	Ca-MHB + 5% LHB 100 mM Tris 44 mM $NaHCO_3$ pH 7.4
Daw 1	6	2	2	4
Daw 2	23	0.5	1	2
		Azithromycin MIC (µg/mL)		
Clinical Breakpoints:		S ≤ 0.5; I = 1; R ≥ 2		
Strain	Capsular Serotype	Ca-MHB + 5% LHB pH 7.2	Ca-MHB + 5% LHB 100 mM Tris pH 7.2	Ca-MHB + 5% LHB 100 mM Tris 44 mM $NaHCO_3$ pH 7.4
D39	2	0.25	0.25	0.0156
		Erythromycin MIC (µg/mL)		
Clinical Breakpoints:		S ≤ 0.25; I = 0.5; R ≥ 1		
Strain	Capsular Serotype	Ca-MHB + 5% LHB pH 7.2	Ca-MHB + 5% LHB 100 mM Tris pH 7.2	Ca-MHB + 5% LHB 100 mM Tris 44 mM $NaHCO_3$ pH 7.4
D39	2	0.125	0.125	0.0156

All MICs were determined by broth microdilution in accordance with CLSI guidelines. MIC plates were incubated in a 5% CO2 incubator. S = Susceptible, NS = Non-Susceptible, I = Intermediate, R = Resistant.

[a]All Clinical Breakpoints are referenced from the CLSI 2014 twenty-fourth informational supplement (*192*) unless otherwise indicated.

Table 4.3c. Antimicrobial susceptibility test in media w/ and w/o $NaHCO_3$ (*Salmonella*).

	Tetracycline MIC (µg/mL)					
Clinical Breakpoints[a]:	S ≤ 4, I = 8, R ≥ 16					
Strain Name	Ca-MHB pH 7.2	Ca-MHB 100 mM Tris pH 7.2	Ca-MHB 100 mM Tris 44 mM $NaHCO_3$ pH 7.4	DMEM pH 7.4	DMEM 100 mM Tris 44 mM $NaHCO_3$ pH 7.4	DMEM 100 mM Tris (w/o $NaHCO_3$) pH 7.4
S. Typhimurium 14028	1	1	4	8	8	1
S. Choleraesuis χ3246	1	1	2	8	4	2
	Azithromycin MIC (µg/mL)					
Clinical Breakpoints:	S ≤ 16, R ≥ 32[(197)]					
Strain Name	Ca-MHB pH 7.2	Ca-MHB 100 mM Tris pH 7.2	Ca-MHB 100 mM Tris 44 mM $NaHCO_3$ pH 7.4	DMEM pH 7.4	DMEM 100 mM Tris 44 mM $NaHCO_3$ pH 7.4	DMEM 100 mM Tris (w/o $NaHCO_3$) pH 7.4
S. Typhimurium 14028	8	8	0.125	2	2	16
S. Choleraesuis χ3246	8	8	0.25	2	2	16
	Erythromycin MIC (µg/mL)					
Clinical Breakpoints:						
Strain Name	Ca-MHB pH 7.2	Ca-MHB 100 mM Tris pH 7.2	Ca-MHB 100 mM Tris 44 mM $NaHCO_3$ pH 7.4	DMEM pH 7.4	DMEM 100 mM Tris 44 mM $NaHCO_3$ pH 7.4	DMEM 100 mM Tris (w/o $NaHCO_3$) pH 7.4
S. Typhimurium 14028	128	128	8	32	32	128
S. Choleraesuis χ3246	128	64	8	32	32	128

All MICs were determined by broth microdilution in accordance with CLSI guidelines. DMEM MICs were incubated in a 5% CO2 incubator. S = Susceptible, NS = Non-Susceptible, I = Intermediate, R = Resistant.

[a]All Clinical Breakpoints are referenced from the CLSI 2014 twenty-fourth informational supplement (*192*) unless otherwise indicated.

Chapter 5

Ex Vivo Antimicrobial Susceptibility Testing

ABSTRACT

Antibiotic-resistant bacterial pathogens progressively impede effective treatment of infections and will require advanced diagnostic strategies to optimize the use of currently available antimicrobials. Determination of antibiotic susceptibility in host microenvironments, such as urine and serum, is an attractive option for improving the accuracy of antibiotic selection. Unfortunately, many pathogens do not grow to sufficient density in host fluids to permit routine susceptibility testing. In this study, we developed a rich-media supplementation and aggregate-disruption strategy which enables growth and testing of clinically relevant Gram-positive and -negative pathogens in healthy pooled urine and serum. This assay provides a convenient phenotypic screen for the potential of a patient isolate to be signaled by its environment to become transiently susceptible or resistant to an antibiotic. Testing performed in host fluids frequently identified treatments that are discordant with the standard testing media, which may impact treatment outcome at similar sites of infection. The assay also identified many viable treatment options which are not predicted to lose efficacy in the microenvironments represented by these testing fluids. Further studies are needed to validate the accuracy of this assay to identify effective treatments for murine in vivo infection models and human sepsis patients.

5.1. INTRODUCTION

The prevalence of antibiotic resistance is growing at a rate which is outpacing novel antibiotic discovery (*1, 203*), with carbapenem and colistin resistance representing particularly urgent threats against our last-line therapeutics (*204-206*). Clinicians therefore need approaches for antimicrobial prescription that can better leverage the large arsenal of currently available antibiotics. One useful strategy is to improve the accuracy of the antimicrobial susceptibility tests (AST) which clinicians rely on to select appropriate individualized therapy. In standard AST, a patient's pathogen isolate is grown in rich media and screened against a panel of relevant antibiotics to identify the most effective treatment. Unfortunately, this method is frequently incorrect, and 10% of AST-recommended therapies will fail, while also excluding roughly 40% of truly effective therapies, in what has been termed the "90-60 rule" (*48-50*). A likely explanation for these incorrect AST predictions is that the pathogens are experiencing transiently altered resistance in the host environment which is not observed when tested in standard culture media (*54*).

Bacterial pathogens commonly exhibit transient altered susceptibility to antimicrobials within conditions that mimic the host microenvironment (*207*). These changes have been confirmed in vivo, or clinically for many pathogens, including *Salmonella (54), Klebsiella, Pseudomonas, Acinetobacter* (*166*), *Enterobacter* (*165*)*, E. coli* (*57*)*,* and *Staphylococcus* (*58*)*.* Susceptibility changes have also been confirmed in a variety of host microenvironments, such as the macrophage phagosome (*54*), urine (*57*), and synovial fluids (*58*). An AST method that can correctly identify altered resistance or susceptibility within the host could permit

targeted prescription based on site of infection, or complete susceptibility (without any transient resistance phenotypes).

Previous studies have successfully demonstrated this phenomenon in human fluids, and even developed universal host-mimicking testing strategies (*207, 208*). However, a convenient testing strategy that is compatible with a wide range of pathogens in human urine and serum would provide an optimal ex vivo diagnostic for susceptibility, and has yet to be demonstrated in the literature. The “Schlichter test” (*209*) is a classic approach which evaluates the efficacy of diluted patient sera (during therapy) against an isolate grown in rich media. This test provides an excellent evaluation of an administered drug’s stability and availability in the patient’s serum, but does not sensitize the bacterial isolate to serum before exposure. Additionally, Thulin et al. (*57*) successfully conducted AST for a single pathogen (*E. coli*) in urine, but do not demonstrate compatibility with other important organisms, such as urinary sepsis pathogens (e.g., *Staphylococcus*, *Pseudomonas*, or *Klebsiella*).

Here, we developed a universal ex vivo assay to evaluate antibiotic susceptibility of environmentally sensitized pathogens in donor human urine and serum. Serum and urine can inhibit high-level growth of pathogens, which is required for robust AST, and was addressed via a universal nutrient supplementation strategy following initial culture sensitization to raw fluids. The assay supported evaluation of a small but diverse collection of significant Gram-positive and -negative human pathogens. These included urinary sepsis patient isolates, and representatives from each of the ESKAPE pathogens (*Enterococcus, Staphylococcus, Klebsiella,*

Acinetobacter, Pseudomonas, and *Enterobacter* species) (*210*) which were tested against a panel of clinically relevant antimicrobials. Large changes in susceptibility were frequently observed for pathogens tested in human fluids, which provides a convenient phenotypic screen for transient resistance that is ready to be evaluated in an in vivo or clinical context.

5.2. RESULTS

5.2.1. Overview of the Universal Ex Vivo Antimicrobial Susceptibility Test

To best recapitulate the host microenvironments, pathogens were cultured in raw donor urine and serum without supplementation whenever possible. During culture in human donor serum (18 h, without aeration, at 37 °C and a 5% CO_2 atmosphere), the majority of evaluated pathogens (10/11) consistently grew to high enough cell densities for use in the AST assay. From a 0.5 mL overnight culture, a minimum density of 5 x 10^7 CFU/mL is required, to have enough cells subcultured at 1 x 10^6 CFU/mL for a 12-drug AST panel. In serum overnight cultures, all pathogens other than *Acinetobacter baumannii* grew to sufficient densities for the AST assay **(Figure 5.1a)**. To consistently reach the requisite density, *A. baumannii* was cultured and tested in heat-inactivated serum with 40% v/v Ca-MHB (cation-adjusted Mueller-Hinton Broth) supplementation. For urine cultures (18 h, with aeration, at 37 °C in ambient atmosphere), all pathogens tested grew to sufficient densities without supplementation **(Figure 5.1a)**.

Although growth of the overnight cultures in test tubes is relatively robust, growth without supplementation in microtiter wells did not provide enough turbidity to clearly determine an MIC (**Figure 5.2b,d**). Further, several pathogens were observed to form resilient aggregates when grown in serum or urine, which impaired accurate enumeration and subculture without adequate agitation to disrupt them. We have thus established a supplementation and aggregate disruption protocol to enable antibiotic susceptibility determination in urine and serum for all pathogens tested (**Figure 5.1b**). A single colony of a pathogen isolate is first inoculated into un-

supplemented raw pooled urine or serum from healthy donors. The culture is incubated at 37 °C for 18 hours (urine is aerated, serum is under 5% CO_2) which potentially serves to “sensitize” the pathogen to the microenvironment prior to antibiotic exposure. Next, the culture is vortexed for 15 seconds in the culture tube, transferred to a microfuge tube, vortexed for 15 more seconds, and then diluted in 10-fold increments to a final concentration of 2 x 10^6 CFU/mL in supplemented fluids, with 5 seconds of vortexing at each step. The subculture is then immediately diluted two-fold into a microtiter dish containing serial dilutions of antibiotics in supplemented urine or serum. These microtiter dishes are then incubated at 37 °C for 20 hours, with 5% CO_2 (serum) or ambient atmosphere (urine), after which the MIC is visually determined based on the loss of turbid growth. The MIC is the lowest drug concentration that inhibits growth.

5.2.2. Evaluation of Supplementation for Growth in Microtiter Assay Plates

To minimize the potential impact of supplementation on microenvironmental signaling, we sought to optimize the timing by comparing the effects of supplementation during specimen overnight culture, or only for subsequent AST. For *ST* (*S.* Typhimurium), growth in serum without supplementation was insufficient for high viability at the end of AST incubation in microtiter plates (2 x 10^8 CFU/mL after 20 hours). However, supplementation of the microtiter dish subculture media was sufficient for high viability (2 x 10^9 CFU/mL after 20 hours), without requiring supplementation of the initial overnight culture (**Figure 5.2a**). This viability resulted in high turbidity in the microtiter dishes, which is absent without supplementation

(**Figure 5.2b**). To evaluate the impact of supplementation on antibiotic susceptibility, *ST* was compared against a small panel of antibiotics with or without culture supplementation prior to testing in supplemented test media (**Figure 5.2c**). Susceptibility in serum was similar with and without supplementation of the initial overnight culture. We also compared the effects of supplementation on assay turbidity between two commonly available rich media, LB (Luria-Bertani) medium or Ca-MHB, in urine and serum for four pathogens. Both media equally supported growth in the microtiter plates, and to a greater extent than un-supplemented urine or serum (**Figure 5.2d**), which may provide future options when testing somewhat fastidious organisms. We elected to proceed with using LB-supplementation in the test media, without overnight culture supplementation.

5.2.3. Antimicrobial MICs Are Markedly Different When Determined Using Ex Vivo Human Fluids, vs Standard Ca-MHB Medium.

A collection of human and veterinary clinical bacterial isolates was evaluated for AST using ex vivo human specimens, compared to host-mimicking tissue-culture media and the standard Ca-MHB medium. Four total media were evaluated, including (i) pooled donor serum, collected from several hundred healthy donors, and frozen before use; (ii) pooled donor urine, collected from 2 or more normal donors in multiple voidings and frozen before use; (iii) Dulbecco's Modified Eagle Medium (DMEM), a tissue culture medium used for mammalian cell growth (*167*); and (iv), Cation-adjusted Mueller-Hinton Broth (Ca-MHB) standard AST broth medium.

Gram-positive (Staphylococcus, Enterococcus). A panel of antimicrobials used in human medicine for treatment of generalized infections and sepsis, was tested for efficacy against clinical isolates of methicillin-resistant and -sensitive *S. aureus*, and *Enterococcus faecium* (**Figure 5.3a**). Assaying in host-mimicking DMEM medium and urine generally increased the susceptibility of *Staphylococcus* to the cephalosporins (ceftriaxone, cephalexin) up to 32-fold; interestingly, this DMEM behavior was loosely mirrored within urine, while not in serum. In both urine and serum, the combination therapy trimethoprim/sulfamethoxazole (co-trimoxazole) exhibited consistent and frequently extreme increases in resistance (in one case > 512-fold more resistant vs standard Ca-MHB for MRSA Blood in urine). **Table 5.1** lists potential therapeutic options for each pathogen tested, including (i) antibiotics which become more effective in one or more host-mimicking or ex vivo medium (classified as “I” or “R” changing to “S” or “I”, with ≥ 8-fold increase in susceptibility); (ii) antibiotics that demonstrate increased resistance in host-mimicking DMEM or ex vivo media (“classified as “S” changing to “I” or “R”, with ≥ 8-fold decrease in susceptibility); and (iii) antibiotics that are susceptible in standard Ca-MHB medium with no change in any other medium (classified as “S” in all conditions and ≤ 4-fold increase in MIC for any medium). For example, treatment of MSSA Newman would likely be effective using imipenem (which is classified as strongly “S” in all conditions, **Table 5.2a**), but may unexpectedly also respond well to cephalexin (classified as “R” in standard media, but “S” in all other media). Conversely, azithromycin would be a poor therapeutic choice (particularly for treatment of urinary

tract infection, 64-fold more resistant in urine) despite apparent sensitivity in standard Ca-MHB media.

Gram-negative Bacteria (Salmonella, Escherichia, Klebsiella, Enterobacter, Pseudomonas, Acinetobacter). Changes in antibiotic susceptibility were also evaluated with a collection of Gram-negative human pathogens, in standard Ca-MHB medium, host-mimicking DMEM medium, and ex vivo human fluids (**Figure 5.3b**). All Gram-negative pathogens demonstrated increased resistance to colistin and tetracycline in host-mimicking DMEM medium, and to azithromycin and ciprofloxacin in urine. Multiple pathogens were also more resistant to streptomycin and co-trimoxazole in urine. Excretion of dietary folate and its metabolites into urine is a potential explanation for some cases of the observed increased resistance to co-trimoxazole (a folate synthesis inhibitor cocktail), as has been previously described for Enterococci (*211, 212*). However this is not expected to be universal in urine, as many pathogens do not utilize exogenous folate (*213-216*) and increased resistance was not observed for all pathogens with urine in the present study. Neither *P. aeruginosa* nor *A. baumannii* exhibited increased resistance to co-trimoxazole in urine (**Table 5.2b**), further suggesting that excreted folate interference is not solely responsible for co-trimoxazole resistance in urine in this study. If a high urine folate level was simply counteracting the effects of co-trimoxazole, all pathogens would be expected to have exhibited increased resistance in urine (although this may indeed be happening in some cases, such as with *Enterococcus*). Relatively fewer changes were observed in serum, although notably a high-level multi-drug resistant urinary sepsis isolate of *K. pneumoniae* (MT3325) demonstrated a 16-fold susceptibility

increase to azithromycin when in serum (**Table 5.2b**), but not in urine. Azithromycin may have been an effective treatment for the lethal *K. pneumoniae* urine isolate, which had few other therapeutic options.

5.2.4. Comparison Summary of Altered MICs Observed Between Ex Vivo or Host-mimicking Media vs Standard Ca-MHB Medium.

We evaluated the percentage of total pathogen-antibiotic combinations that exhibited an altered MIC when tested in host-mimicking or ex vivo conditions, relative to standard Ca-MHB media (**Figure 5.4a**). For the antibiotics and pathogens selected in this study, the majority of MIC results (> 54% in each media) were within 2-fold of the standard Ca-MHB media results, and the fewest changes occurred when testing in serum (64.8% remain the same) compared to urine and host-mimicking media (55% remained the same as Ca-MHB for both). We also evaluated the percentages of MIC changes that would alter clinician decision making by crossing clinical breakpoints. (**Figure 5.4b**). For the pathogens and antibiotics selected in this study, 19.2% (24/125) of pathogen-antibiotic combinations crossed a clinical breakpoint when tested in host-mimicking DMEM media, 15.2% (19/125) in serum, and 19.2% (24/125) in urine. A substantially higher percentage of breakpoint changes was observed within DMEM in this study than in our previous study (currently 19.2%, compared to 6.6% in Ersoy et al. 2017 (*207*)). The panel of antimicrobials selected in this study was designed to include compounds with known susceptibility changes in host-mimicking media, and thus an increased frequency of breakpoint changes was anticipated.

5.3. DISCUSSION

Antibiotic resistant bacteria are responsible for an estimated 2.8 million infections and > 35,000 deaths in the United States per year, and novel resistance is emerging far faster than new therapeutics can be developed (*20, 203*). It is therefore crucial to develop new approaches to better utilize the currently available antimicrobials to treat multi-drug resistant pathogens. Bacterial adaptations to the host microenvironment often lead to changes in antibiotic resistance (*56, 57, 166*), which presents an opportunity to tailor prescriptions to the unique susceptibilities of the pathogen at the site of infection. Towards this end, we have developed an AST method that enables testing directly within donor urine and serum, which is compatible with a small but diverse collection of human pathogens, including the ESKAPE pathogens. In our study, insufficient microbial growth in human fluids was a substantial hurdle for testing a wide range of pathogens. Development of a universal assay was achieved using a convenient supplementation and aggregate disruption protocol to permit accurate inoculation and sufficient growth to perform AST.

We observed many large changes in antimicrobial susceptibility when pathogens are tested in urine or serum, which vary between pathogens and environmental conditions. Due to this variability, a patient's individual pathogen isolate should be tested for its unique responses to the host environment, instead of generalized empirically by class. Further, this pathogen-specific variability precludes the risk that the observed changes are due to fluid-induced degradation of the antimicrobials; if this were the case, all pathogens would likely exhibit similar susceptibility changes relative to standard Ca-MHB media. Therefore, the

susceptibility changes observed represent phenotypic responses by the pathogen to the environment.

During a systemic infection, a pathogen is likely to transit between multiple host microenvironments with diverse signals (*217, 218*), making it prudent to understand which antibiotics a pathogen can become transiently resistant to, regardless of the test media. In that regard, this assay provides a phenotypic screening option that presents many host signals. The ideal therapeutics to select would be those which are highly effective in all media conditions, because the pathogen has not demonstrated an ability to become resistant under any of the host or host-mimicking signals provided by these media. This also provides the best estimate that a pathogen will not be signaled to become resistant, if it transits to an unanticipated environment during infection. Further, if a pathogen's transient sensitivity relies on an active gene (such as an environmental sensor or transcriptional repressor), a simple loss of function mutation could quickly facilitate universal resistance regardless of environmental signaling. Loss of function mutations have been shown to enhance bacterial adaptation in other environments (*219, 220*) and could potentially allow a pathogen to evade transient susceptibility by inactivating the sensor system that leads to it. This possibility makes treatments based on transient susceptibility a higher risk for mutational escape than a universally sensitive antimicrobial if available.

Some of the optimal antimicrobial therapeutics identified include ampicillin, ceftriaxone, cefalexin, linezolid, and vancomycin which when sensitive in standard Ca-MHB, are also always confirmed as sensitive in all test media within this study,

regardless of microenvironmental signaling. If there are few treatment options, such as was the case for *K. pneumoniae* urine, therapeutics that demonstrate media-specific sensitivity (e.g., azithromycin) may be helpful. This is particularly true if the suspected site of infection matches the test media that induced sensitivity, and ideally if the therapeutic can also be safely co-administered with a universally effective therapy (e.g., colistin and azithromycin for *K. pneumoniae* urine). Another strong example is MRSA Blood, for which ciprofloxacin, imipenem, linezolid, tetracycline, or vancomycin are effective in all media, and would potentially be universally effective; cephalexin could also be administered, or ceftriaxone if the pathogen is not infecting the blood.

Conversely, some therapeutics should also be avoided, particularly in suspected UTI, such as azithromycin, ciprofloxacin, streptomycin, and co-trimoxazole, which frequently demonstrate greatly enhanced resistance in urine. An important implication of this site-specific resistance is that the physiology of pathogenesis must be well understood before attempting to leverage transient resistance at a suspected site of infection. For instance, if a pathogen is isolated from the blood, it may only be transiting through, and be actually infecting a target organ with an entirely different microenvironment (*58, 221*), and therefore require a different antimicrobial to treat the source infection**.**

Although this study successfully developed a method of testing AST for a wide range of pathogens in ex vivo fluids, we have not evaluated the clinical relevance of the assay's results. This study is thus limited to providing phenotypic characterization of resistance profiles under ex vivo conditions, and cannot currently

be used to confidently predict treatment success or failure. In addition, the serum microenvironment is expected to substantially differ between the healthy donors used in this study vs. septic patients in the late stages of disease (*222-224*). In light of this, further experiments should assay a pathogen's susceptibility using the patient's own fluid specimens instead of healthy donor specimens, to the extent that sufficient testing volumes are available. Ultimately, clinical trials should be performed to compare the efficacy of standard empirical therapy to that of therapies augmented with ex vivo effective antimicrobials.

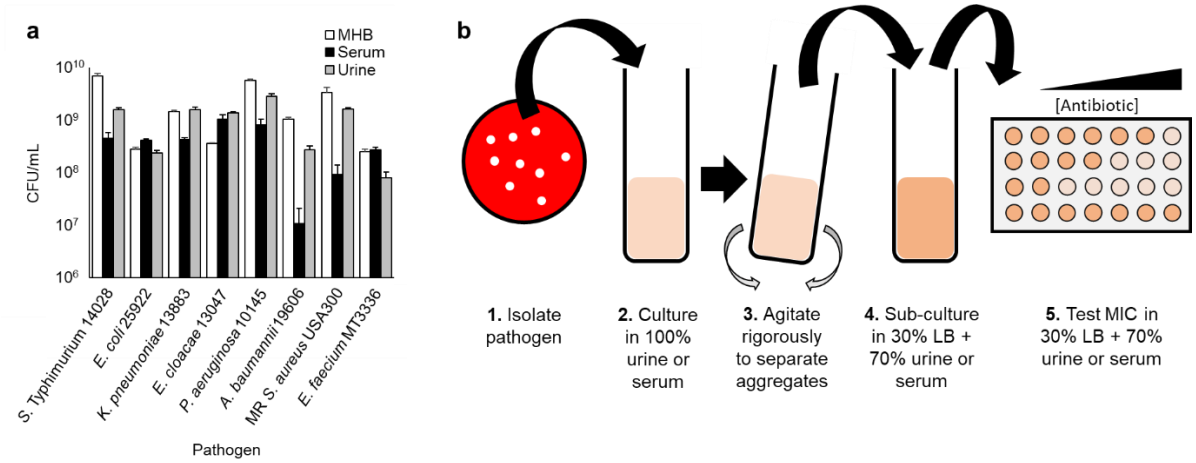

Figure 5.1. Overview of ex vivo antibiotic susceptibility test in human donor fluids. (**a**) Average viability (CFU/mL) of pathogen overnight cultures in Ca-MHB, donor serum, and urine. (**b**) Universal assay strategy for antibiotic susceptibility testing, in which pathogens are isolated, grown in 100% donor fluids, agitated to separate cell aggregates, subcultured into supplemented donor fluids, and tested in supplemented donor fluids against an increasing concentration of various antibiotics. n = 3 biological replicates, error bars represent one standard deviation.

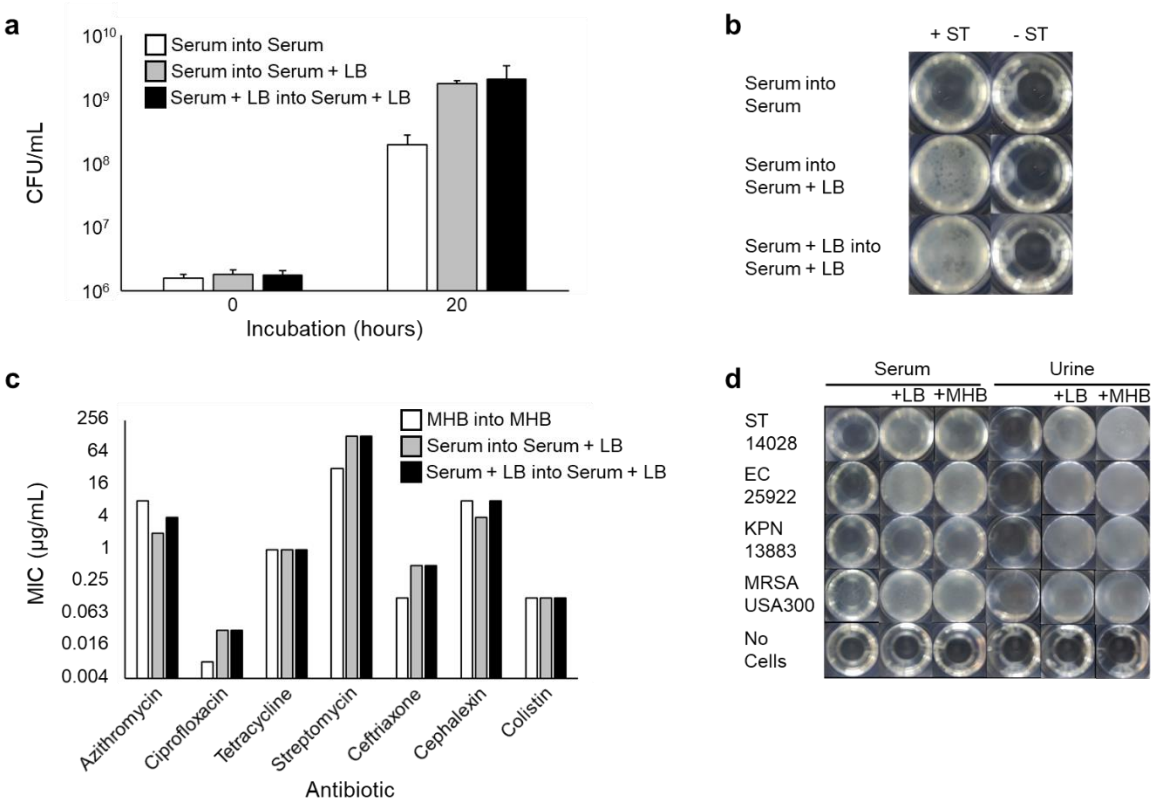

Figure 5.2. Supplementation with rich media enables robust growth for AST in serum and urine. (**a**) Average viability (CFU/mL) of *ST* grown and/or subcultured with 30% LB supplementation in a microtiter plate immediately after subculture (0 h) or after 20 h of growth. (**b**) representative images of subcultures after 20 hours on a microtiter plate, (**c**) MIC (µg/mL) in Ca-MHB, or serum (with and without 30% LB supplementation), (**d**) representative images of urine and serum subcultures of *ST* (*S*. Typhimurium), *EC* (*E. coli*), *KPN* (*K. pneumoniae*), and MRSA in microtiter plates with and without 30% LB or Ca-MHB supplementation. Panel (**a**) average of 3 biological replicates, error bars represent one standard deviation; Panel (**c**) is consensus MIC of three biological replicates.

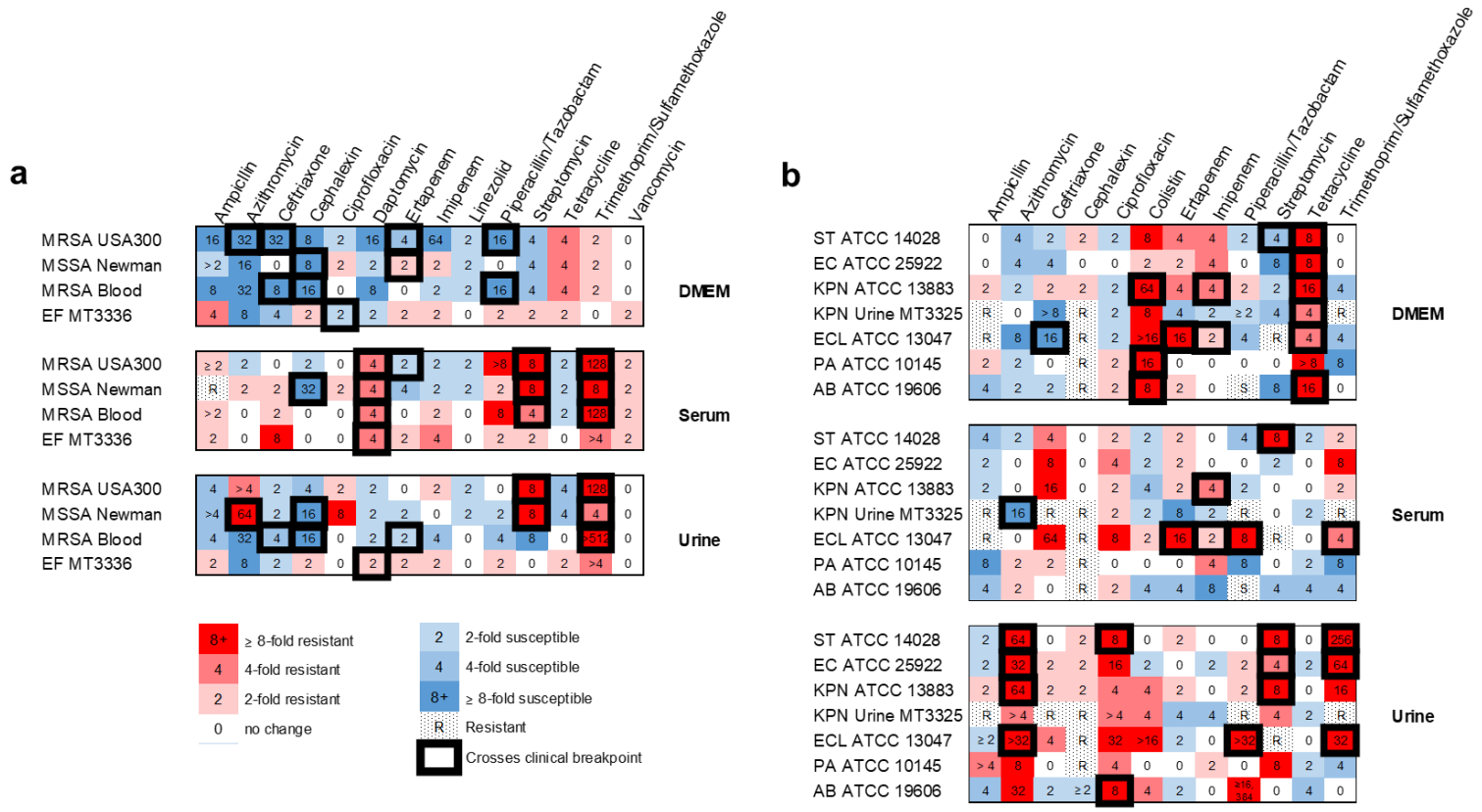

Figure 5.3. Comparison of pathogen-antibiotic combinations that exhibited altered MICs derived from tissue culture media or donor fluids. A panel of antibiotics was screened for altered MICs against (**a**) Gram-positive, and (**b**) Gram-negative bacteria when tested in Dulbecco's Modified Eagle Medium (DMEM), pooled healthy human donor serum, and pooled healthy human donor urine relative to standard Ca-MHB medium, according to CLSI guidelines ((*47, 162*)). Values represent fold-change in MICs when derived in donor fluids relative to standard Ca-MHB medium (test/standard condition). Increased susceptibility depicted in blue; increased resistance depicted in red; changes in clinical breakpoint designation outlined in black. MIC values were obtained from at least 6 independent determinations. Clinical breakpoint concentrations for listed drugs (*189, 190, 192, 193, 225-229*).

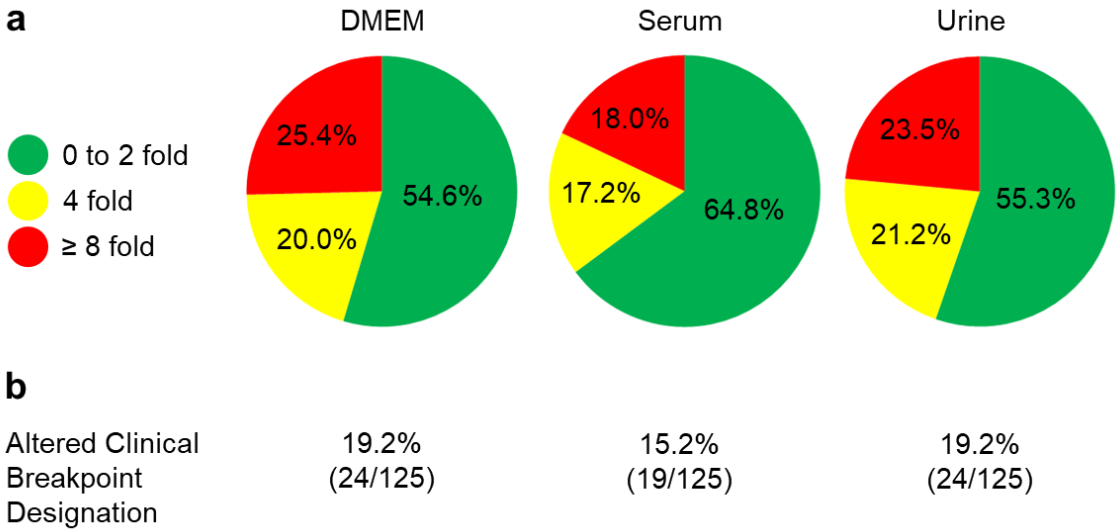

Figure 5.4. Comparison summary of MICs derived from ex vivo fluids compared to standard MHB medium. (**a**) Colored regions depict the fraction of pathogen-antibiotic combinations tested that exhibited a fold-change in MICs (increased susceptibility or resistance) when derived in host-mimicking (DMEM) or ex vivo media (serum, urine) relative to standard MHB medium (test condition); ≤ 2-fold (green), 4-fold (yellow), ≥ 8-fold (red). (**b**) Depicted are percentages of pathogen-antibiotic combinations that resulted in altered MICs that crossed clinical breakpoint designations, used to define isolates as susceptible (“S”), intermediate (“I”), or resistant (“R). Clinical breakpoint concentrations for listed drugs (*189, 190, 192, 193, 225-229*).

Table 5.1. AST in host mimicking and ex vivo media identifies both MICs that cross clinical breakpoint designations which advise on patient therapy, and those that are susceptible in standard MHB with no susceptibility change in any other media.

Drug	Pathogen	Host-mimicking or ex vivo medium	Clinical breakpoint
Increased susceptibility			
Azithromycin	*KPN*[2]; MRSA[1]	DMEM/serum	R to S, I
Ceftriaxone	*ECL*; MRSA[1,2]	DMEM	R to S
Cephalexin	MRSA[2]; MSSA	DMEM/serum/urine	R to S
Piperacillin/Tazobactam	MRSA[1,2]	DMEM	R to S
Decreased susceptibility			
Azithromycin	*EC*; *ECL*; *KPN*[1]; MSSA; *ST*	Urine	S to R
Ciprofloxacin	*AB*; *ST*	Urine	S to R, I
Colistin	*AB*; *KPN*[1]; *PA*	DMEM	S to R
Ertapenem	*ECL*	DMEM/serum	S to R
Piperacillin/Tazobactam	*ECL*	serum/urine	S to R
Streptomycin	*KPN*[1]; MRSA[1]; MSSA; *ST*	serum/urine	S to R, I
Tetracycline	*AB*; *EC*; *KPN*[1]; *ST*	DMEM	S to R, I
Trimethoprim/Sulfamethoxazole	*EC*; *ECL*; MRSA[1,2]; MSSA; *ST*	serum/urine	S to R
No Change			
Ampicillin	*EC*; *EF*; *ST*	DMEM/serum/urine	S to S
Azithromycin	*EF*	DMEM/serum/urine	S to S
Ceftriaxone	MSSA; *ST*	DMEM/serum/urine	S to S
Cephalexin	*EC*; *KNP*[1]; *ST*	DMEM/serum/urine	S to S
Ciprofloxacin	*KPN*[1]; MRSA[1,2]; *PA*	DMEM/serum/urine	S to S
Colistin	*EC*	DMEM/serum/urine	S to S
Ertapenem	*EC*; *KPN*[1]; *ST*	DMEM/serum/urine	S to S
Imipenem	*AB*; *EC*; *EF*; MRSA[1,2]; MSSA; *PA*; *ST*	DMEM/serum/urine	S to S
Linezolid	*EF*; MRSA[1,2]; MSSA	DMEM/serum/urine	S to S
Piperacillin/Tazobactam	*EC*; *EF*; *KPN*[1]; MSSA; *PA*; *ST*	DMEM/serum/urine	S to S
Tetracycline	*EF*; MRSA[1,2]; MSSA	DMEM/serum/urine	S to S
Vancomycin	*EF*; MRSA[1,2]; MSSA	DMEM/serum/urine	S to S

Depicted are pathogen-antibiotic combinations that would guide treatment selection, either sensitive in standard Ca-MHB media with no change in any host-mimicking and ex vivo media, or those with altered susceptibility that crossed clinical breakpoint designations that are used to define isolates as susceptible (“S”), intermediate (“I”), or resistant (“R”). R to S refers to an “R” classification when tested for susceptibility in MHB medium, but an “S” classification in host-mimicking or ex vivo media. *AB* (*A. baumannii*); *EC* (*E. coli*); *ECL* (*E. cloacae*); *EF* (*E. faecium*); *KPN*[1,2] (*K. pneumoniae* ATCC 13883; Urine MT3325); MSSA; MRSA[1,2] (USA300; Blood MT3302); *PA* (*P. aeruginosa*); *ST* (*S.* Typhimurium). Clinical breakpoint concentrations for listed drugs (*189, 190, 192, 193, 225-229*).

Table 5.2a. AST susceptibility results (Gram-positive).

Methicillin-Resistant *Staphylococcus aureus* USA300

	MHB		DMEM		Serum		Urine	
Antibiotic	MIC	Interpretation	MIC	Interpretation	MIC	Interpretation	MIC	Interpretation
Ampicillin	512	R	32	R	>512	R	128	R
Azithromycin	128	R	4	**I**	64	R	>512	R
Ceftriaxone	256	R	8	**S**	256	R	128	R
Cephalexin	256	R	32	R	128	R	64	R
Ciprofloxacin	0.5	S	0.25	S	0.5	**S**	1	S
Daptomycin	1	S	0.063	S	4	**R**	0.5	S
Ertapenem	8	R	2	**S**	4	**I**	8	R
Imipenem	2	S	0.031	S	1	S	4	S
Linezolid	4	S	2	S	2	S	2	S
Piperacillin/Tazobactam	64/4	R	4/4	**S**	>512/4	R	64/4	R
Streptomycin	8	S	2	S	64	**R**	64	**R**
Tetracycline	0.5	S	2	S	0.25	**S**	0.125	**S**
Trimethoprim/Sulfamethoxazole	0.063/1.2	S	0.125/2.4	S	8/152	**R**	8/152	**R**
Vancomycin	1	S	1	S	2	S	1	S

Methicillin-Sensitive *Staphylococcus aureus* Newman

	MHB		DMEM		Serum		Urine	
Antibiotic	MIC	Interpretation	MIC	Interpretation	MIC	Interpretation	MIC	Interpretation
Ampicillin	>512	R	256	R	>512	R	128	R
Azithromycin	1	S	0.063	S	2	S	64	**R**
Ceftriaxone	4	S	4	**S**	8	**S**	2	**S**
Cephalexin	32	R	4	**S**	1	**S**	2	**S**
Ciprofloxacin	0.125	S	0.25	S	0.25	**S**	1	S
Daptomycin	1	S	0.5	**S**	4	**R**	0.5	S
Ertapenem	0.5	S	1	**I**	0.125	S	0.25	S
Imipenem	0.016	S	0.031	S	0.008	S	0.016	S
Linezolid	4	S	2	S	2	S	2	S
Piperacillin/Tazobactam	2/4	S	2/4	S	4/4	**S**	1/4	**S**
Streptomycin	8	S	2	S	64	**R**	64	**R**
Tetracycline	0.5	S	2	S	0.25	**S**	0.125	**S**
Trimethoprim/Sulfamethoxazole	1/19	S	2/38	S	8/152	**R**	4/76	**R**
Vancomycin	1	S	1	S	2	S	1	S

Methicillin-Resistant *Staphylococcus aureus* Blood isolate MT3302

	MHB		DMEM		Serum		Urine	
Antibiotic	MIC	Interpretation	MIC	Interpretation	MIC	Interpretation	MIC	Interpretation
Ampicillin	256	R	32	R	>512	R	64	R
Azithromycin	256	R	8	R	256	R	8	R
Ceftriaxone	64	R	8	**S**	128	R	16	**I**
Cephalexin	128	R	8	**S**	128	R	8	**S**
Ciprofloxacin	0.5	S	0.5	S	0.5	**S**	0.5	S
Daptomycin	1	S	0.125	S	4	**R**	0.5	S
Ertapenem	4	I	4	I	4	I	2	**S**
Imipenem	0.125	S	0.063	S	0.25	S	0.031	S
Linezolid	2	S	1	S	2	S	2	S
Piperacillin/Tazobactam	64/4	R	4/4	**S**	512/4	R	16/4	R
Streptomycin	8	S	2	S	32	**R**	1	S
Tetracycline	0.5	S	2	S	0.25	**S**	0.5	**S**
Trimethoprim/Sulfamethoxazole	0.063/1.2	S	0.125/2.4	S	8/152	**R**	>32/608	**R**
Vancomycin	1	S	1	S	2	S	1	S

***Enterococcus faecium* isolate MT3336**

	MHB		DMEM		Serum		Urine	
Antibiotic	MIC	Interpretation	MIC	Interpretation	MIC	Interpretation	MIC	Interpretation
Ampicillin	0.25	S	1	S	0.5	S	0.5	S
Azithromycin	0.5	S	0.063	S	0.5	S	0.063	S
Ceftriaxone*	8	R	2	R	64	R	4	R
Cephalexin*	64	R	128	R	64	R	128	R
Ciprofloxacin	2	I	1	**S**	2	I	2	I
Daptomycin	4	S	2	S	16	**R**	8	**R**
Ertapenem	8	R	16	R	16	R	16	R
Imipenem	0.5	S	1	S	2	S	1	S
Linezolid	2	S	2	S	2	S	2	S
Piperacillin/Tazobactam	2/4	S	4/4	S	4/4	S	4/4	S
Streptomycin*	32	R	64	R	64	R	32	R
Tetracycline	0.125	S	0.25	S	0.125	S	0.25	S
Trimethoprim/Sulfamethoxazole*	8/152	R	8/152	R	>32/608	R	>32/608	R
Vancomycin	0.5	S	1	S	1	S	0.5	S

Clinical Breakpoints[a]

Antibiotic	*Staphylococcus* spp.	*Enterococcus* spp.
Ampicillin	S ≤ 0.25, R ≥ 0.5[(190)]	S ≤ 8, R ≥ 16
Azithromycin	S ≤ 2, I = 4, R ≥ 8	S ≤ 2, I = 4, R ≥ 8[(225)]
Ceftriaxone	S ≤ 8, I = 16-32, R ≥ 64 [(190)]	Intrinsic Resistance
Cephalexin	S ≤ 8, I = 16, R ≥ 32[(226)]	Intrinsic Resistance
Ciprofloxacin	S ≤ 1, I = 2, R ≥ 4	S ≤ 1, I = 2, R ≥ 4
Daptomycin	S ≤ 1, NS ≥ 2	S ≤ 4, NS ≥ 8
Ertapenem	S ≤ 2, I = 4, R ≥ 8[(190)]	S ≤ 0.5, R > 0.5[(227)]
Imipenem	S ≤ 4, I = 8, R ≥ 16[(190)]	S ≤ 4, R ≥ 8[(227)]
Linezolid	S ≤ 4, R ≥ 8	S ≤ 2, I = 4, R ≥ 8
Piperacillin/Tazobactam	S ≤ 8/4, R ≥ 16/4[(190)]	S ≤ 16, R ≥ 32[(228)]
Streptomycin	S ≤ 8, I = 16, R ≥ 32[(189)]	Intrinsic Resistance
Tetracycline	S ≤ 4, I = 8, R ≥ 16	S ≤ 4, I = 8, R ≥ 16
Trimethoprim/Sulfamethoxazole	S ≤ 2/38, R ≥ 4/76	Intrinsic Resistance
Vancomycin	S ≤ 2, I = 4-8, R ≥ 16	S ≤ 4, I = 8-16, R ≥ 32

MICs (µg/mL) were determined by broth microdilution in accordance with CLSI guidelines. DMEM and Serum MICs were incubated in a 5% CO2 incubator.
S = Susceptible, I = Intermediate, R = Resistant, *Intrinsic Resistance. Bold boxes indicate a change in resistance relative to standard Ca-MHB medium.
Staphylococcus spp. breakpoints were used to interpret *Staphylococcus aureus* MIC values. *Streptococcus pneumoniae* breakpoints were applied to *Streptococcus pneumoniae*, and *Enterococcus* spp. breakpoints used for *Enterococcus faecium*.
[a]All Clinical Breakpoints are referenced from the CLSI 2014 twenty-fourth informational supplement (*192*) unless otherwise indicated.

Table 5.2b. AST susceptibility results (Gram-negative).

***Salmonella* Typhimurium ATCC 14028**

Antibiotic	MHB MIC	MHB Interpretation	DMEM MIC	DMEM Interpretation	Serum MIC	Serum Interpretation	Urine MIC	Urine Interpretation
Ampicillin	1	S	1	S	0.25	S	0.5	S
Azithromycin	4	S	1	S	2	S	256	**R**
Ceftriaxone	0.063	S	0.031	S	0.25	S	0.063	S
Cephalexin	4	S	8	S	4	S	8	S
Ciprofloxacin	0.016	S	0.008	S	0.031	S	0.125	**I**
Colistin Sulfate	0.25	S	2	S	0.125	S	0.25	S
Ertapenem	0.008	S	0.031	S	0.016	S	0.016	S
Imipenem	0.125	S	0.5	S	0.125	S	0.125	S
Piperacillin/Tazobactam	2/4	S	1/4	S	0.5/4	S	2/4	S
Streptomycin	16	I	4	**S**	128	**R**	128	**R**
Tetracycline	1	S	8	**I**	0.5	S	1	S
Trimethoprim/Sulfamethoxazole	0.063/1.2	S	0.063/1.2	S	0.125/2.4	S	16/304	**R**

***Escherichia coli* ATCC 25922**

Antibiotic	MHB MIC	MHB Interpretation	DMEM MIC	DMEM Interpretation	Serum MIC	Serum Interpretation	Urine MIC	Urine Interpretation
Ampicillin	4	S	4	S	4	S	2	S
Azithromycin	4	S	1	S	4	S	128	**R**
Ceftriaxone	0.063	S	0.016	S	0.5	S	0.125	S
Cephalexin	8	S	8	S	8	S	16	S
Ciprofloxacin	0.004	S	0.004	S	0.016	S	0.063	S
Colistin Sulfate	0.25	S	0.5	S	0.125	S	0.125	S
Ertapenem	0.016	S	0.031	S	0.031	S	0.016	S
Imipenem	0.25	S	1	S	0.25	S	0.125	S
Piperacillin/Tazobactam	2/4	S	2/4	S	2/4	S	4/4	S
Streptomycin	8	S	1	S	4	S	32	**R**
Tetracycline	1	S	8	**I**	1	S	0.5	S
Trimethoprim/Sulfamethoxazole	0.063/1.2	S	0.063/1.2	S	0.5/9.5	S	4/76	**R**

***Klebsiella pneumoniae* ATCC 13883**

Antibiotic	MHB MIC	MHB Interpretation	DMEM MIC	DMEM Interpretation	Serum MIC	Serum Interpretation	Urine MIC	Urine Interpretation
Ampicillin	256	R	512	R	128	R	512	R
Azithromycin	4	S	2	S	4	S	256	**R**
Ceftriaxone	0.063	S	0.125	S	1	S	0.125	S
Cephalexin	8	S	16	S	8	S	16	S
Ciprofloxacin	0.031	S	0.016	S	0.063	S	0.125	S
Colistin Sulfate	0.25	S	16	**R**	0.063	S	1	S
Ertapenem	0.016	S	0.063	S	0.031	S	0.031	S
Imipenem	0.5	S	2	**I**	2	**I**	0.5	S
Piperacillin/Tazobactam	2/4	S	4/4	S	1/4	S	4/4	S
Streptomycin	2	S	1	S	2	S	16	**I**
Tetracycline	1	S	16	**R**	1	S	1	S
Trimethoprim/Sulfamethoxazole	0.125/2.4	S	0.031/0.6	S	0.25/4.8	S	2/38	S

***Klebsiella pneumoniae* Urine isolate MT3325**

Antibiotic	MHB MIC	MHB Interpretation	DMEM MIC	DMEM Interpretation	Serum MIC	Serum Interpretation	Urine MIC	Urine Interpretation
Ampicillin	>512	R	>512	R	>512	R	>512	R
Azithromycin	128	R	128	R	8	**S**	>512	R
Ceftriaxone	>512	R	64	R	>512	R	>512	R
Cephalexin	>512	R	>512	R	>512	R	>512	R
Ciprofloxacin	128	R	64	R	256	R	>512	R
Colistin Sulfate	0.125	S	1	S	0.063	S	0.5	S
Ertapenem	256	R	64	R	32	R	64	R
Imipenem	32	R	16	R	16	R	8	R
Piperacillin/Tazobactam	>512/4	R	512/4	R	>512/4	R	>512/4	R
Streptomycin	128	R	32	R	128	R	512	R
Tetracycline	4	S	16	**R**	2	S	2	S
Trimethoprim/Sulfamethoxazole	>32/608	R	>32/608	R	>32/608	R	>32/608	R

***Enterobacter cloacae* ATCC 13047**

Antibiotic	MHB MIC	MHB Interpretation	DMEM MIC	DMEM Interpretation	Serum MIC	Serum Interpretation	Urine MIC	Urine Interpretation
Ampicillin	>512	R	>512	R	>512	R	512	R
Azithromycin	16	S	2	S	16	S	>512	**R**
Ceftriaxone	4	R	0.25	**S**	256	R	16	R
Cephalexin	>512	R	>512	R	>512	R	>512	R
Ciprofloxacin	0.016	S	0.008	S	0.125	S	0.5	S
Colistin Sulfate	32	R	>512	R	64	R	>512	R
Ertapenem	0.25	S	4	**R**	4	**R**	0.125	S
Imipenem	1	S	2	**I**	2	**I**	1	S
Piperacillin/Tazobactam	16/4	S	4/4	S	128/4	**R**	>512/4	**R**
Streptomycin	>512	R	>512	R	>512	R	>512	R
Tetracycline	2	S	8	**I**	2	S	2	S
Trimethoprim/Sulfamethoxazole	1/19	S	0.25/4.8	S	4/76	**R**	32/608	**R**

***Pseudomonas aeruginosa* ATCC 10145**

Antibiotic	MHB MIC	MHB Interpretation	DMEM MIC	DMEM Interpretation	Serum MIC	Serum Interpretation	Urine MIC	Urine Interpretation
Ampicillin*	128	R	256	R	16	R	>512	R
Azithromycin*	64	R	32	R	128	R	512	R
Ceftriaxone*	8	R	8	R	16	R	8	R
Cephalexin*	>512	R	>512	R	>512	R	>512	R
Ciprofloxacin	0.125	S	0.25	S	0.125	S	0.5	S
Colistin Sulfate	0.5	S	8	**R**	0.5	S	0.5	S
Ertapenem*	4	R	4	R	4	R	4	R
Imipenem	0.5	S	0.5	S	2	S	1	S
Piperacillin/Tazobactam	4/4	S	4/4	S	0.5/4	S	4/4	S
Streptomycin	32	R	32	R	32	R	256	R
Tetracycline*	64	R	>512	R	32	R	32	R
Trimethoprim/Sulfamethoxazole*	32/608	R	4/76	R	4/76	R	8/152	R

***Acinetobacter baumannii* ATCC 19606**

Antibiotic	MHB MIC	MHB Interpretation	DMEM MIC	DMEM Interpretation	Serum MIC	Serum Interpretation	Urine MIC	Urine Interpretation
Ampicillin*	256	R	64	R	64	R	64	R
Azithromycin*	16	R	8	R	32	R	512	R
Ceftriaxone	32	I	16	I	32	I	16	I
Cephalexin*	>512	R	>512	R	>512	R	512	R
Ciprofloxacin	0.5	S	1	S	1	S	4	**R**
Colistin Sulfate	0.5	S	4	**R**	0.125	S	2	S
Ertapenem*	4	R	8	R	1	R	2	R
Imipenem	0.25	S	0.25	S	0.031	S	0.25	S
Piperacillin/Tazobactam	≤0.001/4	S	≤0.001/4	S	≤0.001/4	S	16/4	S
Streptomycin	512	R	64	R	128	R	512	R
Tetracycline	2	S	32	**R**	0.5	S	0.5	S
Trimethoprim/Sulfamethoxazole	16/304	R	16/304	R	4/76	R	16/304	R

Clinical Breakpoints[a]

Antibiotic	*Enterobacteriaceae*	*Pseudomonas aeruginosa*	*Acinetobacter* spp.
Ampicillin	S ≤ 8, I = 16, R ≥ 32	Intrinsic Resistance	Intrinsic Resistance
Azithromycin	S ≤ 16, R ≥ 32[(193)]	Intrinsic Resistance	Intrinsic Resistance
Ceftriaxone	S ≤ 1, I = 2, R ≥ 4	Intrinsic Resistance	S ≤ 8, I = 16-32, R ≥ 64
Cephalexin	S ≤ 16, R > 16[(193)]	Intrinsic Resistance	Intrinsic Resistance
Ciprofloxacin	S ≤ 1, I = 2, R ≥ 4 *Salmonella*: S ≤ 0.06, I = 0.125-0.5, R ≥ 1	S ≤ 1, I = 2, R ≥ 4	S ≤ 1, I = 2, R ≥ 4
Colistin Sulfate	S ≤ 2, R ≥ 4[(193)]	S ≤ 2, I = 4, R ≥ 8	S ≤ 2, R ≥ 4
Ertapenem	S ≤ 0.5, I = 1, R ≥ 2	Intrinsic Resistance	Intrinsic Resistance
Imipenem	S ≤ 1, I = 2, R ≥ 4	S ≤ 2, I = 4, R ≥ 8	S ≤ 2, I = 4, R ≥ 8
Piperacillin/Tazobactam	S ≤ 16/4, I = 32/4-64/4, R ≥ 128/4	S ≤ 16/4, I = 32/4-64/4, R ≥ 128/4	S ≤ 16/4, I = 32/4-64/4, R ≥ 128/4
Streptomycin	S ≤ 8, I = 16, R ≥ 32[(189)]	S ≤ 8, R > 16[(229)]	S ≤ 8, R > 16[(229)]
Tetracycline	S ≤ 4, I = 8, R ≥ 16	Intrinsic Resistance	S ≤ 4, I = 8, R ≥ 16
Trimethoprim/Sulfamethoxazole	S ≤ 2/38, R ≥ 4/76	Intrinsic Resistance	S ≤ 2/38, R ≥ 4/76

MICs (µg/mL) were determined by broth microdilution in accordance with CLSI guidelines. DMEM and Serum MICs were incubated in a 5% CO2 incubator.
S = Susceptible, I = Intermediate, R = Resistant, *Intrinsic Resistance. Bold boxes indicate a change in resistance relative to standard Ca-MHB medium.
Enterobacteriaceae breakpoints were used to interpret *Salmonella*, *Escherichia*, *Klebsiella*, and *Enterobacter* MIC values. *Pseudomonas aeruginosa* breakpoints were applied to *Pseudomonas aeruginosa*, and *Acinetobacter* spp. breakpoints used for *Acinetobacter baumannii*.
[a]All Clinical Breakpoints are referenced from the CLSI 2014 twenty-fourth informational supplement (*192*) unless otherwise indicated.

Chapter 6

Conclusions and Future Directions

The emergence of novel pathogens and antimicrobial resistance mechanisms is a natural process that will continue to impact mankind for our foreseeable future. As the human population increases, and we live in higher densities that progressively encroach into the natural world, additional pathogens and pandemics are expected to emerge at an increasing pace (*230, 231*). Further, extended use and misuse of antimicrobials threatens to render them ineffective for treating resistant pathogens, such as multidrug-resistant ESKAPE pathogens (*210, 232*). To make matters even worse, antimicrobial discovery has slowed to a crawl, with the last major class of broad-spectrum antimicrobials (the quinolones) discovered in 1962 (*233*), while pathogens are increasingly becoming resistant to even our “agents of last resort” (e.g. colistin and the carbapenems) (*234, 235*). This presents a true risk that healthcare may return to a “pre-antibiotic era” where even minor infections regain their lethality. To rapidly combat emerging infectious disease, and slow the march of antibiotic resistance, we must devise adaptable point-of-care molecular pathogen identification diagnostics and new approaches to treating antibiotic resistant pathogens using the drugs we already have.

In Chapter 2, we introduced a novel approach to enable accessible rapid molecular diagnostics that could detect existing pathogens, and be quickly adapted for the next pandemic we experienced. In a method we termed smartphone-based real-time loop-mediated isothermal amplification (smaRT-LAMP), we used a smartphone, for the first time, as a stand-alone bacterial pathogen identification diagnostic. In this approach, a smartphone camera measures the fluorescence of a LAMP reaction in real-time, and automatically calculates concentrations of

pathogens in a sample based on the exponential reaction times from a spiked standard curve. All data analysis can be instantly performed using only the smartphone, via a custom-built app named “Bacticount”. The method requires little more than a smartphone, hot plate, carboard box, LEDs, and an aluminum sample holder. In addition to the smartphone, the platform can be manufactured for under $100 USD, yet matches the performance of a gold-standard qPCR thermocycler with the same reaction conditions. Further, the bacterial sample reactions could be performed for roughly $1 USD per sample with results in an hour.

In this chapter, we demonstrated the broad utility of smaRT-LAMP as a bacterial pathogen diagnostic. The assay was extremely sensitive for bacterial DNA, and could frequently detect as few as two genomes per reaction, which equated to 2.5 – 5.0 x 10^3 genomes/mL of sample specimen. Due to the high specificity of LAMP, even very closely related pathogens such as *Salmonella enterica* subsp. *enterica* serovars Typhimurium and Enteritidis could be distinguished from one another, despite sharing a 99% identical genome (*98*). Diverse bacterial pathogens could also be easily identified, and a total of 8 pathogens (6 Gram-negative, and 2 Gram-positive) were accurately identified during this study. Additional bacterial organisms proved facile to include when desired, with new pathogens incorporated into the assay in as little as one week when appropriate LAMP primers were available. This flexible addition of new pathogens into smaRT-LAMP means it can be rapidly adapted in response to novel bacterial pathogens as they emerge.

SmaRT-LAMP also performed very well for a variety of biological specimens – blood, urine, and feces – from murine models of sepsis, and human urinary sepsis

patients. In spiked blood, *ST*, *SPN*, *SA*, *SE*, *EC*, and *YP* showed excellent performance and dose-dependent reaction threshold times, which were successfully applied to murine models of sepsis for these pathogens to determine both pathogen identity and blood bacterial load. Unfortunately, blood specimens require extensive dilution for smaRT-LAMP, which precluded the detection of the very low bacterial loads (1-100 CFU/mL (*63*)) typically found in blood from human bloodstream infection patients. Instead, this assay was successfully used to diagnose urine specimens from urinary sepsis patients, in which bacterial burdens can be much higher than blood. SmaRT-LAMP accurately diagnosed 10 patients with urinary sepsis caused by *EC*, *KPN*, or *PA*, while also correctly identifying five sepsis patients with clinically negative urine specimens. Diagnosis for these patients not only matched the gold-standard clinical results, but was able to do so at a fraction of the time (1 hr vs 18-28 hours) and cost ($1 vs > $100 per test) of the traditional clinical methods.

We had anticipated that smaRT-LAMP would be a flexible and effective diagnostic for novel emergent pathogens, in addition to the well-characterized pathogens evaluated in the first study. In Chapter 3, we leveraged the flexibility and excellent performance of smaRT-LAMP to develop a diagnostic in response to the most recent emergent pandemic pathogen – SARS-CoV-2. Due to the high symptom overlap between SARS-CoV-2 and seasonal influenza (*126*) an assay was developed to differentially diagnose and quantify these pathogens. A collection of published and novel LAMP primer sets was screened, from which two sets each were selected for use against SARS-CoV-2, influenza A, and influenza B. The assay

was developed as a saliva-based test, to avoid the invasive nature of the commonly used nasopharyngeal swab-based diagnostics (*236*), and because saliva viral burdens are typically high (*140*).

Despite representing a large change in experimental design between the initial bacterial DNA-based test to a viral RNA test, smaRT-LAMP performs extremely well as an RNA viral diagnostic. The LOD in saliva is equivalent to the CDC gold-standard CoV-2 RT-qPCR assay ($1x10^3$ genome copies/mL) and meets or exceeds the influenza flu SC2 RT-qPCR assay. SmaRT-LAMP was also able to perfectly distinguish SARS-CoV-2 and influenza viruses from each other, and from relevant viral and bacterial respiratory pathogens. Additionally, the assay was unaffected by mutations in recently emerging SARS-CoV-2 variants, perfectly detecting viral RNA in all five evaluated. Importantly for resource-limited settings, the assay was also robust against delays in sample processing, with no change in SARS-CoV-2 detection after 4 hours of sample storage at room temperature and minimal loss for up to a week at 4°C.

When used to evaluate SARS-CoV-2 human clinical saliva specimens, smaRT-LAMP completely matched the binary (+/-) and quantitative performance of the gold-standard CDC RT-qPCR assay. Fifty saliva specimens were tested, in which 20 were diagnosed as positive for SARS-CoV-2 by smaRT-LAMP, and 30 negative. These fifty specimens were also tested for influenza A and B by both methods, which again were in complete concordance with the standard assay (0/50 specimens were positive for influenza). These diagnoses were performed rapidly, exhibiting a 25-minute reaction time, and instant data analysis for up to 96 reactions

per run, and less than $7 USD per sample. The CoV-2/flu smaRT-LAMP assay is substantially less expensive and therefore more accessible than the current gold-standard molecular approaches. SmaRT-LAMP also does not require sophisticated fluorescent probes which may become limiting when assay demand is high during subsequent COVID/flu seasons (*19*).

Chapters 2 and 3 establish smaRT-LAMP as a powerful diagnostic tool which meets or exceeds the performance of current gold-standard clinical methods for human patient specimens, at a fraction of the time and price. This assay has demonstrated broad success in identifying eight bacterial pathogens, and three viral pathogens in blood, urine, feces, and saliva. SmaRT-LAMP is thus well positioned for global clinical use in diagnosing currently relevant pathogens, and rapid adaptation for novel pathogens as they emerge.

There are many promising future directions for smaRT-LAMP, including increased portability as a home or field diagnostic, and applications for UTI pathogen ID that can serve resource-limited communities. Currently, many of the reagents used for smaRT-LAMP require continuation of the “cold-chain” to remain stable and functional (such as enzymes and dNTPs). This limits the application of the assay to regions with cold-chain access. However, excellent progress has been made by other groups regarding lyophilization of LAMP reagents, such as the simple addition of a 10% trehalose excipient (*237*). If the smaRT-LAMP protocol can be demonstrated to be compatible with this lyophilization approach, the assay could be substantially simplified, and a user may only need to add a liquid specimen (e.g., lysed blood, urine, feces, or raw saliva) to a lyophilized reaction mix before addition

to a heat block. Additionally, the smaRT-LAMP apparatus could be adapted into a simple commercial device that heats the sample, provides UV light excitation (480 nm) and allows the smartphone camera to monitor the reaction. If a convenient device were combined with a simple commercial microfluidics-based lyophilized sample cartridge, smaRT-LAMP would be well suited for home diagnostics and telehealth.

SmaRT-LAMP may also have substantial utility as an inexpensive diagnostic for UTI in pregnant women from low-income communities. UTI is commonly treated empirically as an *E. coli* infection (using antimicrobials such as cephalexin or nitrofurantoin) without full pathogen ID (*22, 238, 239*). However, the high speed and low cost of smaRT-LAMP could enable more accurate diagnosis and better antimicrobial selection when the causative pathogen is intrinsically more resistant to empirical therapies (such as *Klebsiella* and *Pseudomonas,* to nitrofurantoin (*238*)). A further benefit of smaRT-LAMP is that it could also be used to diagnose antimicrobial resistant UTI pathogens by screening for common carbapenem-resistance genes, such as bla_{KPC} or bla_{NDM-1} using previously developed LAMP primer sets that have been effective in a clinical setting (*240*). A clinical study of smaRT-LAMP using urine specimens from pregnant women at low-income obstetric centers would evaluate the accuracy and utility of the approach as a rapid, point-of-care gynecological diagnostic. If the method can indeed identify non-*E. coli*, or antibiotic-resistant pathogens in this population, it could make the accurate prescription decisions enabled by state-of-the-art molecular diagnostics accessible to underserved and needy communities.

Accurately identifying a pathogen is an important early step toward treatment, and has been thoroughly addressed by smaRT-LAMP. However, the increased prevalence of antibiotic resistance necessitates additional testing for accurate therapeutic intervention with antimicrobials. Although the rate of novel antimicrobial development is being outpaced by the emergence of resistance (*203, 241*), clinicians can likely leverage the large array of currently available therapies (*242*) if there is a better understanding of how pathogens respond to antimicrobials while within the host. Pathogens often need to change their physiology in response to the host environment in order to survive, which can come with inadvertent trade-offs regarding their resistance to antimicrobials. By testing the resistance of a patient's isolate in host-like conditions (host mimicking, or ex vivo fluids), clinicians can identify which therapeutics are likely to succeed, and prescribe those. Considering the complexity of host microenvironmental responses, and the large array of currently available therapeutics, it seems unlikely that pathogens will be able to acquire complete resistance to all available therapies while still retaining viability within the host. Solving the antibiotic resistance problem may thus become a matter of improving susceptibility testing to identify the transient susceptibilities in various host microenvironments.

In Chapter 4, we described a host-mimicking AST approach that was compatible with a wide range of human and veterinary bacterial pathogens (16 Gram-positive, and 24 Gram-negative pathogen isolates) and four different host-mimicking media. When tested in these media, substantial alterations in susceptibility were common, and observed with a unique pattern for each individual

isolate in each condition. Overall, in one third of the antibiotic/pathogen/media combinations tested, the resistance changed by 4-fold or more within host-mimicking media, and in 8.2% (107/1311) the change was substantial enough to alter clinical prescription decisions. When appropriate murine infection models were available, the large changes in susceptibility frequently predicted the correct treatment outcome, often in contrast to the standard test media. For example, ciprofloxacin was able to treat murine infections with a lethal human MRSA isolate, despite predicted failure using standard testing. In many cases, the host-mimicking signal in the tissue-culture test media DMEM was determined to be sodium bicarbonate. When the standard MHB test media was supplemented with bicarbonate, it too became host-mimicking in many cases, indicating that this inexpensive and widely-available additive can be used to improve the accuracy of the standard test.

The host-mimicking media experiments demonstrated that specific environmental growth conditions could drastically alter antimicrobial susceptibility in a large number of clinically significant pathogens. We therefore attempted in Chapter 5 to tailor this approach to host conditions by using ex vivo human fluids (urine and serum) which contain the full assortment of soluble molecular signals found in these host microenvironments. While developing this assay, many pathogens were unable to grow robustly enough in human fluids for AST, or formed aggregates that impeded accurate viability measurements and resultant subculture. These issues were resolved by supplementation of the testing media, and use of a simple aggregate disruption protocol. This ex vivo AST method was compatible with all of a small, but diverse panel of seven Gram-negative, and four Gram-positive human

pathogens, including several that were lethal to the patients from whom they were isolated.

With donor human fluids, large changes (8-fold or more) were observed in 18% of pathogen/antibiotic combinations tested for serum, and 23.9% for urine. A commonly used antimicrobial cocktail (trimethoprim/sulfamethoxazole) frequently lost a large degree of efficacy in human fluids (in one case becoming more than 512-fold less effective). For a lethal, extremely multi-drug resistant *Klebsiella* urinary sepsis isolate, ex vivo AST identified an additional treatment option, wherein azithromycin became substantially effective in serum. Because pathogens frequently transit between multiple host sites (*243*), the safest antimicrobial therapy may be one which demonstrates high-level efficacy ("susceptibility") in all conditions. The results of this assay have not been confirmed either clinically or in vivo, however it does provide a phenotypic assay to screen against the capacity for a pathogen to become resistant to specific antimicrobials in multiple relevant host microenvironments.

Now that a universally compatible ex vivo AST assay has been developed, it will be important to tailor it to human sepsis patients, and evaluate its accuracy using both in vitro murine models of infection and in clinical trials with human sepsis patients. Because sepsis represents a dramatic aberration in host biochemistry (*223, 224*), the accuracy of this ex vivo assay may be enhanced by testing a patient's pathogen isolate in their own septic urine or serum specimens. If changes in blood or urine biochemistry signal differential susceptibility during sepsis compared to

healthy donors, then AST using patient specimens would likely provide ideal accuracy, allowing optimal therapeutic prescription efficacy.

Murine in vivo challenge experiments will be a crucial next step in confirming the accuracy of the transient resistance phenotypes identified by ex vivo AST. Any large susceptibility changes that have been observed to cross a clinical breakpoint with a pathogen that is lethal to a mouse should be evaluated. Some strong examples of these include azithromycin against *Klebsiella pneumoniae* MT 3325, which should be able to treat a purely septic infection without a urinary component; or conversely an azithromycin treatment for MSSA Newman in a urinary tract infection model. If the murine experiments prove successful, then human clinical trials would be the most meaningful confirmation possible for this assay. Two potentially strong clinical models would be important, depending on the number of available recruits. Initially, a smaller cohort of sepsis or chronic UTI patients could be enrolled, and treated with either the empirical therapy, or the empirical therapy plus an antimicrobial that is identified by ex vivo AST to become efficacious at the confirmed site of infection. Alternatively, if a large enough cohort can be enrolled to make a statistically significant difference observable, ex vivo AST could be used to test confirmed susceptible therapies; patients in the test group would be treated with an antimicrobial that is susceptible in all conditions, including the ex vivo fluids and standard testing media. With a large enough cohort, substantially more positive response is expected to be observed when using the ex vivo AST-confirmed antimicrobials, than with antimicrobials selected using only standard AST methods.

Host-mimicking and ex vivo AST also provides an exciting opportunity to revisit potentially effective antimicrobial libraries, to identify any compounds that may have failed during initial activity screening with the standard MHB testing medium. This idea also extends to any previously approved compound, either with unexpected antimicrobial efficacy (*244*) or compounds that have been typically presumed to be ineffective in all environments but are actually effective at the infection site (*56, 208*). Such re-screening may allow the rate of antibiotic discovery to return to a pace that can somewhat compete again with the emergence of novel resistance.

Together, smaRT-LAMP and the host-mimicking/ex vivo AST assays are intended to provide additional tools for clinicians to use against the seemingly inexorable onslaught of novel pathogens and antimicrobial resistance mechanisms. SmaRT-LAMP makes the accuracy of molecular diagnostics accessible to underserved populations, in a manner that also drastically improves diagnosis speed, and is flexible enough to be deployed rapidly against novel pathogens when they emerge. Host-mimicking AST improves the accuracy of antimicrobial prescription selection, while ex vivo AST enhances that accuracy to the precise site of infection. Bacterial and viral infectious diseases present innumerable threats to human health, and we must utilize diagnostic tools such as these to rapidly identify these pathogens and their cryptic weaknesses.

“If you know the enemy and know yourself,

you need not fear the result of a hundred battles.”

– Sun Tzu, The Art of War.

Chapter 7

Materials and Methods†

†This chapter contains excerpts reproduced with permission, from Ersoy SC, Heithoff DM, Barnes L, Tripp GK, House JK, Marth JD, Smith JW, and Mahan MJ. (2017). Correcting a fundamental flaw in the paradigm for antimicrobial susceptibility testing. *EBioMedicine*. 20(2017) 173-181,

†This chapter contains excerpts reproduced with permission from Barnes L, Heithoff DM, Mahan SP, Fox GN, Zambrano A, Choe J, Fitzgibbons LN, Marth JD, Fried J, Soh HT, and Mahan MJ. (2018). Smartphone-based pathogen diagnosis in urinary sepsis patients. *EBioMedicine*. 36(2018) 73-82.

†This chapter contains excerpts reproduced with permission from Heithoff DM, Barnes L, Mahan SP, Fox GN, Arn KE, Ettinger S, Bishop AM, Fitzgibbons LN, Fried JC, Low DA, Samuel CE, and Mahan MJ (2021). Transforming the Smartphone into a Stand-alone Point-of-Care Diagnostic for SARS-CoV-2 and Influenza. *In Preparation.*

CHAPTER 2 MATERIALS AND METHODS

7.1. Bacterial strains and media.

Gram-negative bacterial isolates tested included *Salmonella* sp., *Salmonella* Typhimurium ATCC 14028 (*ST*), and *S. enteritidis* 4973 (SE) (*245, 246*), *Escherichia coli* (*EC*) strain ATCC 25922 (*EC*), *Yersinia pseudotuberculosis* YPIII/pIB1 (*YP*) (*247*), *Klebsiella pneumoniae* strain ATCC 13883 (*KPN*), and *Pseudomonas aeruginosa* strain ATCC 10145 (*PA*). Gram-positive bacterial isolates analyzed included *S. aureus* USA300 (*SA*), a community-associated methicillin-resistant isolate causing the most MRSA infections in the U.S. (*248*), and *S. pneumoniae* D39 (ser. 2) (*SPN*) [41]. *ST*, *SE*, *YP*, *EC*, *KPN*, and *PA* (*54, 207*) were streaked from frozen stocks onto Luria-Bertani (LB) agar plates and single colonies were inoculated into LB broth and incubated overnight with shaking at 37 °C. All incubations of *YP* were at 28 °C. *SPN* was streaked from frozen stocks onto Todd-Hewitt (TH) broth agar plates containing 2% yeast extract and incubated overnight at 37 °C in a 5% CO_2 incubator. Single colonies were inoculated into TH broth containing 2% yeast extract and incubated overnight without shaking at 37 °C in a 5% CO_2 incubator. *SA* was streaked from frozen stocks onto Tryptic Soy (TS) agar plates and incubated overnight at 37 °C. Single colonies were inoculated into TS broth and incubated overnight with shaking at 37 °C.

7.2. gDNA preparation.

gDNA was prepared by growing bacteria as described above and pelleting approximately 1×10^{10} total cells. Cells were resuspended in 0.5 mL TE buffer, 10

µL 10% SDS, 10 µL 10 mg/mL DNase-free RNase, mixed and incubated 1 h at 37 °C. Next, 10 µL 10 mg/mL proteinase K was added and samples were incubated 2 h at 65 °C. Samples were then extracted with an equal volume of chloroform/isoamyl alcohol and spun 5 m at 16,000 ×g in a microcentrifuge. The aqueous phase was transferred to a fresh tube and DNA was extracted twice with phenol/ chloroform/isoamyl alcohol (25:24:1) and spun 5 m at 16,000 ×g. The aqueous phase was transferred to a fresh tube and DNA was extracted with 2.5 vol 100% ethanol and 0.1 vol 3M sodium acetate. Precipitate was washed once with 70% ethanol, supernatant was removed and pellet was dried briefly in a DNA speed vac. Pellets were resuspended in 100 µL ultrapure H_2O, aliquoted and stored at −20 °C until use.

7.3. LAMP reaction conditions.

7.3.1. LAMP reagents

Betaine, calcein, KCl, MgSO4, MnCl2, (NH4)2SO4, and Triton X-100 were purchased from Millipore Sigma (St. Louis, MO). Bst 2.0 WarmStart DNA polymerase was purchased from New England Biolabs (Beverly, MA), deoxynucleotide triphosphates from Promega (Madison, WI), Tris (pH 7.5) from Invitrogen (Carlsbad, CA), Nuclease-free water, DMSO, NaOH, and polysorbate 20 from ThermoFisher (Waltham, MA). Tris (pH 8.8) was purchased from VWR (Radnor, PA), and PCR tubes with optically clear lid strips from Bio-Rad (Hercules, CA). Primers were purchased from Integrated DNA Technologies (Coralville, IA).

7.3.2. Oligonucleotide primers

Table 2.4 provides a list of oligonucleotide primer sequences. All synthetic oligos were purchased from Integrated DNA Technologies (Coralville, IA). Previously designed primers targeting the *recF* gene of *Salmonella* sp. (*96*) were employed with the addition of loop primers chosen to accelerate the reaction by priming strand displacement synthesis (*249*). The set of primers consisted of two outer (F3 and B3), two inner (FIP and BIP), and two loop primers (F-Loop and B-Loop). Additional published primer sets were selected for other pathogens: *ST rfbJ* (*112*); *SE sdfI* (*111*); *YP inv* (*115*); *EC glxK* (*250*), *KPN fimD* (*110*), *PA oprI* (*110*), *SPN lytA* (*114*) (a F-Loop primer was developed for the *SPN lytA* set); *SA* 16S rRNA (*113*).

7.3.3. Reaction conditions

We generated a 2× LAMP reagent “master mix” containing 40mM Tris (pH 8.8), 20 mM KCl, 16 mM MgSO4, 20 mM (NH4)2SO4, 0.2% v/v polysorbate 20, 1.6 M betaine, 2.8 mM for each of the four deoxynucleotide triphosphates, 0.58 U/µL of Bst WarmStart DNA polymerase, 0.4 µM each of F3, B3 primers, 3.2 µM each of FIP, BIP primers, 1.6 µM each of F-Loop, B-Loop primers, 750 µM MnCl2, and 37.6 µM calcein. All reactions were conducted at 65 °C for 50 m.

7.4. Lysis protocol.

7.4.1. Purified gDNA

20 µL of purified pathogen gDNA stock was diluted to specified concentrations, mixed 1:1 with 20 µL of LAMP master mix (at 2× final concentration), and split into 19 µL aliquots between qPCR-LAMP and smaRT-LAMP.

7.4.2. CFU in buffer and blood

For analysis of CFU in buffer and blood, a modified alkaline treatment was used (*251*). A 2 µL sample was vortexed for 15 s after mixture with 78 µL (*252*) of lysis mix (50 mM NaOH and 0.5% Triton X-100 in the final 80 µL lysate volume), then pulse-spun for 3 s on a microcentrifuge, and heated at 100 °C for 10m on an aluminum heat block. After cooling on ice for 2m, samples were centrifuged for 2m at 16,000 x g and 40 µL of supernatant removed to another tube. To neutralize, 6.4 µL of 1M Tris-HCl (pH 7.5) was added, vortexed briefly, and centrifuged for 2 m. 40 µL of supernatant was added to tubes containing 40 µL of 2× LAMP master mix and mixed by pipetting. The resultant lysate was split into two 38 µL aliquots that were analyzed by a Bio-Rad thermocycler and smaRT-LAMP with the Bacticount app.

7.4.3. CFU in urine and feces

Urine and feces samples were analyzed similar to buffer and blood, with the omission of centrifugation and pellet-removal steps. After heating at 100 °C and cooling on ice, the 80 µL lysates were neutralized with 12.8 µL of 1M Tris-HCl (pH 7.5), vortexed briefly to mix, and 40 µL of lysate was mixed with 40 µL 2× LAMP master mix before splitting into two aliquots for analysis.

7.5. Preparation of pathogen samples in spiked buffer and uninfected murine Specimens.

For LOD buffer analysis, serial dilutions of *S.* Typhimurium cells (10^1 to 10^5 CFU/mL) were spiked into buffer. Briefly, 1 mL samples of the stated concentrations were reduced to 2 µL via sequential centrifugation. Blood from uninfected mice was collected by tail bleed into BD Microtainer PST tubes with lithium heparin (Becton

Dickinson, cat. no. 365985). Urine was collected into sterile microfuge tubes. Feces (0.1 g) was collected into sterile microfuge tubes, resuspended in 0.3 mL reaction buffer, and the mixture was pulse-spun in a microcentrifuge for 5 s to pellet large particulates. Bacteria were diluted into reaction buffer (20 mM Tris, pH 7.5), or spiked into blood, feces, or urine, collected from uninfected mice, respectively, at specified concentrations. Mice: 8–12 wk. old male and female C57BL/6 J mice (Jackson Labs, Bar Harbor, ME) were used for all infections and blood, urine, and feces specimen collections.

7.6. Animal infection protocols and specimen collection.

7.6.1. Gram-negative pathogens

All Gram-negative strains were grown overnight in LB. *ST* and *SE* bacterial strains were pelleted by centrifugation, washed, and suspended in sterile 0.2 M sodium phosphate buffer (pH 8.1). Mice were orally infected with *ST* via gastric intubation at a dose of 2×10^7 cells ($20 \times LD_{50}$) and whole blood was sampled at days 6 (pre-sepsis), 8 (sepsis), and 10 (severe sepsis) post-infection. For intraperitoneal (i.p.) infections, a $20\times LD_{50}$ dose of *SE* (10^3 cells) or *YP* (5×10^5 cells) in 100 µL 0.15M NaCl was administered and whole blood was collected from the tail vein of septic mice at day 5 post-infection. *EC*, was suspended in sterile phosphate buffered saline (PBS) and mice were infected via the i.p. route at a dose of $1–2 \times 10^7$ bacteria ($20\times LD_{50}$) in 100 µL volume. Blood was taken for analyses at 48 h post-infection (severe sepsis). A dose of $20 \times LD_{50}$ ensures that virtually all infected animals will undergo sepsis.

7.6.2. Gram-positive pathogens

SPN cultures were diluted 1:10 into fresh TH broth and sub-cultured to mid-log phase (A_{600} = 0.4), pelleted in a microfuge at 16,000 ×g for 2 m, washed, and suspended in 0.15 M NaCl. i.p. injection of 1 to 2 × 10^4 cells (20× LD_{50}) was done in 100 µL 0.15 M NaCl. Whole blood was collected from the tail vein of septic mice at 48 h post-infection into microtainer tubes. *SA* cultures were diluted 1:100 into fresh TS broth and sub-cultured to mid-log phase (A_{600} = 0.4), pelleted in a microfuge at 16,000 × g for 2 m, washed, and suspended in 0.15 M NaCl. Intravenous (i.v.) injection into the retroorbital sinus of 1–2 × 10^8 cells (20× LD_{50}) was done in 100 µL 0.15 M NaCl. Whole blood was collected from the tail vein of septic mice at 48 h post-infection into microtainer tubes. Institutional Animal Care and Use Committee of the University of California, Santa Barbara approved studies undertaken herein.

7.7. Urine specimens from human sepsis patients.

Human specimens were collected at Santa Barbara Cottage Hospital, Santa Barbara, CA. Patients were selected who met the clinical criteria for sepsis based on fever, increased heart rate, and/or elevated white blood cell count, and had a suspected urinary source of their severe infection. Some of these patients had severe sepsis, with evidence of end organ dysfunction or septic shock. Upon presentation at the hospital, urine and blood specimens were collected from patients before antibiotic administration. A comparative urine bacterial analysis was performed between smaRT-LAMP and clinical diagnostics carried out by the hospital managing patient care. Pathogen ID in the urine and blood of sepsis patients was

determined by the hospital microbiology laboratory. The bacterial load in urine specimens was assessed by both direct colony count, and smaRT-LAMP utilizing primer sets directed against the urine pathogen identified in the clinical setting. The bacterial load in the urine of human sepsis patients with clinically negative urine cultures (below the standard threshold for infection of 10^5 CFU) (*37, 72*) was determined by the hospital microbiology laboratory (clinical culture) versus an academic laboratory examining CFU by direct colony count, qPCR-LAMP, and smaRT-LAMP, utilizing *E. coli* primer sets. A linear fit of standard curves with a clinically relevant bacterial burden (5×10^4 –5×10^7 CFU/mL) was used to determine LAMP-based CFUs. LAMP-based assays were sometimes inhibited in cloudy urine specimens (precipitated phosphate crystals and/or pyuria) (*37*), but inhibition was relieved by a 1:10 dilution of the specimen in 20 mM Tris-HCl (pH 7.5). Institutional Human Subjects Use Committees of the University of California, Santa Barbara and Santa Barbara Cottage Hospital approved studies undertaken herein.

7.8. Data analysis.

Real-Time LAMP traces were automatically generated at the end of each run for each sample by the qPCR thermocycler and the Bacticount app. Trace files were transferred to a personal computer (PC), where MATLAB was used (described in detail in the Supplementary Methods section) to find the maximum of the derivative taken over a coarse time stepper (i.e., a chosen length of time over which to average the derivative). The resultant Tt value was linearly related to the logarithm of

the input concentration and used to determine the concentration of bacteria in septic murine samples using standard curves with a minimum of 10 reaction replicates per concentration at 5×10^6 CFU/reaction and below. All steps of this process can be automatically performed by the Bacticount app without using a PC.

7.9. Hardware of smaRT-LAMP platform.

All experiments were performed in low-profile 0.2-mL PCR strips (Bio-Rad cat. no. TLS-0801) covered with optical flat strips (Bio-Rad cat. no. TLS-0803). Sample tubes were placed in an aluminum sample block (LightLabs cat. no. A-7079) on a hot plate (HP30A digital aluminum hotplate, Torrey Pines Scientific, Carlsbad, CA). A cardboard box large enough to cover the hot plate was painted black and two flexible cables of 96 W, 480 nm, 672 lm, 96-LEDs (DealeXtreme cat. no. 180563) were affixed to the inside top cover of the box. LEDs were powered using a single output DC power supply (UA8001A, Agilent Technologies, Santa Clara, CA). A Samsung Galaxy S7 smartphone (Samsung Electronics Co., Ltd.) was outfitted with a 520 ± 10 nm bandpass filter (Edmund Optics cat. no. 65–699) for visual detection of emitted green light (**Figure 2.6**). All qPCR reactions were performed on a Bio-Rad CFX96 qPCR Thermocycler.

7.10. Development and function of Bacticount android application.

7.10.1. Bacticount android application

The Bacticount smartphone application was built on a Samsung Galaxy S7 phone using the developer tools in Android Studio IDE, Android SDK (Android), and

OpenCV library. The app can be downloaded and installed from the Google Play Store; the user is then prompted to install the “OpenCV Manager” application, which is employed to handle complex algorithms such as image rendering, histogram generation, and back-calculations. Upon opening the app, the user is initially presented with an option for a step-by-step tutorial. In addition to the tutorial, the user is given a choice to “Start Bacterial Analysis”; when selected, the user is prompted to pick the correct sample type (Blood, Urine, or Feces). The user can then follow a three-step analysis procedure: 1) record a standard curve for the pathogen in spiked samples; 2) record a sample reaction from unknown analytes; and 3) select and view results to analyze a sample reaction using a specific standard curve to instantly determine bacterial burden (**Figure 2.7a–c**).

7.10.2. Running standard curve and unknown sample reactions

When running a standard curve or unknown sample reaction, the app launches a specialized viewfinder, allowing the user to carefully center the reaction vials in the view-frame of the phone's camera, such that their intensity can be analyzed over time. After entering a name, the user must load samples and press “start”, which begins a timer to correct for lost reaction time while setting up the box and aiming the camera (**Figure 2.7d, e**). When the user selects “Begin Recording Amplification,” the application proceeds to take one photograph of the amplification reaction every 10 s over the course of a 50 m period (**Figure 2.1b**, Supplemental **Figure 2.7f**). The app performs image processing for each of the vials outlined in the viewfinder to extract the average green intensity of each pixel, which is stored in a matrix. For the “1. Record Standard Curve” option, the software also prompts the

user to align each reference sample with a provided sample map so that the input starting concentrations of DNA are known. The standard curve is determined through a linear regression fit of Tt vs. $\log_{10}$[conc], which is stored as a .pasc file for determining the results in future tests. When the user has selected the “2. Record Sample” option, the app will record traces for each sample, to be analyzed later. The numerical sample traces and collected time-stamped photos are saved as a .parr file and as .jpeg files, respectively, which may be extracted by the user to any computer.

7.10.3. Automated data analysis

When the user selects “3. Select and view results”, the app will prompt the user to choose a standard curve that has been recorded as outlined in the previous section with known standard concentrations. After data processing and analysis (described in the Supplementary Methods section), the Tt of unknown test samples are related to their initial concentrations via the standard curve. On its final screen, the app displays the number of bacterial CFU in each reaction vial (**Figure 2.7 g–i**).

7.11. Supplementary Methods.

7.11.1 Determination of T_t

The first step in manipulating the signal curve is the application of a smoothing filter that averages each point with the ten surrounding point values. Though this will help correct for small changes in the measured fluorescence, it will not account for variations in amplification efficiencies, ground-phase minima, or plateau-phase maxima. To combat such behavioral deviances between samples, we defined T_t as the time when the maximum of the derivative of a coarse model of the real-time curve occurs. Based on the first derivative maximum (FDM) method

(*251*), the coarse derivative technique avoids falsely assigning T_t to errant noise in the finite first-derivative curve and accounts for sample-dependent variations in amplification efficiencies or time-course minima and maxima. Instead of computing the signal difference on a point-to-point scale, the coarse derivative takes the difference over a coarse time-stepper (i.e., a chosen length of time over which to average). The coarse differential of a given system U with time step δt, where time $t_k = k\delta t$, is:

Equation 1

$$\frac{\partial U}{\partial t} = \frac{U^{k+1,N} - U^{k,N}}{\delta t}$$

***Equation 1*.** Coarse derivative function used to differentiate an output signal U according to a set time-stepper δt.

In our case, the optimal δt was empirically determined to be the average rise time from the ground phase to the plateau phase, or 220 s. Using the average rise time as a time-stepper allows us to compute the timescale derivative of our fluorescence measurements in a way that is more tractable than attempting a finite first derivative, yet commensurate with the measured trends. T_t is hence defined as the time of maximum signal change over a 220 s time step.

7.11.2 Detection of Amplification

During automated analysis, sample signal curves are evaluated with a built-in feature that determines whether amplification has occurred based on the behavior of positive and negative controls. A positive sample must demonstrate an increase in fluorescent signal that indicates complete amplification (calculated as the sum of the

positive first derivative values for each trace, which if beyond a preset threshold value indicates amplification). This approach distinguishes the large rise in signal typical of amplification from small rises that can occur as background fluorescence increases during a run. Importantly, the preset threshold value is different between blood (which is highly turbid, damping the rise in fluorescence) and urine or feces samples (which are substantially less turbid).

Equation 2

$$Sample\ Threshold\ Value\ (dU) = \int_{0}^{3000} \frac{dU}{dt}; dU > 0$$

Equation 2*.* Integral function used to sum the increases in sample output signal U, over the signal output trace, for all positive changes in fluorescence from 0 to 3000 s. Amplification is positive if this value exceeds a preset threshold value.

7.11.3 Determination of sample CFU from a standard curve

During automated analysis, a simple linear regression model is used to calculate bacterial burden, based on the slope and y-intercept of a line fitted to a standard curve of T_t as a function of $\log_{10}$ [CFU], in spiked blood, urine, or feces.

Equation 3

$$\left(\log_{10}\left(\frac{CFU}{Reaction}\right)\right) = m\,(T_t) + b$$

Equation 3**.** Determination of CFU from a linear curve, used to determine murine bacterial burdens. The $\log_{10}$ of the bacterial burden is equal to the slope of the standard curve *m*, multiplied by the T_t, plus the y-intercept *b*.

CHAPTER 3 MATERIALS AND METHODS

7.12. Study Design.

Human saliva samples spiked with SARS-CoV-2 or influenza viruses were analyzed with the smaRT-LAMP detection system in comparison to gold-standard RT-qPCR. These analyses were used as the basis for smaRT-LAMP detection of SARS-CoV-2 from self-collected clinical samples obtained from patients with COVID-19.

7.13. Strains.

Coronavirus strains and gRNA: SARS-CoV-2: USA-WA and Hong Kong; Human seasonal coronavirus: HCoV-OC43, HCoV-229E, HCoV-NL63, and HCoV-HKU1; SARS-CoV-1; and MERS-CoV (see supplement). SARS-CoV-2 variant gRNA: B.1.1.7 (UK), P.1 (Brazil, B.1.1.28.1), B.1.526 (NY), B.1.429 (CAL.20C) and B.1.617.2 (India). Influenza virus strains: influenza A (H1N1) and influenza B (Yamagata). Bacterial respiratory pathogens: (*144, 207*) *Streptococcus pneumoniae*, *Staphylococcus aureus, Pseudomonas aeruginosa* and *Klebsiella pneumoniae.*

7.14. Primer Gene Targets.

SmaRT-LAMP primers target the SARS-CoV-2 nucleocapsid (N) and ORF1ab genes; influenza primers target genes encoding matrix protein (M1) and polymerase (PB1) for influenza A; and M1 and nonstructural protein (NS1) for influenza B (**Table 3.1**). Primers for CDC 2019-nCoV RT-qPCR analysis targets the

SARS-CoV-2 N gene, (*137*) while the influenza SARS-CoV-2 (Flu SC2) RT-qPCR multiplex assay targets M1 for influenza A and NS2 for influenza B (*139*).

7.15. Minimizing Lamp Primer-Dimer Amplification.

Since its discovery more than two decades ago, LAMP diagnostics have been limited by primer-dimer amplification (false-positives) due to the requirement of six primers per target (*122-124*). This technical hurdle was overcome by the development of smaRT-LAMP experimental conditions which effectively eliminate primer-dimer amplification as described in the supplement (**Figure 3.4**).

7.16. Overview Of The smaRT-LAMP Platform.

The smaRT-LAMP protocol involves assembly of the reaction mixture at room temperature in 96-well plates and, transfer to a 70 ^{o}C heat block, which initiates both the reverse transcription and LAMP reactions (**Figure 3.5**). Image data are collected and analyzed by a smartphone running the free, custom-built “Bacticount” app available through the Google Play store, transforming the smartphone into a stand-alone device for quantitative diagnostics. The entire detection system can be fabricated for less than $100 USD (in addition to the cost of the smartphone; ~$200 USD used; ~$400 USD new), and can simultaneously analyze up to 96 samples, at a cost of < $7 USD/test (**Table 3.2**).

7.17. Analysis of Virus Present in Saliva.

7.17.1 Spiked saliva.

Known numbers of inactivated SARS-CoV-2 as well as several viral and bacterial respiratory pathogens were added to virus-negative human saliva and serial dilutions made using saliva diluent. Samples were analyzed using smaRT-LAMP and RT-qPCR to assess specificity and sensitivity of the assay.

7.17.2. Patient saliva.

Saliva specimens were collected at Santa Barbara Cottage Hospital, Santa Barbara, CA. Two sub-groups (symptomatic and asymptomatic) of participants were enrolled: the symptomatic group consisted of recruited patients who tested positive for SARS-CoV-2 with symptoms, and the asymptomatic patients were recruited from the same community, through negative admission screening testing for SARS-CoV-2 infection. Patient saliva specimens were collected in sterile plastic tubes and stored frozen at - 20 ^{o}C on site. Upon transport to UC Santa Barbara, frozen specimens were thawed on ice, heat-inactivated at 95 ^{o}C for 30 min, aliquoted and stored frozen at - 80 ^{o}C. For processing, saliva samples were thawed on ice and reaction mix was assembled at room temperature. Human subjects approval was obtained from the Institutional Human Subjects Use Committee of the University of California, Santa Barbara and the Institutional Review Board of Santa Barbara Cottage Hospital. To assess real-world detection of virus in patient saliva samples, we carried out a temporal analysis of patient saliva samples stored up to a week at 4°C and 25°C using smaRT-LAMP.

7.18. SmaRT-LAMP Sensitivity and Specificity.

SmaRT-LAMP can simultaneously detect SARS-CoV-2, influenza A and/or B viruses via addition of cognate primers to individual wells, which is clinically important when CoV-2 and influenza viruses are co-circulating as the two disease syndromes are very similar (*125*). Sensitivity and specificity tests were performed using contrived saliva specimens as recommended under FDA Emergency Use Authorization (EUA) guidelines as described in the supplement (*136*). Sensitivity was determined as the largest serial dilution of viral stock giving a signal in $\geq$ 19/20 biological replicates. Specificity was evaluated using 10^5 and 10^6 genome copies/mL of designated viral or bacterial pathogens, respectively, or using undiluted viral stocks quantified by the 50% tissue culture infective dose assay [$TCID_{50}$, the highest dilution causing a cytopathic effect in one-half of tissue culture samples] (*253*). Specificity was determined by the presence or absence of signal (binary + or - call) in 20/20 biological replicates for all respiratory pathogens except SARS-CoV-2 variants (10/10 biological replicates).

7.19. Data Analysis.

The Bacticount app enables the smartphone to serve as a stand-alone diagnostic for sensitivity (binary +/- call) and quantitative detection of microbial titers as adapted from Barnes et al (*144*). Real-time LAMP traces were automatically generated for each sample and used to calculate the threshold time (Tt) and concentration by the Bacticount app on the smartphone. Tt is linearly related to the logarithm of the input concentration and is used to determine the concentration of

virus in saliva samples using standard curves. Alternatively, trace files from the phone were transferred to a personal computer (PC), where a custom MATLAB script was used to determine the Tt and calculate the resultant virus concentration using standard curves with Microsoft Excel.

7.20. Statistical Analyses.

SmaRT-LAMP and RT-qPCR molecular diagnostic sensitivity and specificity were determined by comparing the proportion of samples that amplified with cognate vs. non-cognate primers (or no template), using Chi-square (Epicalc 2000 version 1.02, 1998 Brixton Books).

7.21. Supplementary Methods.

7.21.1. Strains

Coronavirus: The following reagents were obtained from BEI Resources, NIAID, NIH or ATCC: inactivated SARS-CoV-2 isolate from USA-WA1/2020 (NR-52286); genomic RNA from SARS-CoV-2, isolate Hong Kong/VM20001061/2020 (NR-52388); genomic RNA from SARS-CoV-1 (NR-52346); inactivated Middle East Respiratory Syndrome coronavirus MERS-CoV EMC/2012 (NR-50549). Human seasonal coronavirus: HCoV-OC43 (VR-1558); HCoV-229E (VR-740); HCoV-NL63 (NR-470); and genomic RNA from HCoV-HKU1 (VR-3262SD). SARS-CoV-2 variant genomic RNA was obtained from Carolina Arias and Zach Aralis (University of California, Santa Barbara): B.1.1.7 (UK), P.1 (Brazil, B.1.1.28.1), B.1.526 (NY), B.1.429 (CAL.20C) and B.1.617.2 (India). Influenza virus: influenza A Virus, A/San

Diego/1/2009 (H1N1)pdm09 (NR-15241) and influenza B virus, B/Christchurch/33/2004 (Yamagata Lineage) (NR-36526) were obtained from BEI Resources. The viral genomic RNA and virus stocks were aliquoted and stored at -80 °C. Stocks were not thawed and frozen more than three times. Bacterial respiratory pathogens: (*144, 207*) Gram-positive *S. pneumoniae* and *S. aureus* were obtained from Jamey Marth (Sanford-Burnham-Prebys Medical Discovery Institute). Gram-negative *P. aeruginosa* and *K. pneumoniae* were obtained from the ATCC.

7.21.2. Oligonucleotide Primers

Table 3.1. lists the oligonucleotide primer sequences used in this study. The smaRT-LAMP primer sets consist of two outer (F3 and B3), two inner (FIP and BIP), and two loop primers (F-Loop and B-Loop). Primers for smaRT-LAMP analysis target the SARS-CoV-2 nucleocapsid (N) and ORF1ab genes; influenza primers target genes encoding matrix protein (M1) and polymerase (PB1) for influenza A; and M1 and nonstructural protein (NS1) for influenza B. SARS-CoV-2 LAMP primer sets targeting ORF1ab and N genes (sets 9 and 16, respectively) were used for all analyses in this study. Alternative SARS-CoV-2 LAMP primers sets targeting ORF1ab and N genes have been validated for smaRT-LAMP (sets 15 and 3, respectively). Primers for CDC 2019-nCoV RT-qPCR analysis targets the SARS-CoV-2 N gene, (*137*) while the influenza SARS-CoV-2 (Flu SC2) RT-qPCR multiplex assay targets M1 for influenza A; and NS2 for influenza B (*139*).

New smaRT-LAMP primer sets (SARS-CoV-2, set 9; influenza A, set A5a; and influenza B, sets B5, B7) were designed as follows. A minimum of 42 genome sequences each for SARS-CoV-2, influenza A, and influenza B were downloaded

from the NCBI virus genome database (SARS-CoV-2) or NCBI Influenza Virus Database (influenza A and B), and aligned using CLC sequence viewer (version 6.8.1), to identify conserved regions and consensus target sequences for primer design. Loop primers were designed for SARS-CoV-2 alternative primer set 15 adapted from Ganguli et al. (*147*). Influenza A primer set A6 was adapted from Poon et. al (*148*) by designing loop primers and using consensus sequences to redesign primers.

7.21.3. LAMP reagents

Calcein, KCl, $MnCl_2$, $(NH_4)_2SO_4$, and Triton X-100 were purchased from Millipore Sigma (St. Louis, MO). Bst 2.0 WarmStart DNA polymerase, WarmStart RTx reverse transcriptase, isothermal amplification buffer, $MgSO_4$, RNase inhibitor (murine) and deoxynucleotide triphosphates were purchased from New England Biolabs (Beverly, MA); 1M Tris (pH 7.5) from Invitrogen (Carlsbad, CA); and, nuclease-free water, DMSO, NaOH, and polysorbate 20 (Tween-20) from ThermoFisher (Waltham, MA). PCR strip tubes with optically clear lid strips were purchased from Bio-Rad (Hercules, CA). Oligonucleotide primers were purchased from Integrated DNA Technologies (IDT, Coralville, IA).

7.21.4. Optimal primer design and reaction conditions

Optimization of target RNA stability and cDNA synthesis favors target gene vs. primer-dimer amplification (**Figure 3.4**). Parameters include: (i) primer design to reduce primer-dimers; (ii) reaction chemistry favoring primer binding to target; (iii) primer melting; and (iv) RNase inhibitor addition to saliva specimens. Primer design: SARS-CoV-2 LAMP primer sequences were derived from published reports (*145,*

146) and/or designed and optimized with PrimerExplorer v.5.0 (http://primerexplorer.jp/lampv5e/index.html) (**Table 3.1**). All candidate primers were subsequently screened for the likelihood of primer-dimer formation via Integrated DNA Technology Oligo Analyzer software (v3.1) (http://eu.idtdna.com/analyzer/Applications/OligoAnalyzer/), and primers with large negative ΔG (- 9 kcal/mol), which are associated with high primer-dimer potential, were further optimized to obtain a more-positive ΔG by base sliding or deletion, particularly within 8 bp of the 5' and 3' ends of primers (*123*). Candidate primers were then screened for specificity via a comparative BLAST homology search of a coronavirus (HCoV-229E, HCoV-NL63), β coronavirus (HCoV-HKU1, HCoV-OC43, SARS-Cov-1, MERS) and influenza A (H1N1) and B (Yamagata) virus genomes in the NCBI data base.

Restrictive reaction chemistry: Standard manufacturer recommendations (https://www.neb.com) were modified to more restrictive conditions to diminish primer-dimer formation/amplification by reducing the reaction mix (50 µL) Mg^{2+} concentration (from 8.0 mM to 5.7 mM); addition of 40 mM Tris-HCl pH 7.5 to saliva sample mix (25 µL); and increasing reaction temperature (from 65 ^{o}C to 70 ^{o}C). Primer melting: To reduce primer-dimer formation in the "master mix", primers were individually heated to 70 ^{o}C, cooled to room temperature, and added immediately prior to the addition of reverse transcriptase and DNA polymerase. RNase inhibitor: To reduce RNA degradation, RNase inhibitor was added to saliva specimen samples prior to their addition to the master mix. The resultant reaction mix vessels were loaded on a heat block at 70 ^{o}C to initiate reverse transcription and LAMP reactions,

while the smaRT-LAMP app simultaneously records fluorescence following viral DNA amplification. In summary, the smaRT-LAMP protocol favors target RNA stability and cDNA synthesis, while effectively eliminating primer-dimer self-amplification (false positives) that has hindered LAMP-based diagnostics.

7.21.5. SmaRT-LAMP reaction conditions

The smaRT-LAMP reaction mix was assembled at room temperature in 50 µL total reaction volume containing 25 µL "sample mix" (20 µL saliva specimen with RNA stabilizers), 25 µL "master mix" (containing lysis reagents, primers and polymerase enzymes) in PCR strip tubes (BioRad). The resultant smaRT-LAMP reaction mix (50 µL) was transferred to a 70 ^{o}C heat-block for lysis and amplification, which was monitored by the free, custom-built Bacticount app adapted from (*144*) on Samsung Galaxy S7 or S9 phones.

The order of assembly of LAMP reagents is critical to improve LAMP performance and reduce primer-dimer self-amplification (false positives). Sample mix is comprised of 20 µL saliva and 5 µL RNase inhibitor/Tris-HCL buffer (2.5 µl 400 mM Tris-HCl, pH 7.5 [final specimen mix concentration of 40mM Tris-HCl]), 1.25 µL RNase inhibitor (40 U/µL), and 1.25 µL nuclease-free water. Master mix and sample mix volumes are scaled up 10% relative to the actual volumes need to test a given sample number (reagent volumes for 96 samples are given in **Table 3.2**). Order and composition of master mix (25 µL) assembly is as follows: (i) 5 µL of 10X isothermal amplification buffer (final reaction concentrations of 20 mM Tris-HCl, 10 mM $(NH_4)_2SO_4$, 50 mM KCl, 2 mM $MgSO_4$, 0.1% polysorbate 20, pH 8.8 @ 25^{O}C), supplemented with 1.85 µL of 100 mM $MgSO_4$ and 0.5 µL 40% polysorbate 20 [final

reaction concentrations of 5.7 mM and 0.5% (w/v), respectively]); (ii) 7 µL deoxynucleotide triphosphates (10 mM each; 1.4 mM final reaction concentration); (iii) 2 µL fluorescence detection reagent: calcein and $MnCl_2$ [final reaction concentrations of 20 µM and 0.4 mM, respectively]; and (iv) 7.7 µL oligonucleotide primers (2 gene targets, using two LAMP primer sets per reaction): 0.34 µL x 2 of F3 and B3 (30 µM); 0.26 mL x 2 of FIP and BIP (300 µM); 1.3 µL x 2 of F-Loop and B-Loop (30 µM) [final reaction concentrations of 0.2 µM, 1.6 µM, and 0.80 µM, respectively]. (v) In order to reduce primer-dimer formation, primers were heated individually at 70 ^{o}C for 5 m and allowed to cool to room temperature; and added to master mix just prior to enzyme addition (primer dimers occur with no primer melting and earlier primer addition to master mix). (vi) High concentration *Bst* 2.0 WarmStart DNA polymerase was added (0.64 U/µL) together with RTx WarmStart reverse transcriptase (0.6 U/µL). (vii) Specimen mix is added to master mix and the resultant reaction mix was transferred to a 70 ^{o}C heat block for amplification. Negative controls consisted of confirmed clinically-negative saliva from Cottage Hospital. For patient saliva testing, heat-treated aliquots were removed from - 80 ^{o}C storage, thawed on ice and added to sample mix at room temperature. Specimen stability as a function of time and temperature was assessed in this study.

7.21.6. RT-qPCR reaction conditions

The CDC 2019-nCoV RT-qPCR (*137*) and Flu SC2 RT-qPCR (*139*) tests contains primers and probes for SARS-CoV-2; and SARS-CoV-2, influenza A and B, respectively. SARS-CoV-2 was evaluated using SARS-CoV-2, influenza A, or influenza B primer and probes (IDT) and the LUNA cell-ready probe one step RT-

qPCR kit (NEB). RT-qPCR was performed using 10 µL saliva sample as per manufacturer recommendations.

7.21.7 SmaRT-LAMP platform hardware

SmaRT-LAMP hardware was adapted from Barnes et al. (*144*) Experiments were performed in low-profile 0.2-mL PCR strips (Bio-Rad cat. no. TLS-0801) covered with optical flat strips (Bio-Rad cat. no. TLS-0803). Sample tubes were placed in an aluminum sample block (LightLabs cat. no. A-7079) on a hot plate (HP30A digital aluminum hot plate, Torrey Pines Scientific, Carlsbad, CA). A cardboard box covering the hot plate was painted black and a flexible LED cable of 96 W, 480 nm, 672 lumens, 96-LEDs (DealeXtreme cat. no. 180563) was affixed to the inside top cover of the box to excite the calcein dye at 480 nm. LEDs were powered using a single output DC power supply (UA8001A, Agilent Technologies, Santa Clara, CA). A Samsung Galaxy S7 or S9 smartphone (Samsung Electronics Co., Ltd.) was outfitted with a 520 ± 10 nm bandpass filter (Edmund Optics cat. no. 65-699) for visual detection of emitted green light. All RT-qPCR reactions were performed on a Bio-Rad CFX96 qPCR Thermocycler.

7.21.8 Bacticount application

The Bacticount mobile phone application for monitoring and analyzing the smaRT-LAMP assay was built on a Samsung Galaxy S7 and S9 phone and can be downloaded and installed free of charge from the Google Play Store or www.bacticount.com. The main screen offers a choice to “Start Bacterial or Viral Analysis” and the user is prompted to pick the sample type; i.e., blood, urine, feces, or saliva (**Figure 3.6**). The user follows a three-step procedure: 1) Record Standard

Curve for a pathogen of interest in contrived (spiked) samples (e.g., SARS-CoV-2; influenza); 2) Record Sample; and 3) Select and view results where the app displays the sample results in a binary manner as follows: “Pathogen Detected” - designated as red circle; or, “No Pathogen Found” - designated as green circle on the “Reaction Results” screen. Further, by clicking on the red circle that appears if a pathogen is detected, the app then displays the viral load in copies/mL on the “Detailed Reaction Results” screen.

7.21.9. Establishing standard curve, unknown sample reactions, and data analysis

When running a sample reaction, the app launches a specialized viewfinder, allowing the user to center the reaction vials in the view-frame of the phone’s camera, such that their intensity can be analyzed over time as adapted from (*144*) for up to 96 sample wells (**Figure 3.6**). After entering the sample name, the user loads samples and presses “OK”, which starts a timer to measure lost reaction time while setting up the box and aiming the camera. When the user selects “Begin Recording Amplification,” the application proceeds to capture one photograph of the amplification reaction every 10 s over the entire course of the allotted reaction time. The user has three options: 1. Record Standard Curve option, the software also prompts the user to align each reference sample with a provided sample map so that the input starting concentrations of nucleic acid are known. The standard curve is determined through a linear regression fit of T_t vs. $\log_{10}$[conc], which is stored as a ‘.pasc file’ for determining the results in future tests. 2. Record Sample option, the app will record traces for each sample. The numerical sample traces and collected time-stamped photos are saved as a ‘.parr file’ and as ‘.jpeg files’, respectively,

which may be extracted by the user to any computer. 3. Select and view results option, the app will prompt the user to choose a standard curve that has been recorded as outlined in the previous section with known standard concentrations. After data processing and analysis, the T_t of unknown test samples are related to their initial concentrations via the standard curve. On its final screen, the app displays the viral load for each positive reaction well that was initially scored in a binary manner as either positive (red) or negative (green).

7.21.10. SmaRT-LAMP sensitivity and specificity assays

Sensitivity and specificity tests were performed using contrived saliva specimens as recommended under FDA Emergency Use Authorization (EUA) guidelines (*136*). Sensitivity: Limit of detection (LOD) was evaluated following serial dilution of viral and genomic RNA (genome copies/mL) or viral stocks quantified by the 50% tissue culture infective dose assay [$TCID_{50}$, the highest dilution causing a cytopathic effect in one-half of tissue culture samples] (*253*). Viral pathogens quantified by $TCID_{50}$/mL include: influenza A, 1.4×10^5 $TCID_{50}$/mL; influenza B, 8.0×10^4 $TCID_{50}$/mL; HCoV-NL63, 8.0×10^3 $TCID_{50}$/mL; HCoV-229E, 8.0×10^5 $TCID_{50}$/mL; HCoV-OC43: 4.5×10^4 $TCID_{50}$/mL. LOD was determined by the largest serial dilution giving a signal in $\geq$ 19/20 biological replicates. Specificity: Cross-reactivity tests were performed with contrived saliva specimens using EUA recommended amounts of 10^5 and 10^6 copies/mL specimen for viral and bacterial pathogens, respectively; or via undiluted viral stocks quantified by $TCID_{50.}$ (*136*) Specificity was determined by the presence or absence of signal (binary +/- call). n= 10 biological

replicates for SARS-CoV-2 variants; n = 20 biological replicates for all other pathogens.

CHAPTER 4 MATERIALS AND METHODS

7.22. Bacterial Strains and Media.

Staphylococcal clinical isolates analyzed included USA300, a community-associated methicillin-resistant *Staphylococcus aureus* (*SA*) isolate causing the most MRSA infections in the United States (*248*); and 9 isolates from human sepsis patients (Santa Barbara Cottage Hospital, 2016) with various host sites of pathogen origin including blood, wound, urine, sputum (termed MRSA Blood [MT3302]; Wound [MT3315]); MSSA (Blood [MT3305]; Wound [MT3307]; Urine [MT3309]; Sputum [MT3314]); and CoNS (*S. epidermidis*, blood [MT3320]; *S. lugdunensis*, blood [MT3317]; *S.warneri*, blood [MT3321]). *S. pneumoniae* (*SPN*) clinical isolates included D39 (ser. 2) (*254*), and 5 *SPN* isolates derived from the nasopharynx of children with sickle cell anemia at risk for invasive pneumococcal disease (Daw 1 [serotype 6]; Daw 2 [serotype 23]; Daw 19 [serotype 6]; Daw 20 [serotype 11]; Daw 25 [serotype 35C]) (*255, 256*). Gram-negative bacterial isolates included *Salmonella* spp., *Salmonella* Typhimurium ATCC 14028, TY1212; and var. 5 (04)-9639; S. Dublin Lane; S. Newport (03)-721; S. Choleraesuis χ3236 (*245, 246*); E. coli ATCC 25922; UPEC J96; UPEC ECR12; UPEC ATCC 11775; APEC χ7126; A96 χ7117; EPEC χ2927); RDEC-1 χ2862; EPEC JPN 15; *Yersinia pseudotuberculosis* (YPIII/pIB1; IP32953; IP2515; IP2666) (*247*); *Shigella flexneri* ATCC 29903; *Providencia stuartii* ATCC 29914; *Citrobacter freundii* ATCC 8090; *Klebsiella pneumoniae* ATCC 13883; *Pseudomonas aeruginosa* ATCC 10145. All *Staphylococcus* strains were isolated on Tryptic Soy Broth Agar (TSA) incubated at 37 °C in ambient air. *S. pneumoniae* strains were isolated on Columbia Sheep's

Blood Agar (CSBA) and grown in Todd-Hewitt Broth (THB) supplemented with 2% yeast extract incubated at 37 °C in a 5% CO_2 incubator. Gram negative bacteria were isolated on Luria-Bertani (LB) agar (*257*) incubated at 37 °C or 28 °C (*Yersinia*) in ambient air. Standard AST broth medium is Mueller–Hinton Broth (MHB) supplemented with $CaCl_2$ and $MgCl_2$ to make cation-adjusted MHB (Ca-MHB) (*162*). AST was also performed in Dulbecco's Modified Eagle Medium (DMEM (*167*); High Glucose [Life Technologies]); Lacks medium (*168*); modified Lacks medium (MLM) (*170*); or low phosphate, low magnesium medium (LPM) (*53*). DMEM cultures were incubated in a 5% CO_2 incubator; all other conditions were incubated in ambient air. To facilitate growth, DMEM was supplemented with 5% LB broth for *Staphylococci*, and 5% Lysed Horse Blood (LHB) for *S. pneumoniae*; MLM was supplemented with 5% THB for *S. pneumoniae* D39.

7.23. MIC Assays.

The minimum inhibitory concentration (MIC) was determined according to the Clinical and Laboratory Standards Institute (CLSI) guidelines by either broth or agar dilution (*47, 162*). For determination of MIC in alternative media conditions, bacteria were obtained from overnight culture (*Staphylococci* and Gram-negative bacteria) or after a 4 h incubation period (*S. pneumoniae*) in specified medium and diluted into same medium containing 2-fold serial dilutions of antibiotics. To control for the potential effects of pH and media composition for LPM pH 5.5 comparisons, antibiotic resistance and clinical breakpoint designations were calculated by comparing the MIC in LPM medium divided by the MIC in MHB medium at both pH

5.5 and pH 7 (unbuffered) (ratio of LPM pH 5.5/pH 7.0 to MHB pH 5.5/pH 7.2) (*54*). MIC values were derived after 20 h incubation, and were the result of at least 6 independent determinations.

7.24. Sodium Bicarbonate Susceptibility Assays.

Strains were grown in MHB pH 7.2; unbuffered; MHB adjusted to pH 7.2 with 100 mM Tris(hydroxymethyl)aminomethane (Fisher Scientific); and DMEM liquid pH 7.4 (containing 44 mM $NaHCO_3$; Difco/Becton Dickinson). All other media conditions were adjusted to pH 7.4 with 100 mM Tris including: MHB medium w/$NaHCO_3$; and $NaHCO_3$- free powdered DMEM w/wo $NaHCO_3$. Bacteria were grown overnight in specified medium and diluted as described above. For *S. pneumoniae* isolates, $NaHCO_3$ assays were performed in MHB medium in the CO_2 incubator due to viability considerations since *S. pneumoniae* isolates tested did not grow in either MHB medium with $NaHCO_3$ in ambient air; or in DMEM in the absence of $NaHCO_3$ in the CO_2 incubator. MIC values were the result of at least 6 independent determinations.

7.25. Virulence Assays.

7.25.1. Intraperitoneal (i.p.) Infection

S. Typhimurium 14028 (dose of 10^2 CFU) and *S. pneumoniae* Daw 25 (dose of 9×10^7 CFU) were grown overnight in LB or Todd-Hewitt medium with 2% yeast extract, respectively, and sub-cultured to $A_{600} = 0.4$, resuspended in 0.15M NaCl, and administered to mice via the i.p. route of infection.

7.25.2. Intravenous (i.v.) Infection

MRSA USA300 (dose 1 × 10^8 CFU), MRSA Blood (MT3302; dose 1.5 × 10^8 CFU) and MSSA Wound (MT3307; dose of 2 × 10^8 CFU) were grown overnight in TSB and sub-cultured to A_{600} = 0.4; and *K. pneumoniae* ATCC 13883 (dose of 2 × 10^8 CFU) were grown overnight in LB medium. Strains were resuspended in 0.15 M NaCl and administered i.v. to mice by retro-orbital injection.

7.25.3. Antibiotic Treatment

Infected mice were treated (or mock-treated) with the following dosing regimens beginning 2 h post-infection: azithromycin (100 mg/kg/day), ceftiofur (40 mg/kg/day), ceftriaxone (50 mg/kg/day), cephalothin (200 mg/kg/day), ciprofloxacin (30 mg/kg/day), colistin (30 mg/kg/day), co-trimoxazole (15 mg/kg/day), daptomycin (10 mg/kg/day), erythromycin (100 mg/kg/day), tetracycline (100 mg/kg/day), or trimethoprim (30 mg/kg/day).

7.25.4. Bacterial Clearance

Mice infected with MSSA Wound (MT3307; dose of 4 × 10^8 CFU) were treated with azithromycin or co-trimoxazole. All drug doses were delivered once every 24 h except cephalothin, ciprofloxacin, colistin, and co-trimoxazole, which were delivered once every 12 h; ceftriaxone and ceftiofur were given every 12 h for MRSA Blood (MT3302) experiments. All drugs were delivered by the i.p. route with the exception of cephalothin (subcutaneous). Mouse survival was assessed for 10 days post-infection. Equal numbers of male and female 10- to 12- week-old litter-mate C57BL/6J mice were used in all virulence studies. Institutional Animal Care

and Use Committee of the University of California, Santa Barbara approved all mouse research protocols undertaken herein.

7.26. Statistical Analysis.

Statistical significance for difference in proportions of animal survival was calculated using Chi-square (Epi Info 7, CDC). For all statistical analyses, a significance level (P) of < 0.05 was considered to be statistically significant. Degrees of statistical significance are presented as $^{***}P < 0.001$, $^{**}P < 0.01$, or $^{*}P < 0.05$.

CHAPTER 5 MATERIALS AND METHODS

7.27. Bacterial Strains and Media.

Staphylococcal clinical isolates analyzed included methicillin-resistant *Staphylococcus aureus* (MRSA USA300), a methicillin-sensitive *Staphylococcus aureus* (MSSA Newman), and an isolate from a human sepsis patient termed MRSA Blood (MT3302) (*207*). An *E. faecium* urinary sepsis isolate was included (Santa Barbra Cottage Hospital, Santa Barbara, CA, 2018). Gram-negative bacterial isolates included *Salmonella* Typhimurium ATCC 14028; *E. coli* ATCC 25922; *Klebsiella pneumoniae* ATCC 13883; a multidrug-resistant urinary sepsis isolate MT3325 (Pacific Diagnostic Laboratories, Lompoc, CA, 2017); *Enterobacter cloacae* ATCC 13047; *Pseudomonas aeruginosa* ATCC 10145; *Acinetobacter baumannii* ATCC 19606. All *Staphylococcus* strains were isolated on Tryptic Soy Broth Agar (TSA) incubated at 37 °C in ambient air. *E. cloacae* was isolated on Luria-Bertani (LB) agar (*257*) incubated at 37 °C in ambient air. Gram-negative bacteria were isolated on LB agar incubated at 37 °C in ambient air. Standard AST medium is Mueller-Hinton Broth, supplemented with $CaCl_2$ and $MgCl_2$ to generate cation-adjusted MHB (Ca-MHB) (*162*). AST was also performed in Dulbecco's Modified Eagle Medium (DMEM (*167*) High Glucose [Life Technologies]); pooled normal human serum (Millipore Sigma, product S1-Liter); pooled normal human urine (Innovative Research, Novi, MI, product IRHUURE1000ML). DMEM and serum cultures were incubated in a 5% CO_2 incubator; all other conditions were incubated in ambient air. To facilitate growth, DMEM was supplemented with 5% LB broth for *Staphylococci*; serum was supplemented with 30% LB for all strains on the microtiter

dish, or 40% Ca-MHB for *Acinetobacter* following serum heat inactivation (30 min in a 56 °C water bath); urine was supplemented with 30% LB for most strains on the microtiter dish. Robust growth of *Enterococcus* required supplementation with 30% TSB for all media, on the microtiter dish. Urine and serum stocks arrived frozen from the supplier, 1 L stocks were thawed at 4 °C for 2 d until fully thawed, and split into single-use aliquots. Aliquots of urine and serum were stored frozen at -20 °C, and thawed in a water bath at 37 °C immediately before use.

7.28. MIC Assays.

The minimum inhibitory concentration (MIC) was determined according to the Clinical and Laboratory Standards Institute (CLSI) guidelines by broth microdilution (*47, 162*). For determination of MIC in host-mimicking media or human fluids, bacteria were obtained from overnight cultures grown in 100% raw specified medium (to sensitize the isolate to the medium) and diluted into the same medium containing 2-fold serial dilutions of antibiotics (typically supplemented with 30% LB for human fluids to facilitate growth on the microtiter dish). To further facilitate universal growth of pathogens, all strains in all conditions were inoculated to $1x10^6$ CFU/mL instead of the typical $5x10^5$ CFU/mL used in broth microdilution AST. MIC values were derived after 20 h of incubation and were the result of at least 6 independent determinations.

7.29. Disruption of Aggregates for Viability and AST Assays in Human Fluids.

Human pathogens were frequently found to form robust aggregates when grown in human fluids, which impede the reproducible and accurate viability measurements necessary for consistent inoculation in AST. To correct for this, all pathogen cultures were vortexed following culture (0.5 mL in 16 mm glass culture tubes) on high for 15 s, immediately transferred to a 1.5 mL microfuge tubes, vortexed again for 15 s on high, and immediately diluted in 10-fold increments to the final desired concentrations (vortexing for 5 s between each dilution step). Cultures were then immediately spread on agar plates for viability determination, or immediately inoculated onto a microtiter dish for AST. In **figure 5.1a**, *S. aureus* Ca-MHB overnight culture viability was evaluated after growth on a microtiter dish following direct colony inoculation.

7.30. Microtiter Plate Imaging.

Microtiter plates were imaged using a Samsung Galaxy S7 smartphone (Samsung Electronics Co., Ltd.), with a macroscopic lens (Easy-Macro, Manchester, MA) affixed to the front camera. All microtiter plate wells were imaged individually from below, using white light reflective illumination while inside an AlphaImager gel imaging cabinet.

REFERENCES

1. D. R. Dodds, Antibiotic resistance: A current epilogue. *Biochemical pharmacology* **134**, 139-146 (2017).
2. R. Kolter, G. P. Van Wezel, Goodbye to brute force in antibiotic discovery? *Nature microbiology* **1**, 1-2 (2016).
3. R. Rosenberg, Detecting the emergence of novel, zoonotic viruses pathogenic to humans. *Cellular and Molecular Life Sciences* **72**, 1115-1125 (2015).
4. D. E. Morris, D. W. Cleary, S. C. Clarke, Secondary Bacterial Infections Associated with Influenza Pandemics. *Frontiers in Microbiology* **8**, 1041 (2017).
5. H. Hiyoshi, C. R. Tiffany, D. N. Bronner, A. J. Bäumler, Typhoidal Salmonella serovars: ecological opportunity and the evolution of a new pathovar. *FEMS Microbiology Reviews* **42**, 527-541 (2018).
6. S. E. Majowicz *et al.*, The Global Burden of Nontyphoidal Salmonella Gastroenteritis. *Clinical Infectious Diseases* **50**, 882-889 (2010).
7. S. M. Faruque *et al.*, Emergence and evolution of Vibrio cholerae O139. *Proceedings of the National Academy of Sciences* **100**, 1304-1309 (2003).
8. D. M. Morens, A. S. Fauci, The 1918 Influenza Pandemic: Insights for the 21st Century. *The Journal of Infectious Diseases* **195**, 1018-1028 (2007).
9. T. Girum, A. Wasie, A. Worku, Trend of HIV/AIDS for the last 26 years and predicting achievement of the 90–90-90 HIV prevention targets by 2020 in Ethiopia: a time series analysis. *BMC infectious diseases* **18**, 1-10 (2018).
10. T. S. Alexander, Human immunodeficiency virus diagnostic testing: 30 years of evolution. *Clinical and Vaccine Immunology* **23**, 249-253 (2016).
11. E. Petersen *et al.*, Comparing SARS-CoV-2 with SARS-CoV and influenza pandemics. *The Lancet infectious diseases* **20**, e238-e244 (2020).
12. J. Nicholls, X. P. DONG, G. Jiang, M. Peiris, SARS: clinical virology and pathogenesis. *Respirology* **8**, S6-S8 (2003).
13. S. S. Shrestha *et al.*, Estimating the Burden of 2009 Pandemic Influenza A (H1N1) in the United States (April 2009–April 2010). *Clinical Infectious Diseases* **52**, S75-S82 (2011).
14. D. B. Jernigan *et al.*, Detecting 2009 Pandemic Influenza A (H1N1) Virus Infection: Availability of Diagnostic Testing Led to Rapid Pandemic Response. *Clinical Infectious Diseases* **52**, S36-S43 (2011).
15. A. Chafekar, B. C. Fielding, MERS-CoV: Understanding the Latest Human Coronavirus Threat. *Viruses* **10**, 93 (2018).
16. A. Rojek, P. Horby, J. Dunning, Insights from clinical research completed during the west Africa Ebola virus disease epidemic. *The Lancet Infectious Diseases* **17**, e280-e292 (2017).
17. P. Cherpillod *et al.*, Ebola virus disease diagnosis by real-time RT-PCR: a comparative study of 11 different procedures. *Journal of Clinical Virology* **77**, 9-14 (2016).
18. N. Sinnott-Armstrong, D. Klein, B. Hickey, Evaluation of group testing for SARS-CoV-2 RNA. *MedRxiv*,

https://www.medrxiv.org/content/10.1101/2020.1103.1127.20043968v20043961 (2020).
19. T. L. Sandri *et al.*, Complementary methods for SARS-CoV-2 diagnosis in times of material shortage. *Scientific reports* **11**, 1-8 (2021).
20. Centers for Disease Control and Prevention, *Antibiotic resistance threats in the United States, 2019*. (US Department of Health and Human Services, Centres for Disease Control and …, 2019).
21. E. Charani, J. Cooke, A. Holmes, Antibiotic stewardship programmes—what's missing? *Journal of antimicrobial chemotherapy* **65**, 2275-2277 (2010).
22. M. C. O'Grady *et al.*, Empirical treatment of urinary tract infections: how rational are our guidelines? *Journal of Antimicrobial Chemotherapy* **74**, 214-217 (2019).
23. S. Leekha, C. L. Terrell, R. S. Edson, in *Mayo Clinic Proceedings*. (Elsevier, 2011), vol. 86, pp. 156-167.
24. I. Yelin *et al.*, Personal clinical history predicts antibiotic resistance of urinary tract infections. *Nature medicine* **25**, 1143-1152 (2019).
25. S. Moreno-Gamez *et al.*, Imperfect drug penetration leads to spatial monotherapy and rapid evolution of multidrug resistance. *Proceedings of the National Academy of Sciences* **112**, E2874-E2883 (2015).
26. L. Nguyen, Antibiotic resistance mechanisms in M. tuberculosis: an update. *Archives of toxicology* **90**, 1585-1604 (2016).
27. Y. Yang *et al.*, Review of Antibiotic Resistance, Ecology, Dissemination, and Mitigation in U.S. Broiler Poultry Systems. *Frontiers in Microbiology* **10**, (2019).
28. E. M. Wellington *et al.*, The role of the natural environment in the emergence of antibiotic resistance in Gram-negative bacteria. *The Lancet infectious diseases* **13**, 155-165 (2013).
29. A. A. DeNegre, M. L. Ndeffo Mbah, K. Myers, N. H. Fefferman, Emergence of antibiotic resistance in immunocompromised host populations: A case study of emerging antibiotic resistant tuberculosis in AIDS patients. *PloS one* **14**, e0212969 (2019).
30. L. J. Sherrard, M. M. Tunney, J. S. Elborn, Antimicrobial resistance in the respiratory microbiota of people with cystic fibrosis. *The Lancet* **384**, 703-713 (2014).
31. T. Cai *et al.*, Asymptomatic Bacteriuria Treatment Is Associated With a Higher Prevalence of Antibiotic Resistant Strains in Women With Urinary Tract Infections. *Clinical Infectious Diseases* **61**, 1655-1661 (2015).
32. A. S. Lee *et al.*, Methicillin-resistant Staphylococcus aureus. *Nature reviews Disease primers* **4**, 1-23 (2018).
33. L. K. Logan, R. A. Weinstein, The Epidemiology of Carbapenem-Resistant Enterobacteriaceae: The Impact and Evolution of a Global Menace. *The Journal of Infectious Diseases* **215**, S28-S36 (2017).
34. X. Zhen, C. Stålsby Lundborg, X. Sun, S. Gu, H. Dong, Clinical and Economic Burden of Carbapenem-Resistant Infection or Colonization Caused by Klebsiella pneumoniae, Pseudomonas aeruginosa, Acinetobacter baumannii: A Multicenter Study in China. *Antibiotics* **9**, 514 (2020).

35. R. O'Hanlon, M. L. Shaw, Baloxavir marboxil: the new influenza drug on the market. *Current opinion in virology* **35**, 14-18 (2019).
36. P. C. Taylor *et al.*, Neutralizing monoclonal antibodies for treatment of COVID-19. *Nature Reviews Immunology*, 1-12 (2021).
37. J. A. Simerville, W. C. Maxted, J. J. Pahira, Urinalysis: a comprehensive review. *American family physician* **71**, 1153-1162 (2005).
38. J. F. Cohen, N. Bertille, R. Cohen, M. Chalumeau, Rapid antigen detection test for group A streptococcus in children with pharyngitis. *Cochrane Database of Systematic Reviews*, (2016).
39. N. Kohmer *et al.*, The comparative clinical performance of four SARS-CoV-2 rapid antigen tests and their correlation to infectivity in vitro. *Journal of Clinical Medicine* **10**, 328 (2021).
40. M. A. Poritz *et al.*, FilmArray, an automated nested multiplex PCR system for multi-pathogen detection: development and application to respiratory tract infection. *PloS one* **6**, e26047 (2011).
41. P. Khan, L. M. Aufdembrink, A. E. Engelhart, Isothermal SARS-CoV-2 diagnostics: Tools for enabling distributed pandemic testing as a means of supporting safe reopenings. *ACS Synthetic Biology* **9**, 2861-2880 (2020).
42. T. Moehling, G. Choi, L. Dugan, M. Salit, R. Meagher, LAMP diagnostics at the point-of-care: Emerging trends and perspectives for the developer community. *Expt Rev Molec Diagnostics* **21**, 43-61 (2021).
43. N. Tomita, Y. Mori, H. Kanda, T. Notomi, Loop-mediated isothermal amplification (LAMP) of gene sequences and simple visual detection of products. *Nature protocols* **3**, 877-882 (2008).
44. Y. Furuse, Genomic sequencing effort for SARS-CoV-2 by country during the pandemic. *International Journal of Infectious Diseases* **103**, 305-307 (2021).
45. A. Rambaut *et al.*, A dynamic nomenclature proposal for SARS-CoV-2 lineages to assist genomic epidemiology. *Nature microbiology* **5**, 1403-1407 (2020).
46. A. van Belkum *et al.*, Innovative and rapid antimicrobial susceptibility testing systems. *Nature Reviews Microbiology* **18**, 299-311 (2020).
47. I. Wiegand, K. Hilpert, R. E. Hancock, Agar and broth dilution methods to determine the minimal inhibitory concentration (MIC) of antimicrobial substances. *Nature protocols* **3**, 163 (2008).
48. J. F. Mohr, A. Wanger, J. H. Rex, Pharmacokinetic/pharmacodynamic modeling can help guide targeted antimicrobial therapy for nosocomial gram-negative infections in critically ill patients. *Diagnostic microbiology and infectious disease* **48**, 125-130 (2004).
49. G. V. Doern, S. M. Brecher, The clinical predictive value (or lack thereof) of the results of in vitro antimicrobial susceptibility tests. *Journal of Clinical Microbiology* **49**, S11-S14 (2011).
50. J. H. Rex, M. A. Pfaller, Has antifungal susceptibility testing come of age? *Clinical infectious diseases* **35**, 982-989 (2002).
51. V. Nizet, The accidental orthodoxy of Drs. Mueller and Hinton. *EBioMedicine* **22**, 26-27 (2017).

52. D. K. Mercer *et al.*, Antimicrobial susceptibility testing of antimicrobial peptides to better predict efficacy. *Frontiers in Cellular and Infection Microbiology* **10**, 326 (2020).
53. B. K. Coombes, N. F. Brown, Y. Valdez, J. H. Brumell, B. B. Finlay, Expression and secretion of Salmonella pathogenicity island-2 virulence genes in response to acidification exhibit differential requirements of a functional type III secretion apparatus and SsaL. *Journal of Biological Chemistry* **279**, 49804-49815 (2004).
54. J. Z. Kubicek-Sutherland *et al.*, Host-dependent induction of transient antibiotic resistance: a prelude to treatment failure. *EBioMedicine* **2**, 1169-1178 (2015).
55. R. A. Dorschner *et al.*, The mammalian ionic environment dictates microbial susceptibility to antimicrobial defense peptides. *The FASEB Journal* **20**, 35-42 (2006).
56. S. C. Ersoy *et al.*, Bicarbonate resensitization of methicillin-resistant Staphylococcus aureus to β-lactam antibiotics. *Antimicrobial agents and chemotherapy* **63**, (2019).
57. E. Thulin, M. Thulin, D. I. Andersson, Reversion of high-level mecillinam resistance to susceptibility in Escherichia coli during growth in urine. *EBioMedicine* **23**, 111-118 (2017).
58. S. Dastgheyb, J. Parvizi, I. M. Shapiro, N. J. Hickok, M. Otto, Effect of biofilms on recalcitrance of staphylococcal joint infection to antibiotic treatment. *The Journal of infectious diseases* **211**, 641-650 (2015).
59. S. S. Magill, G. Dumyati, S. M. Ray, S. K. Fridkin, Evaluating epidemiology and improving surveillance of infections associated with health care, United States. *Emerging infectious diseases* **21**, 1537 (2015).
60. World Health Organization, Worldwide country situation analysis: response to antimicrobial resistance. (2015).
61. A. M. Caliendo *et al.*, Better tests, better care: improved diagnostics for infectious diseases. *Clinical Infectious Diseases* **57**, S139-S170 (2013).
62. N. A. Feasey, G. Dougan, R. A. Kingsley, R. S. Heyderman, M. A. Gordon, Invasive non-typhoidal salmonella disease: an emerging and neglected tropical disease in Africa. *The Lancet* **379**, 2489-2499 (2012).
63. O. Opota, K. Jaton, G. Greub, Microbial diagnosis of bloodstream infection: towards molecular diagnosis directly from blood. *Clinical microbiology and infection* **21**, 323-331 (2015).
64. J. R. Andrews, E. T. Ryan, Diagnostics for invasive Salmonella infections: current challenges and future directions. *Vaccine* **33**, C8-C15 (2015).
65. S. G. Beal *et al.*, Evaluation of the nanosphere verigene gram-positive blood culture assay with the VersaTREK blood culture system and assessment of possible impact on selected patients. *Journal of clinical microbiology* **51**, 3988-3992 (2013).
66. C. Leli *et al.*, Rapid identification of bacterial and fungal pathogens from positive blood cultures by MALDI-TOF MS. *International Journal of Medical Microbiology* **303**, 205-209 (2013).

67. T. Ly, J. Gulia, V. Pyrgos, M. Waga, S. Shoham, Impact upon clinical outcomes of translation of PNA FISH-generated laboratory data from the clinical microbiology bench to bedside in real time. *Therapeutics and clinical risk management* **4**, 637 (2008).
68. A. J. Blaschke *et al.*, Rapid identification of pathogens from positive blood cultures by multiplex polymerase chain reaction using the FilmArray system. *Diagnostic microbiology and infectious disease* **74**, 349-355 (2012).
69. F. Cockerill III *et al.*, Optimal testing parameters for blood cultures. *Clinical infectious diseases* **38**, 1724-1730 (2004).
70. N. Mancini *et al.*, The era of molecular and other non-culture-based methods in diagnosis of sepsis. *Clinical microbiology reviews* **23**, 235-251 (2010).
71. H. Salimnia *et al.*, Evaluation of the FilmArray blood culture identification panel: results of a multicenter controlled trial. *Journal of Clinical Microbiology* **54**, 687-698 (2016).
72. A. Rabinovitch *et al.*, Urinalysis and collection, transportation, and preservation of urine specimens: approved guideline. *Contract No.: NCCLS Document GP16-A2*, (2001).
73. A. L. Flores-Mireles, J. N. Walker, M. Caparon, S. J. Hultgren, Urinary tract infections: epidemiology, mechanisms of infection and treatment options. *Nature reviews microbiology* **13**, 269-284 (2015).
74. National Institutes of Health, Bladder Health for Older Adults. https://www.nia.nih.gov/health/bladder-health-older-adults (2018).
75. M. Davenport *et al.*, New and developing diagnostic technologies for urinary tract infections. *Nature Reviews Urology* **14**, 296-310 (2017).
76. C. W. Seymour *et al.*, Time to treatment and mortality during mandated emergency care for sepsis. *New England Journal of Medicine* **376**, 2235-2244 (2017).
77. A. Greenbaum *et al.*, Imaging without lenses: achievements and remaining challenges of wide-field on-chip microscopy. *Nature methods* **9**, 889-895 (2012).
78. S. Feng, D. Tseng, D. Di Carlo, O. B. Garner, A. Ozcan, High-throughput and automated diagnosis of antimicrobial resistance using a cost-effective cellphone-based micro-plate reader. *Scientific reports* **6**, 1-9 (2016).
79. X. Liu, T.-Y. Lin, P. B. Lillehoj, Smartphones for cell and biomolecular detection. *Annals of biomedical engineering* **42**, 2205-2217 (2014).
80. S. Cho, T. San Park, T. G. Nahapetian, J.-Y. Yoon, Smartphone-based, sensitive µPAD detection of urinary tract infection and gonorrhea. *Biosensors and Bioelectronics* **74**, 601-611 (2015).
81. T. Laksanasopin *et al.*, A smartphone dongle for diagnosis of infectious diseases at the point of care. *Science translational medicine* **7**, 273re271-273re271 (2015).
82. S.-J. Yeo *et al.*, Smartphone-based fluorescent diagnostic system for highly pathogenic H5N1 viruses. *Theranostics* **6**, 231 (2016).
83. Y. S. Jiang *et al.*, Portable platform for rapid in-field identification of human fecal pollution in water. *Water research* **131**, 186-195 (2018).

84. A. Priye *et al.*, A smartphone-based diagnostic platform for rapid detection of Zika, chikungunya, and dengue viruses. *Scientific reports* **7**, 1-11 (2017).
85. J. E. Kong *et al.*, Highly stable and sensitive nucleic acid amplification and cell-phone-based readout. *ACS nano* **11**, 2934-2943 (2017).
86. H. Im *et al.*, Digital diffraction analysis enables low-cost molecular diagnostics on a smartphone. *Proceedings of the National Academy of Sciences* **112**, 5613-5618 (2015).
87. W. Chen *et al.*, Mobile platform for multiplexed detection and differentiation of disease-specific nucleic acid sequences, using microfluidic loop-mediated isothermal amplification and smartphone detection. *Analytical chemistry* **89**, 11219-11226 (2017).
88. G. L. Damhorst *et al.*, Smartphone-imaged HIV-1 reverse-transcription loop-mediated isothermal amplification (RT-LAMP) on a chip from whole blood. *Engineering* **1**, 324-335 (2015).
89. A. Ganguli *et al.*, Hands-free smartphone-based diagnostics for simultaneous detection of Zika, Chikungunya, and Dengue at point-of-care. *Biomedical microdevices* **19**, 1-13 (2017).
90. S.-C. Liao *et al.*, Smart cup: a minimally-instrumented, smartphone-based point-of-care molecular diagnostic device. *Sensors and Actuators B: Chemical* **229**, 232-238 (2016).
91. R. Snodgrass *et al.*, KS-Detect–validation of solar thermal PCR for the diagnosis of Kaposi's sarcoma using pseudo-biopsy samples. *PLoS One* **11**, e0147636 (2016).
92. R. D. Stedtfeld *et al.*, Gene-Z: a device for point of care genetic testing using a smartphone. *Lab on a Chip* **12**, 1454-1462 (2012).
93. D. Shin *et al.*, Mobile nucleic acid amplification testing (mobiNAAT) for Chlamydia trachomatis screening in hospital emergency department settings. *Scientific reports* **7**, 1-10 (2017).
94. A. Tichopad, M. Dilger, G. Schwarz, M. W. Pfaffl, Standardized determination of real-time PCR efficiency from a single reaction set-up. *Nucleic acids research* **31**, e122-e122 (2003).
95. Y. Mori, M. Kitao, N. Tomita, T. Notomi, Real-time turbidimetry of LAMP reaction for quantifying template DNA. *Journal of biochemical and biophysical methods* **59**, 145-157 (2004).
96. A. S. Patterson *et al.*, Microfluidic chip-based detection and intraspecies strain discrimination of Salmonella serovars derived from whole blood of septic mice. *Applied and environmental microbiology* **79**, 2302-2311 (2013).
97. R. A. Edwards, G. J. Olsen, S. R. Maloy, Comparative genomics of closely related salmonellae. *Trends in microbiology* **10**, 94-99 (2002).
98. N. R. Thomson *et al.*, Comparative genome analysis of Salmonella Enteritidis PT4 and Salmonella Gallinarum 287/91 provides insights into evolutionary and host adaptation pathways. *Genome research* **18**, 1624-1637 (2008).
99. K. De Rauw, L. Detemmerman, J. Breynaert, D. Piérard, Detection of Shiga toxin-producing and other diarrheagenic Escherichia coli by the BioFire FilmArray® Gastrointestinal Panel in human fecal samples. *European Journal of Clinical Microbiology & Infectious Diseases* **35**, 1479-1486 (2016).

100. R. Khare *et al.*, Comparative evaluation of two commercial multiplex panels for detection of gastrointestinal pathogens by use of clinical stool specimens. *Journal of clinical microbiology* **52**, 3667-3673 (2014).
101. J. Delzell, M. LeFevre, Urinary tract infections during pregnancy. *American family physician* **61**, 713-720 (2000).
102. N. Gupta, B. M. Limbago, J. B. Patel, A. J. Kallen, Carbapenem-resistant Enterobacteriaceae: epidemiology and prevention. *Clinical infectious diseases* **53**, 60-67 (2011).
103. S. S. Kanj, Z. A. Kanafani, in *Mayo Clinic Proceedings*. (Elsevier, 2011), vol. 86, pp. 250-259.
104. A.-P. Magiorakos *et al.*, Multidrug-resistant, extensively drug-resistant and pandrug-resistant bacteria: an international expert proposal for interim standard definitions for acquired resistance. *Clinical microbiology and infection* **18**, 268-281 (2012).
105. N. J. Loman *et al.*, High-throughput bacterial genome sequencing: an embarrassment of choice, a world of opportunity. *Nature Reviews Microbiology* **10**, 599-606 (2012).
106. S. Peacock, Health care: Bring microbial sequencing to hospitals. *Nature News* **509**, 557 (2014).
107. K. Hayashida, K. Kajino, L. Hachaambwa, B. Namangala, C. Sugimoto, Direct blood dry LAMP: a rapid, stable, and easy diagnostic tool for Human African Trypanosomiasis. *PLoS Negl Trop Dis* **9**, e0003578 (2015).
108. T. Yoshikawa *et al.*, Direct detection of human herpesvirus 6B by the LAMP method using newly developed dry-reagents. *Journal of virological methods* **201**, 65-67 (2014).
109. L. Diaz *et al.*, in *2017 ASABE Annu Intl Meeting*. (Amer Soc Agricultural and Biological Engineers, 2017), pp. 1.
110. Y. Kang *et al.*, Etiologic diagnosis of lower respiratory tract bacterial infections using sputum samples and quantitative loop-mediated isothermal amplification. *PloS one* **7**, e38743 (2012).
111. J. L. Yang *et al.*, Simple and rapid detection of Salmonella serovar Enteritidis under field conditions by loop-mediated isothermal amplification. *Journal of applied microbiology* **109**, 1715-1723 (2010).
112. M. Okamura *et al.*, Rapid, sensitive, and specific detection of the O4 group of Salmonella enterica by loop-mediated isothermal amplification. *Avian diseases* **53**, 216-221 (2009).
113. Z. Xu *et al.*, Development and application of loop-mediated isothermal amplification assays on rapid detection of various types of staphylococci strains. *Food Research International* **47**, 166-173 (2012).
114. D. W. Kim *et al.*, The enhanced pneumococcal LAMP assay: a clinical tool for the diagnosis of meningitis due to Streptococcus pneumoniae. *PLoS One* **7**, e42954 (2012).
115. T. Horisaka *et al.*, Sensitive and specific detection of Yersinia pseudotuberculosis by loop-mediated isothermal amplification. *Journal of clinical microbiology* **42**, 5349-5352 (2004).

116. World Health Organization, WHO Coronavirus (COVID-19) Dashboard. https://covid19.who.int/. 2021.
117. N. Ravi, D. Cortade, E. Ng, S. Wang, Diagnostics for SARS-CoV-2 detection: A comprehensive review of the FDA-EUA COVID-19 testing landscape. *Biosensors Bioelectronics* **165**, 112454 (2020).
118. O. Vandenberg, D. Martiny, O. Rochas, A. van Belkum, Z. Kozlakidis, Considerations for diagnostic COVID-19 tests. *Nat Rev Microbiol*, 1-13 (2020).
119. G. Guglielmi, Rapid coronavirus tests: a guide for the perplexed. *Nature* **590**, 202-205 (2021).
120. R. Weissleder, H. Lee, J. Ko, M. Pittet, COVID-19 diagnostics in context. *Sci Transl Med* **12**, (2020).
121. R. Augustine *et al.*, Rapid antibody-based COVID-19 mass surveillance: relevance, challenges, and prospects in a pandemic and Post-Pandemic world. *J Clin Med* **9**, 3372 (2020).
122. S. Desmarais, T. Leitner, A. Barron, Quantitative experimental determination of primer–dimer formation risk by free-solution conjugate electrophoresis. *Electrophoresis* **33**, 483-491 (2012).
123. R. Meagher, A. Priye, Y. Light, C. Huang, E. Wang, Impact of primer dimers and self-amplifying hairpins on reverse transcription loop-mediated isothermal amplification detection of viral RNA. *Analyst* **143**, 1924-1933 (2018).
124. Y. Zou, M. Mason, J. Botella, Evaluation and improvement of isothermal amplification methods for point-of-need plant disease diagnostics. *PloS one* **15**, e0235216 (2020).
125. Centers for Disease Control and Prevention, Testing guidance for clinicians when SARS-CoV-2 and influenza viruses are co-circulating. https://www.cdc.gov/flu/professionals/diagnosis/testing-guidance-for-clinicians.htm. 2021.
126. E. A. Belongia, M. T. Osterholm, COVID-19 and flu, a perfect storm. *Science* **368**, 1163 (2020).
127. R. Rubin, What happens when COVID-19 collides with flu season? *JAMA* **324**, 923-925 (2020).
128. K. Servick, Coronavirus creates a flu season guessing game. *Science* **369**, 890-891 (2020).
129. X. Chen *et al.*, The microbial coinfection in COVID-19. *Appl Microbiol Biotech* **104**, 7777-7785 (2020).
130. J. Contreras-Naranjo, Q. Wei, A. Ozcan, Mobile phone-based microscopy, sensing, and diagnostics. *IEEE J Selected Topics Quantum Electronics* **22**, 1-14 (2015).
131. M. Citartan, T.-H. Tang, Recent developments of aptasensors expedient for point-of-care (POC) diagnostics. *Talanta* **199**, 556-566 (2019).
132. X. Xu *et al.*, Advances in smartphone-based point-of-care diagnostics. *Proc IEEE* **103**, 236-247 (2015).
133. A. Ozcan, Mobile phones democratize and cultivate next-generation imaging, diagnostics and measurement tools. *Lab on a Chip* **14**, 3187-3194 (2014).

134. D. Ong, M. Poljak, Smartphones as mobile microbiological laboratories. *Clini Microbiol Infect* **26**, 421-424 (2020).
135. S. O'Dea, Number of smartphone users worldwide from 2016 to 2023. https://www.statista.com/statistics/330695/number-of-smartphone-users-worldwide/ (2021).
136. U.S. Food and Drug Administration, Molecular diagnostic template for laboratories. *https://www.fda.gov/medical-devices/coronavirus-disease-2019-covid-19-emergency-use-authorizations-medical-devices/in-vitro-diagnostics-euas (updated July 28, 2020)*. 2021.
137. Centers for Disease Control and Prevention, CDC's diagnostic test for COVID-19 only and supplies. *https://www.cdc.gov/coronavirus/2019-ncov/lab/virus-requests.html*. 2020.
138. Centers for Disease Control and Prevention, SARS-CoV-2 variant classifications and definitions. *https://www.cdc.gov/coronavirus/2019-ncov/cases-updates/variant-surveillance/variant-info.html*. 2021.
139. Centers for Disease Control and Prevention, CDC's influenza SARS-CoV-2 multiplex assay and required supplies. *https://www.cdc.gov/coronavirus/2019-ncov/lab/multiplex.html*. 2021.
140. A. L. Wyllie *et al.*, Saliva or nasopharyngeal swab specimens for detection of SARS-CoV-2. *New England Journal of Medicine* **383**, 1283-1286 (2020).
141. E. Williams, K. Bond, B. Zhang, M. Putland, D. Williamson, Saliva as a non-invasive specimen for detection of SARS-CoV-2. *J Clin Microbiol* **58**, e00776-00720 (2020).
142. I. Hernández-Neuta *et al.*, Smartphone-based clinical diagnostics: towards democratization of evidence-based health care. *J Internal Med* **285**, 19-39 (2019).
143. J. Hollander, B. Carr, Virtually perfect? Telemedicine for COVID-19. *New Engl J Med* **382**, 1679-1681 (2020).
144. L. Barnes *et al.*, Smartphone-based pathogen diagnosis in urinary sepsis patients. *EBioMedicine* **36**, 73-82 (2018).
145. J. Broughton *et al.*, CRISPR–Cas12-based detection of SARS-CoV-2. *Nat Biotech* **38**, 870-874 (2020).
146. V. Thi *et al.*, A colorimetric RT-LAMP assay and LAMP-sequencing for detecting SARS-CoV-2 RNA in clinical samples. *Sci Transl Med* **12**, 1-13 (2020).
147. A. Ganguli *et al.*, Rapid isothermal amplification and portable detection system for SARS-CoV-2. *Proc Natl Acad Sci USA* **117**, 22727-22735 (2020).
148. L. Poon *et al.*, Detection of human influenza A viruses by loop-mediated isothermal amplification. *J Clin Microbiol* **43**, 427-430 (2005).
149. A. Rambaut *et al.*, Preliminary genomic characterisation of an emergent SARS-CoV-2 lineage in the UK defined by a novel set of spike mutations. https://virological.org/t/preliminary-genomic-characterisation-of-an-emergent-sars-cov-2-lineage-in-the-uk-defined-by-a-novel-set-of-spike-mutations/563 (2020).
150. A. O'Toole *et al.*, pangolin: lineage assignment in an emerging pandemic as an epidemiological tool. https://cov-lineages.org/global_report.html (2021).

151. H. Tegally *et al.*, Detection of a SARS-CoV-2 variant of concern in South Africa. *Nature* **592**, 438-443 (2021).
152. F. Naveca *et al.*, Phylogenetic relationship of SARS-CoV-2 sequences from Amazonas with emerging Brazilian variants harboring mutations E484K and N501Y in the Spike protein. https://virological.org/t/phylogenetic-relationship-of-sars-cov-2-sequences-from-amazonas-with-emerging-brazilian-variants-harboring-mutations-e484k-and-n501y-in-the-spike-protein/585 (2021).
153. X. Deng *et al.*, Transmission, infectivity, and antibody neutralization of an emerging SARS-CoV-2 variant in California carrying a L452R spike protein mutation. *medRxiv*, https://www.medrxiv.org/content/10.1101/2021.1103.1107.21252647v21252641 (2021).
154. J. Cadena *et al.*, Detection of the new SARS-CoV-2 variant B. 1.526 with the Spike E484K mutation in South America. 2021 (10.21203/rs.3.rs-248965/v1).
155. World Health Organization, Tracking SARS-CoV-2 variants. *https://www.who.int/en/activities/tracking-SARS-CoV-2-variants (accessed June 10, 2021)* 2021.
156. United States Department of Health and Human Services Centers for Disease Control and Prevention, Antibiotic resistance threats in the United States, 2013. *Threat Report*, 50-52 (2013).
157. World Health Organization, "Antimicrobial resistance global report on surveillance: 2014 summary," (World Health Organization, 2014).
158. World Health Assembly, *Antimicrobial resistance.*, (67.25, R (Ed.), Sixty-seventh World Health Assembly., 2014).
159. PCAST, National action plan for combatting antibiotic-resistant bacteria. *Washington, DC: White House*, (2015).
160. World Health Organization, Standardization of methods for conducting microbic sensitivity tests: second report of the Expert Committee on Antibiotics [meeting held in Geneva from 11 to 16 July 1960]. (1961).
161. S. M. Diene, J.-M. Rolain, Carbapenemase genes and genetic platforms in Gram-negative bacilli: Enterobacteriaceae, Pseudomonas and Acinetobacter species. *Clinical Microbiology and Infection* **20**, 831-838 (2014).
162. Clinical and Laboratory Standards Institute, *Methods for Dilution Antimicrobial Susceptibility Tests for Bacteria That Grow Aerobically (Approved standard-ninth edition)*. (2012).
163. European Committee on Antimicrobial Susceptibility Testing, EUCAST definitions of clinical breakpoints and epidemiological cut-off values. (2014).
164. V. L. Yu *et al.*, An international prospective study of pneumococcal bacteremia: correlation with in vitro resistance, antibiotics administered, and clinical outcome. *Clinical Infectious Diseases* **37**, 230-237 (2003).
165. V. I. Band *et al.*, Antibiotic failure mediated by a resistant subpopulation in Enterobacter cloacae. *Nature microbiology* **1**, 1-9 (2016).
166. L. Lin *et al.*, Azithromycin synergizes with cationic antimicrobial peptides to exert bactericidal and therapeutic activity against highly multidrug-resistant gram-negative bacterial pathogens. *EBioMedicine* **2**, 690-698 (2015).

167. R. Dulbecco, Plaque production by polyoma virus. *Virology* **8**, 396-397 (1969).
168. S. Lacks, Integration efficiency and genetic recombination in pneumococcal transformation. *Genetics* **53**, 207 (1966).
169. M.-C. Trombe, C. Clavé, J.-M. Manias, Calcium regulation of growth and differentiation in Streptococcus pneumoniae. *Microbiology* **138**, 77-84 (1992).
170. L. J. Hathaway *et al.*, Capsule type of Streptococcus pneumoniae determines growth phenotype. *PLoS Pathog* **8**, e1002574 (2012).
171. O. Steele-Mortimer, The Salmonella-containing vacuole—moving with the times. *Current opinion in microbiology* **11**, 38-45 (2008).
172. T. L. Holland, C. Arnold, V. G. Fowler, Clinical management of Staphylococcus aureus bacteremia: a review. *Jama* **312**, 1330-1341 (2014).
173. D. Yahav, L. Farbman, L. Leibovici, M. Paul, Colistin: new lessons on an old antibiotic. *Clinical microbiology and infection* **18**, 18-29 (2012).
174. V. Cano *et al.*, K lebsiella pneumoniae survives within macrophages by avoiding delivery to lysosomes. *Cellular microbiology* **17**, 1537-1560 (2015).
175. S. Carryn *et al.*, Intracellular pharmacodynamics of antibiotics. *Infectious Disease Clinics* **17**, 615-634 (2003).
176. Mayo Clinic, Bicarbonate, Serum. http://www.mayomedicallaboratories.com/test-catalog/Clinical+and+Interpretive/876 (2017).
177. C. S. Deutschman, K. J. Tracey, Sepsis: current dogma and new perspectives. *Immunity* **40**, 463-475 (2014).
178. L. Hermansen, J.-B. Osnes, Blood and muscle pH after maximal exercise in man. *Journal of applied physiology* **32**, 304-308 (1972).
179. T. Rosenthal, The effect of temperature on the pH of blood and plasma in vitro. *Journal of Biological Chemistry* **173**, 25-30 (1948).
180. E. Newbrun, C. I. Hoover, M. I. Ryder, Bactericidal action of bicarbonate ion on selected periodontal pathogenic microorganisms. *Journal of periodontology* **55**, 658-667 (1984).
181. V. Pader *et al.*, Staphylococcus aureus inactivates daptomycin by releasing membrane phospholipids. *Nature microbiology* **2**, 1-8 (2016).
182. P. G. Ambrose *et al.*, Pharmacokinetics-pharmacodynamics of antimicrobial therapy: it's not just for mice anymore. *Clinical Infectious Diseases* **44**, 79-86 (2007).
183. M. R. Deziel *et al.*, Effective antimicrobial regimens for use in humans for therapy of Bacillus anthracis infections and postexposure prophylaxis. *Antimicrobial Agents and Chemotherapy* **49**, 5099-5106 (2005).
184. N. M. Vega, J. Gore, Collective antibiotic resistance: mechanisms and implications. *Current opinion in microbiology* **21**, 28-34 (2014).
185. R. A. Sorg *et al.*, Collective resistance in microbial communities by intracellular antibiotic deactivation. *PLoS biology* **14**, e2000631 (2016).
186. R. Logan, R. S. Funk, E. Axcell, J. P. Krise, Drug-drug interactions involving lysosomes: mechanisms and potential clinical implications. *Expert opinion on drug metabolism & toxicology* **8**, 943-958 (2012).

187. S. Carlsson, N. Wiklund, L. Engstrand, E. Weitzberg, J. Lundberg, Effects of pH, nitrite, and ascorbic acid on nonenzymatic nitric oxide generation and bacterial growth in urine. *Nitric oxide* **5**, 580-586 (2001).
188. D. L. Paterson, R. A. Bonomo, Extended-spectrum β-lactamases: a clinical update. *Clinical microbiology reviews* **18**, 657-686 (2005).
189. Societe Francaise de Microbiologie, Comite de l'Antibiogramme de la Societe Francaise de Microbiologie (CASFM). (2012).
190. Clinical and Laboratory Standards Institute, Performance standards for antimicrobial resistance testing; twenty-second informational supplement. (2012).
191. Clinical and Laboratory Standards Institute, Minimum inhibitory concentration (MIC) breakpoints for veterinary pathogens. (2013).
192. Clinical and Laboratory Standards Institute, Performance standards for antimicrobial resistance testing; twenty-fourth informational supplement. (2014).
193. European Committee on Antimicrobial Susceptibility Testing, Breakpoint tables for interpretation of MICs and zone diameters. Version 6.0., (2016).
194. P. Fuchs, A. Barry, S. Brown, Interpretive criteria and quality control parameters for testing of susceptibilities of Haemophilus influenzae and Streptococcus pneumoniae to trimethoprim and trimethoprim-sulfamethoxazole. The antimicrobial susceptibility testing OC group. *J Clin Microbiol* **35**, 125-131 (1997).
195. D. Landman, C. Georgescu, D. A. Martin, J. Quale, Polymyxins revisited. *Clinical microbiology reviews* **21**, 449-465 (2008).
196. R. Wise, J. Andrews, J. Ashby, Activity of daptomycin against Gram-positive pathogens: a comparison with other agents and the determination of a tentative breakpoint. *Journal of Antimicrobial Chemotherapy* **48**, 563-567 (2001).
197. European Committee on Antimicrobial Susceptibility Testing, Breakpoint tables for interpretation of MICs and zone diameters. (2016).
198. Food and Drug Administration, Guidance for Industry Microbiological Data for Systemic Antibacterial Drug Products—Development, Analysis, and Presentation. *Center for Drug Evaluation and Research (CDER), US Department of Health and Human Services*, (2009).
199. J. A. Washington, P. K. Yu, In vitro antibacterial activity of spectinomycin. *Antimicrobial agents and chemotherapy* **2**, 427-430 (1972).
200. I. Stock, B. Wiedemann, Natural antibiotic susceptibilities of Edwardsiella tarda, E. ictaluri, and E. hoshinae. *Antimicrobial agents and chemotherapy* **45**, 2245-2255 (2001).
201. H. Hao *et al.*, Susceptibility breakpoint for enrofloxacin against swine Salmonella spp. *Journal of clinical microbiology* **51**, 3070-3072 (2013).
202. R. S. Singer *et al.*, Relationship between phenotypic and genotypic florfenicol resistance in Escherichia coli. *Antimicrobial agents and chemotherapy* **48**, 4047-4049 (2004).
203. E. Martens, A. L. Demain, The antibiotic resistance crisis, with a focus on the United States. *The Journal of antibiotics* **70**, 520-526 (2017).

204. A. Y. Guh *et al.*, Epidemiology of carbapenem-resistant Enterobacteriaceae in 7 US communities, 2012-2013. *JAMA* **314**, 1479-1487 (2015).
205. K. R. Woodworth *et al.*, Vital signs: containment of novel multidrug-resistant organisms and resistance mechanisms—United States, 2006–2017. *Morbidity and Mortality Weekly Report* **67**, 396 (2018).
206. M. A. E.-G. El-Sayed Ahmed *et al.*, Colistin and its role in the Era of antibiotic resistance: an extended review (2000–2019). *Emerging microbes & infections* **9**, 868-885 (2020).
207. S. C. Ersoy *et al.*, Correcting a fundamental flaw in the paradigm for antimicrobial susceptibility testing. *EBioMedicine* **20**, 173-181 (2017).
208. S. C. Ersoy *et al.*, Scope and predictive genetic/phenotypic signatures of bicarbonate (NaHCO3) responsiveness and β-lactam sensitization in methicillin-resistant Staphylococcus aureus. *Antimicrobial agents and chemotherapy* **64**, e02445-02419 (2020).
209. J. Schlichter, H. MacLean, A method of determining the effective therapeutic level in the treatment of subacute bacterial endocarditis with penicillin: a preliminary report. *American heart journal* **34**, 209-211 (1947).
210. D. M. De Oliveira *et al.*, Antimicrobial resistance in ESKAPE pathogens. *Clinical microbiology reviews* **33**, e00181-00119 (2020).
211. M. Zervos, D. Schaberg, Reversal of the in vitro susceptibility of enterococci to trimethoprim-sulfamethoxazole by folinic acid. *Antimicrobial agents and chemotherapy* **28**, 446-448 (1985).
212. K. T. Wisell, G. Kahlmeter, C. G. Giske, Trimethoprim and enterococci in urinary tract infections: new perspectives on an old issue. *Journal of antimicrobial chemotherapy* **62**, 35-40 (2008).
213. D. Fernández-Villa, M. R. Aguilar, L. Rojo, Folic acid antagonists: antimicrobial and immunomodulating mechanisms and applications. *International journal of molecular sciences* **20**, 4996 (2019).
214. J. Hamilton-Miller, Reversal of activity of trimethoprim against Gram-positive cocci by thymidine, thymine and 'folates'. *Journal of Antimicrobial Chemotherapy* **22**, 35-39 (1988).
215. S. Bushby, Trimethoprim-sulfamethoxazole: in vitro microbiological aspects. *Journal of Infectious Diseases* **128**, S442-S462 (1973).
216. S. Bushby, G. Hitchings, Trimethoprim, a sulphonamide potentiator. *British journal of pharmacology and chemotherapy* **33**, 72-90 (1968).
217. J. Barrila *et al.*, Modeling host-pathogen interactions in the context of the microenvironment: three-dimensional cell culture comes of age. *Infection and immunity* **86**, e00282-00218 (2018).
218. H. Praetorius, The Bacteria and the Host: A Story of Purinergic Signaling in Urinary Tract Infections. *American Journal of Physiology-Cell Physiology*, (2021).
219. A. K. Hottes *et al.*, Bacterial adaptation through loss of function. *PLoS genetics* **9**, e1003617 (2013).
220. S. B. Andersen, R. L. Marvig, S. Molin, H. K. Johansen, A. S. Griffin, Long-term social dynamics drive loss of function in pathogenic bacteria. *Proceedings of the National Academy of Sciences* **112**, 10756-10761 (2015).

221. C. J. Mathews, V. C. Weston, A. Jones, M. Field, G. Coakley, Bacterial septic arthritis in adults. *The Lancet* **375**, 846-855 (2010).
222. T. van der Poll, F. L. van de Veerdonk, B. P. Scicluna, M. G. Netea, The immunopathology of sepsis and potential therapeutic targets. *Nature Reviews Immunology* **17**, 407 (2017).
223. A. Jyoti, S. Kumar, V. K. Srivastava, S. Kaushik, S. G. Singh, Neonatal sepsis at point of care. *Clinica Chimica Acta*, (2021).
224. M. Singer *et al.*, The third international consensus definitions for sepsis and septic shock (Sepsis-3). *JAMA* **315**, 801-810 (2016).
225. R. Fass, Erythromycin, clarithromycin, and azithromycin: use of frequency distribution curves, scattergrams, and regression analyses to compare in vitro activities and describe cross-resistance. *Antimicrobial agents and chemotherapy* **37**, 2080-2086 (1993).
226. Cephalexin Capsules USP [Product Insert]. Sellersville, PA: Teva Pharmaceuticals (2012).
227. European Committee on Antimicrobial Susceptibility Testing, Breakpoint tables for interpretation of MICs and zone diameters. Version 9.0, 2019. (2019).
228. A. Hällgren *et al.*, Antimicrobial susceptibility patterns of enterococci in intensive care units in Sweden evaluated by different MIC breakpoint systems. *Journal of Antimicrobial Chemotherapy* **48**, 53-62 (2001).
229. SFM Antibiogram Committee, Comité de l'Antibiogramme de la Société Française de Microbiologie report 2003. *International Journal of Antimicrobial Agents* **21**, 364-391 (2003).
230. M. Di Marco *et al.*, Opinion: Sustainable development must account for pandemic risk. *Proceedings of the National Academy of Sciences* **117**, 3888-3892 (2020).
231. T. Wu, The socioeconomic and environmental drivers of the COVID-19 pandemic: A review. *Ambio*, 1-12 (2021).
232. B. Malik, S. Bhattacharyya, Antibiotic drug-resistance as a complex system driven by socio-economic growth and antibiotic misuse. *Scientific reports* **9**, 1-12 (2019).
233. A. Emmerson, A. Jones, The quinolones: decades of development and use. *Journal of Antimicrobial Chemotherapy* **51**, 13-20 (2003).
234. R. Aminov, History of antimicrobial drug discovery: Major classes and health impact. *Biochemical pharmacology* **133**, 4-19 (2017).
235. E. P. Lesho, M. Laguio-Vila, in *Mayo Clinic Proceedings*. (Elsevier, 2019), vol. 94, pp. 1040-1047.
236. E. Pasomsub *et al.*, Saliva sample as a non-invasive specimen for the diagnosis of coronavirus disease 2019: a cross-sectional study. *Clinical Microbiology and Infection* **27**, 285. e281-285. e284 (2021).
237. C. Carter, K. Akrami, D. Hall, D. Smith, E. Aronoff-Spencer, Lyophilized visually readable loop-mediated isothermal reverse transcriptase nucleic acid amplification test for detection Ebola Zaire RNA. *Journal of virological methods* **244**, 32-38 (2017).

238. N. F. Abou Heidar, J. A. Degheili, A. A. Yacoubian, R. B. Khauli, Management of urinary tract infection in women: A practical approach for everyday practice. *Urology annals* **11**, 339 (2019).
239. R. Orenstein, E. S. Wong, Urinary tract infections in adults. *American family physician* **59**, 1225 (1999).
240. S. Lahiri *et al.*, Evaluation of LAMP-based assays for carbapenemase genes. *Journal of Medical Microbiology* **68**, 1431-1437 (2019).
241. L. Freire-Moran *et al.*, Critical shortage of new antibiotics in development against multidrug-resistant bacteria—Time to react is now. *Drug resistance updates* **14**, 118-124 (2011).
242. M. I. Hutchings, A. W. Truman, B. Wilkinson, Antibiotics: past, present and future. *Current opinion in microbiology* **51**, 72-80 (2019).
243. R. Lood, K. W. Waldetoft, P. Nordenfelt, Localization-triggered bacterial pathogenesis. *Future microbiology* **10**, 1659-1668 (2015).
244. M. A. Farha, E. D. Brown, Drug repurposing for antimicrobial discovery. *Nature microbiology* **4**, 565-577 (2019).
245. D. M. Heithoff *et al.*, Intraspecies variation in the emergence of hyperinfectious bacterial strains in nature. *PLoS Pathog* **8**, e1002647 (2012).
246. D. M. Heithoff *et al.*, Human Salmonella clinical isolates distinct from those of animal origin. *Applied and Environmental Microbiology* **74**, 1757-1766 (2008).
247. J. Z. Kubicek-Sutherland, D. M. Heithoff, S. C. Ersoy, W. R. Shimp, M. J. Mahan, Immunization with a DNA adenine methylase over-producing Yersinia pseudotuberculosis vaccine confers robust cross-protection against heterologous pathogenic serotypes. *Vaccine* **32**, 1451-1459 (2014).
248. D. J. Diekema *et al.*, Continued emergence of USA300 methicillin-resistant Staphylococcus aureus in the United States: results from a nationwide surveillance study. *Infection Control & Hospital Epidemiology* **35**, 285-292 (2014).
249. K. Nagamine, T. Hase, T. Notomi, Accelerated reaction by loop-mediated isothermal amplification using loop primers. *Molecular and cellular probes* **16**, 223-229 (2002).
250. L. M. Diaz, Point-of-Care Electroflotation of Dispersed, Low Tolerance Pathogens Improves Detection Rates by Loop Mediated Isothermal Amplification. *University of Hawai'i at Mānoa*, (2017).
251. J. Beige *et al.*, Clinical evaluation of a Mycobacterium tuberculosis PCR assay. *Journal of clinical microbiology* **33**, 90-95 (1995).
252. IT Union, ICT facts and figures. https://www.itu.int/en/ITU-D/Statistics/Documents/facts/ICTFactsFigures2013-e.pdf (2013).
253. A. Klimov *et al.*, Influenza virus titration, antigenic characterization, and serological methods for antibody detection. *In Influenza Virus, Springer*, 25-51 (2012).
254. J. A. Lanie *et al.*, Genome sequence of Avery's virulent serotype 2 strain D39 of Streptococcus pneumoniae and comparison with that of unencapsulated laboratory strain R6. *Journal of bacteriology* **189**, 38-51 (2007).

255. N. C. Daw *et al.*, Nasopharyngeal Carriage of Penicillin-resistantStreptococcus pneumoniae in Children With Sickle Cell Disease. *Pediatrics* **99**, e7-e7 (1997).
256. R. Carter *et al.*, Genomic analyses of pneumococci from children with sickle cell disease expose host-specific bacterial adaptations and deficits in current interventions. *Cell host & microbe* **15**, 587-599 (2014).
257. R. Davis, D. Botstein, J. Roth, *Advanced Bacterial Genetics.*, Advanced Bacterial Genetics (Cold Spring Harbor Laboratory Press, Plainview, NY, 1980).